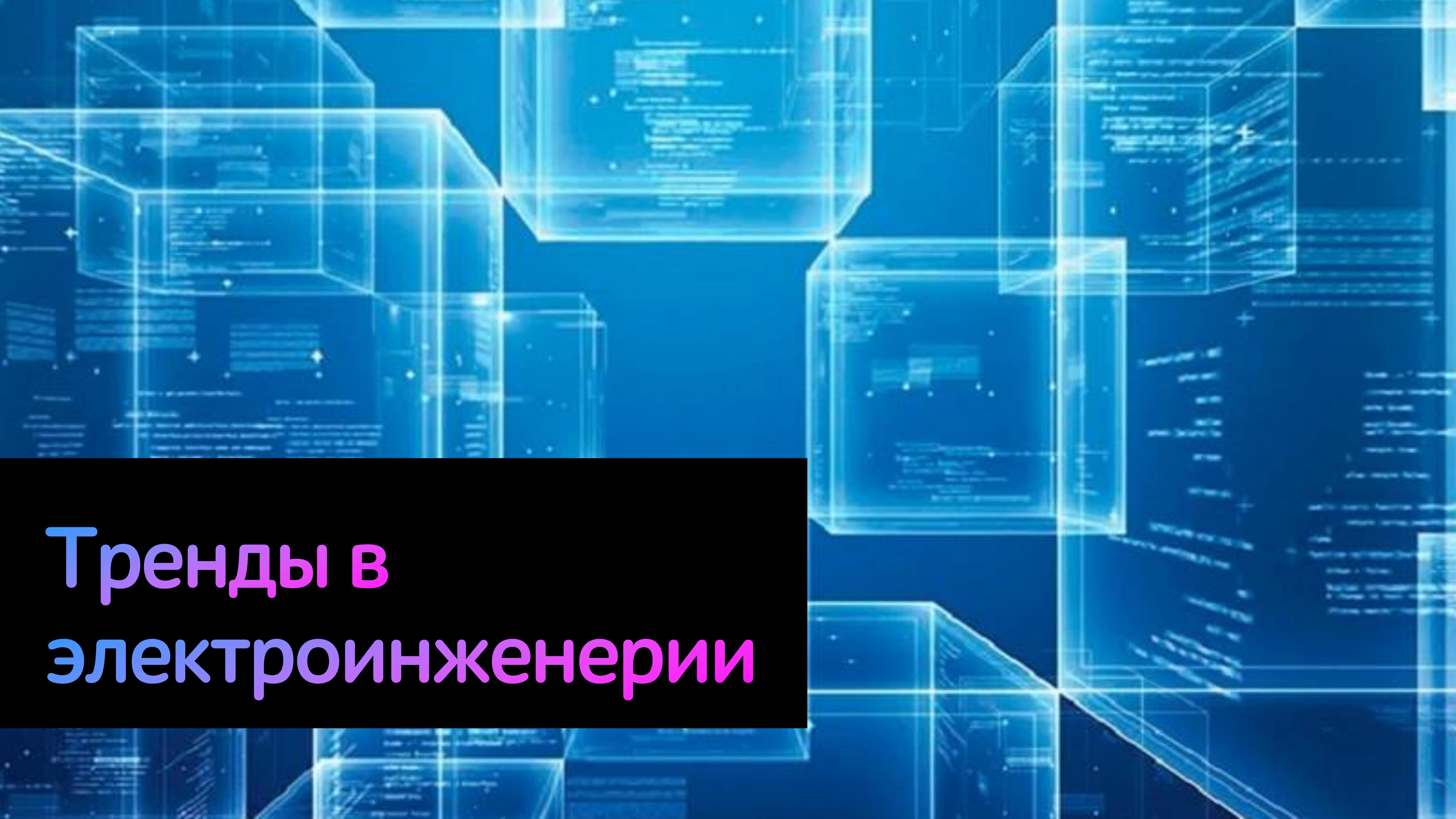


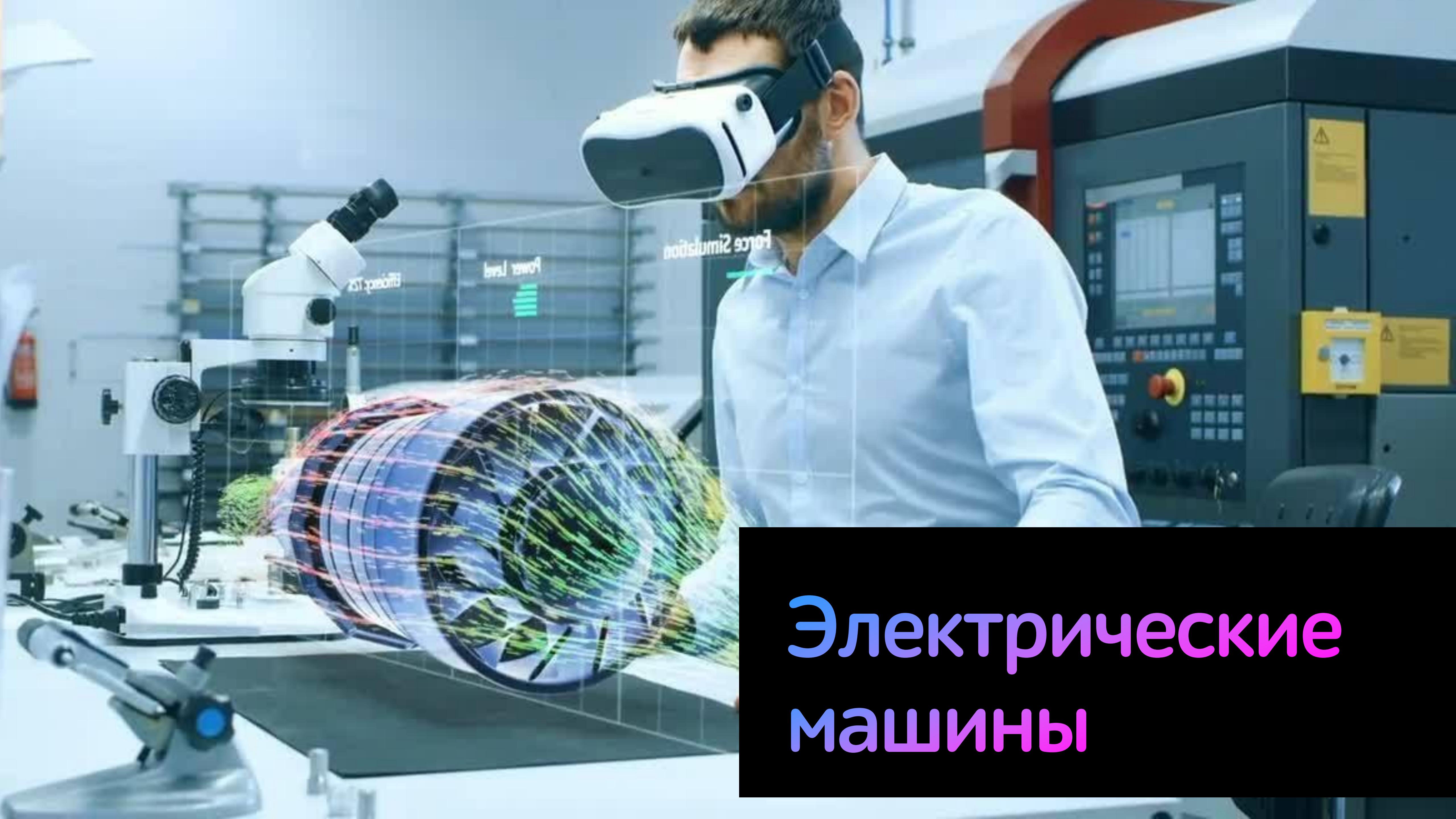
Интеллектуальное управление и тренды в электроинженерии

К.Т.Н., доцент
Университет ИТМО
Демидова Галина Львовна



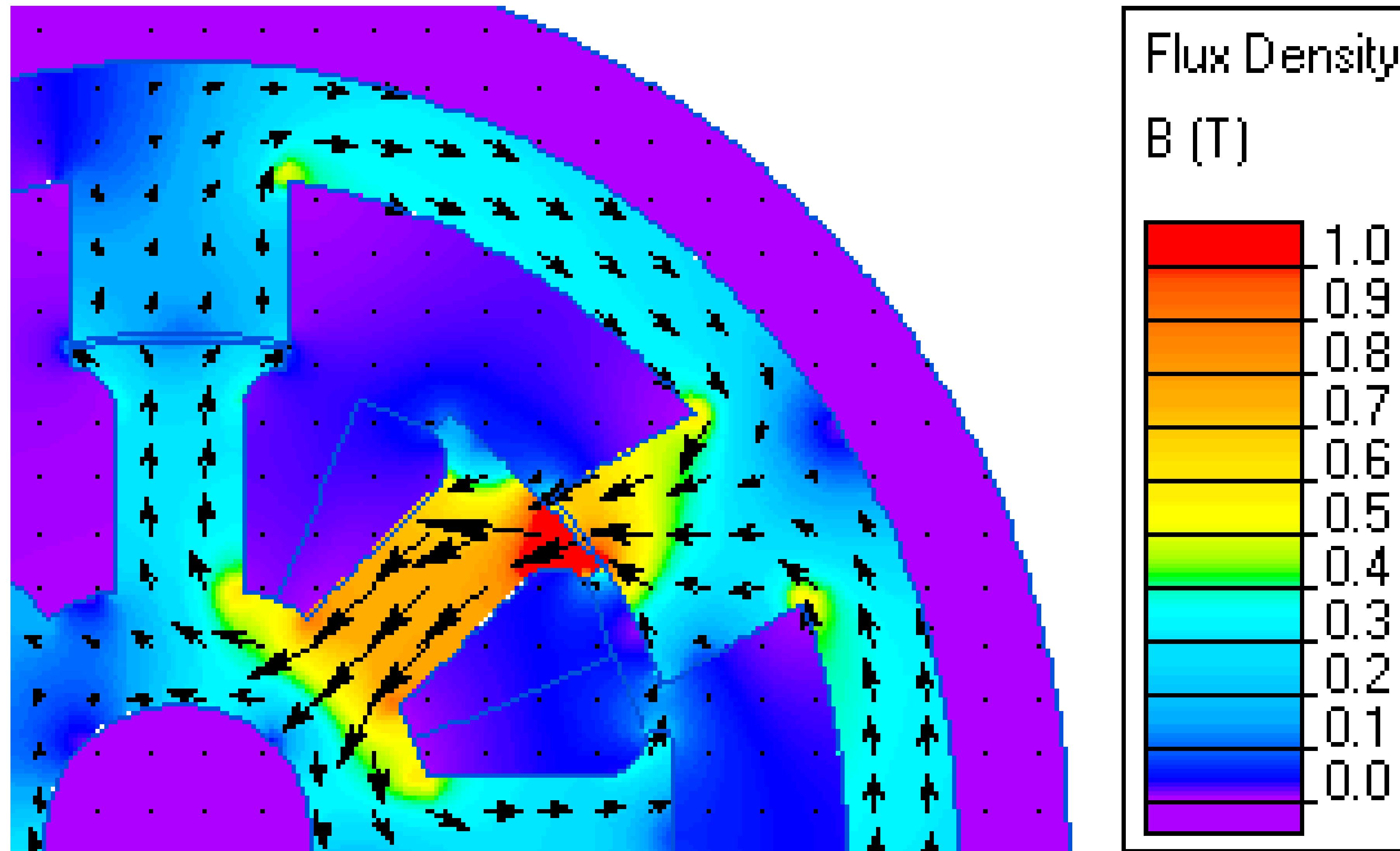
Тренды в электроинженерии





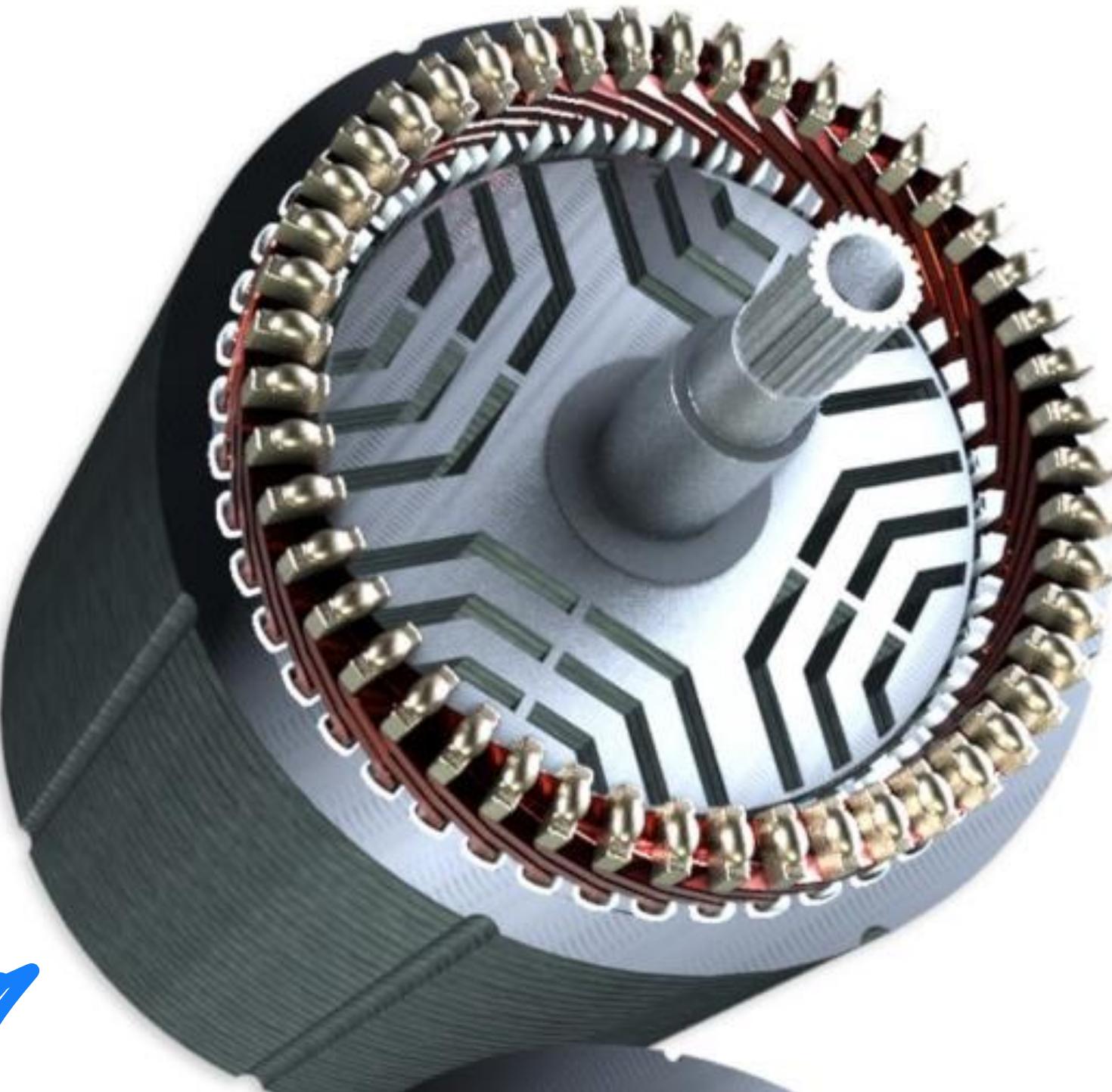
Электрические машины

Дизайн электрических машин



Синхронные реактивные электрические машины

- ротор состоит только из электрической стали
- данные машины дешевы в производстве
- достаточно легкое охлаждение
- подразделяют на
 - синхронные реактивные машины (SynRM)
 - вентильно-индукторные машины (SRM)



Синхронные реактивные машины

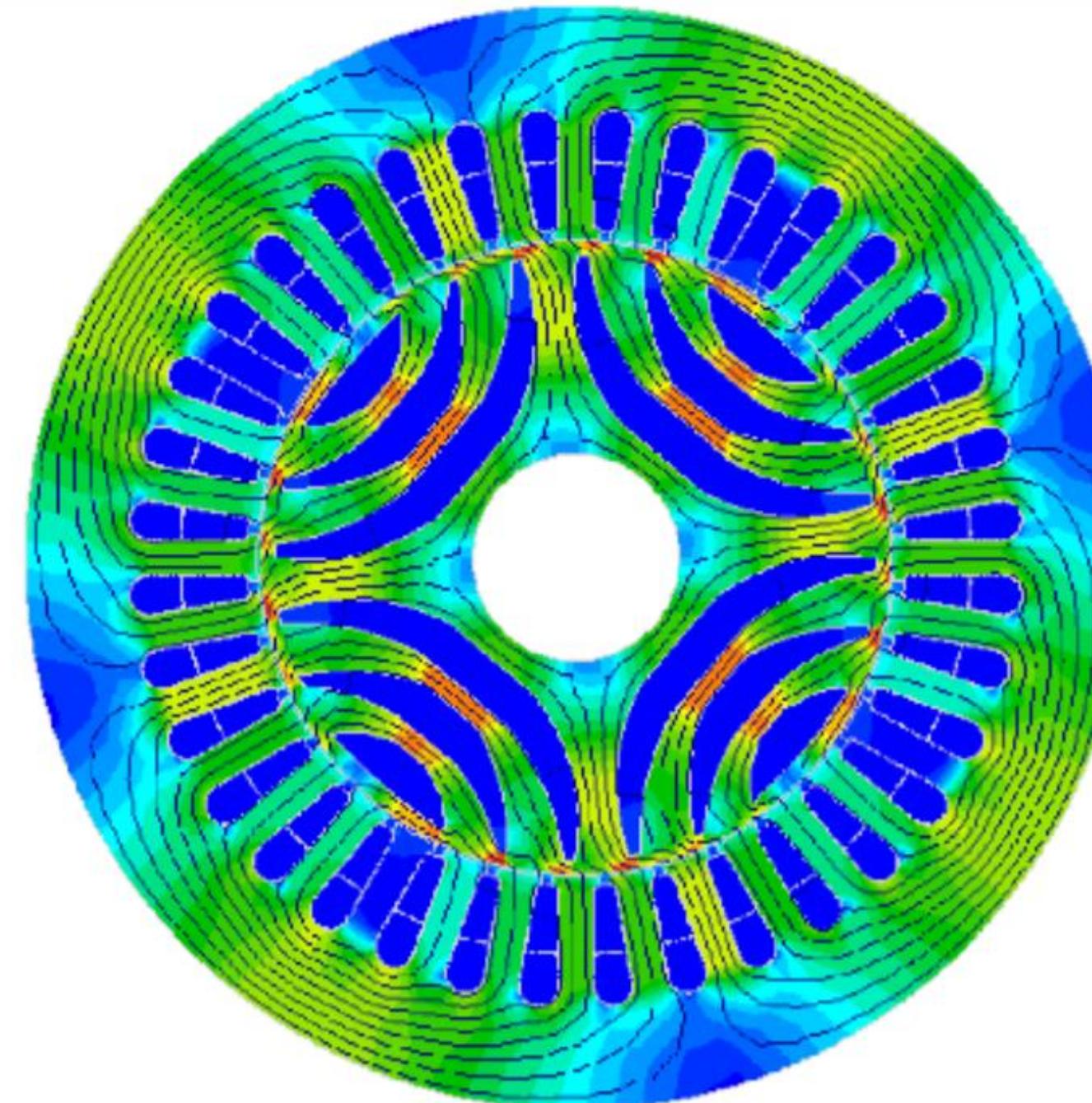
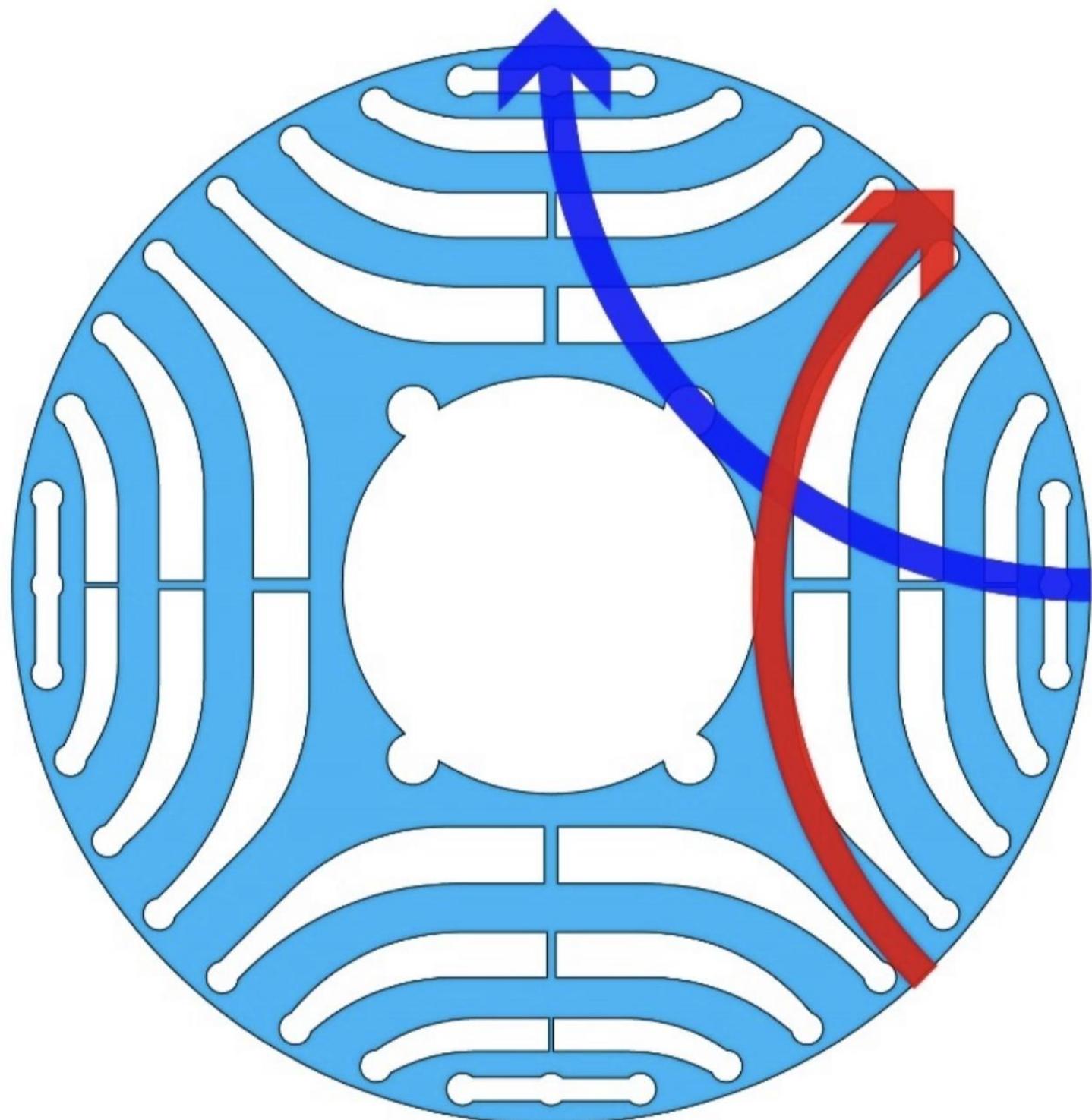
- Конструкция и производственный процесс SRM аналогичен всем асинхронным двигателям. Существенное отличие имеет только конструкция ротора, ротор SRM анизотропный (не симметричный)



Что такое реактивный?

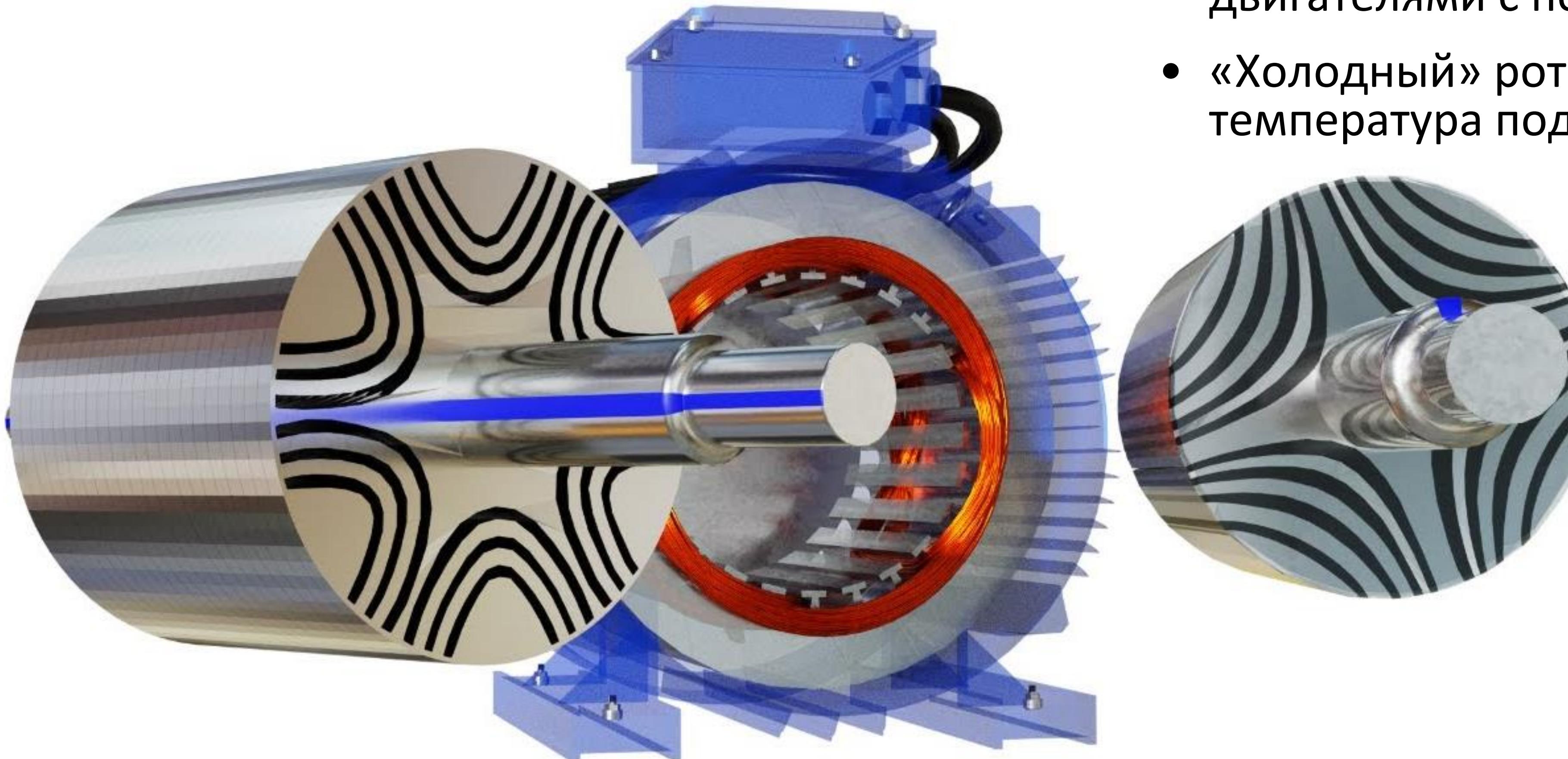
High Magnetic Reluctance

Low Magnetic Reluctance



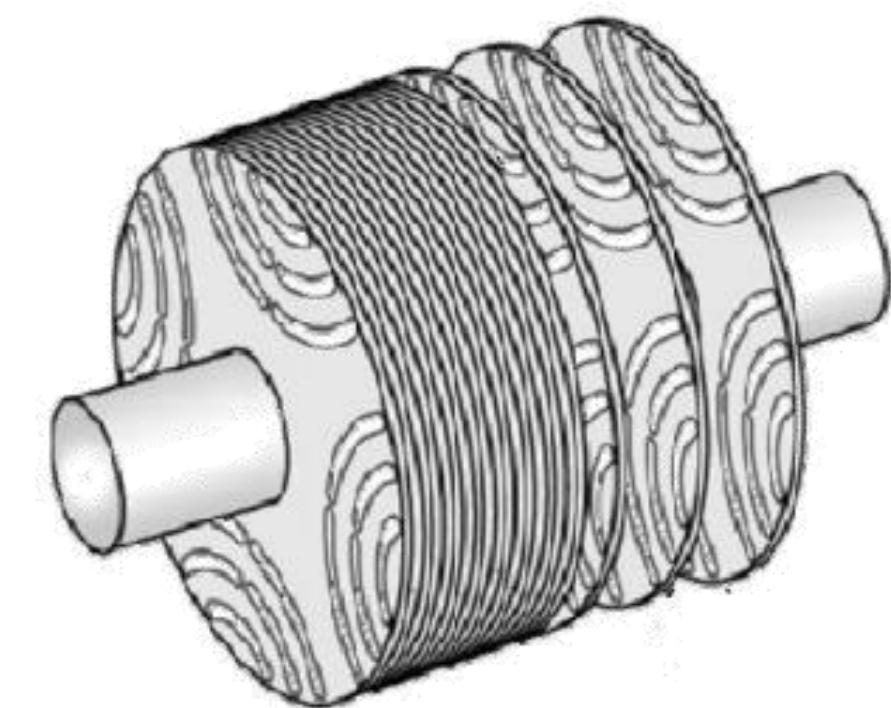
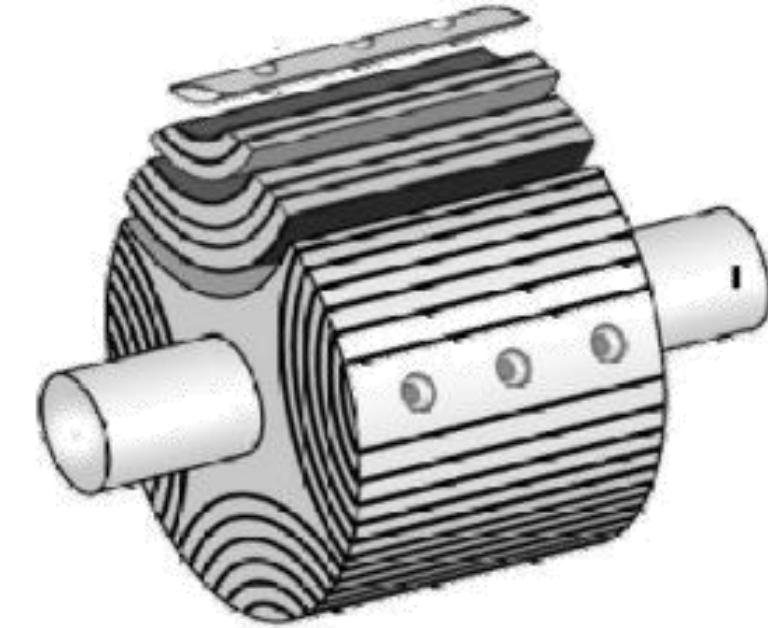
Синхронные реактивные электрические машины

- Ротор без постоянных магнитов.
- Отсутствие основных потерь ротора (I^2R), максимально возможная эффективность.
- Отсутствие проскальзывания ротора (дополнительные потери)
- Простота обслуживания по сравнению с двигателями с постоянными магнитами.
- «Холодный» ротор (низкая рабочая температура подшипника).

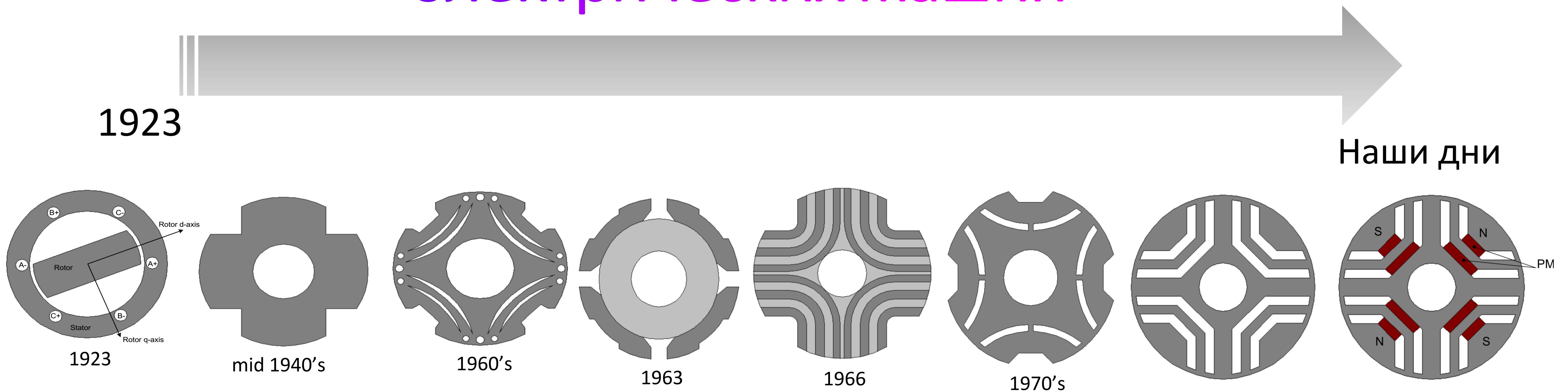


Синхронные реактивные электрические машины

- Синхронные реактивные электрические машины сочетают в себе характеристики двигателя с постоянными магнитами с простотой и удобством обслуживания асинхронного двигателя.
- Ротор не имеет ни магнитов, ни обмоток и в связи с этим практически отсутствуют потери мощности.
- Техническое обслуживание так же просто, как и в асинхронных двигателях.



Эволюция роторов синхронных реактивных электрических машин



Received January 13, 2021, accepted January 23, 2021, date of publication January 26, 2021, date of current version February 4, 2021.
Digital Object Identifier 10.1109/ACCESS.2021.3054766

A Novel Modular Permanent Magnet-Assisted Synchronous Reluctance Motor

ZEYU LIU¹, YAN HU, JIACHENG WU, BINGYI ZHANG, AND GUIHONG FENG

¹School of Electrical Engineering, Shenyang University of Technology, Shenyang 110870, China

Corresponding author: Yan Hu (huyans@163.com)

ABSTRACT This paper proposes a novel modular permanent magnet-assisted synchronous reluctance motor (MPMA-SynRM) structure. The rotor is composed of two types of rotor modules that are axially combined. This article analyses and explains the combined angle of the axial assembly of different rotor modules. The MPMA-SynRM rotor module is optimized using a differential evolution algorithm and the MPMA-SynRM space vector diagram is established to give the torque calculation an analytical expression. Whether there is axial magnetic isolation between different rotors is analysed, and various segment numbers, pole arc coefficients, and length ratios are used for different rotor modules to affect the electromagnetic influence of the MPMA-SynRM's cogging torque. Detailed analyses of the MPMA-SynRM loss, efficiency, and permanent magnet demagnetization state are given. The no-load back EMF, power factor, efficiency, eddy current loss, and cogging torque of the MPMA-SynRM with traditional Nd-Fe-B permanent magnet motors and permanent magnet auxiliary synchronous reluctance motors are compared, and a prototype is made to prove the performance of this motor.

INDEX TERMS Permanent magnet motors, permanent magnet-assisted synchronous reluctance motor, rare earth magnets, ferrite magnets, finite element method, design optimization, rotor structure.

I. INTRODUCTION

Permanent magnet motors have many advantages, such as a high power, high efficiency, direct drive, etc. Thus, they are widely used in industry, transportation, and aerospace. Motor torque density has been significantly improved since utilizing the Nd-Fe-B permanent magnetic materials [1]. Due to the high price and limited supply of rare earth permanent magnet materials, permanent magnet motor development has been restricted. Therefore, a high-performance synchronous motor with few rare earth elements or one without any rare earth elements has become a prominent research area for many scholars.

The inner rotor permanent magnet-assisted synchronous reluctance motor (PMA-SynRM) has many advantages. It has the benefits of an interior permanent magnet machine (IPM) and a reluctance synchronous motor (SynRM), such as a low cost, a low permanent magnet material consumption, and a high efficiency. It has been used in new energy vehicles [2], [3] and various industrial fields [1]. Related scholars have determined that PMA-SynRM has good constant power operating characteristics [4], [5]. Ferrite permanent magnet materials cannot demagnetize at high temperatures.

The associate editor coordinating the review of this manuscript and approving it for publication was Giovanni Angiulli[✉].

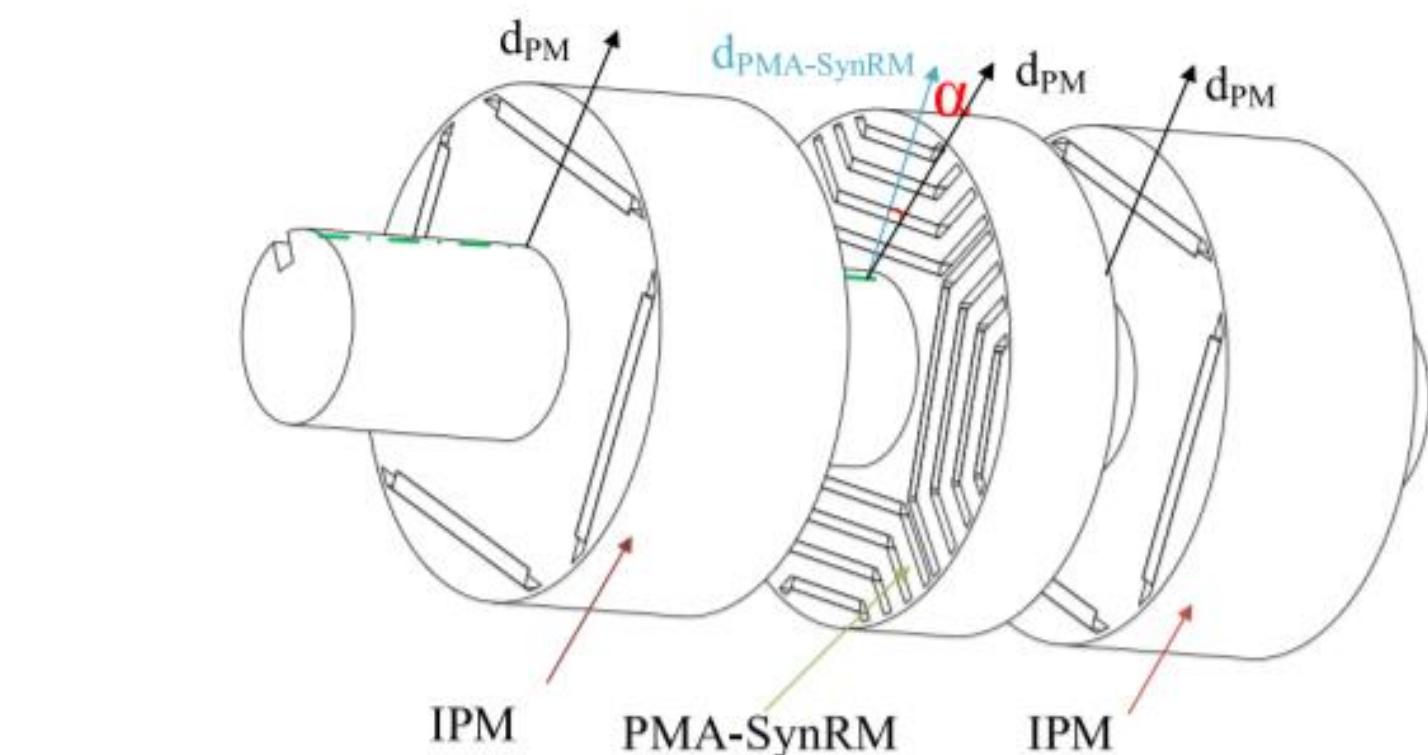
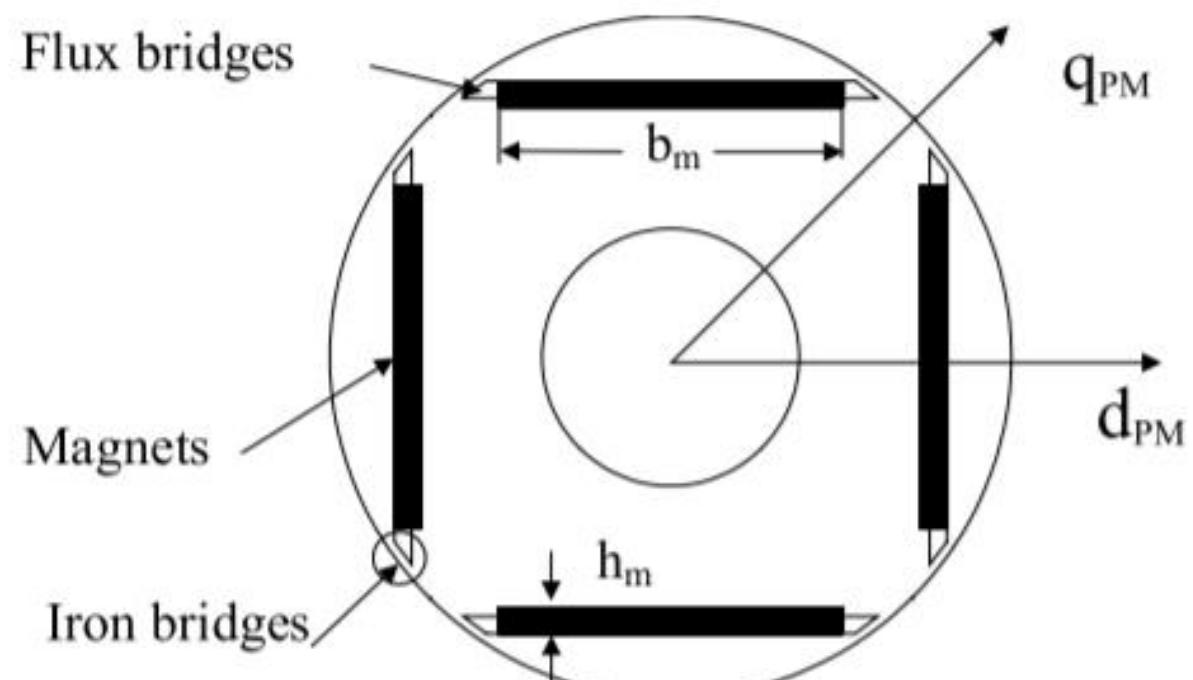
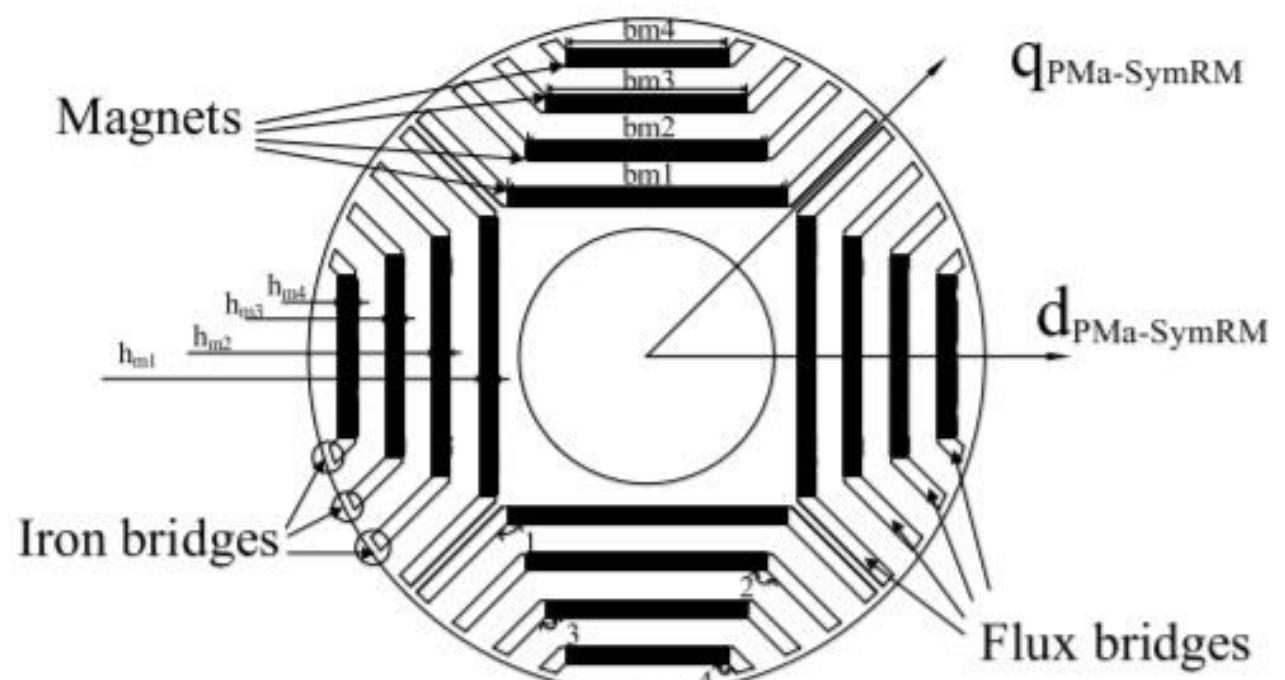


FIGURE 1. Novel modular permanent magnet-assisted synchronous reluctance motor.



Z. Liu, Y. Hu, J. Wu, B. Zhang and G. Feng,
"A Novel Modular Permanent Magnet-Assisted Synchronous Reluctance Motor,"
in *IEEE Access*, vol. 9, pp. 19947-19959,
2021, doi: 10.1109/ACCESS.2021.3054766



PMA-SynRM rotor lamination

FIGURE 3. Permanent magnet synchronous rotor module lamination.

TABLE 1. Main structural parameters.

Item	Unit	Value
Outer diameter of stator	mm	130
Outer diameter of rotor	mm	80
Permanent material 1	-	N38SH/1.22T
Permanent material 2	-	Y35/0.42T
Steel sheet	-	DW470/1.8T

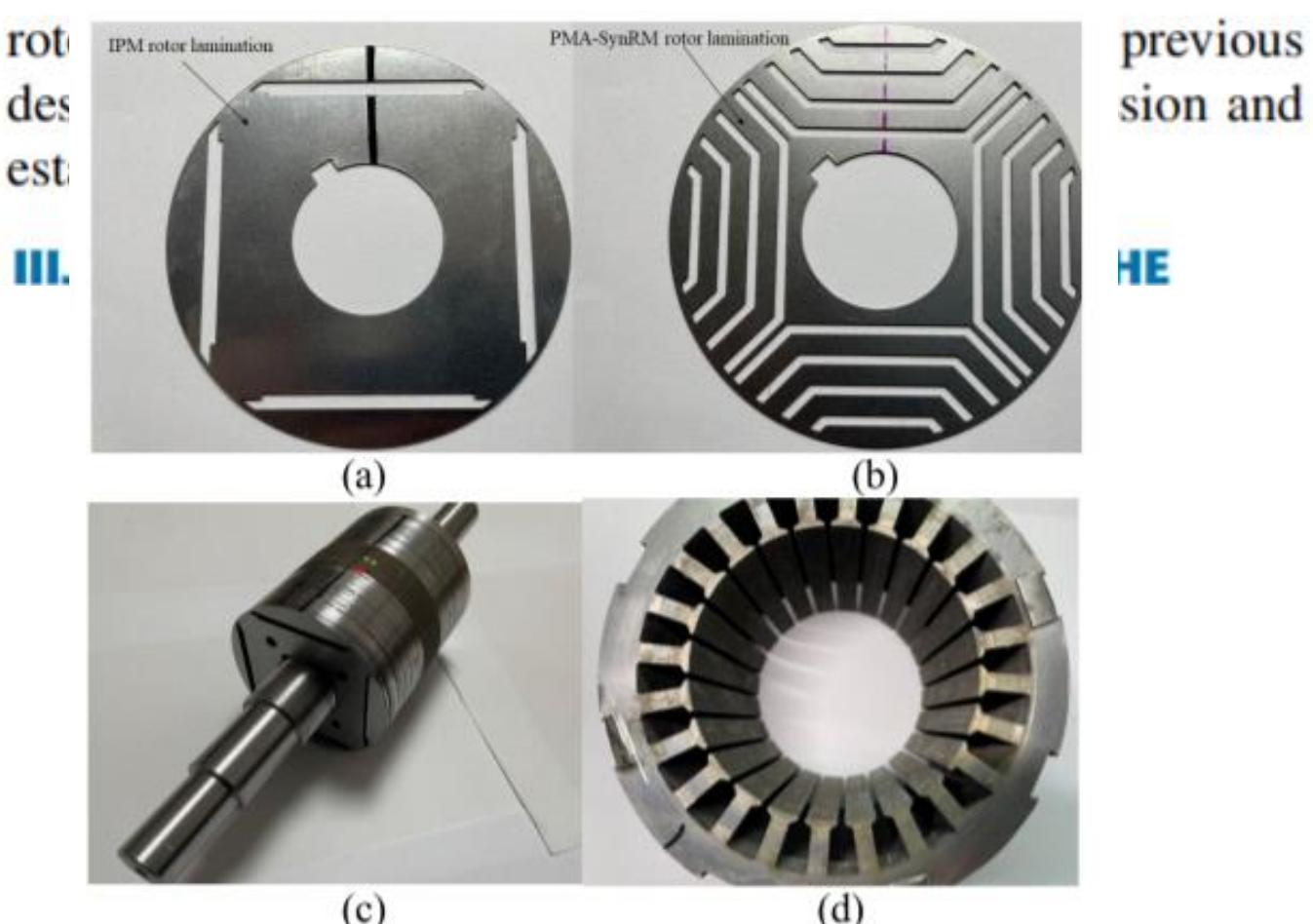


FIGURE 26. Manufactured prototype machine (a) Permanent magnet synchronous rotor module lamination (b) Permanent magnet synchronous rotor module lamination (c) Novel modular permanent magnet-assisted synchronous reluctance motor (d) stator.

Review

A Review of Synchronous Reluctance Motor-Drive Advancements

Hamidreza Heidari ^{1,*}, Anton Rassölkin ^{1,2}, Ants Kallaste ¹, Toomas Vaimann ^{1,2}, Ekaterina Andriushchenko ¹, Anouar Belahcen ^{1,3} and Dmitry V. Lukichev ²

¹ Department of Electrical Power Engineering and Mechatronics, Tallinn University of Technology, Ehitajate tee 5, 19086 Tallinn, Estonia; anton.rassolkin@taltech.ee (A.R.); ants.kallaste@taltech.ee (A.K.); toomas.vaimann@taltech.ee (T.V.); ekandr@taltech.ee (E.A.); anouar.belahcen@taltech.ee (A.B.)

² Faculty of Control Systems and Robotics, ITMO University, 197101 Saint Petersburg, Russia; lukichev@itmo.ru

³ Department of Electrical Engineering and Automation, Aalto University, P.O. Box 15500 Aalto, Finland

* Correspondence: haheid@taltech.ee; Tel.: +372-56139797

Abstract Recent studies show that synchronous reluctance motors (SynRMs) present promising technologies. As a result, research on trending SynRMs drive systems has expanded. This work disseminates the recent developments of design, modeling, and more specifically, control of these motors. Firstly, a brief study of the dominant motor technologies compared to SynRMs is carried out. Secondly, the most prominent motor control methods are studied and classified, which can come in handy for researchers and industries to opt for a proper control method for motor drive systems. Finally, the control strategies for different speed regions of SynRM are studied and the transitions between trajectories are analyzed.

Keywords: synchronous reluctance motor; efficiency map analysis; efficient motor technology; efficient control strategy; direct torque control; field-oriented control; predictive torque control; sensorless control; maximum torque per ampere; field-weakening



Citation: Heidari, H.; Rassölkin, A.; Kallaste, A.; Vaimann, T.; Andriushchenko, E.; Belahcen, A.; Lukichev, D.V. A Review of Synchronous Reluctance Motor-Drive Advancements. *Sustainability* **2021**, *13*, 729. <https://doi.org/10.3390/su13020729>

Received: 11 December 2020
Accepted: 8 January 2021
Published: 13 January 2021

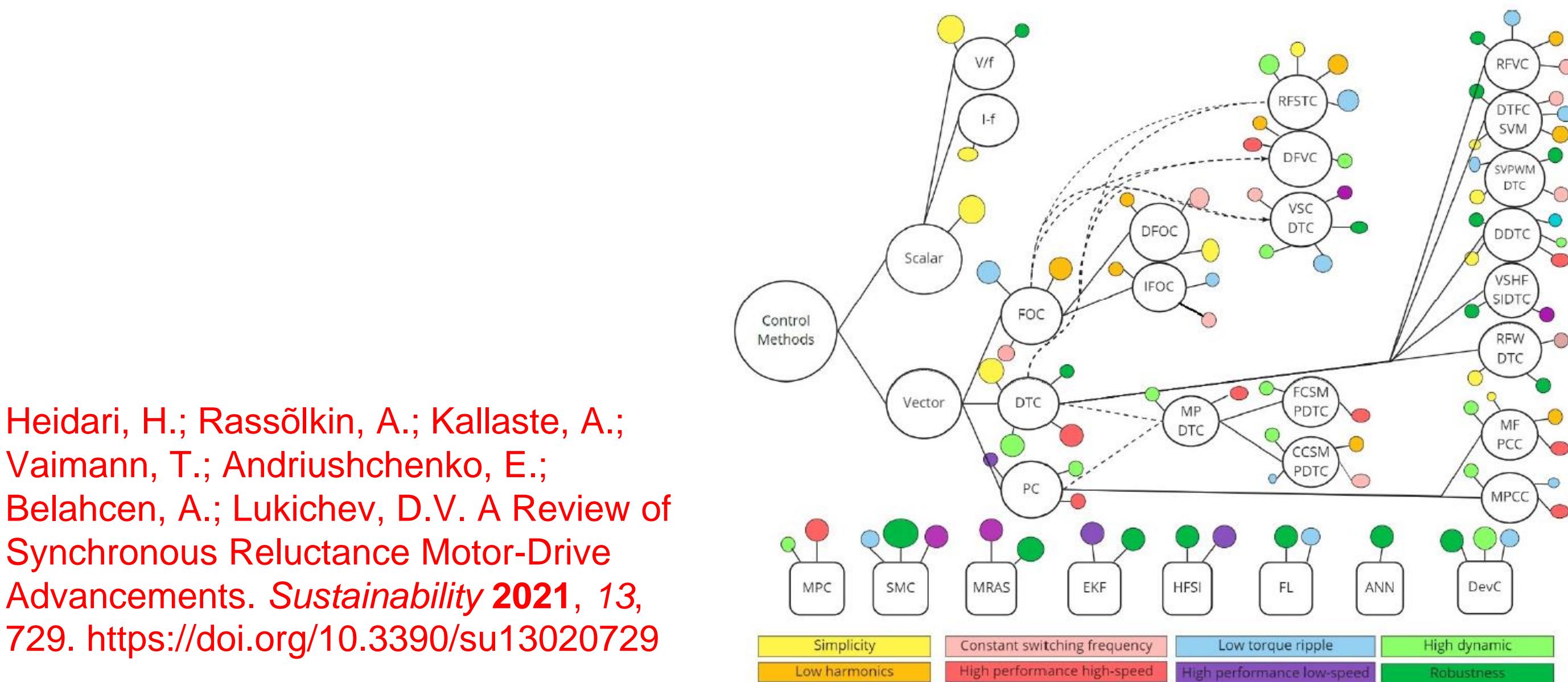
Publisher's Note: MDPI stays neutral with regard to jurisdictional claims in published maps and institutional affiliations.



Copyright © 2021 by the authors. Licensee MDPI, Basel, Switzerland. This article is an open access article distributed under the terms and conditions of the Creative Commons Attribution (CC BY) license (<https://creativecommons.org/licenses/by/4.0/>).

Table 1. A comparison of motor technologies in highlighted features.

Motor Type	Stator and Rotor Structure Sample	Different Types	Main Applications	Superiorities	Drawback(s)
IM		<ul style="list-style-type: none"> • copper rotor • aluminum rotor • wound rotor • rotor skewing 	Industrial applications (pump, fan, traction, etc.)	+ low cost of material and manufacturing process + line-start capability	– low power factor – highly probable bearing fault
PMSM		<ul style="list-style-type: none"> • interior PM [42] • surface-mounted PM [43] • line-start PMSM 	precise control and high-speed performance (traction, robotics, aerospace, medical, etc.)	+ high performance in wide speed range operation	– rare-earth material usage
SynRM		<ul style="list-style-type: none"> • line-start SynRM • skewed rotor • rotor with asymmetric flux barriers 	Industrial applications (pump, fan, traction, etc.)	+ reliable and highly efficient due to cold rotor operation + high dynamic + high overloadability + very high-speed capability	– high torque ripple – severe low power factor
PMsynRM		<ul style="list-style-type: none"> • rotor skewing • asymmetric rotor structure • different barrier structure and PM material 	Traction applications	+ very high performance without rare-earth PMs	– hard manufacturing and installment process



Heidari, H.; Rassölkin, A.; Kallaste, A.; Vaimann, T.; Andriushchenko, E.; Belahcen, A.; Lukichev, D.V. A Review of Synchronous Reluctance Motor-Drive Advancements. *Sustainability* **2021**, *13*, 729. <https://doi.org/10.3390/su13020729>

Figure 8. Motor control methods classification.

Optimal Rotor Design of Synchronous Reluctance Machines Considering the Effect of Current Angle

Hegazy Rezk ^{1,2,*}, Kotb B. Tawfiq ^{3,4,5}, Peter Sergeant ^{3,4} and Mohamed N. Ibrahim ^{3,4,6}

- ¹ College of Engineering at Wadi Aldawaser, Prince Sattam Bin Abdulaziz University, Wadi Aldawaser 11991, Saudi Arabia
 - ² Electrical Engineering Department, Faculty of Engineering, Minia University, Minia 61111, Egypt
 - ³ Department of Electromechanical Systems and Metal Engineering, Ghent University, 9000 Ghent, Belgium; kotb.basem@ugent.be (K.B.T); Peter.Sergeant@UGent.be (P.S.); m.nabil@ugent.be (M.N.I.)
 - ⁴ FlandersMake@UGent—corelab EEDT-MP, 3001 Leuven, Belgium
 - ⁵ Department of Electrical Engineering, Faculty of Engineering, Menoufia University, Menoufia 32511, Egypt
 - ⁶ Electrical Engineering Department, Kafrelsheikh University, Kafrelsheikh 33511, Egypt
- * Correspondence: h.rezk@psau.edu.sa

Abstract The torque density and efficiency of synchronous reluctance machines (SynRMs) are greatly affected by the geometry of the rotor. Hence, an optimal design of the SynRM rotor geometry is highly recommended to achieve optimal performance (i.e., torque density, efficiency, and power factor). This paper studies the impact of considering the current angle as a variable during the optimization process on the resulting optimal geometry of the SynRM rotor. Various cases are analyzed and compared for different ranges of current angles during the optimization process. The analysis is carried out using finite element magnetic simulation. The obtained optimal geometry is prototyped for validation purposes. It is observed that when considering the effect of the current angle during the optimization process, the output power of the optimal geometry is about 3.32% higher than that of a fixed current angle case. In addition, during the optimization process, the case which considers the current angle as a variable has reached the optimal rotor geometry faster than that of a fixed current angle case. Moreover, it is observed that for a fixed current angle case, the torque ripple is affected by the selected value of the current angle. The torque ripple is greatly decreased by about 34.20% with a current angle of 45° compared to a current angle of 56.50°, which was introduced in previous literature.



Citation: Rezk, H.; Tawfiq, K.B.; Sergeant, P.; Ibrahim, M.N. Optimal Rotor Design of Synchronous Reluctance Machines Considering the Effect of Current Angle. *Mathematics* **2021**, *9*, 344. <https://doi.org/10.3390/math9040344>

Academic Editor: Jinfeng Liu
Received: 17 January 2021
Accepted: 5 February 2021
Published: 9 February 2021

Publisher's Note: MDPI stays neutral with regard to jurisdictional claims in published maps and institutional affiliations.



Copyright: © 2021 by the authors. Licensee MDPI, Basel, Switzerland. This article is an open access article distributed under the terms and conditions of the Creative Commons Attribution (CC BY) license (<https://creativecommons.org/licenses/by/4.0/>).

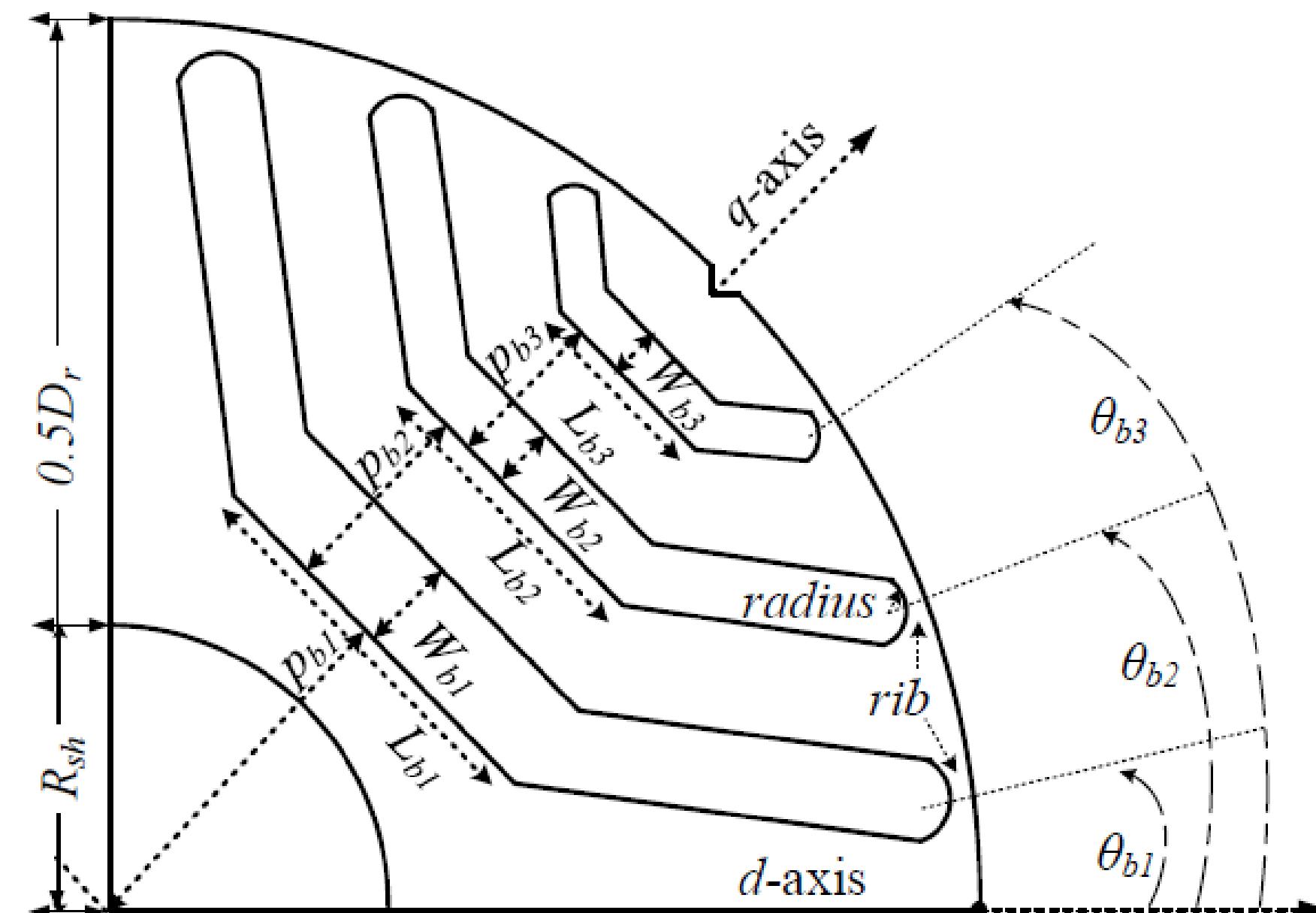
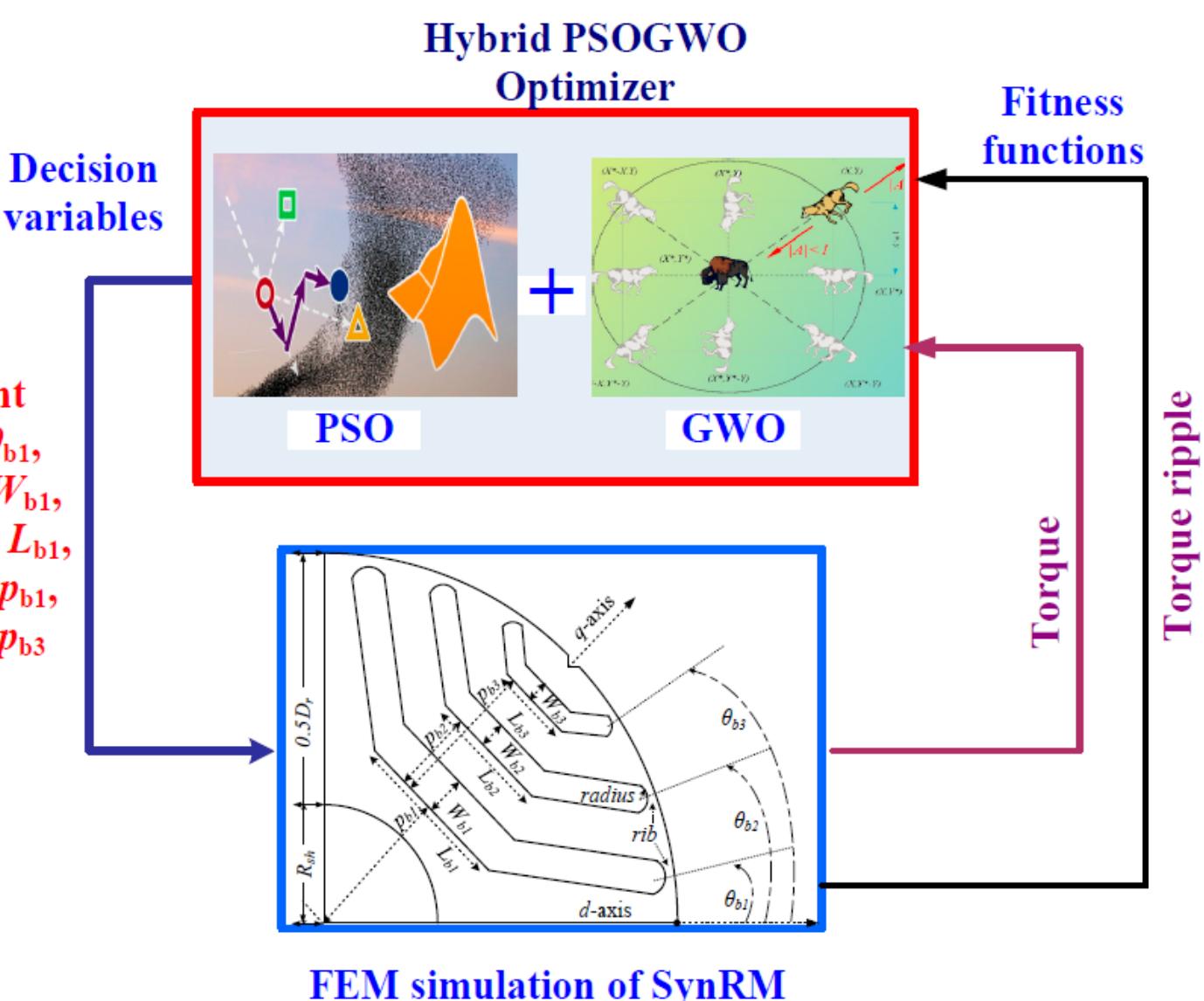


Figure 1. Rotor geometry of one pole of synchronous reluctance machines (SynRM).



Rezk, H.; Tawfiq, K.B.; Sergeant, P.; Ibrahim, M.N. Optimal Rotor Design of Synchronous Reluctance Machines Considering the Effect of Current Angle. *Mathematics* **2021**, *9*, 344. <https://doi.org/10.3390/math9040344>

Figure 2. Flow chart of the optimization process.

Плюсы и минусы синхронной реактивной электрической машины

SynRM

- Отсутствуют потери в меди
- SynRM синхронная машина и работает на синхронной скорости.
- Ротор SynRM имеет простую конструкцию, нет магнитов и короткозамкнутой обмотки.
- SynRM имеет низкую стоимость производства
- Более высокая эффективность при той же номинальной мощности

Асинхронный двигатель

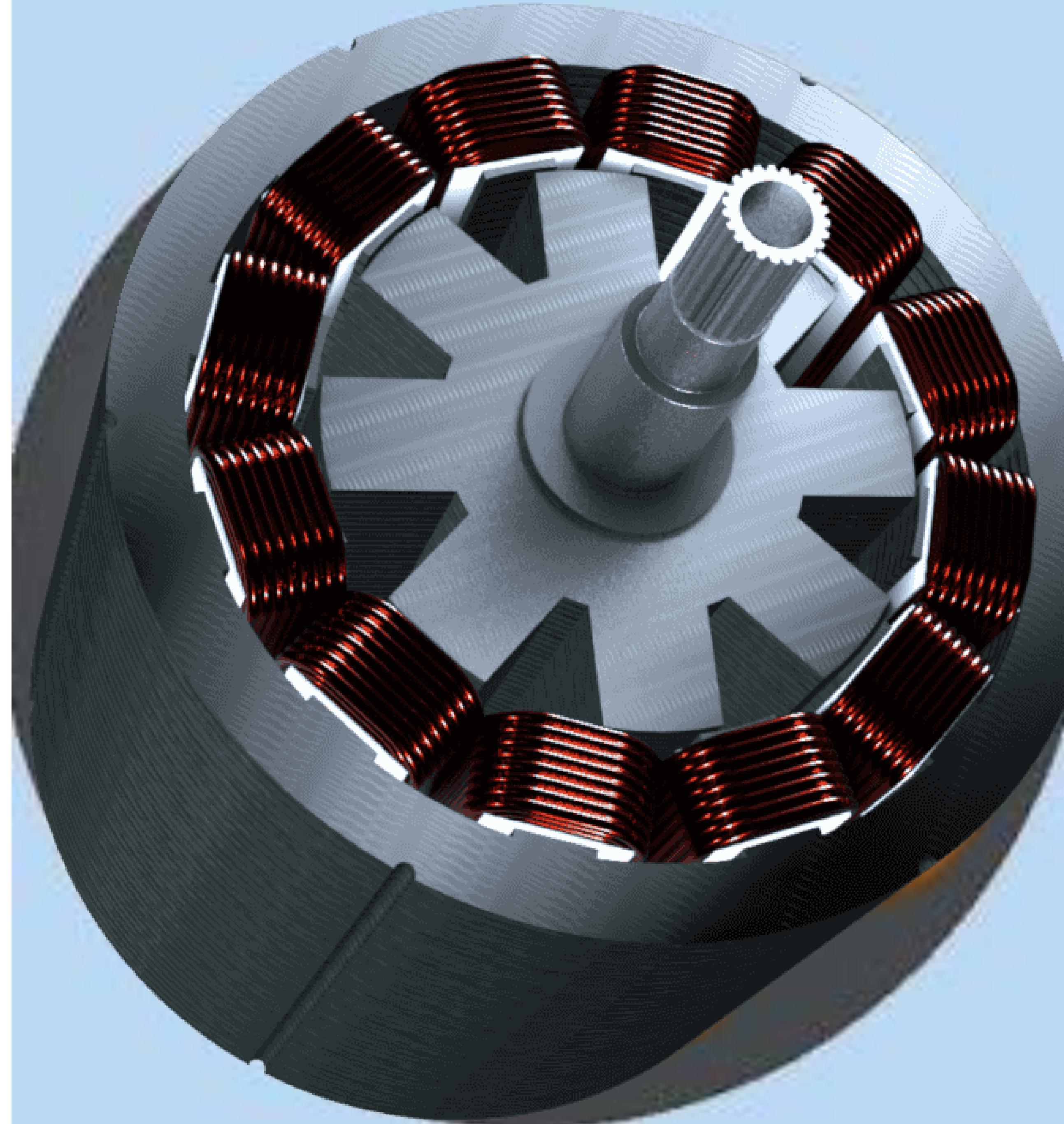
- Потери в меди.
- Асинхронный двигатель всегда работает на скорости меньше, чем его синхронная скорость.
- В асинхронном двигателе обмотка ротора представляет собой короткозамкнутую обмотку.
- Асинхронный двигатель имеет высокую стоимость производства.
- Меньший КПД при той же мощности

Недостатки SynRM

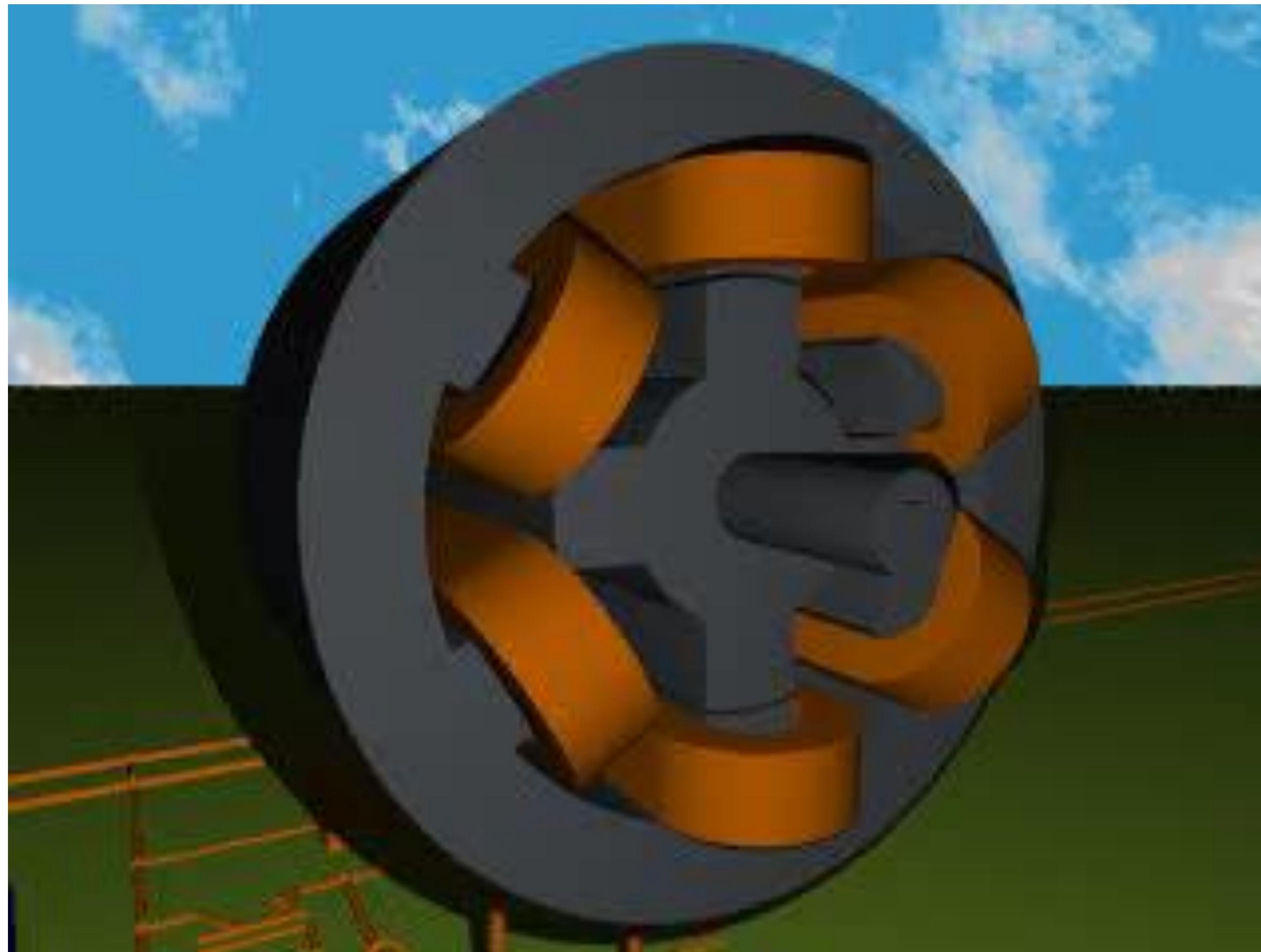
- SynRM не может запуститься самостоятельно.
- квадратичная) зависимость врачающего момента от напряжения сети.
- низкий коэффициент мощности .

Вентильно-индукторная электрическая машина

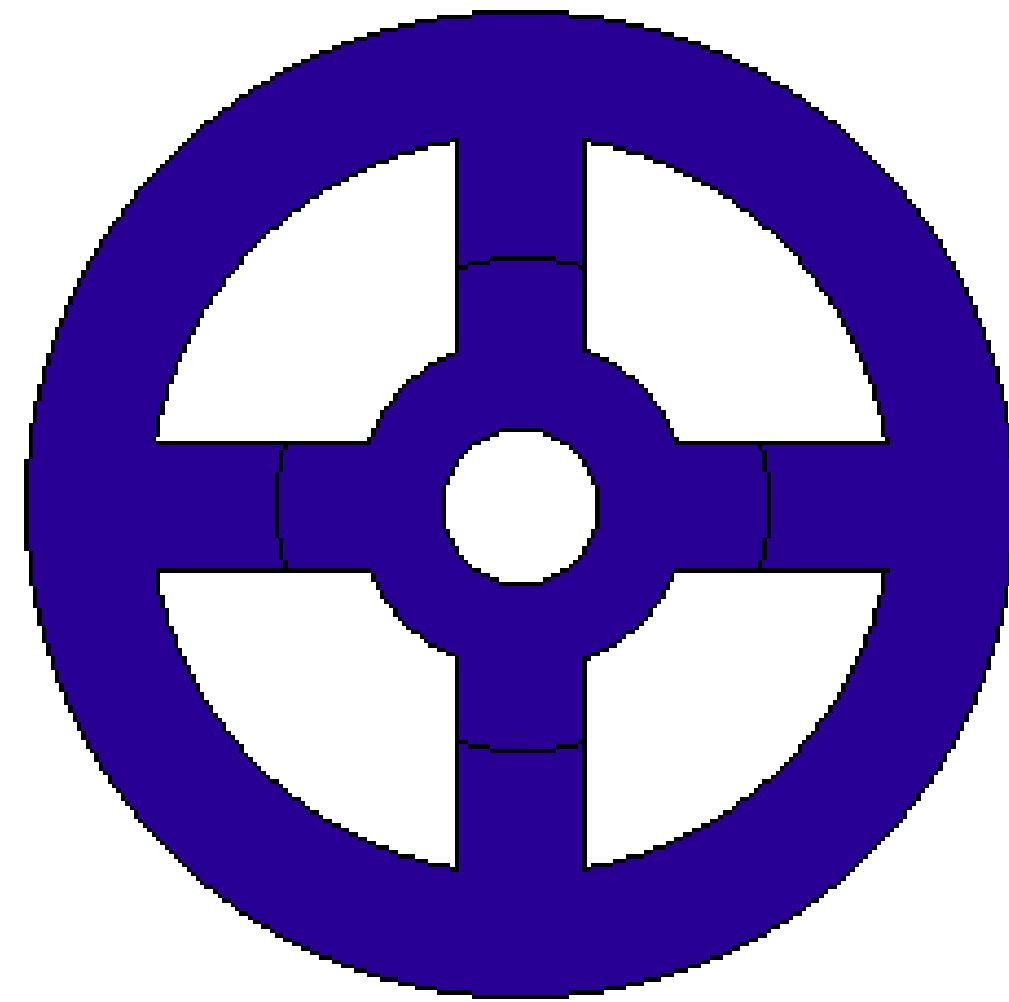
- высокая технологичность и за счет этого низкая трудоемкость производства двигателя;
- экономия активных материалов до 30%;;
- низкая себестоимость машины;
- экологическая чистота производства;
- упрощенная и более надежная по сравнению с преобразователем частоты для асинхронного электропривода схема;
- широкие функциональные возможности;
- высокие энергетические показатели.



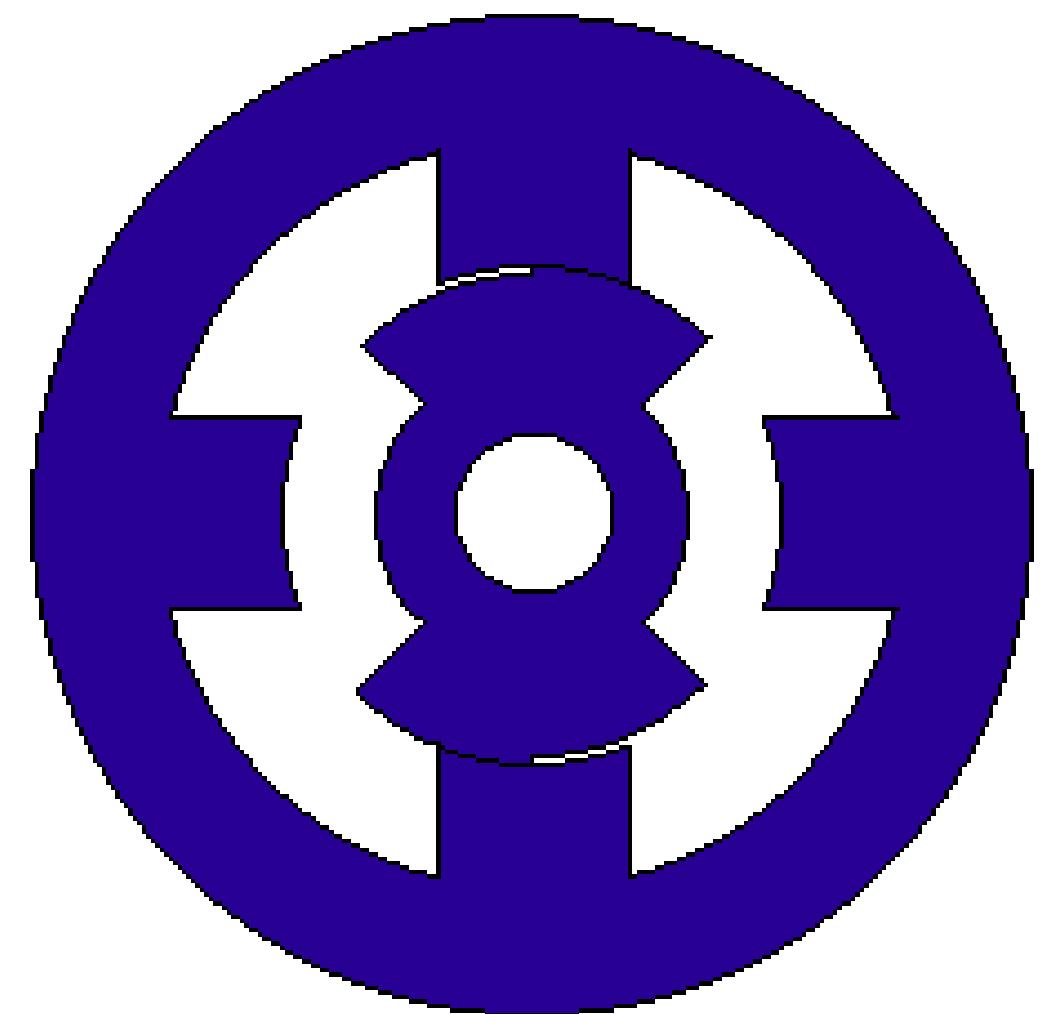
Вентильно-индукторная электрическая машина



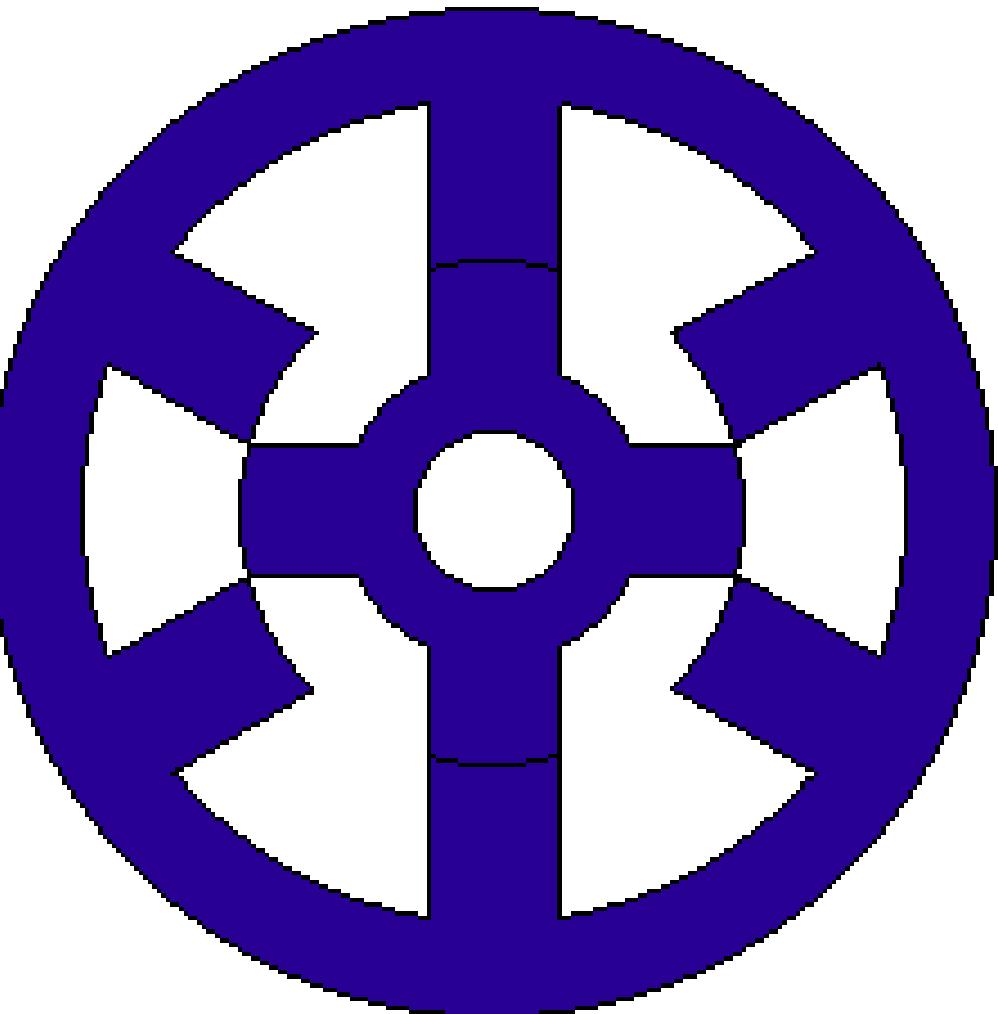
Вентильно-индукторная электрическая машина



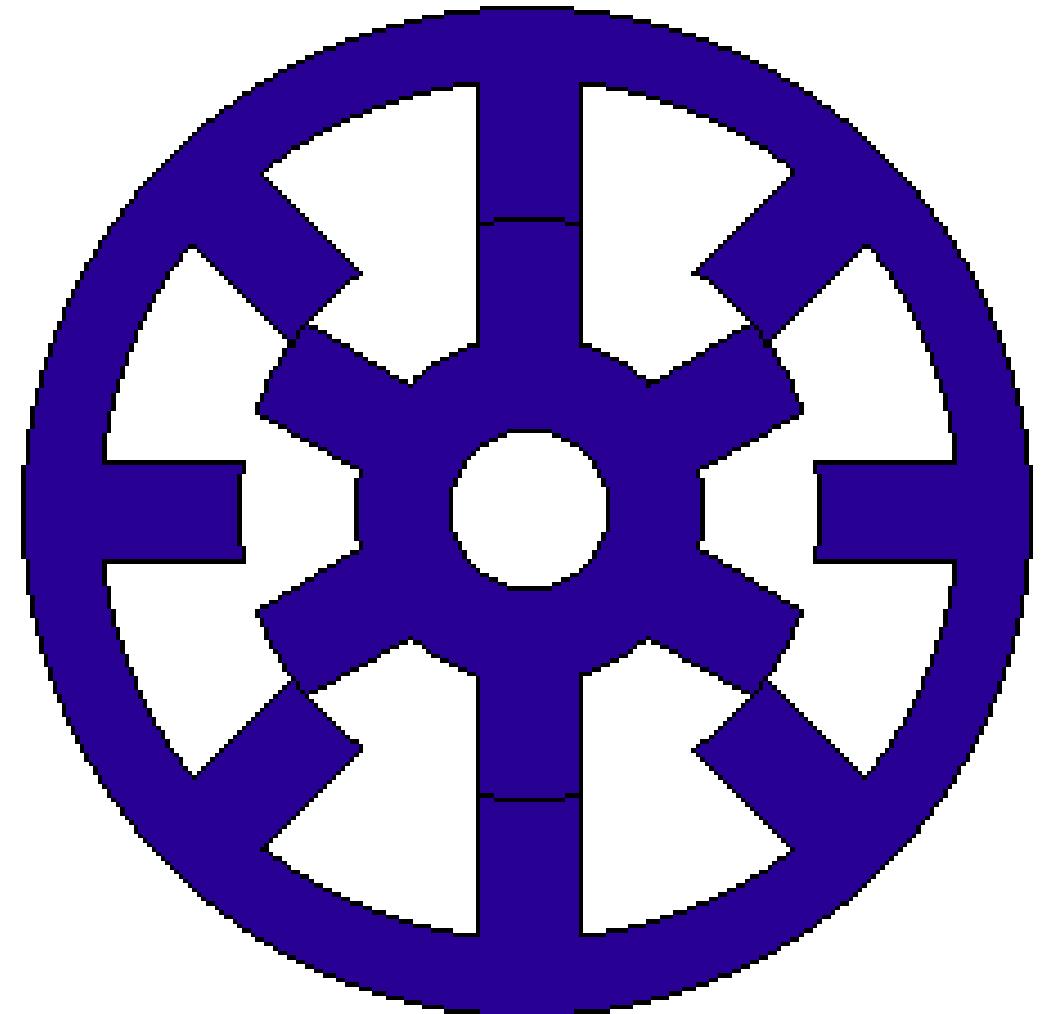
Однофазный
двигатель



Двухфазный
двигатель



Трехфазный
двигатель

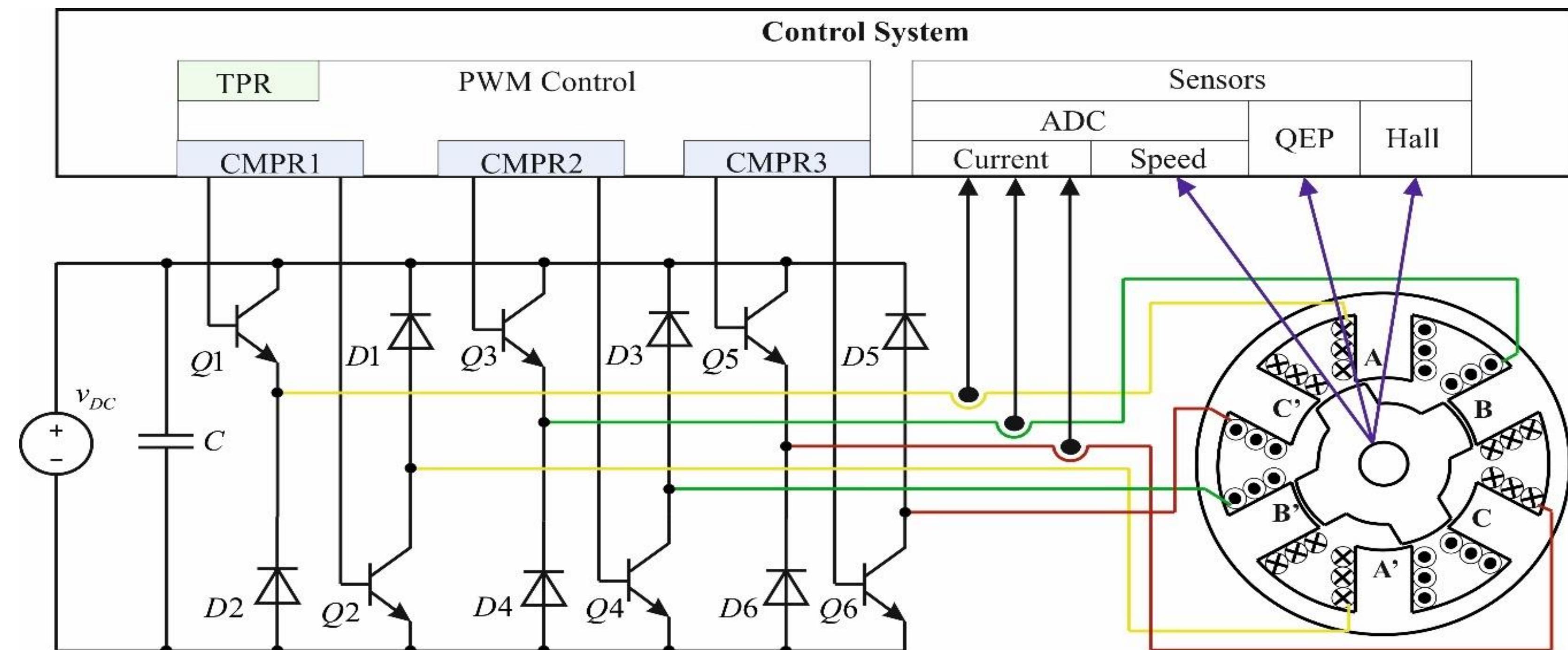


Четырехфаз-
ный
двигатель

Вентильно-индукторная электрическая машина

Достоинства:

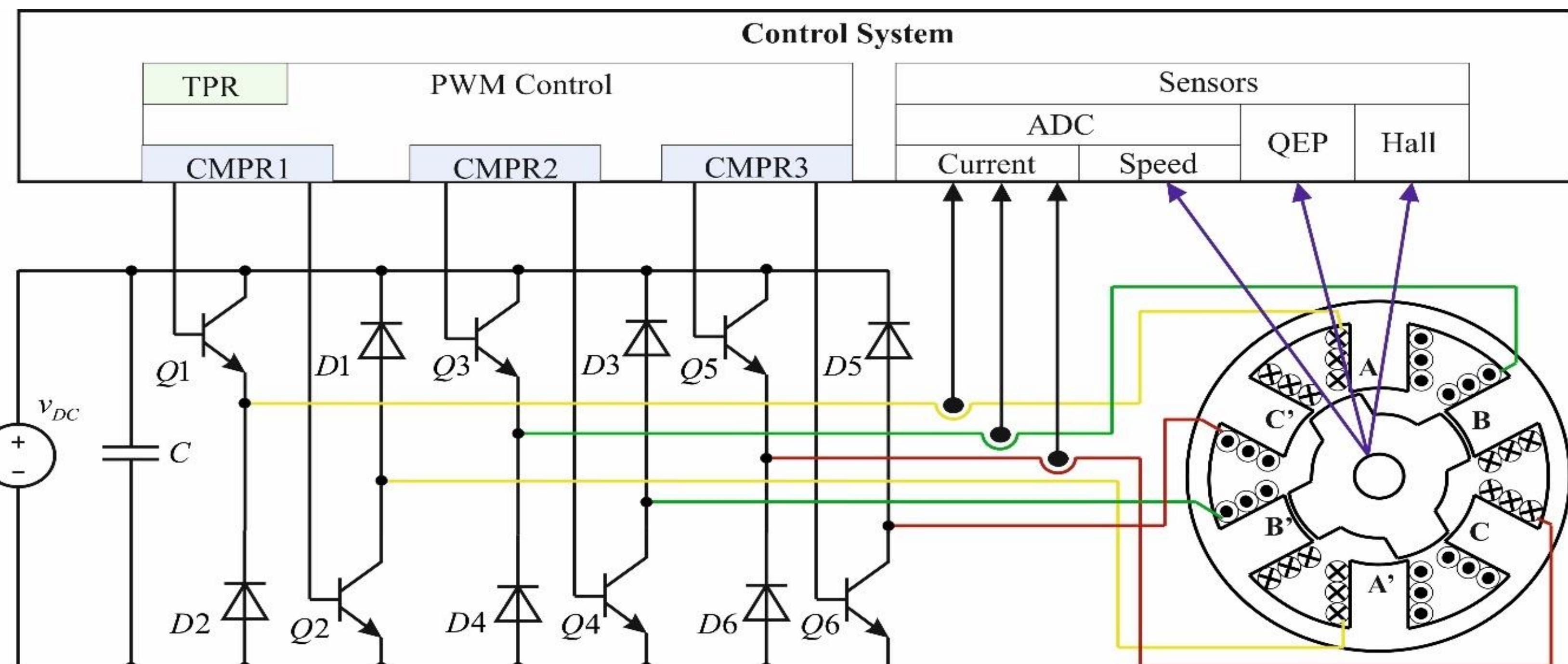
- Очень простая конструкция и изготовление машины
- Самосенсорное управление во всем диапазоне скоростей
- Высокая надежность двигателя
- Нулевые потери в режиме ожидания



Вентильно-индукторная электрическая машина

Недостатки:

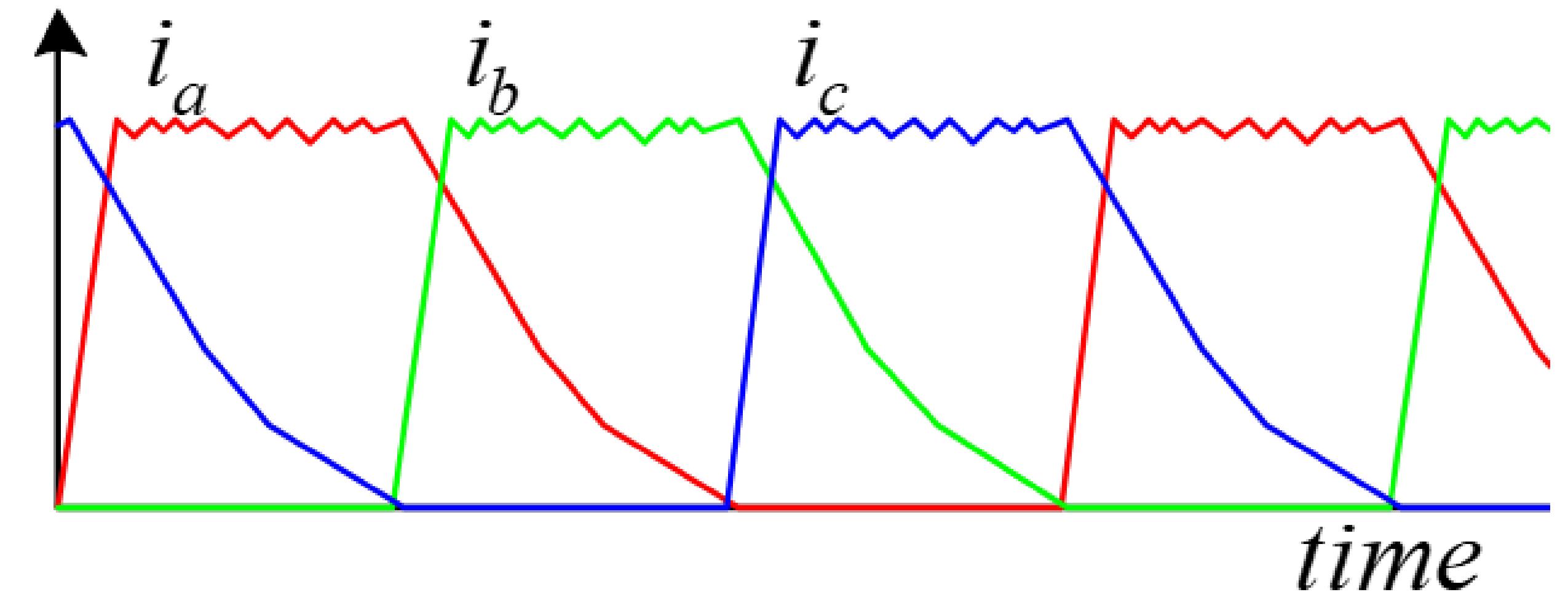
- Высокая стоимость силового преобразователей
- Высокие пульсации крутящего момента
- Требуется возбуждение в режиме генератора
- Акустический шум



Вентильно-индукторная электрическая машина

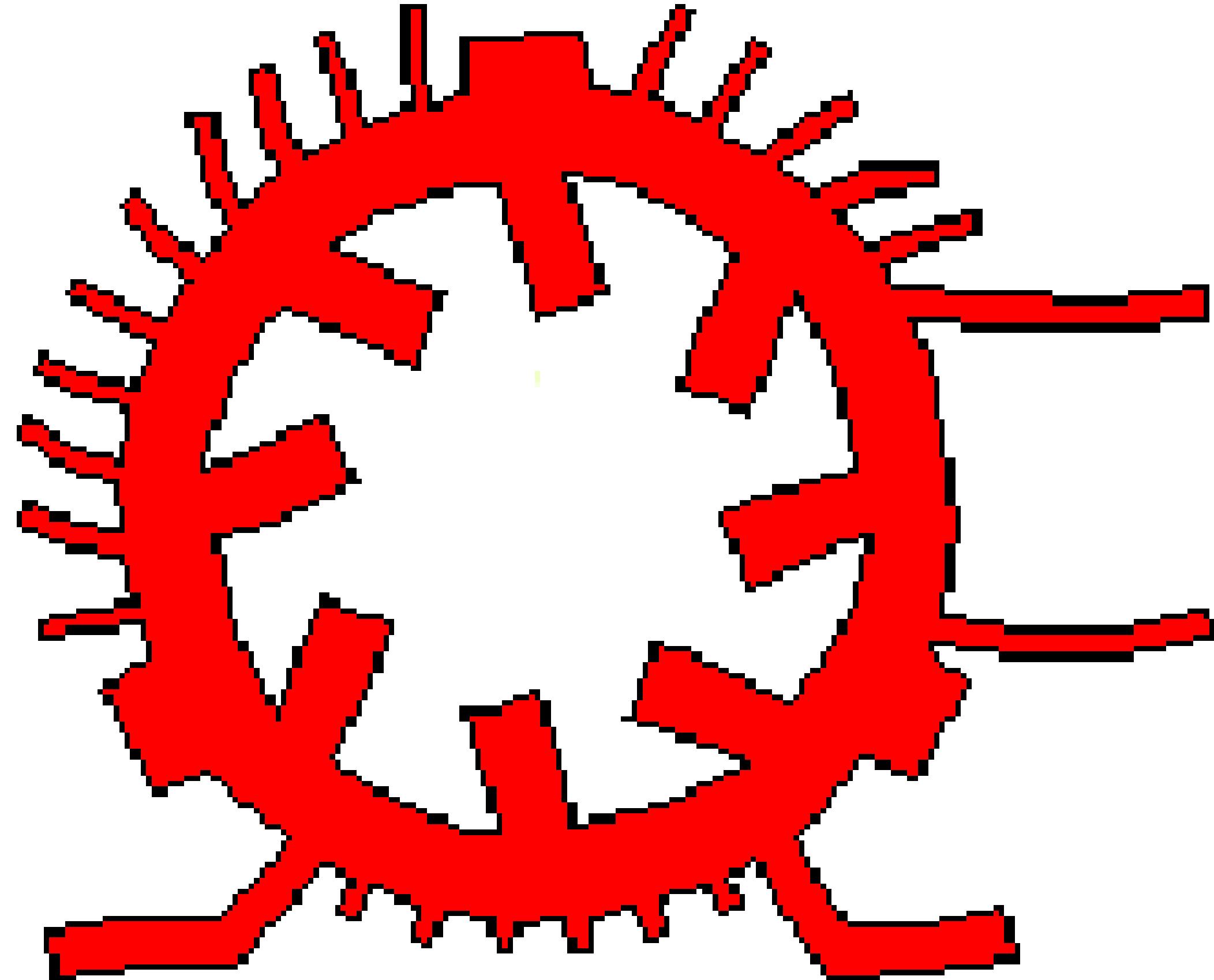
- Можем отрегулировать углы коммутации
- Мы можем настроить уровень тока
- Мы не можем использовать обычные ПИ-регуляторы тока из-за нелинейности двигателя.
- Лучшая производительность была достигнута при использовании системы управления с прогнозированием.

Высокие пульсации
момента



Вентильтрансформаторная электрическая машина

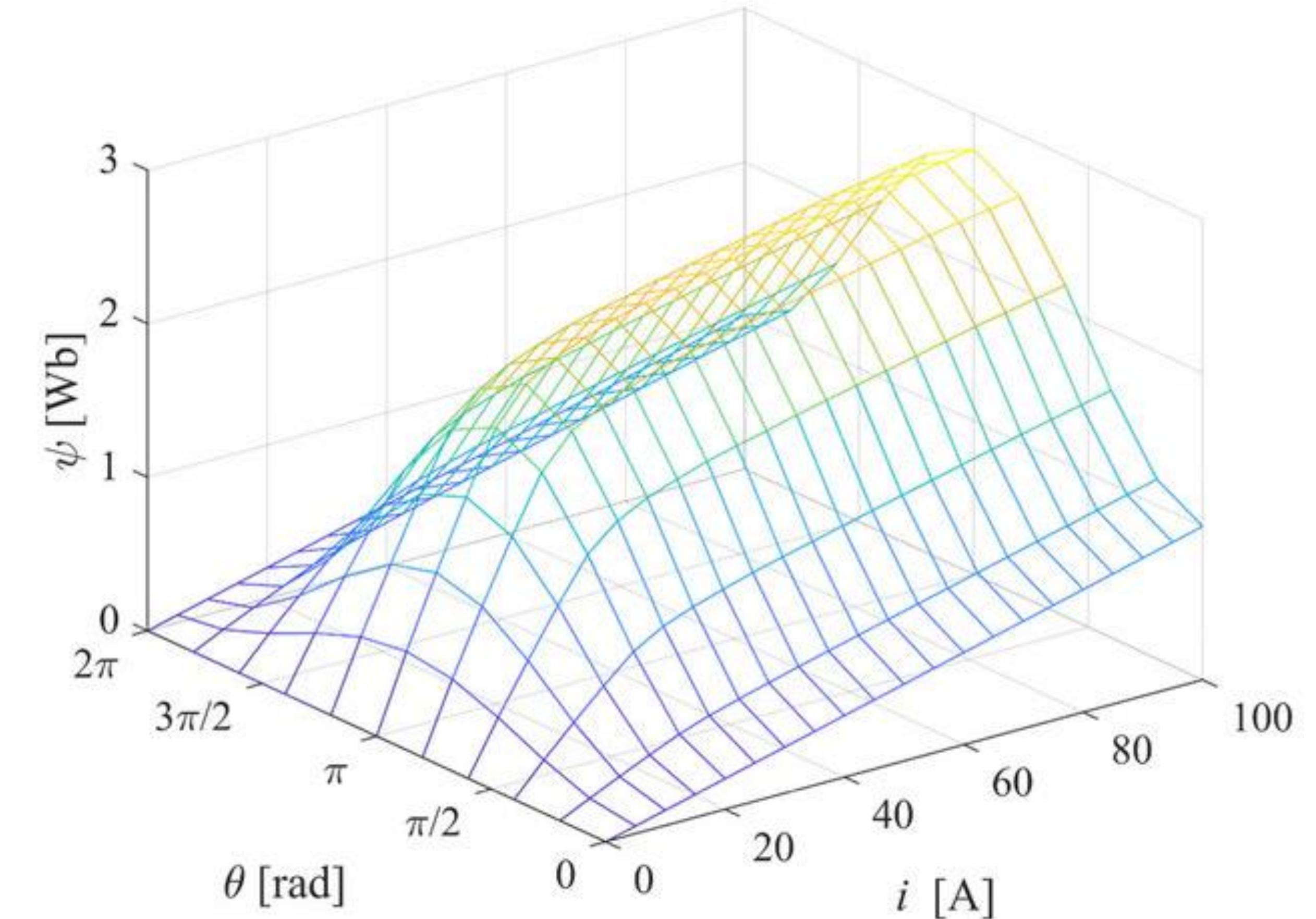
- Акустический шум



Vibration modes and acoustic noise entitled "An investigation into vibration in switched reluctance motors" by Pragasen Pillay & William Cai at the IAS conference in St. Louis 1998.

Вентильно-индукторная электрическая машина

- Нелинейная поверхность намагничивания



Online Magnetization Surface Identification for a Switched Reluctance Motor

Alecksey Anuchin
Department of Electric Drives
Moscow Power Engineering Institute
Moscow, Russia
anuchin.alecksey@gmail.com

Evgeniy Stolyarov
Department of Electric Drives
Moscow Power Engineering Institute
Moscow, Russia
stolyarovevgen@mail.ru

Abstract—The precise control of switched reluctance motor requires information about the magnetization surface as a function of rotor angular position and current. The surface can be obtained performing offline tests; however, it demands specialized mechanical equipment and time for commissioning. Moreover, the magnetization surface may be changed with the varying of the rotor and stator temperatures, which affect their dimensions and, therefore, the airgap variation. That is why the online estimation of the magnetization surface is desirable. This paper proposes the identification method operating in parallel with the model predictive current control system utilizing the magnetization map. Any error between the referenced and obtained currents is used to correct the reference points of the two-dimensional array representing the magnetization surface. The proposed method was examined using a simulation model and operated online in parallel with the primary control system driving the electrical machine.

Keywords—switched reluctance motor, magnetization surface, identification, model predictive control

I. INTRODUCTION

Over the past three decades, switched reluctance motors (SRM) have received much attention due to intensive development of power electronics technology and IGBTs components in particular. In terms of 3D-printing, SRM is considered as one of the best candidates to be the first commercial 3D-printed machine [1] and modular designed machine [2]–[5]. However, the electric drives based on SRM demonstrate a considerably high level of noises, vibrations, and torque ripples. The problem of torque ripples affecting both noise and vibration has been successfully solved using appropriate control techniques as reported in [6]–[8]. The best results were obtained by implementing the following two methods: (1) the direct instantaneous torque control [9] and (2) the model predictive control (MPC) [10], [11]. Both methods utilize a magnetization map as a function of rotor angular position and current or torque surface. The torque surface of the SRM can be derived from the magnetization surface and used for precise control.

The methods to obtain the magnetization surface of an SRM using special test benches are called offline methods [12], [13]. Other approaches, where the motor parameters

Andrei Bogdanov
Faculty of Control System and Robotics
ITMO University
Saint-Petersburg, Russia
ambogdanov@itmo.ru

Dimid Surnin
Department of Electric Drives
Moscow Power Engineering Institute
Moscow, Russia
dimidsumin@gmail.com

Yuriy Vagapov
Faculty of Art, Science and Technology
Wrexham Glyndwr University
Wrexham, UK
y.vagapov@glyndwr.ac.uk

are identified under normal SRM operation, are introduced as online methods [14]. Offline methods are applied to determine the magnetization map over the entire rotor revolution, whereas online methods provide the data correction within the drive operating region only. The method reported in [14] records the voltage command data and feedback data from current sensors to build up a magnetization map. However, the sensed data always contain noise and should be filtered.

Implementation of the continuous control set (CCS) MPC of the switched reluctance drive using lookup tables [15] of the magnetization surface required solution of two problems. The first is the proper selection of representation form for the magnetization surface. In general, the magnetization surface has a high nonlinearity; it cannot be expressed as a Fourier or Tailor series with a reasonable number of coefficients to provide a desired accuracy [16]. Therefore, the best option is to use a lookup table with some interpolation method for the estimation of flux linkage between the table reference points. The lookup table can be easily adjusted using experimental data, whereas the online correction of Fourier or Tailor series coefficients is a more sophisticated procedure.

The second problem is that the accuracy of current stabilization strictly depends on the precision of the magnetization map. This feature of the CCS MPC was selected for analysis and development to use in the online identification of the magnetization surface proposed in this paper.

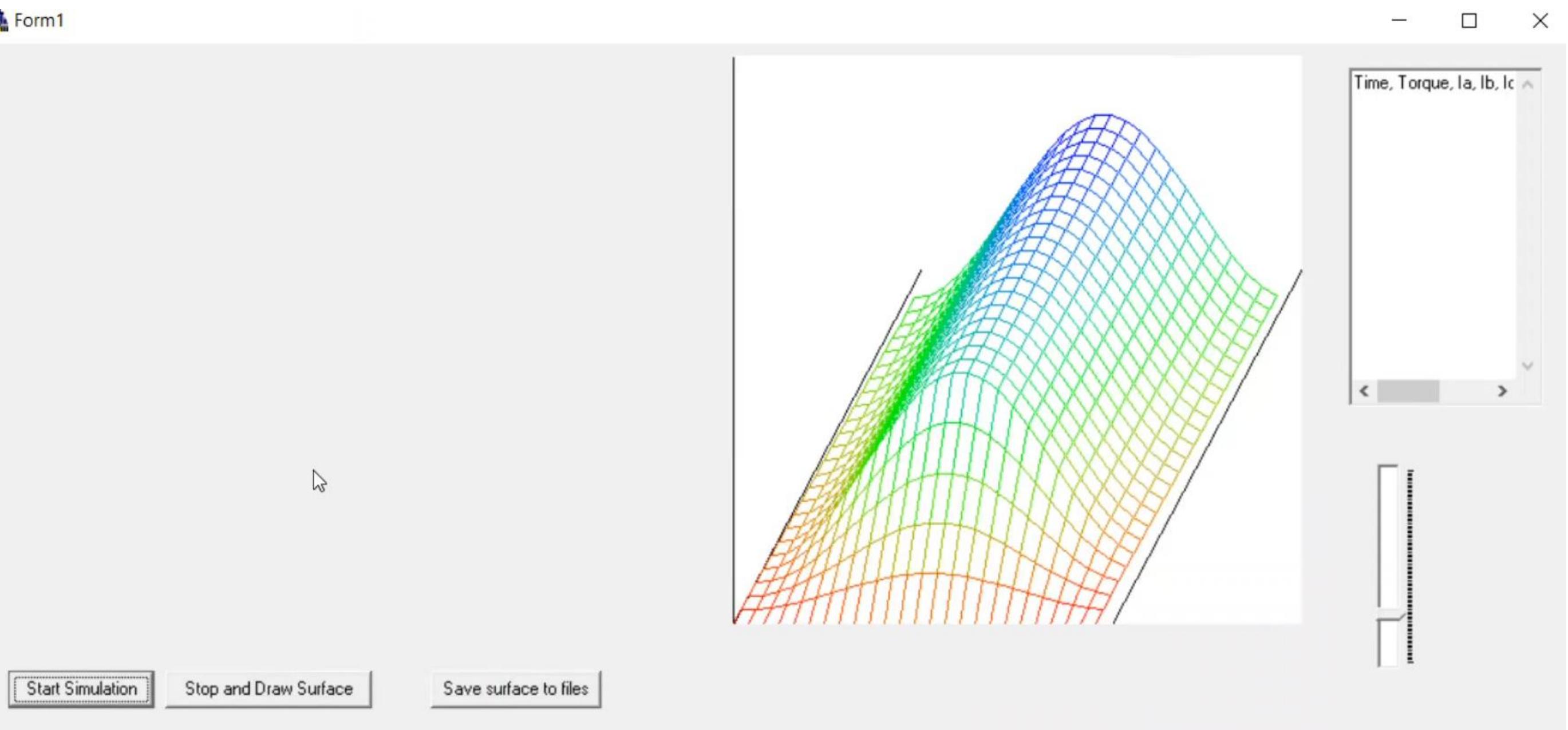
The proposed method operates in parallel with the CCS MPC utilizing a magnetization map. Any error between the referenced and obtained currents is processed to correct the reference points in the two-dimensional array representing the magnetization surface as a function of rotor angular position and flowing current.

II. CONTINUOUS CONTROL SET MODEL PREDICTIVE CONTROL FOR SRM

Each phase of SRM has described by the voltage balance equation [17]:

$$\frac{d\psi}{dt} = v - iR, \quad (1)$$

where v is the applied voltage, i is the flowing current, R is the phase resistance, and ψ is the flux linkage of the



A. Anuchin, A. Bogdanov, G. Demidova, E. Stolyarov, D. Surnin and Y. Vagapov, "Online Magnetization Surface Identification for a Switched Reluctance Motor," 2020 55th International Universities Power Engineering Conference (UPEC), 2020, pp. 1-5, doi: 10.1109/UPEC49904.2020.9209832.

A Mathematical Torque Ripple Minimization Technique Based on a Nonlinear Modulating Factor for Switched Reluctance Motor Drives

Ashwani Kumar Rana[✉], Student Member, IEEE, and A. V. Ravi Teja[✉], Member, IEEE

Abstract—This article presents a method to reduce the torque ripple in an 8/6 four-phase switched reluctance motor (SRM). The proposed scheme introduces a nonlinear modulating factor dependent on the rotor position and magnitude of the phase currents. This factor manipulates the currents in two adjacent phases during commutation and reduces the torque ripple effectively. Unlike the conventionally available torque-sharing functions, the proposed method instantaneously modulates every phase current obtained mathematically based on the other phase current in order to maintain the net torque constant. The proposed method requires minimal offline analysis and offers maximum possible torque with a minimal ripple. The method is simple and easy to implement due to a low computational burden. The proposed algorithm is implemented using MATLAB/Simulink software and is also validated experimentally on a 0.6-hp 8/6 SRM using a field-programmable-gate-arrays-based hardware setup developed in the laboratory. Typical results are presented and compared with the existing techniques. A torque ripple of $\approx 8\%$ has been achieved.

Index Terms—Field-programmable gate arrays (FPGA), nonlinear modulating factor, switched reluctance motor (SRM), torque control, torque ripple, torque sharing function.

NOMENCLATURE

T_e	Motor electric torque.
β_r, β_s	Rotor and stator pole arcs.
L_{min}, L_{max}	Minimum and maximum inductance of motor.
$\theta_{off}, \theta_{on}$	Turn-OFF and turn-ON angles.
θ_0	Zero slope angle.
θ_s	Angle at which inductance is maximum.
θ_r	Start angle of positive inductance region.
θ_t	End angle of negative inductance region.
$\theta_a, \theta_b, \theta_c, \theta_d$	Actual phase angles.
i_a, i_b, i_c, i_d	Actual phase currents.

Manuscript received October 3, 2020; revised December 18, 2020 and January 20, 2021; accepted February 19, 2021. Date of publication March 10, 2021; date of current version October 27, 2021. This work was supported by the Department of Science and Technology (SERB), Government of India, under Grant SRG/2019/001356. (Corresponding author: A. V. Ravi Teja.)

The authors are with the Department of Electrical Engineering, Indian Institute of Technology Ropar, Rupnagar 140001, India (e-mail: 2017ee002@iitrpr.ac.in; reviteja009@yahoo.co.in).

Color versions of one or more figures in this article are available at <https://doi.org/10.1109/TIE.2021.3063871>.

Digital Object Identifier 10.1109/TIE.2021.3063871

$i_a^*, i_b^*, i_c^*, i_d^*$ Reference phase currents.
 ω_r Rotor speed (electrical).
 T_a, T_b, T_c, T_d Motor per phase torque.

I. INTRODUCTION

A SWITCHED reluctance motor (SRM) is a special type of variable reluctance motor designed for rugged operation. Being lightweight, an SRM has the capability of driving high torque, which makes it attractive in the fields of electric vehicle and aerospace applications. The SRM has a simple manufacturing process, which makes it cheaper as compared to other motors. It is also fault tolerant, reliable, and have a high power density. The major issue limiting the SRM is the high torque ripple and its associated effects on the motor [1]. Its rugged construction and low cost is motivating industries and researchers to contribute in the development of algorithms to tackle the torque ripple issues. Husain [2] presented a broad and critical review of the origin of torque ripple and the approaches adopted by various researchers to minimize the torque ripple. The impact of the torque ripple on the efficiency of the SRM and its associated issues with respect to electric vehicle application are presented in [3] and [4]. To reduce the torque ripple in the SRM, various other approaches are adopted in literature such as torque-sharing function (TSF) [5]–[11], iterative learning-based methods [12]–[14], direct torque control, direct instantaneous torque control, flux control, [15]–[20], predictive control [21], [22], fuzzy control [23], [24], and sliding mode control [25], [26].

In TSF-based methods, a predefined torque function (linear or nonlinear) [5] is applied for every phase and the ripple is computed. The function with minimum ripple is selected for the given conditions. The torque ripple also depends on the turn-OFF angle, which is again computed based on the machine geometry and rigorous offline analysis [6]. In [7]–[9], some modified TSF's are proposed with online and offline data to reduce the torque ripple. Based on the obtained machine characteristics, a current-/torque-sharing function is determined using curve-fitting/lookup tables. Hence, these algorithms not only require offline analysis specific to that particular machine but also increase the computational overhead on the controller [9]–[11]. These techniques cannot reduce the torque ripple effectively because the torque is approximated to follow a predefined function, which in reality is not the case. Therefore, the torque

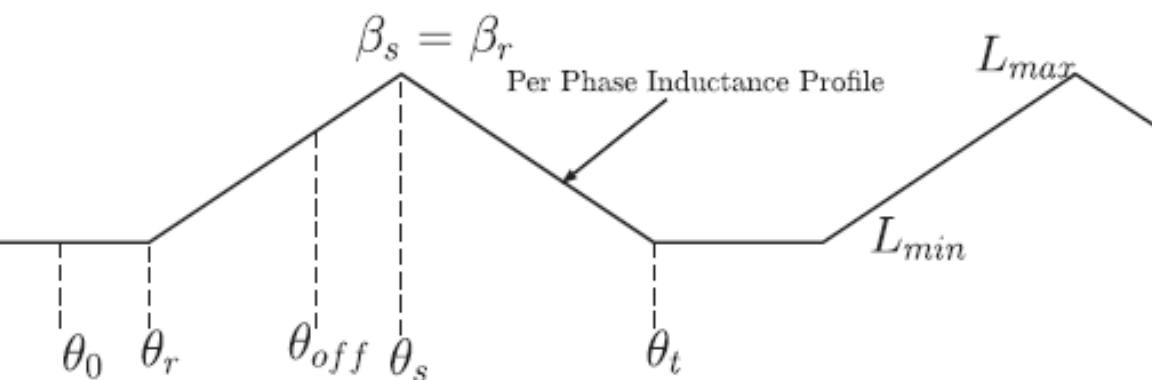


Fig. 1. Per phase inductance (linear) profile.

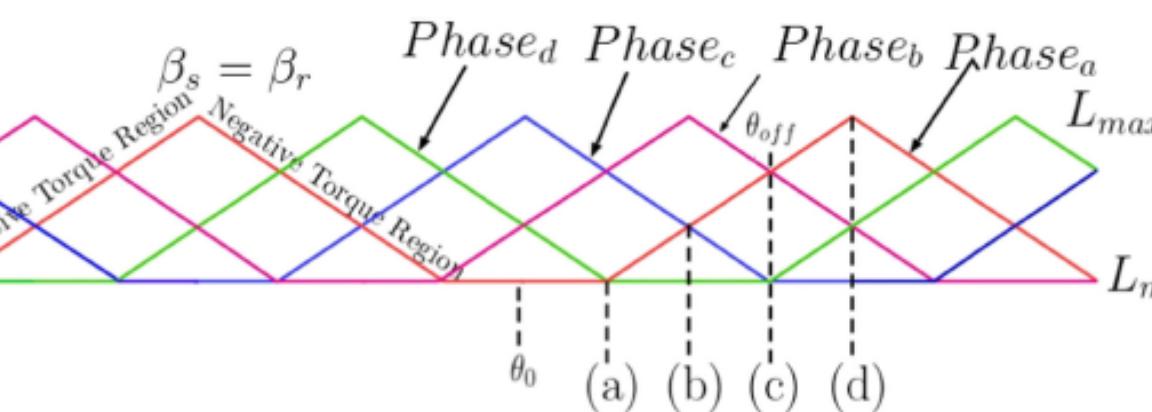


Fig. 2. Inductance (linear) profile of all four phases.

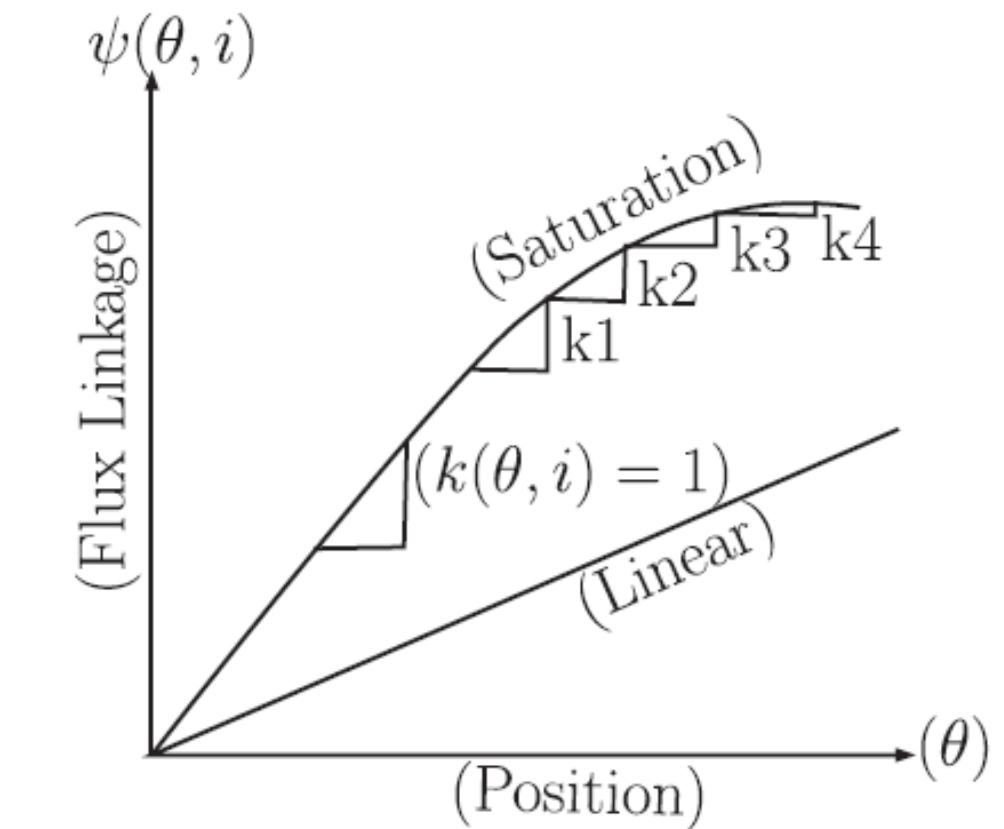


Fig. 3. Per phase flux linkage profile.

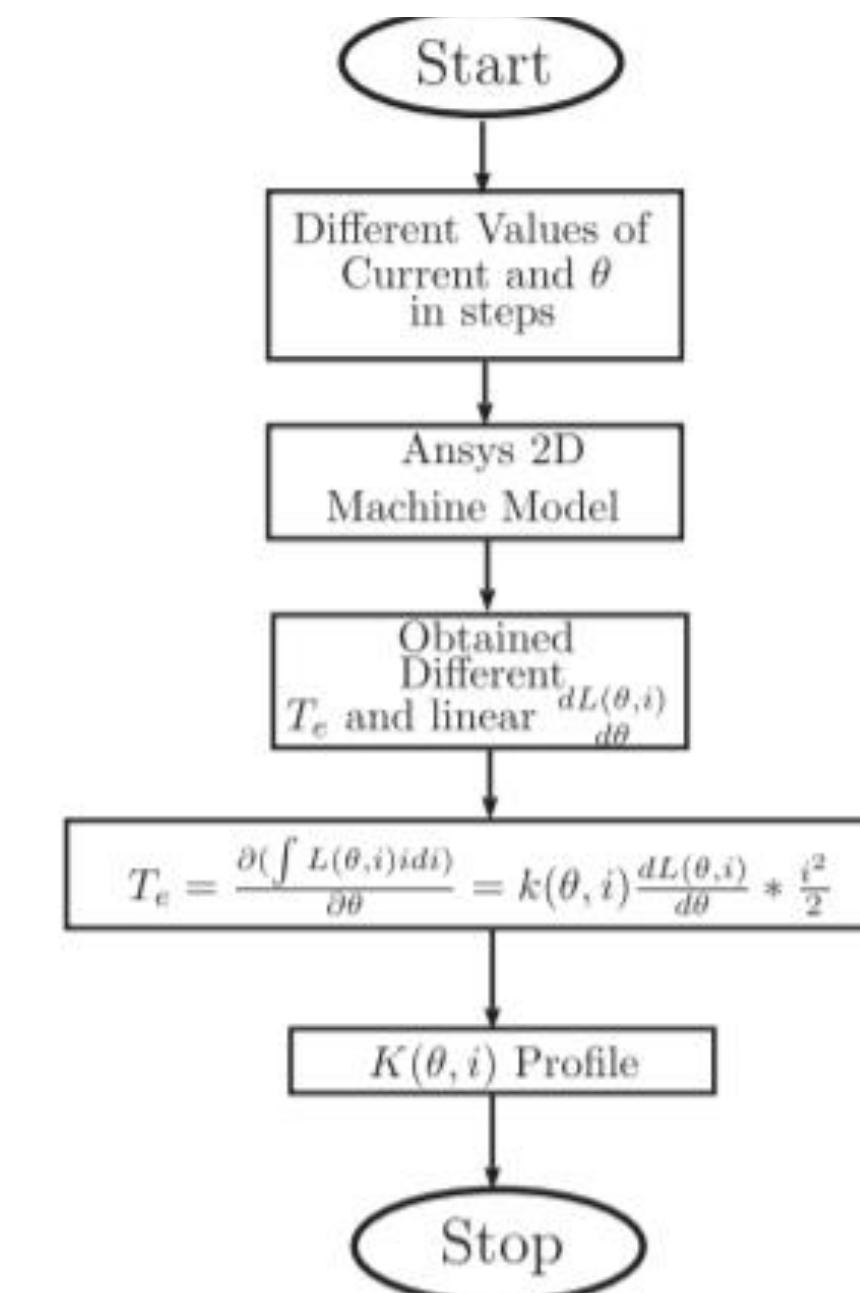


Fig. 6. Flow chart for the $K(\theta, i)$ profile generation.

A. K. Rana and A. V. R. Teja, "A Mathematical Torque Ripple Minimization Technique Based on a Nonlinear Modulating Factor for Switched Reluctance Motor Drives," in *IEEE Transactions on Industrial Electronics*, vol. 69, no. 2, pp.

1356–1366, Feb. 2022, doi:

10.1109/TIE.2021.3063871.

Development and Performance Analysis of Segmented-Double-Stator Switched Reluctance Machine

He Cheng, Member, IEEE, Shuo Liao, and Wenju Yan, Member, IEEE

Abstract—This paper investigates the design methods and performance optimization of segmented-double-stator switched reluctance machine (SDS-SRM). Firstly, two segmented U-shaped single-stator SRMs are introduced, including inner-rotor and outer-rotor constructions. In order to enhance the torque and power density, these two kinds of single-stator SRMs are combined together to constitute an SDS-SRM. Then, the relationships of torque ripple coefficient with the mechanical offset angles of the inner and outer rotor teeth are investigated to obtain the optimal rotor structure, and the corresponding conduction phase sequences for double-stator excitation mode are also analyzed. Furthermore, the flux distributions of the inner and outer stators with different coil magnetic polarities configurations are researched, and it reveals that the phase windings both on inner and outer stators with NSSNNSSN polarities have better magnetic field decoupling characteristics. To evaluate the final topology of the proposed SDS-SRM, the static magnetic characteristics and dynamic performances are presented. Finally, the SDS-SRM prototype is manufactured and tested to validate the theory and simulation analyses.

Index Terms—Double-stator, segmented stator, switched reluctance motor (SRM), magnetic characteristics

I. INTRODUCTION

Due to robust construction, good overload capability, inherent fault tolerance, low cost and wide speed range, switched reluctance machines (SRMs) have been widely used in home appliance, wind power generation, industrial drive and transportation electrification applications [1]-[6]. However, in comparison to permanent magnet motor (PMM), the disadvantages of SRMs, such as low torque density, high torque ripple and large acoustic noise, prohibit their widespread use in some fields where high drive performances are required [7], [8].

Manuscript received September 7, 2020; revised December 1, 2020, January 3, 2021 and January 22, 2021; accepted January 31, 2021. This work was supported in part by the National Natural Science Foundation of China under Grant 51707192, in part by Natural Science Foundation of Jiangsu Province under Grant BK20200654 and in part by the Project funded by China Postdoctoral Science Foundation under 2020M671642.

H. Cheng, S. Liao and W. J. Yan are with the School of Electrical and Power Engineering, China University of Mining and Technology, Xuzhou 221116, China (e-mail: chenghecumt@163.com; 125784358@qq.com; yanwenju09@126.com). (Corresponding author: Wenju Yan.)

Thus, in order to solve issues above, varieties of segmented structures in SRMs have been proposed, mainly including segmented-stator and segmented-rotor topologies [9]-[16]. In [9], based on the concepts of maximum energy conversion, a novel stator segmented structure is put forward, and it can produce over 20% torque compared to the conventional SRM. A kind of U-shaped segmented-stator hybrid excitation SRMs assisted with permanent magnets is investigated in [10]. The research reveals that the proposed motor produces higher electromagnetic torque with the help of the permanent magnets. In [11] and [12], the influences of the pole number and flux gap width between E-core segmented stators on the electromagnetic performance have been researched, and the torque ripples for modular machines are significantly reduced, and so do the iron loss and radial force. For segmented-rotor SRM, two segmented SRMs with single tooth winding and multitooth winding are designed and show similar capabilities in [13], but have significantly greater torque ripple than the PM machine. In [14] and [15], the design methodology and principles for high-performance segmented rotor SRM are proposed, and it finds that slot/pole combination and rotor pole numbers have a significant effect on its performance parameters such as efficiency, speed range, and overload capability. Furthermore, an E-core stator and segmented-rotor SRM is studied and the analysis indicates that this motor has low steel consumption, high torque production, high power and torque densities, and strong starting capability [16].

In addition to employing modular motor structure, double-stator construction is another effective means to enhance the torque and power density for different types of motors [17]-[25]. In [18], it demonstrates that with the identical copper losses, the proposed double stator SFMM can deliver 29.5% higher torque than its single stator counterpart. In [22], a double stator wound field switched flux (WFSF) machine is proposed, and this motor exhibits 19% higher torque than the conventional WFSF machine. In [23], The double stator switched reluctance machine (DS-SR) and double stator multitoothed switched reluctance machine (DS-MSR) can offer higher torque density than the single-stator SR counterpart by 46.1% and 183.2%, respectively. In [24] and [25], it shows that the DSSRM migrates the advantages of a conventional SRM while substantially improving its high torque/power density. This is due to two main features of DSSRM structure, first increased copper area, and second flux cancelation and rerouting. In [26], a new double-stator SRM (DSSRM) is introduced, and the proposed design is based on optimization of

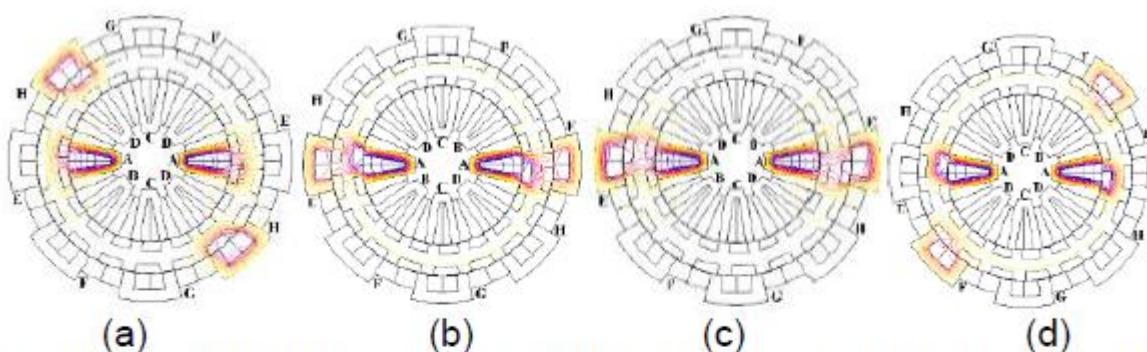


Fig. 9 Flux distributions for SDS-SRM-1 and SDS-SRM-4 when the rotor position is at 1.5° and 4.5° (a) SDS-SRM-1 at 1.5° (b) SDS-SRM-1 at 4.5° (c) SDS-SRM-4 at 1.5° (d) SDS-SRM-4 at 4.5°

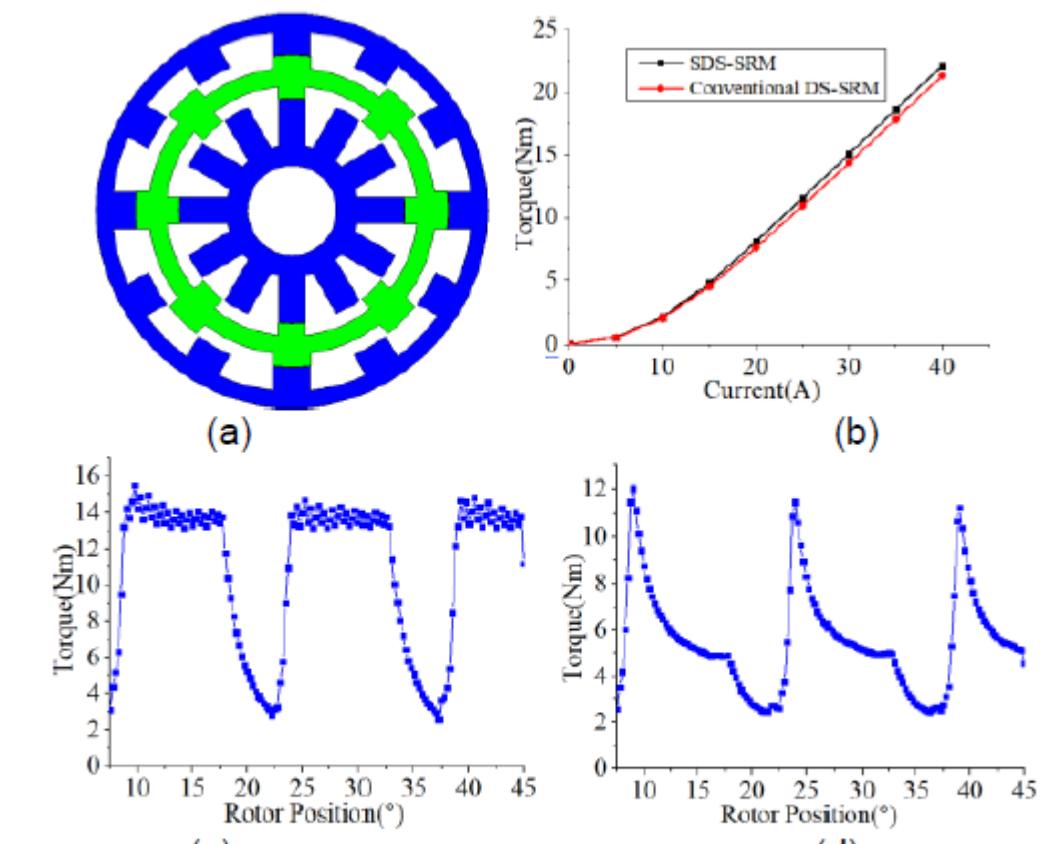


Fig. 10 Flux distribution for SDS-SRM-2 and SDS-SRM-3 when the rotor position is at 1.5° or 4.5° (a) SDS-SRM-2 at 1.5° (b) SDS-SRM-2 at 4.5° (c) SDS-SRM-3 at 1.5° (d) SDS-SRM-3 at 4.5°

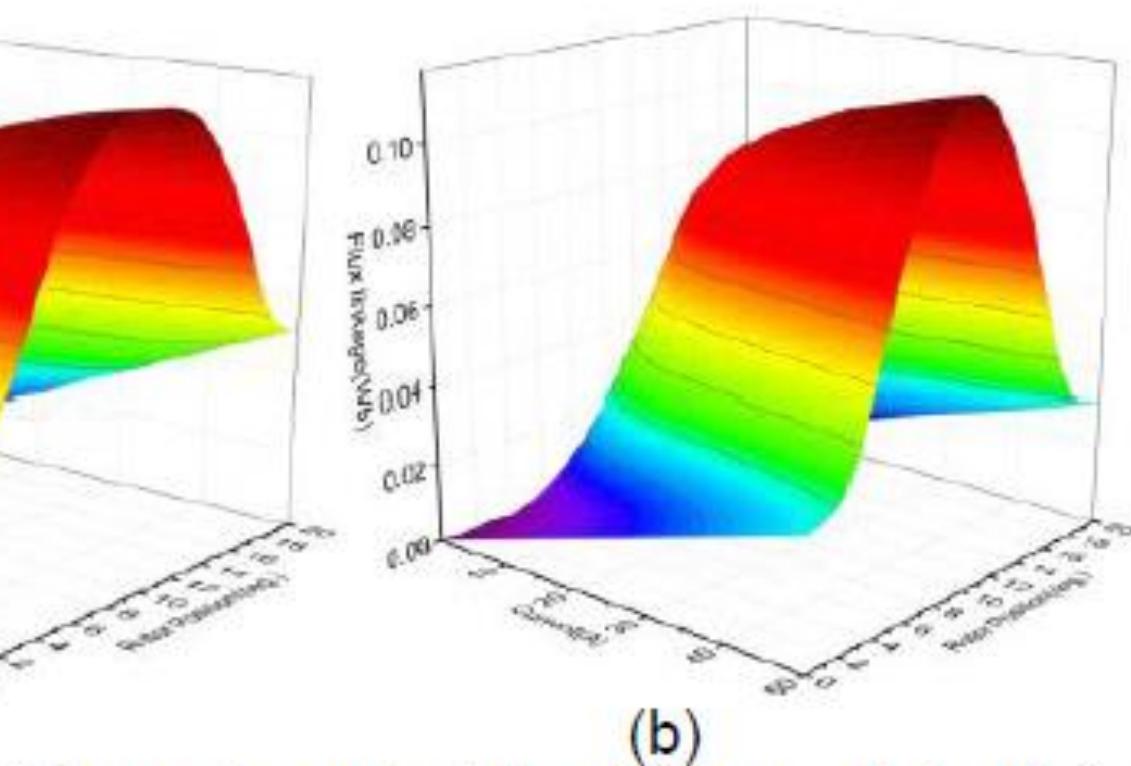
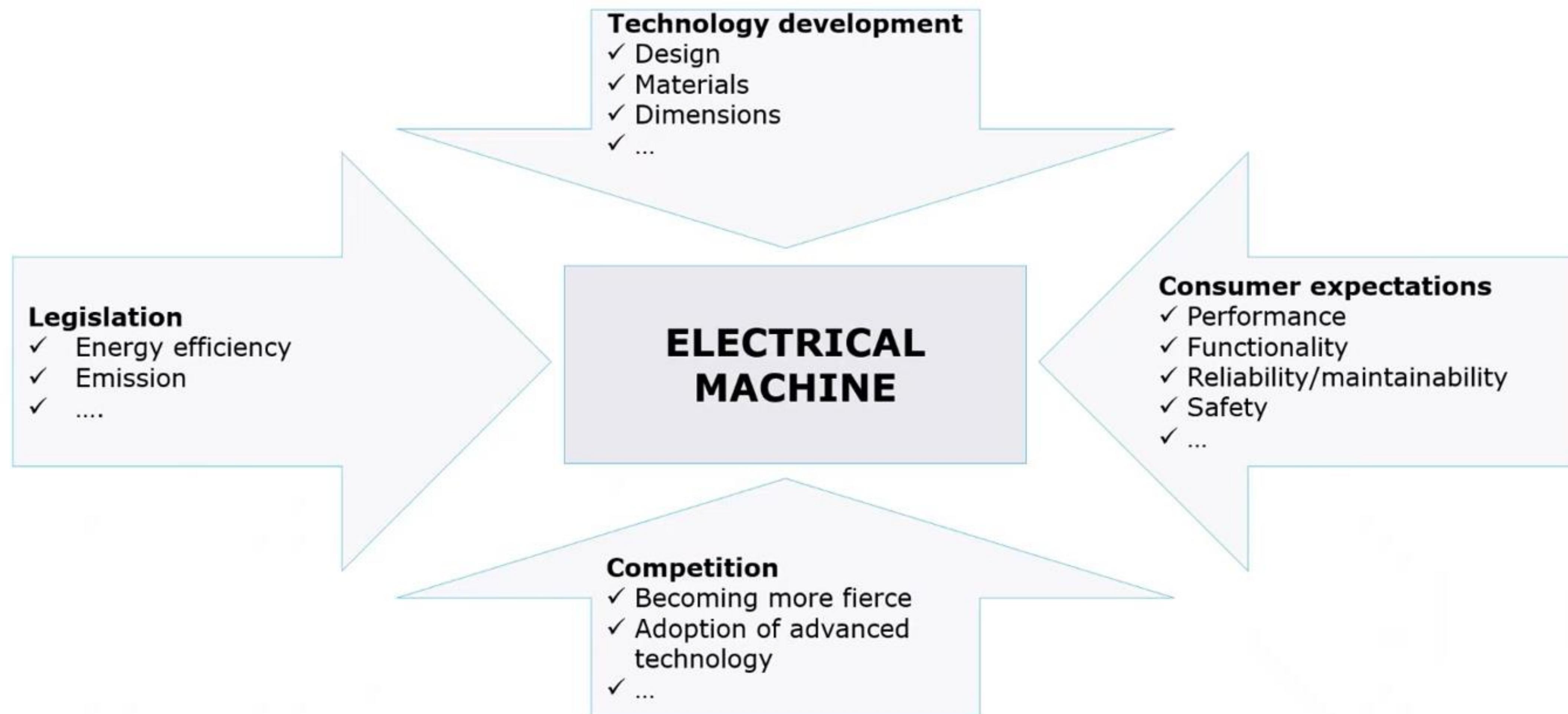


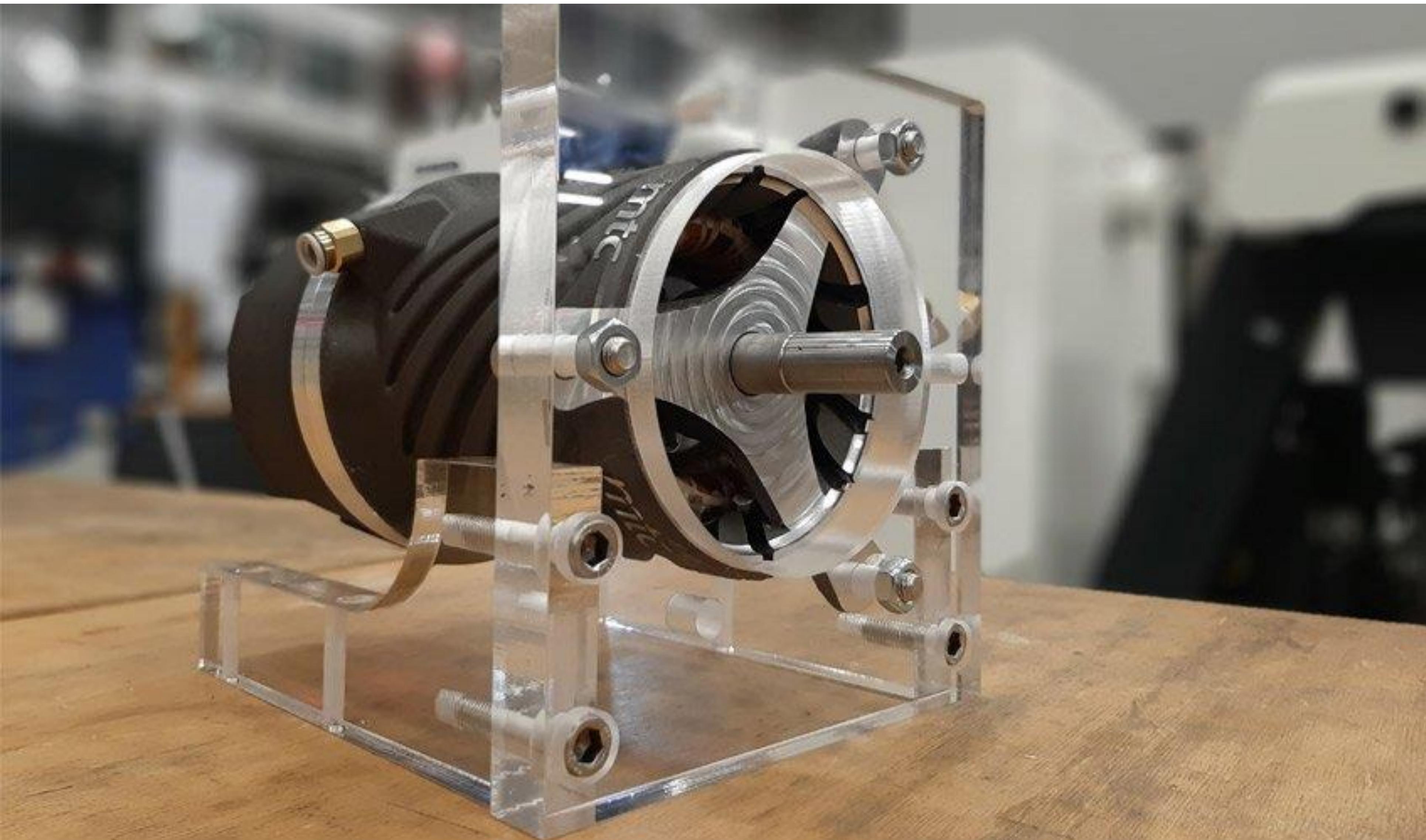
Fig. 13 Static phase flux linkage characteristics (a) inner stator (b) outer stator

H. Cheng, S. Liao and W. Yan, "Development and Performance Analysis of Segmented-Double-Stator Switched Reluctance Machine," in IEEE Transactions on Industrial Electronics, vol. 69, no. 2, pp. 1298-1309, Feb. 2022, doi: 10.1109/TIE.2021.3059554.

Дизайн электрических машин



Аддитивные технологии в производстве электрических машин



Аддитивные технологии в производстве электрических машин

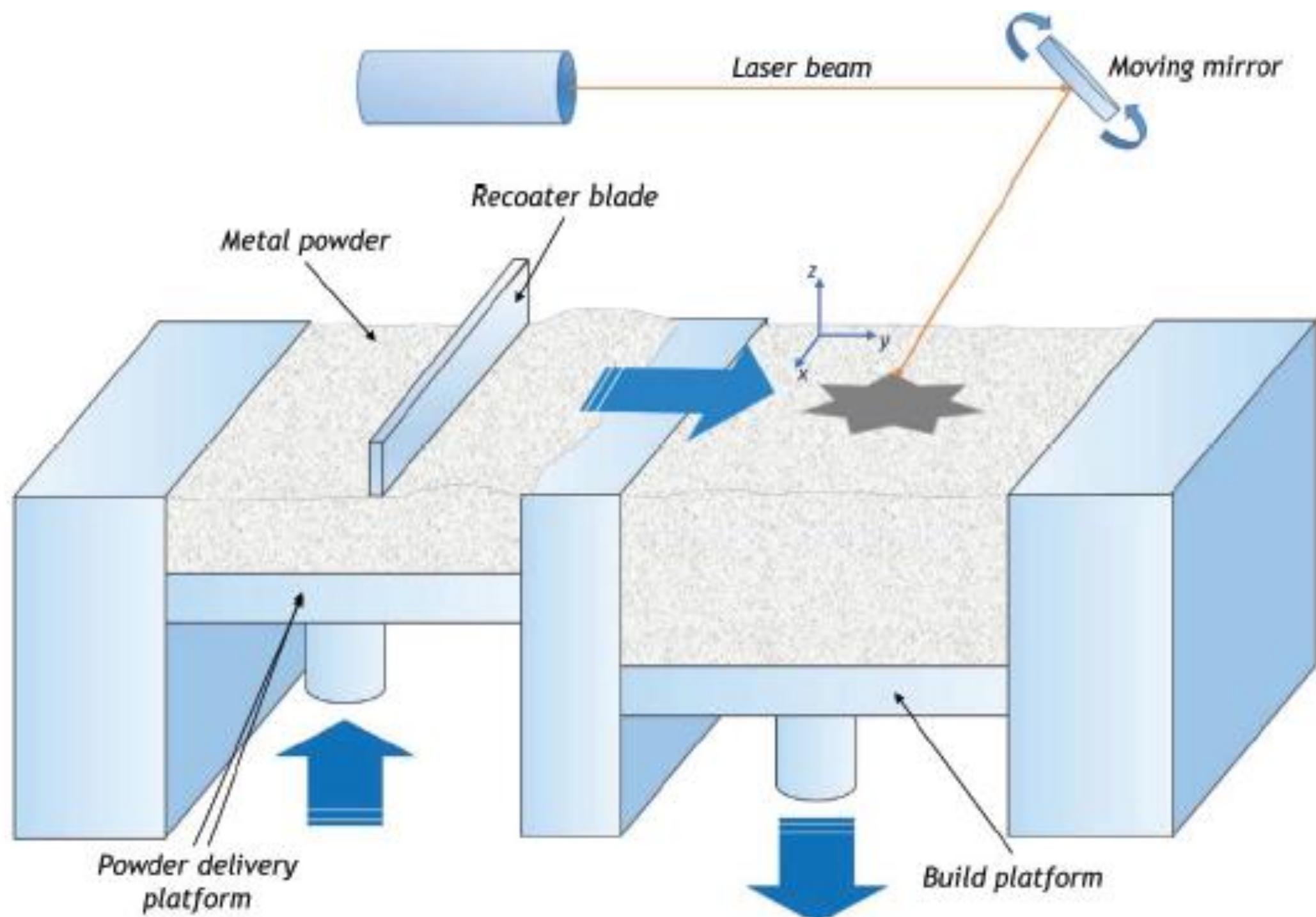


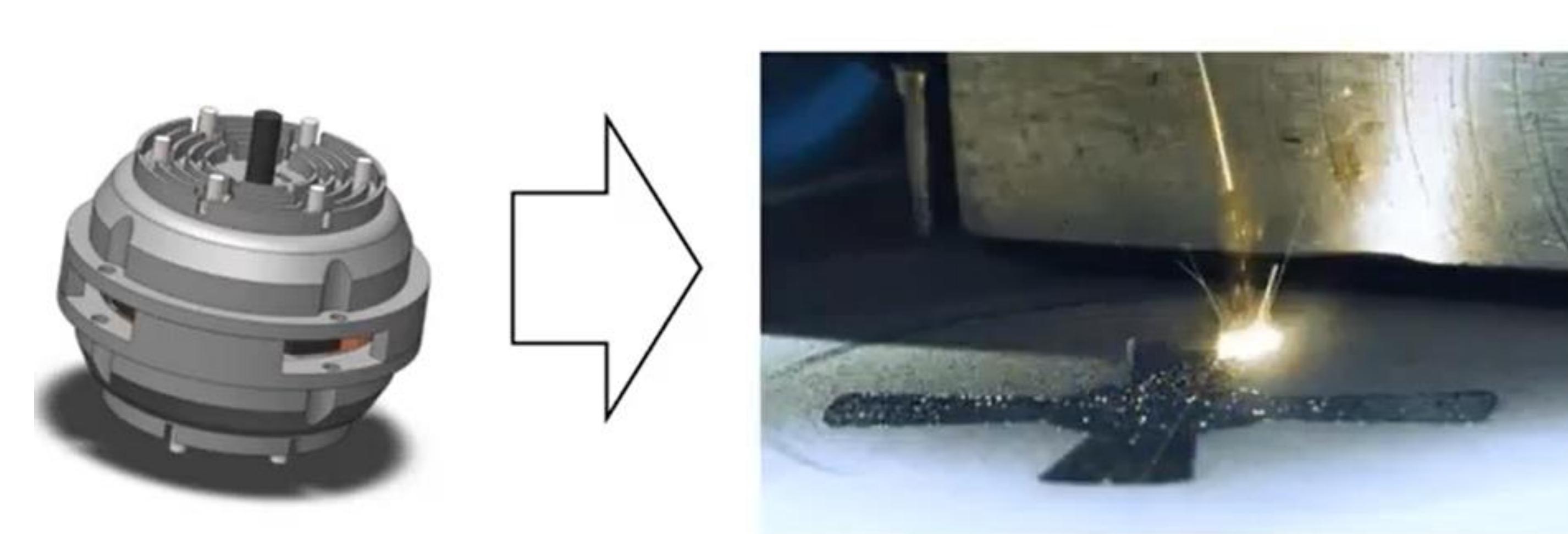
Fig.5. Selective laser melting build process. [21]



(c) TalTech

Аддитивные технологии в производстве электрических машин

- **Computed-aided-design (CAD)** software or 3D object scanners to direct hardware to deposit material, layer upon layer, in precise geometric shapes. As its name implies, additive manufacturing adds material to create an object



Аддитивные технологии в производстве электрических машин

- Новые возможности для инноваций в **мелкосерийном производстве** благодаря более быстрому и дешевому прототипированию, сокращению времени выполнения заказа и более коротким цепочкам поставок.
- Новая технология, позволяющая производить компоненты и целые сборки без использования инструментов непосредственно из файла САПР.
- Создание сложных систем с помощью обычного процесса занимает много времени, а сборка всей системы воедино требует большого количества человека-часов, но с помощью 3D-печати можно значительно сократить время прототипирования.
- Устранение участия человека позволит улучшить производственные допуски и упростить изготовление и, в конечном итоге, позволит использовать методологию «пресс-печати».



Technologies for Additive Manufacturing of Electrical Machines

Hans Tiismus¹, Student Member, IEEE, Ants Kallaste¹, Member IEEE, Toomas Vaimann¹, Member IEEE,

Anton Rassõlkin¹, Member IEEE, Anouar Belahcen^{1,2}, Member IEEE

¹Tallinn University of Technology, Tallinn, Estonia

²Aalto University, Espoo, Finland

Abstract — Additive manufacturing (AM) technology is considered an essential component of the Industry 4.0 revolution, due to its capability for decentralized production of highly customizable complex objects. Its design and fabrication freedom also suggest for the production capacity of goods with embedded electromechanical components and even electrical machines with enhanced performance. Currently, due to the maturity of homo-material and limited multi-material capabilities of current AM systems, prototyping of 3D printed electrical machines has taken the path of manual assembly of printed components. For fully printed end-user products containing integrated electromechanical components to emerge, evolution of the multi-material printing systems is required. This paper discusses the technical demands of additively manufacturing electrical machines and current promising technologies on the horizon to bring us one step closer to mass produced fully 3D printed electrical machines.

Index Terms — Electric machines, Manufacturing processes, Magnetic materials, Three-dimensional printing

I. INTRODUCTION

ADITIVE manufacturing or 3D printing is the common term for a class of technologies that produce functional components or entire assemblies from a CAD file in a layer by layer fashion. This radically different approach from subtractive methods plays a significant role in the vision of industry 4.0 by improving the capabilities of traditional manufacturing systems. Coupled with unprecedented data acquisition and analysis capacity of the Internet of Things (IoT), the fourth industrial revolution can potentially redefine the industry as we know it today, enabling for example:

- Mass personalization of goods – real-time customer feedback alongside unparalleled design and production freedom of AM allows customization of products according to individual needs and their viable small-scale production. [1]
- Decentralized production – production workload can be distributed over automated factories via utilization of cloud services. [2]
- On demand production – digital inventories will replace physical inventories when parts are produced on-demand, when actually needed. [3]

These upgrades will provide immense opportunities

towards the realization of sustainable manufacturing with highly efficient resource usage, simplified logistics and individualized products. For achieving the full functionality of industry 4.0 smart factories, printing of goods containing electro-mechanical and electronic elements must be completed as a single uninterrupted process without any additional manual post-processing or assembly. This level of automated integration is not currently possible due to several limitations of the AM technology, as 3D printing of electromechanical systems is notably difficult due to high precision moving parts and multiple diverse materials involved. State of the art printing technology is currently capable of industrial level production of only homo-material components, which could be utilized with present or novel next generation motor designs for enhancing performance.

With the AM technologies finally shifting from rapid prototyping into large scale production, the value of AM market is anticipated to jump from \$ 9.5B (2018) to \$ 26.2B (2022) worldwide [4], and the research and development of AM technologies is expected to accelerate even further – possibly unlocking industrial level multi-material 3D printing capabilities in the near future.

II. STATE OF THE ART OF ADDITIVELY MANUFACTURED ELECTRICAL MACHINES

Until now, the design of EMs had mostly been limited to 2D, mainly due to the manufacturing constraints employed by the industry. Previously, independently from the lamination industry, different motors with powder metallurgy cores have been shown to benefit from three-dimensional flux paths: such as claw pole or pancake motors or designs involved in transverse flux. [5] These designs can also be realized with AM, with more refined geometries. The main advantage of AM lies in its capacity for realizing finite walls (up to 60 μm) and achieving partially hollow structures: improving motor cooling capacity, moment of inertia and material efficiency. Coupling these possibilities with the industrial level capacity of AM platforms and topology optimization capabilities of current computational systems finally have a case at pushing 3D machines into mainstream. Electrical machines can be divided into three major branches

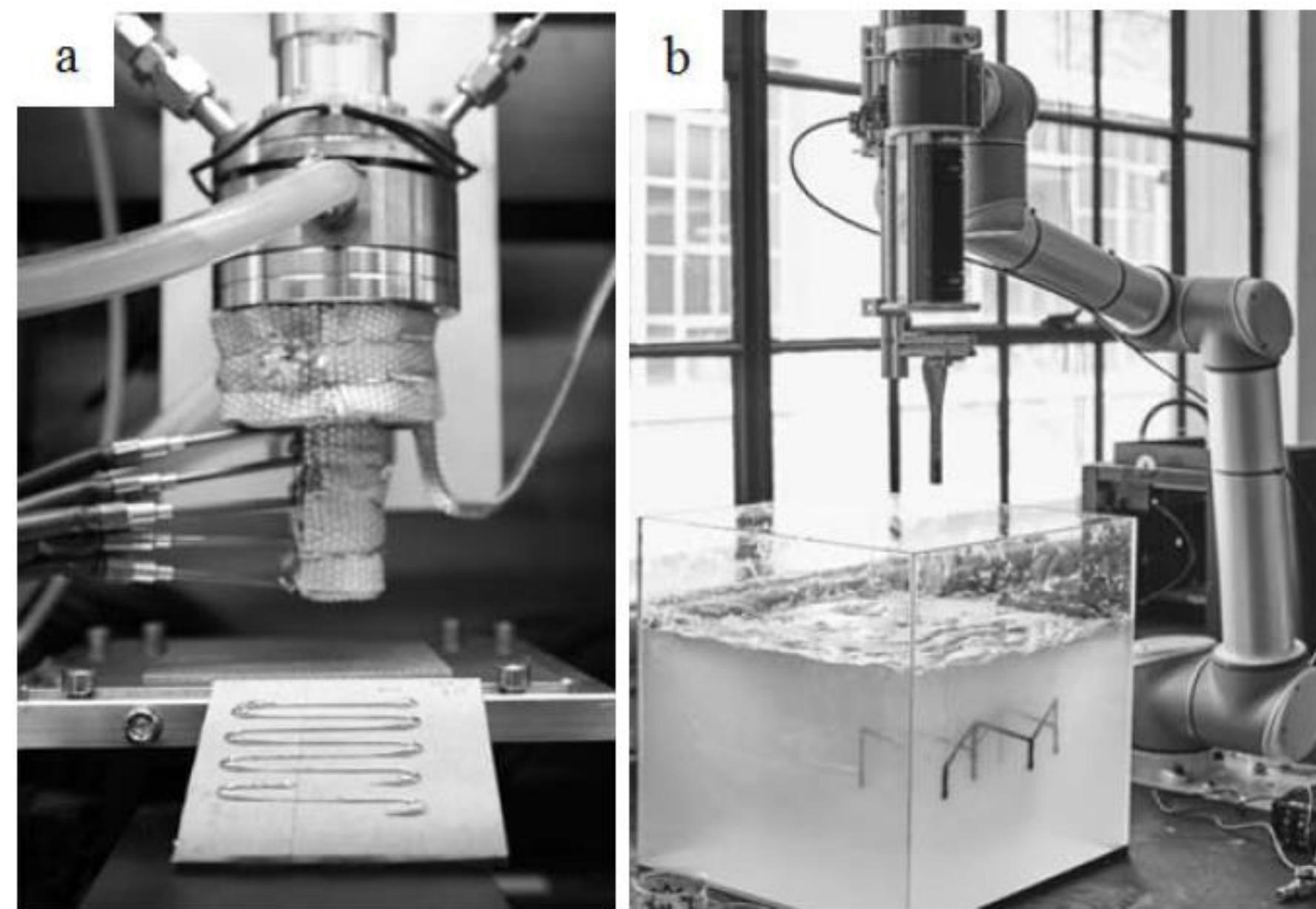


Fig.4. (a) Direct metal writing reinvents metal additive manufacturing [18], (b) Rapid Liquid Printing system [20].

H. Tiismus, A. Kallaste, T. Vaimann, A. Rassõlkin and A. Belahcen, "Technologies for Additive Manufacturing of Electrical Machines," 2019 20th International Conference of Young Specialists on Micro/Nanotechnologies and Electron Devices (EDM), 2019, pp. 651-655, doi: 10.1109/EDM.2019.8823462.

Challenges of Additive Manufacturing of Electrical Machines

Hans Tiismus, Ants Kallaste, Member, IEEE, Anouar Belahcen, Senior Member, IEEE, Anton Rassölkin, Member, IEEE, Toomas Vaimann, Member, IEEE

Abstract – 3D printing or additive manufacturing (AM) technology is considered an essential component of the Industry 4.0 revolution due to its improved capabilities over traditional manufacturing systems, facilitating the shift towards next generation smart factories. The three-dimensional fabrication freedom also suggests a new epoch in the design of electrical machines, as the process can finally be liberated from the constraints of 2D laminations. Despite the multi-material nature of 3D printing electrical machines, due to the availability and maturity of dedicated metal printing systems, most of the research and development on the field is concentrated on material optimization and rapid prototyping on these systems. In this paper we present the challenges of 3D printing electrical machines with current manufacturing systems and solutions offered by different authors. Challenges of selective laser melting (SLM) fabrication are discussed in greater detail due to its recognition and popularity in the electrical machine community.

Index Terms – additive manufacturing, electrical machines, electrical steel, hot isostatic pressing, material properties, selective laser melting

I. INTRODUCTION

NEXT generation industry demands resource efficient management of personnel, fabrication and logistics. The additive process is material economical by the virtue of its capacity for optimized part topology and its refined internal structure. The fabrication freedom, free of pre-prepared moulds, dies or stamps, also suggests streamlined prototyping, production and logistics of industry 4.0 factories, ultimately ushering towards mass-personalized goods. [1] It is vital for these end-products to contain additional features, such as embedded electrical or electromechanical components to truly shift the industry to a new era. Fully 3D printed end-user products have been shown to exhibit multiple benefits over traditionally manufactured products, such as: three-dimensional multi-physical designs (including mechanical, electrical, thermal and magnetic considerations) [2], fully recyclable constructions [3] and smart material utilization [4]. The prospects and the recent shift of AM technologies from

This research work has been supported by Estonian Ministry of Education and Research (Project PSG137).

H. Tiismus, T. Vaimann, A. Kallaste and Anton Rassölkin are with the Department of Electrical Power Engineering and Mechatronics, Tallinn University of Technology, Estonia (e-mail: biasad@tlu.ee)

A. Belahcen is with Department of Electrical Engineering and Automation, Aalto University, Espoo, Finland and with the Department of Electrical Power Engineering and Mechatronics, Tallinn University of Technology, Estonia (e-mail: anouar.belahcen@aalto.fi)

rapid prototyping into large scale production has sparked its flourishing growth and the sector is expected to triple in the next few years, from the value of \$ 9.5 B (2018) to \$ 26.2 B (2022) worldwide [5]. Presently, AM research community is ever-growing, developing new printing technologies and improving the existing ones to resolve its main drawbacks of [4]:

- Relatively slow manufacturing speed
- Internal defects from layer-by-layer fabrication
- Limited multi-material capabilities
- Necessary post-production of printed parts

The same limitations apply to additive manufacturing of electrical machines as well. This paper focuses on the current challenges and latest progress made in additive manufacturing of electrical machines.

II. ADDITIVELY MANUFACTURED ELECTRICAL MACHINES

Electrical machines can be divided into three major branches according to driving phenomena of their operation: electrostatic, piezoelectric and electromagnetic motors. Although 3D printing capabilities have been demonstrated for all three types of devices [6], [7], [8], this paper focuses on the electromagnetic motor (EM), as these machines are the most common and functional. AM has been proposed to open a new epoch in the EM design – as it can finally be elevated above the constraints of 2D laminations. Previously, different motors with powder metallurgy cores have been shown to benefit from three-dimensional flux paths: such as claw pole or pancake motors or designs involved in transverse flux. [9] These designs can also be realized with AM, however with more refined geometries. The main advantage of 3D printing lies in its capacity for realizing finite walls (up to 60 µm) and achieving partially hollow structures: improving motor cooling capacity, moment of inertia and material efficiency. [7] Coupling these possibilities with the industrial level capacity of AM platforms and topology optimization capabilities of current computational systems, we finally have a case at pushing 3D machines into mainstream.

3D printing EMs is a technically demanding procedure, due to tight tolerances for fitting moving parts and their structural makeup of multiple dissimilar materials. EMs require both electromagnets for the controllable generation of magnetic fields and ferromagnetic flux guides for the amplification of magnetic interactions inside the machine.

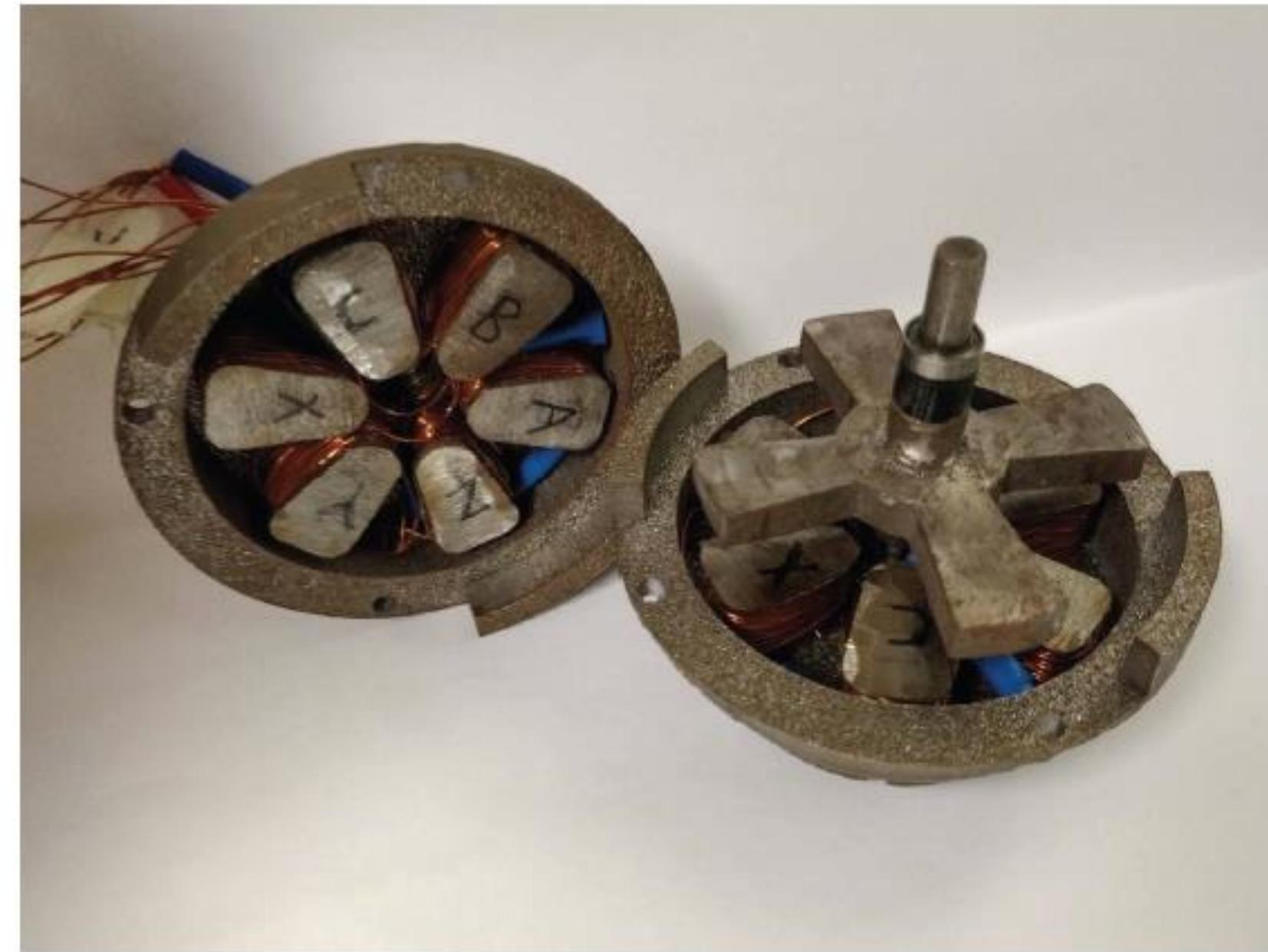


Fig. 3 SLM fabricated stator halves and rotor alongside inserted bearings and hand-wound electromagnets.

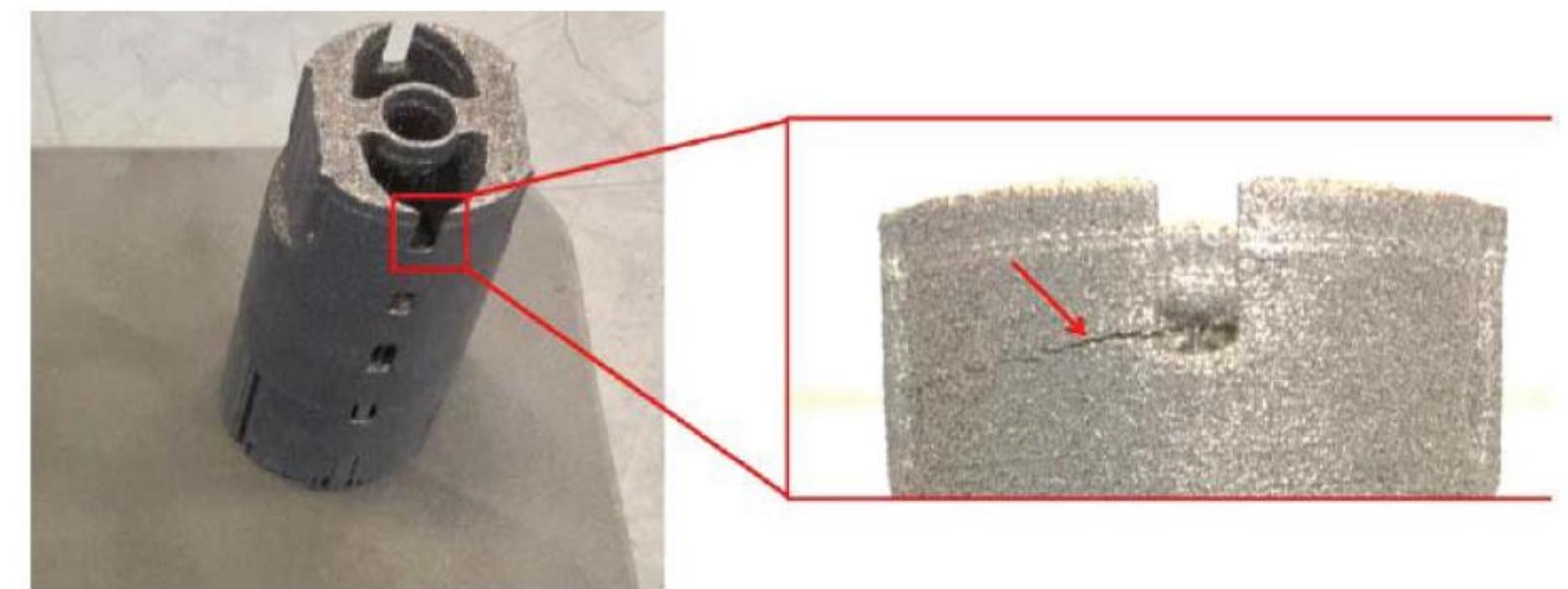


Fig. 6. SLM fabricated rotor with optimized torque density. Zoomed region shows the presence of the crack. [19]

Control Challenges of 3D Printed Switched Reluctance Motor

Anton Rassõlkin, Ants Kallaste, Toomas Vaimann, Hans Tiismus
Department of Electrical Power Engineering and Mechatronics
Tallinn University of Technology
Tallinn, Estonia
anton.rassolkin@taltech.ee

Abstract— Additive manufacturing, also known as 3D printing, is opening up new ground for innovations in low-volume production due to faster and cheaper prototyping, reduced lead time and shorter supply chains. Using the 3D printing in design of electrical machines is also facing different challenges in control of machines. This paper discusses material and manufacture drawbacks caused by Selective Laser Melting technology, mainly mechanical defects. Special attention is paid to control algorithms of first prototypes and design of converter. Moreover, an overview of control strategies for small Switched Reluctance Motors is presented.

Keywords— machine control, microcontrollers, motors

I. INTRODUCTION

Nowadays the electrical machine design is pushed forward by the need of increased energy efficiency, progress of system integration and devices mobility that has led also to investigation of alternative production methods for electrical machines. Additive manufacturing (AM) is a relatively new technology, which enables the tool-free production of components and entire assemblies directly from a CAD file. Today, the technology is still not widely used in industrial production, but it is gaining more and more popularity. In electrical machine research community, the quality, reliability, and performance of 3D printed machines is growing dramatically. Using the additive manufacturing process to produce highly complicated structures is fairly novel.

Particularly, the AM advantage in prototyping is coming out when producing smaller size machines [1]. The conventional manufacturing methods raise the costs for small parts due to the necessary manual production steps. The main advantages of 3D printing process lies in the possibility of manufacturing complex designs, including fine walls down to 60 µm and high up to several centimetres [2]. This allows the manufacturing of parts with complex inner structures and offers the possibility to realize complete hollow structures [3]. It is also possible to reduce the machine weight by designing the machine without excessive material, which is needed in a conventional design [4]. This is especially useful for rotor design, as it is possible to reduce the machine moment of inertia, resulting in machines with shorter acceleration time and high dynamics. However, using the 3D printing in design of electrical machines nowadays is facing different challenges, which have to be solved in the future. For example, in [5] it is given that the 3D printed rotor mechanical strength may not be as high as expected and this type of machine is not suitable for use in the high speed operation. In [4] it is stated that in the future more

investigations of the electromagnetic behaviour of additively manufactured materials are needed. Besides, realizable function integration like cooling effects or lightweight designs are required to establish the additive manufacturing as a standard process in industrial process chains.

There are several variations of machine types that could be manufactured by the printing method, but the most attractive and simplest ones are the switched reluctance and the synchronous reluctance machine. Nevertheless, AM is facing huge amount of challenges that need to be addressed to reach to the point where the 3D printed machine could be competing with the conventional machines produced for special application in small series.

The main objective of the paper is highlight control challenges of 3D printed switched reluctance motor.

II. FEATURES OF SELECTIVE LASER MELTING

Selective Laser Melting (SLM) is emerging across a broad range of sectors, including automotive, medical and aerospace, for the creation of functional metallic parts. The process involves melting metal powders layer by layer by laser and consolidating them into fully dense objects. For the practicality of the SLM process for manufacturing electrical machines, specific mechanical and electromagnetically properties need to be achieved [6]. Until now the design of standard electrical motors has mostly been limited to two-dimensions, mainly due to constraints imposed by the manufacturing processes employed. The possibility offered by AM to extend the design to the three-dimensional space introduces new opportunities towards the fabrication of compact, highly performing electrical machines.

Despite the advantages of the additive manufacturing process over traditional methods, concerns exist regarding the reliability and strength of 3D printed objects. Mechanical integrity of the printed objects becomes particularly relevant for rotors employed in high speed motors, as even relatively small structural inconsistencies are likely to lead to propagation of cracks in the rotor and failure in its integrity [7]. It has been shown that increasing the melting laser energy input promotes densification of the part by improving powder melting and reducing melt-pool instabilities (e.g., balling), however the formation micro cracks is also increased due to increased thermal stresses. An example of micro cracks is shown on Fig. 1 (a).

Printing the magnetic material suitable for electrical machine is a challenging task, as the material is required to achieve good magnetic properties: small hysteresis loop and high permeability, and it has to show high electrical resistivity to decrease the eddy currents. Iron-silicon (Fe-Si)

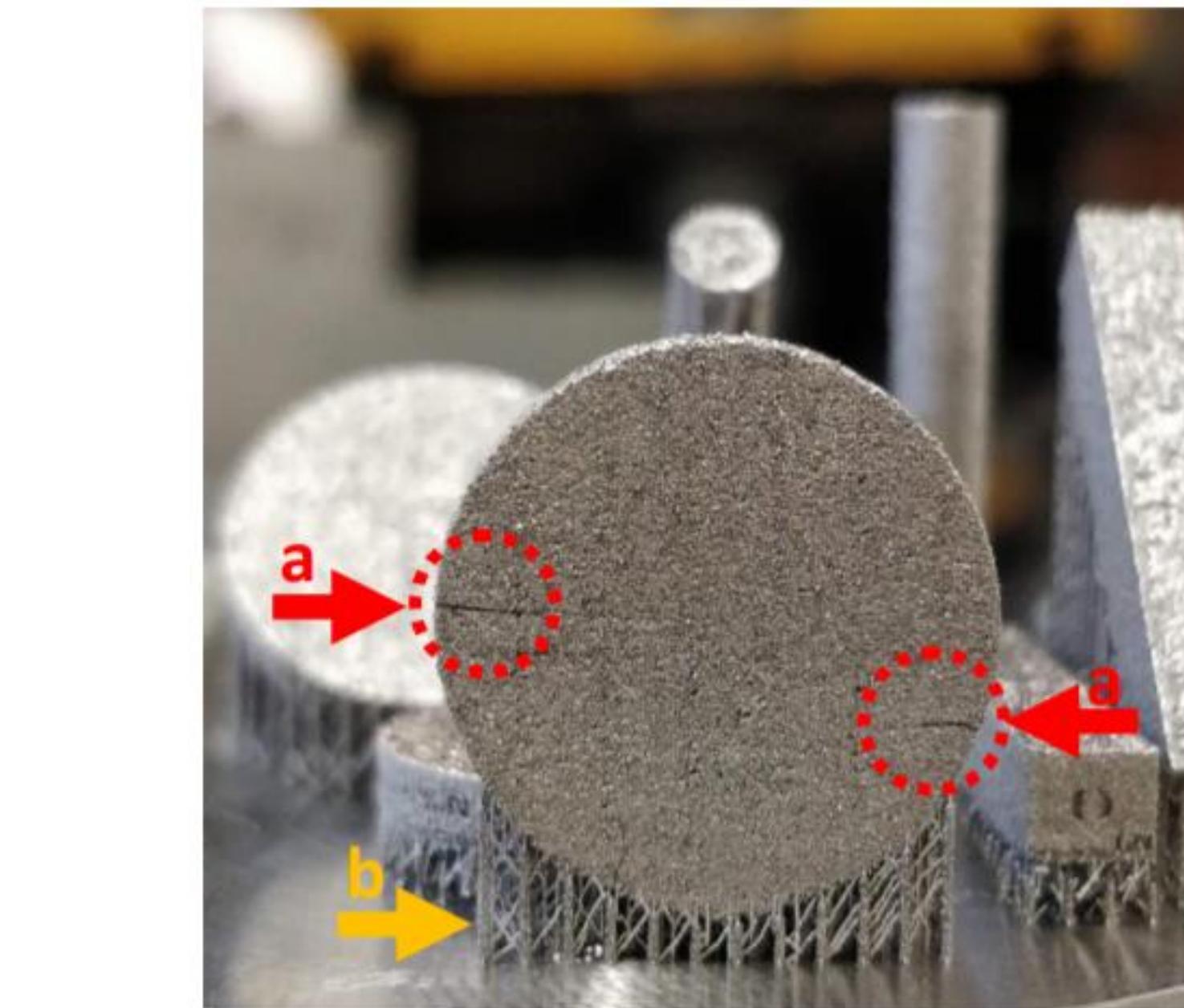
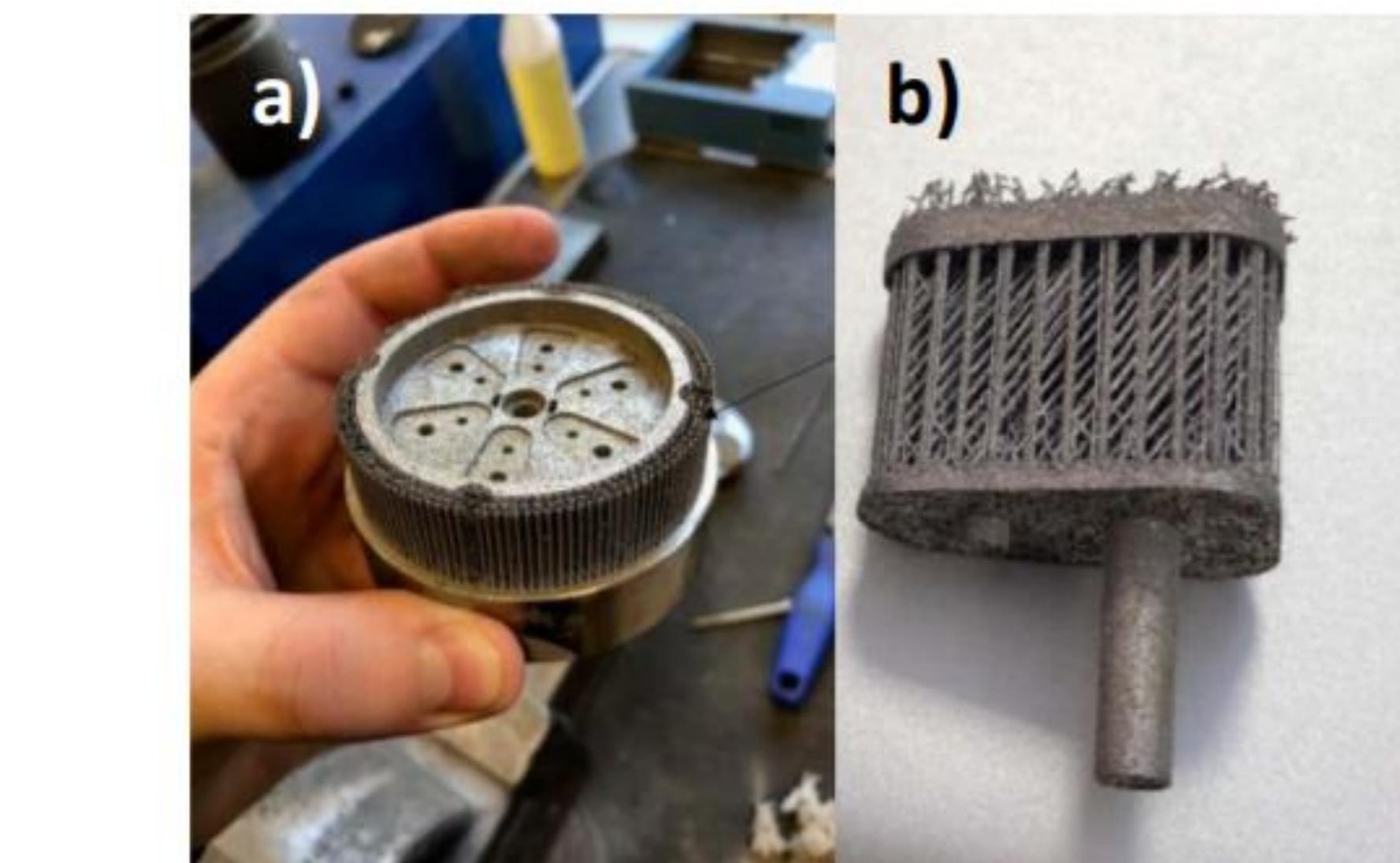


Fig. 1. Common defect of additive manufacturing cracks (a) and supports (b) for printing.

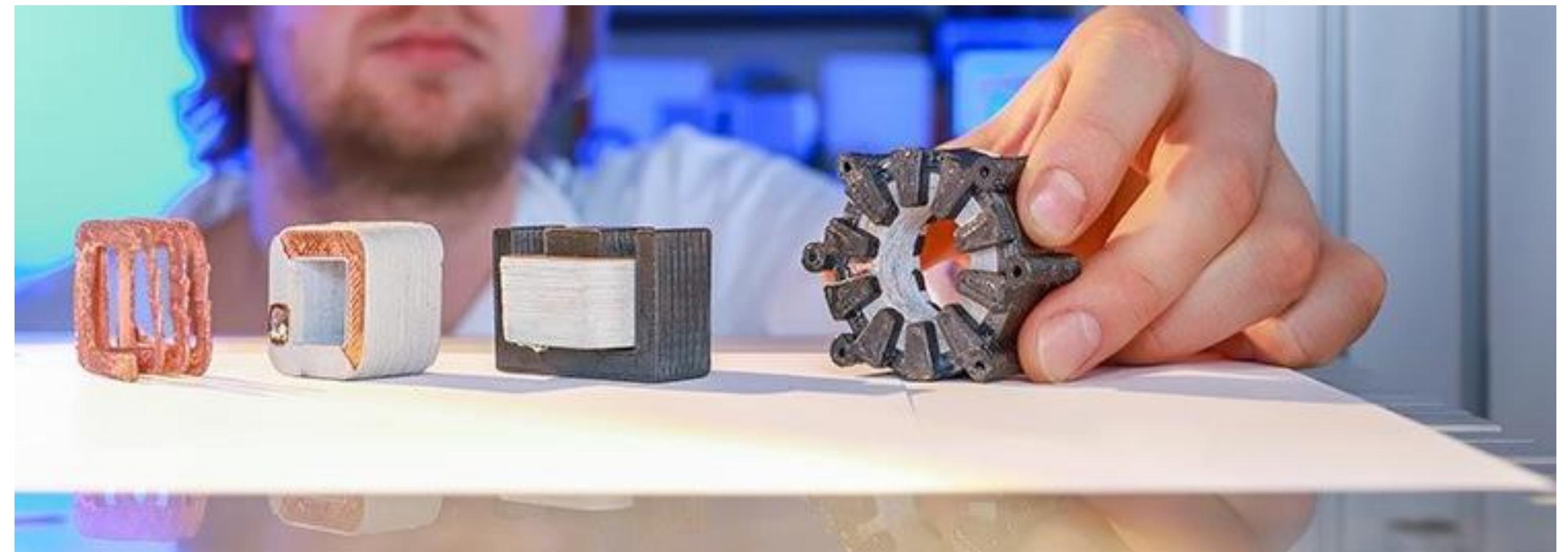


A. Rassõlkin, A. Kallaste, T. Vaimann and H. Tiismus, "Control Challenges of 3D Printed Switched Reluctance Motor," 2019 26th International Workshop on Electric Drives: Improvement in Efficiency of Electric Drives (IWED), 2019, pp. 1-5, doi: 10.1109/IWED.2019.8664282.

Аддитивные технологии в производстве электрических машин

Достоинства

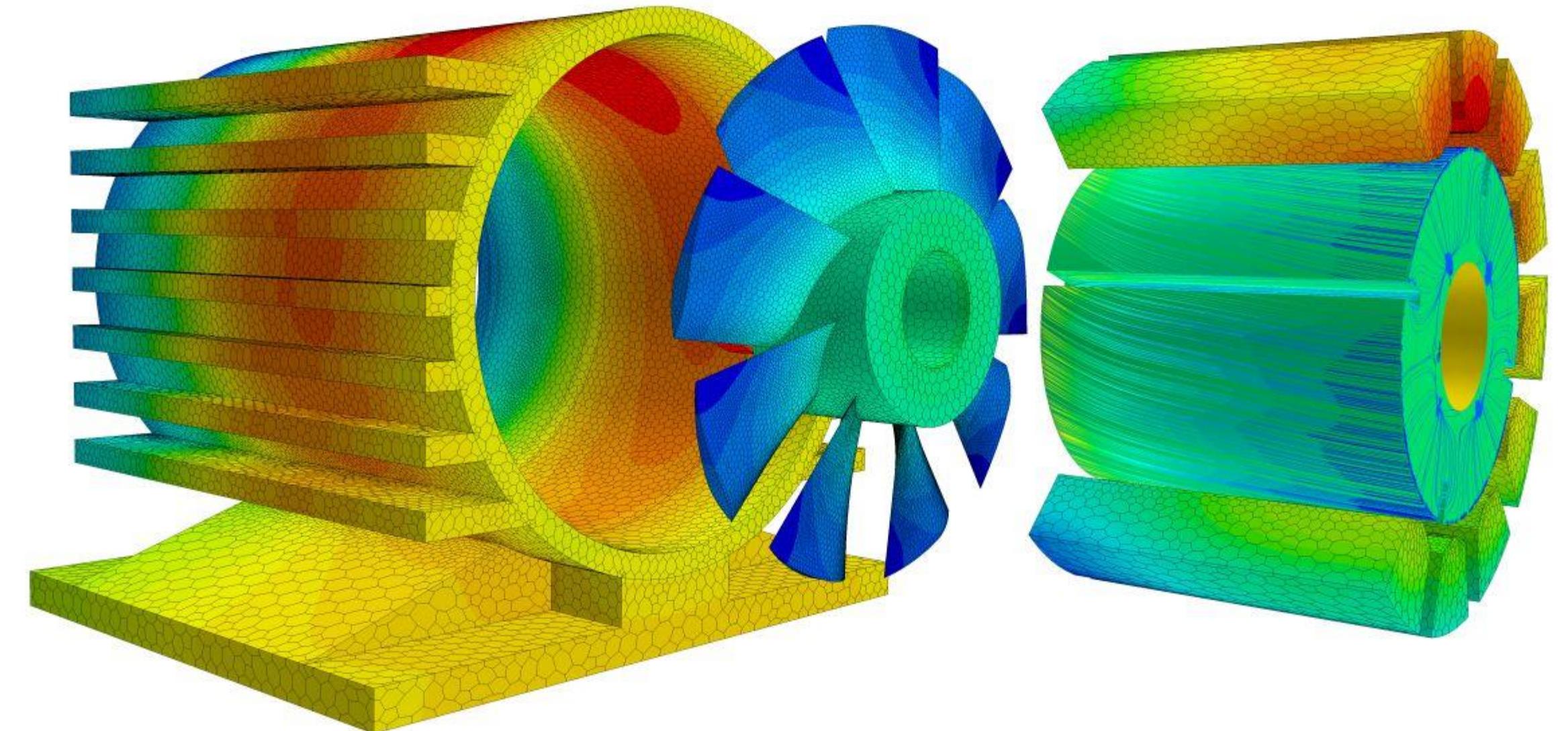
- Индивидуализация
- Свобода дизайна
- Скорость
- Никаких инструментов и форм не требуется



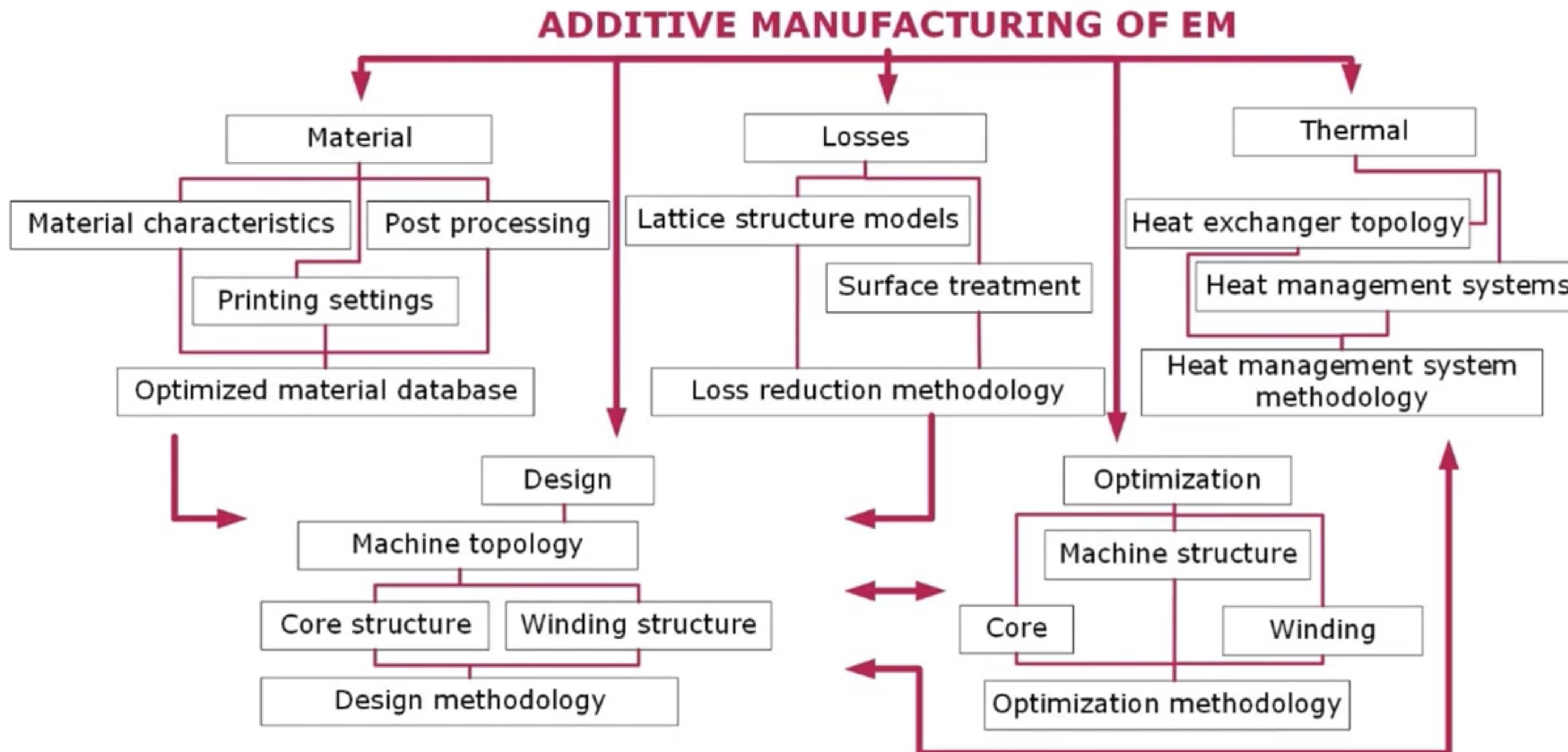
Аддитивные технологии в производстве электрических машин

Недостатки

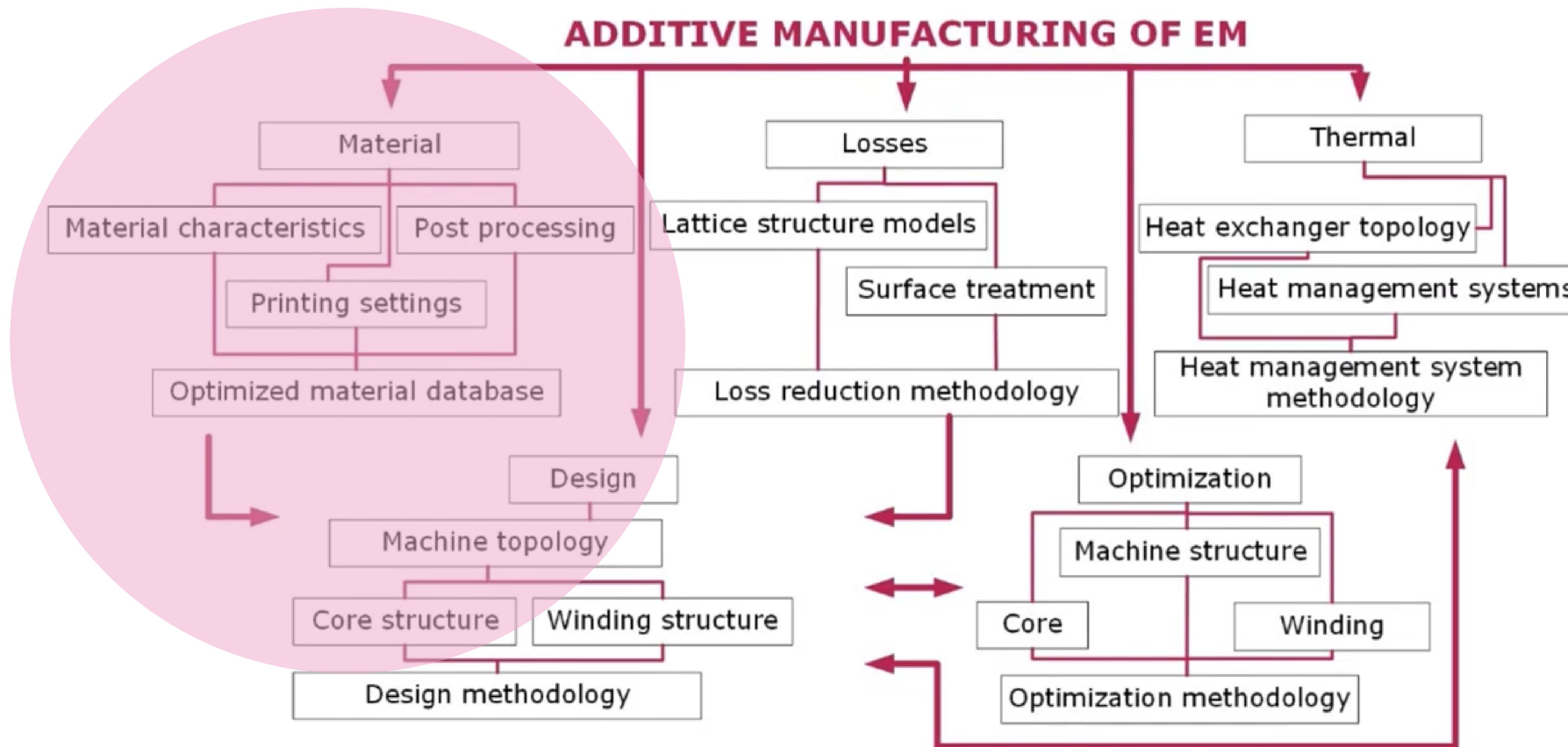
- Неизбежность доработки
- Невозможность промышленного массового производства
- Ограниченные возможности работы с некоторыми материалами



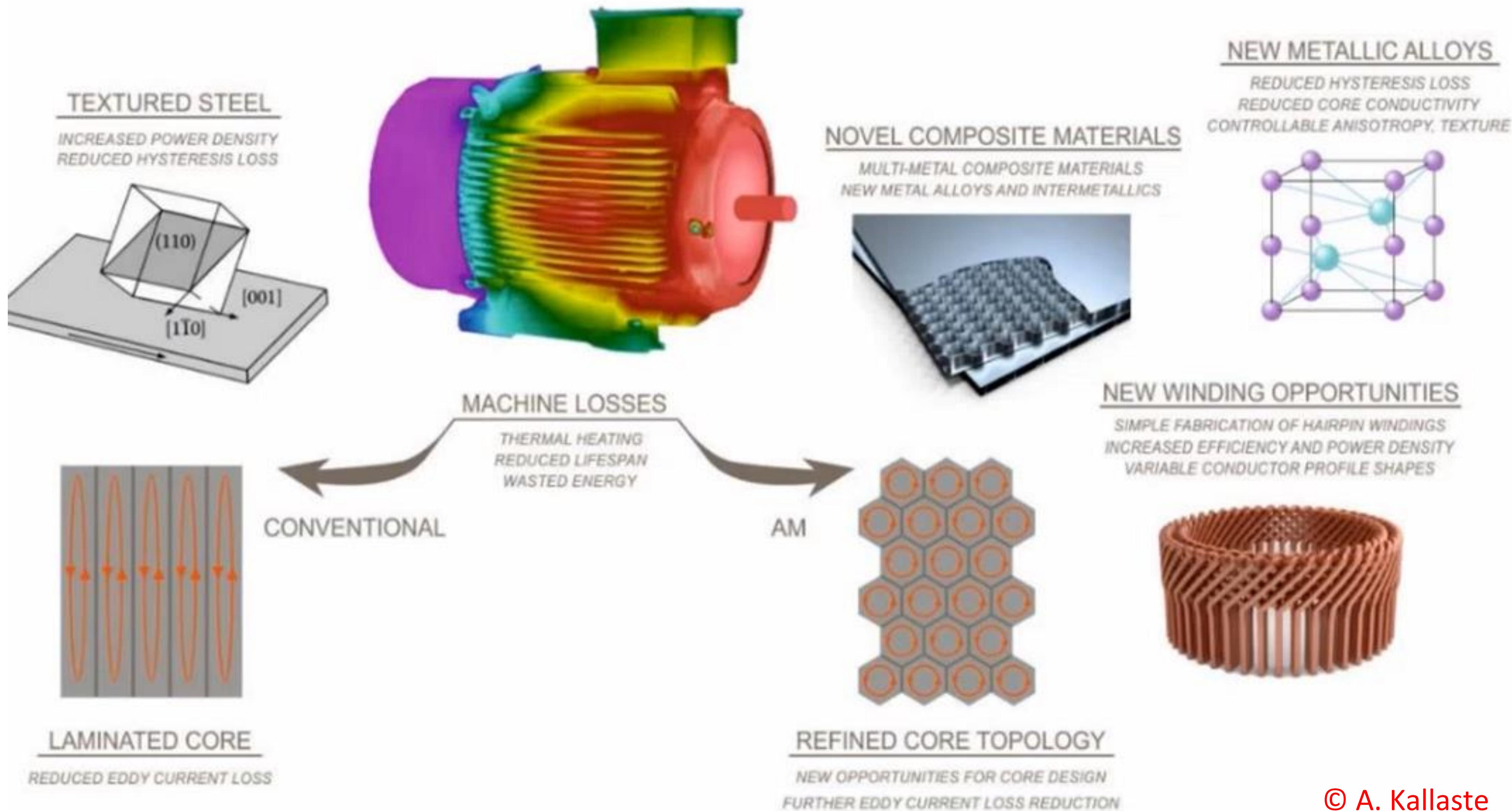
Аддитивные технологии в производстве электрических машин



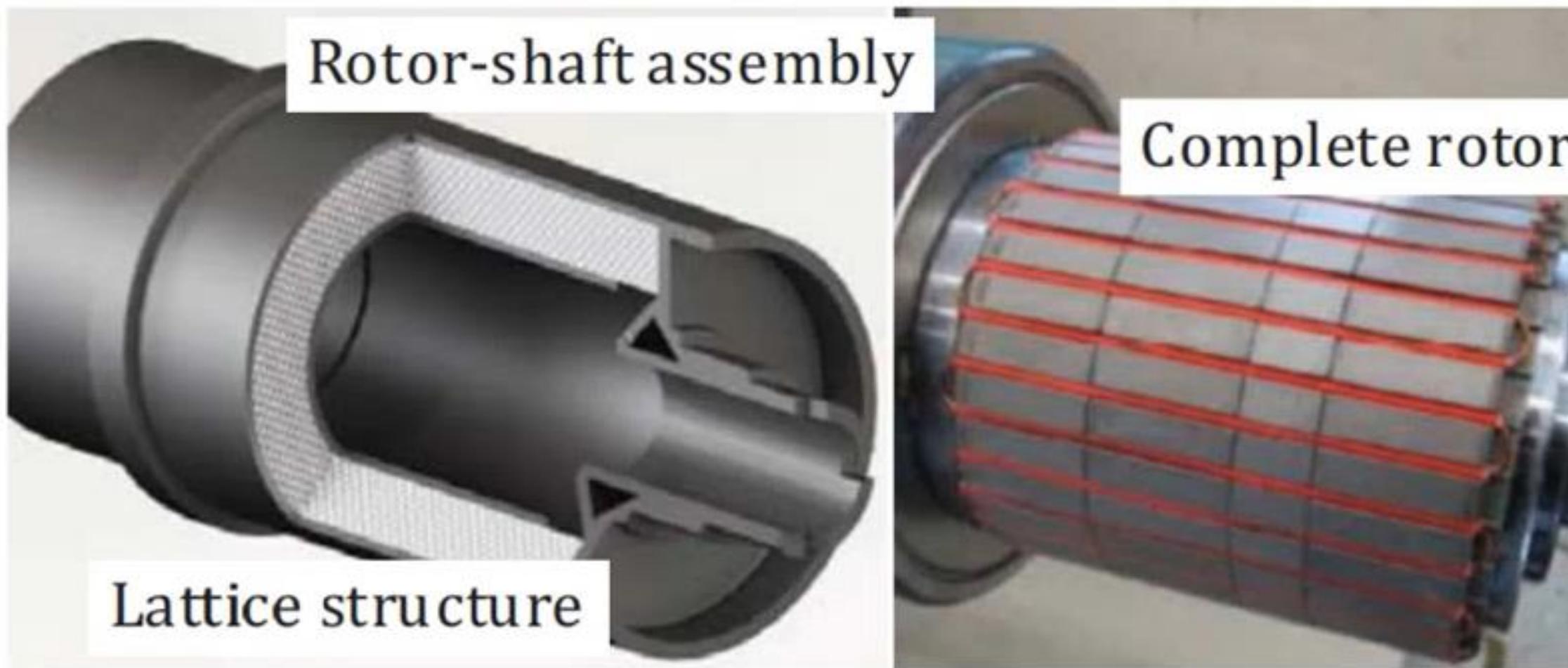
Аддитивные технологии в производстве электрических машин



Аддитивные технологии в производстве электрических машин



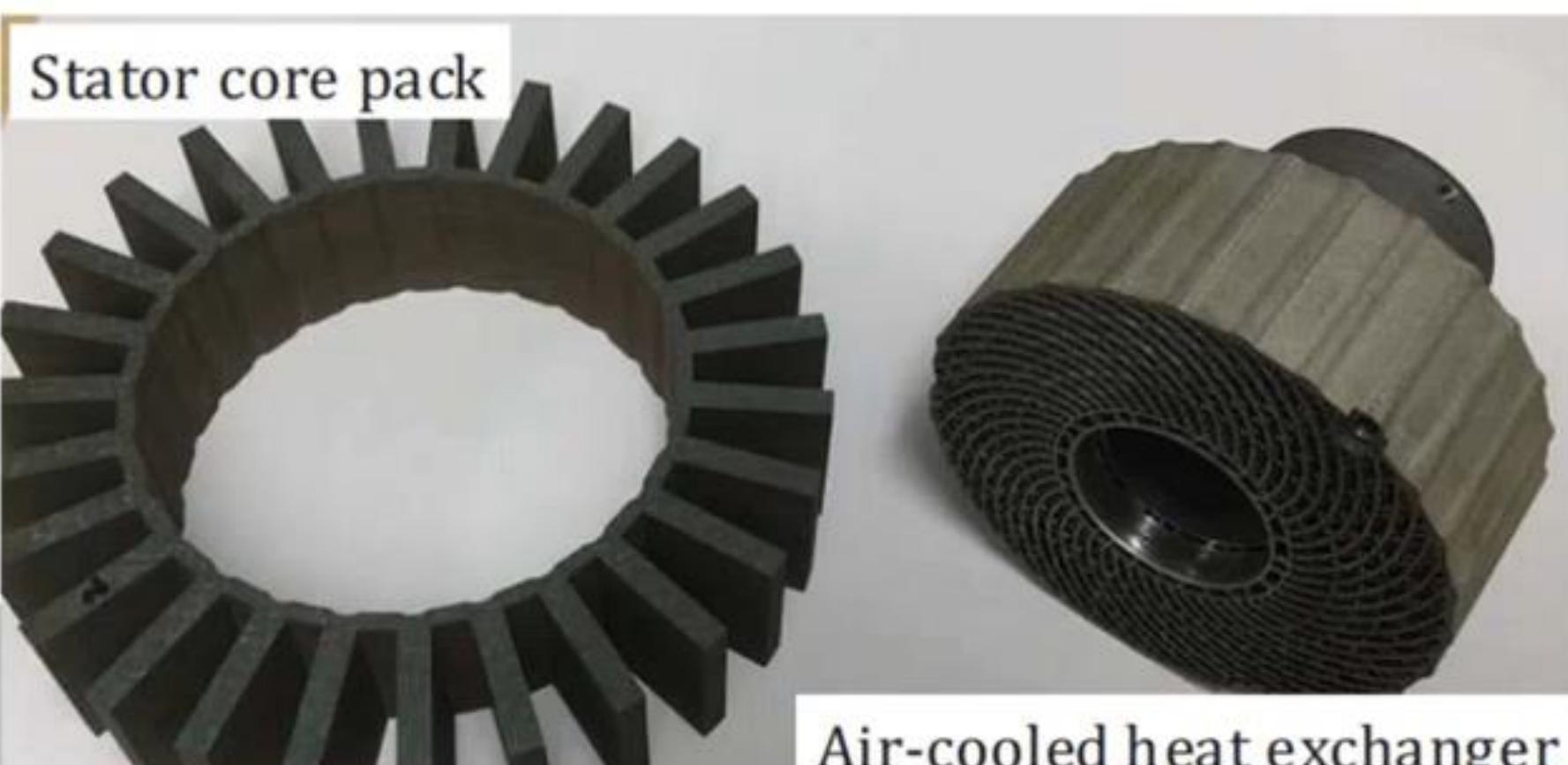
Разработчики - Аддитивные технологии в производстве электрических машин



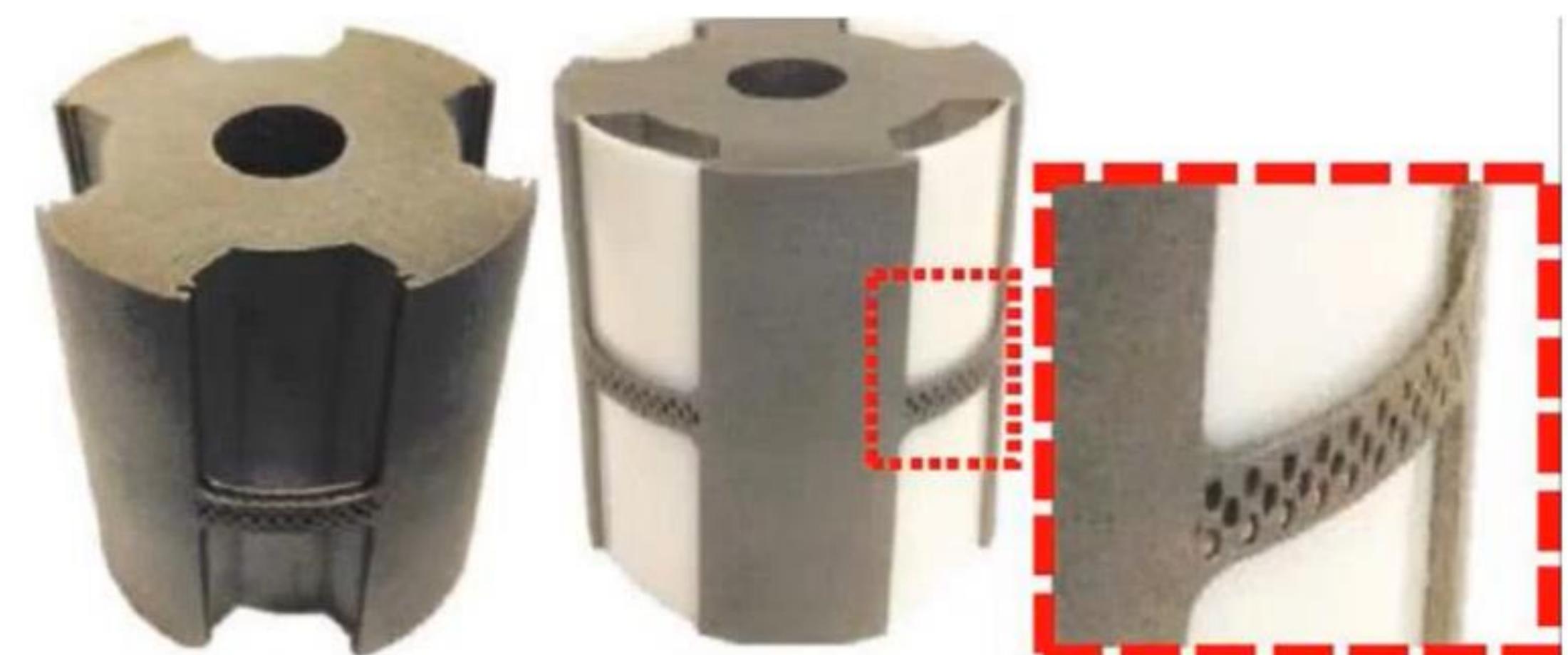
Paderborn University, Karlsruhe Institute for Technology and Leibniz University Hannover



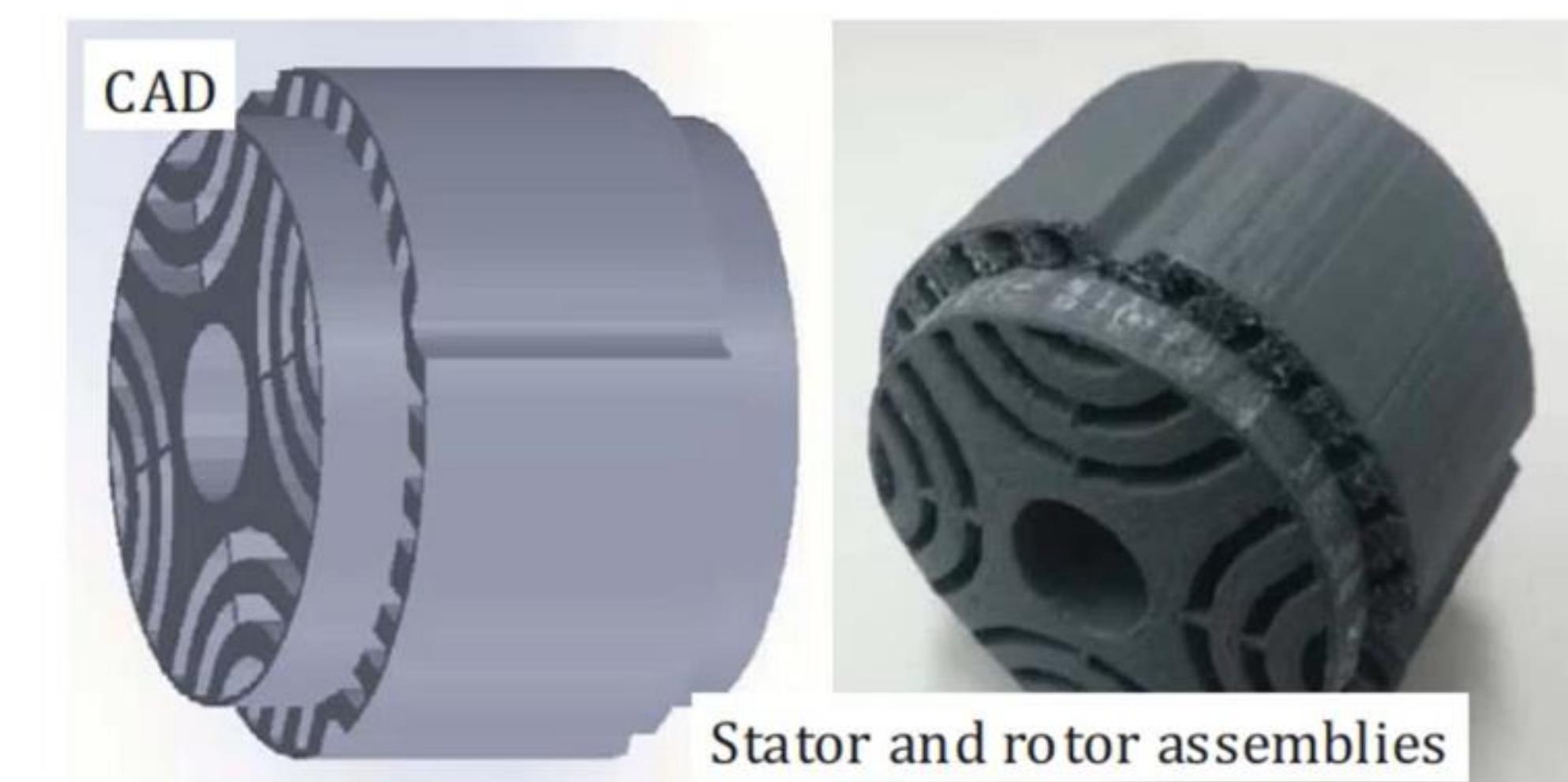
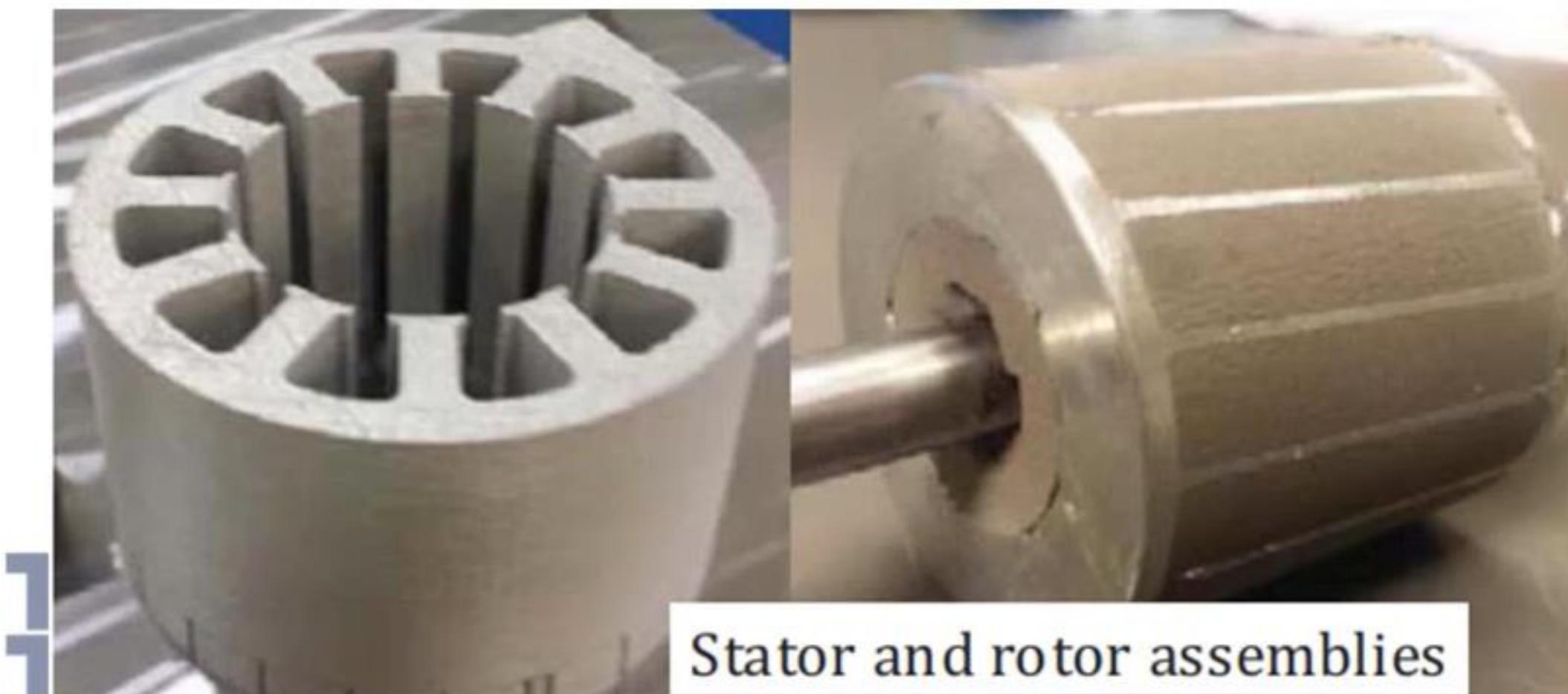
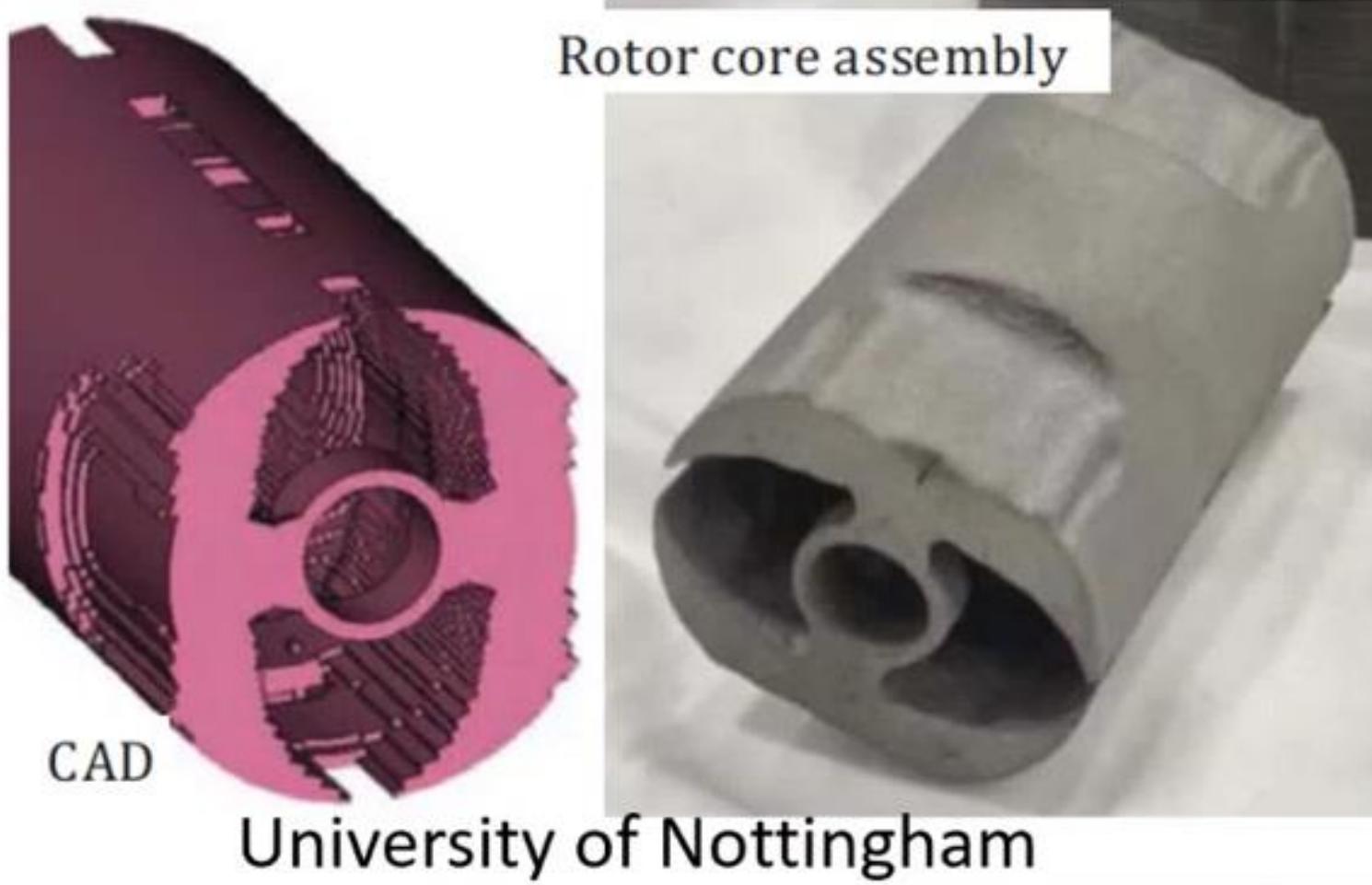
Newcastle University



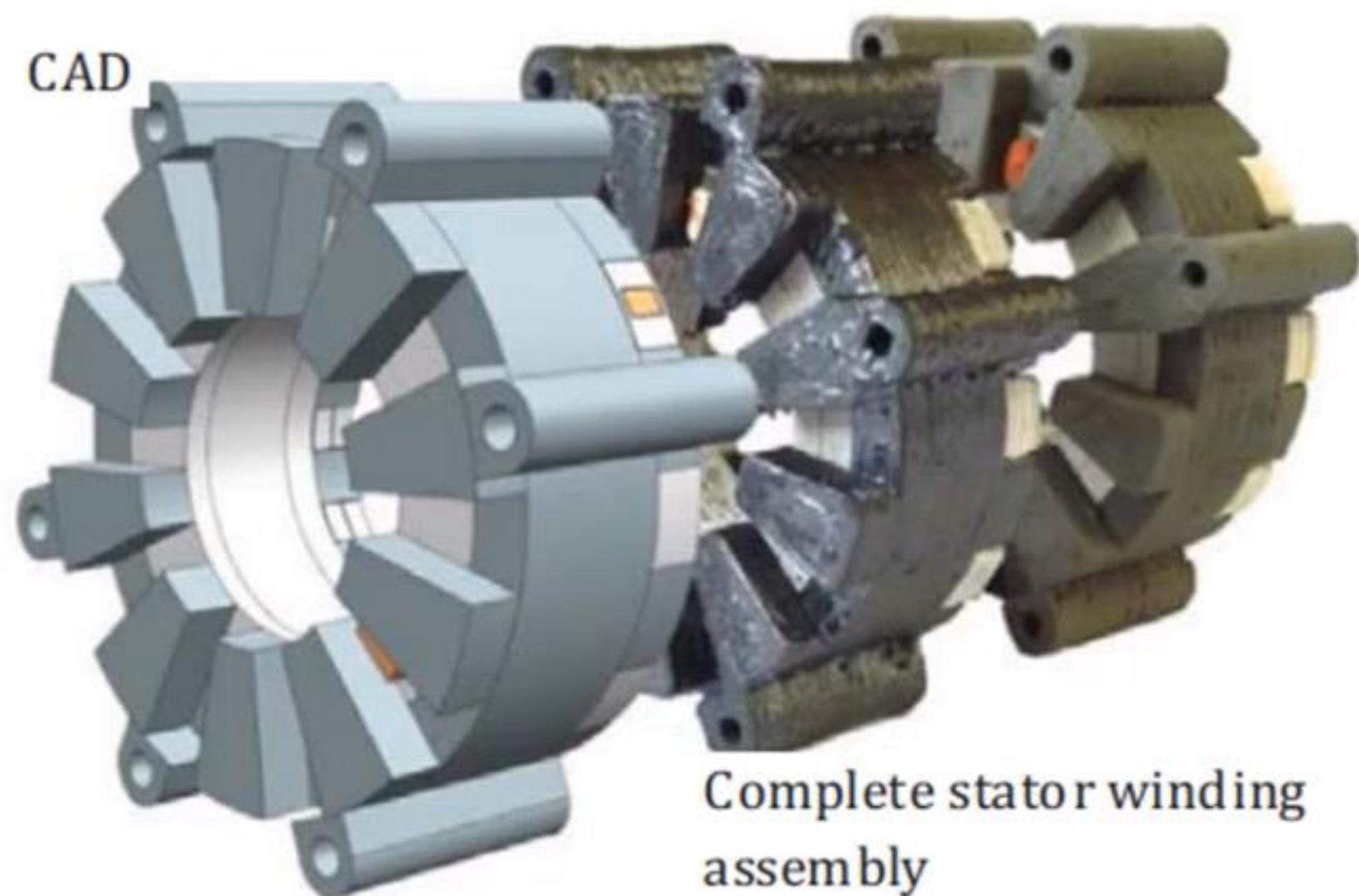
Newcastle University



Разработчики - Аддитивные технологии в производстве электрических машин



Разработчики - Аддитивные технологии в производстве электрических машин



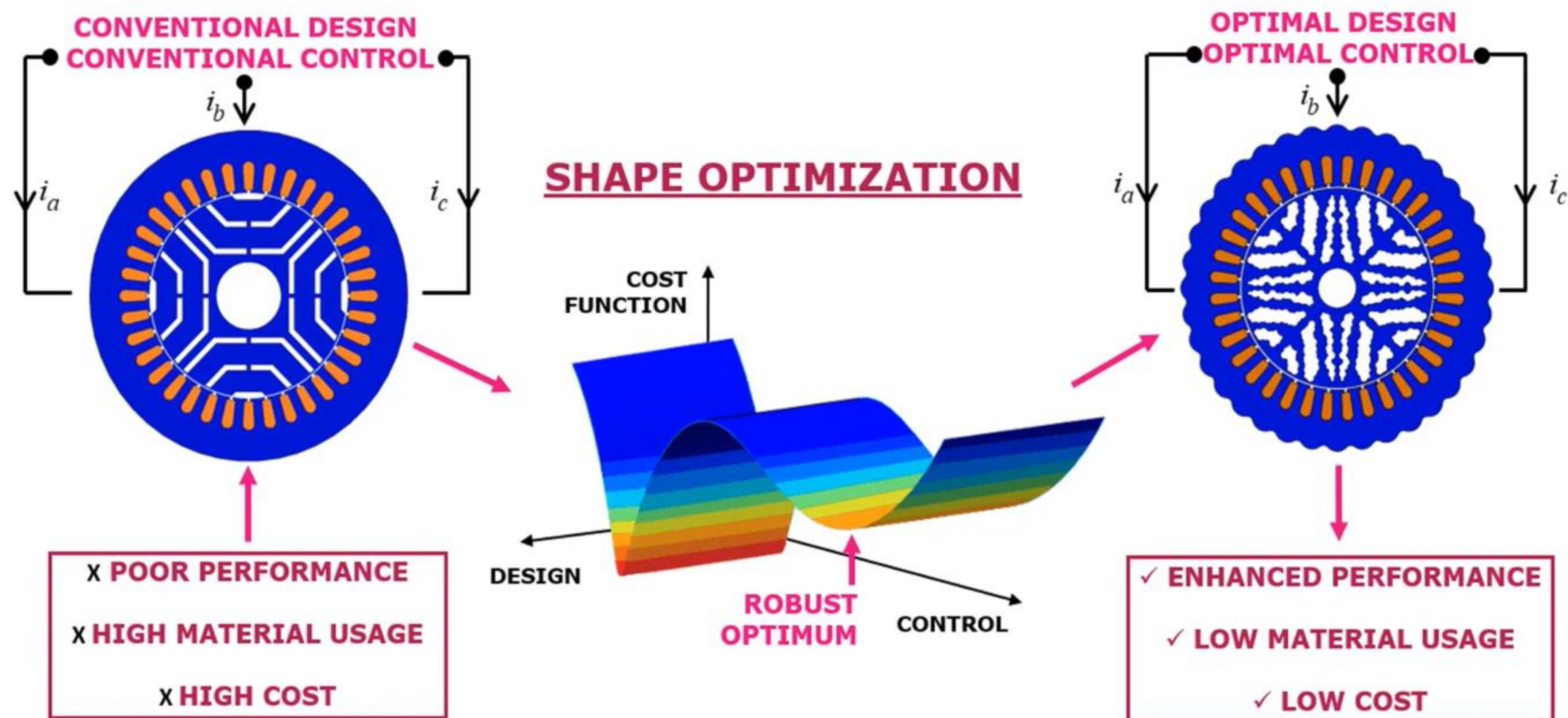
Chemnitz University of Technology



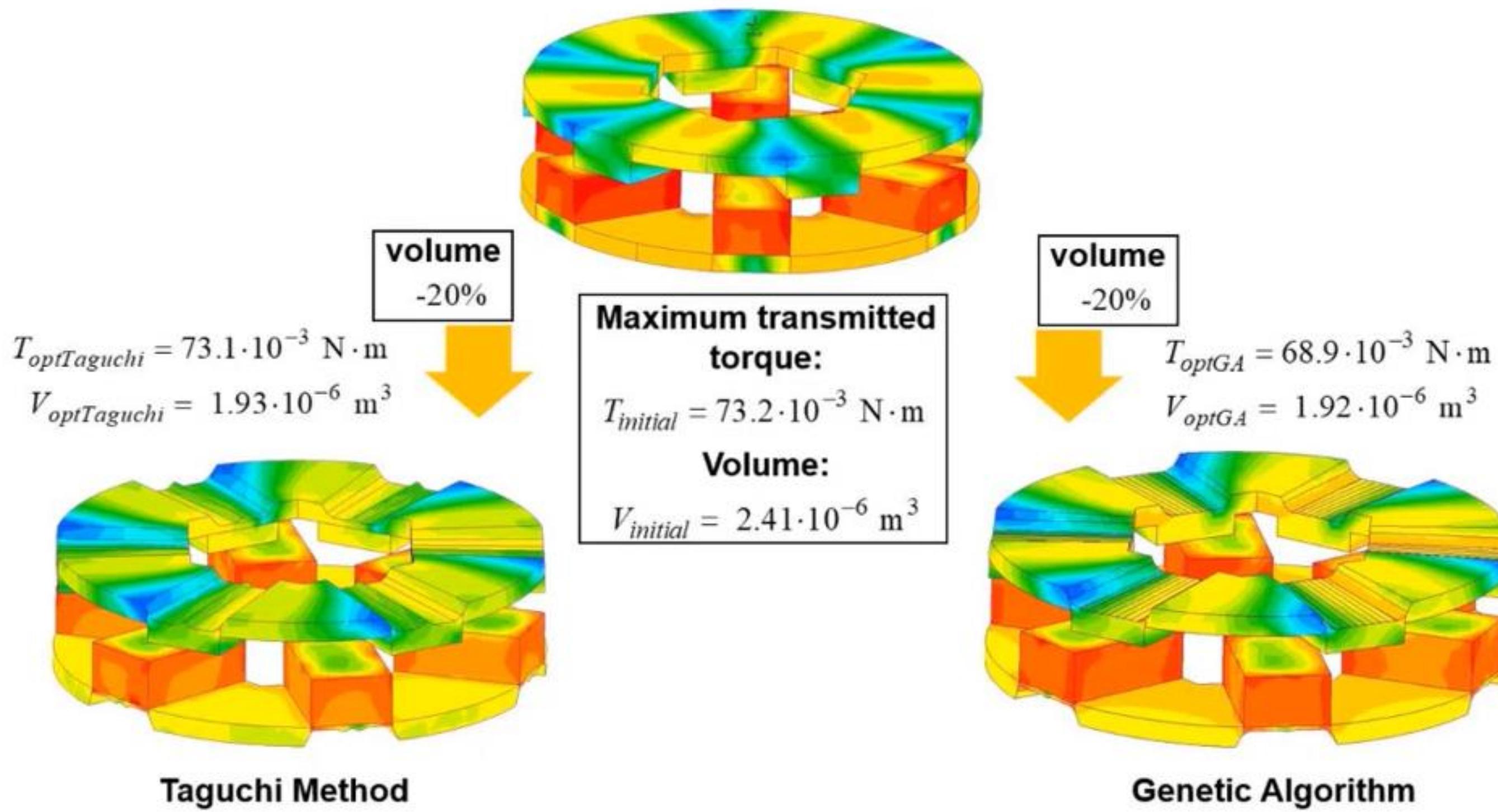
Persimmon Technologies Corporation



Оптимизация электрических машин



Оптимизация электрических машин



Periodica Polytechnica Electrical Engineering and Computer Science

Design Optimization of Permanent Magnet Clutch with Ārtap Framework

Ekaterina Andriushchenko^{1*}, Jan Kaska², Ants Kallaste¹, Anouar Belahcen³, Toomas Vaimann¹, Anton Rassõlkin¹

¹ Department of Electrical Power Engineering and Mechatronics, School of Engineering, Tallinn University of Technology, Ehitajate tee 5, 19086 Tallinn, Estonia

² Department of Electrical and Computational Engineering, Faculty of Electrical Engineering, University of West Bohemia, Univerzitní 2732/8, 301 00 Pilsen, Czech Republic

³ Department of Electrical Engineering and Automation, School of Electrical Engineering, Aalto University, Otakaari 1B, 02150 Espoo, Finland

* Corresponding author, e-mail: ekandr@taltech.ee

Received: 09 August 2020, Accepted: 14 September 2020, Published online: 09 March 2021

Abstract

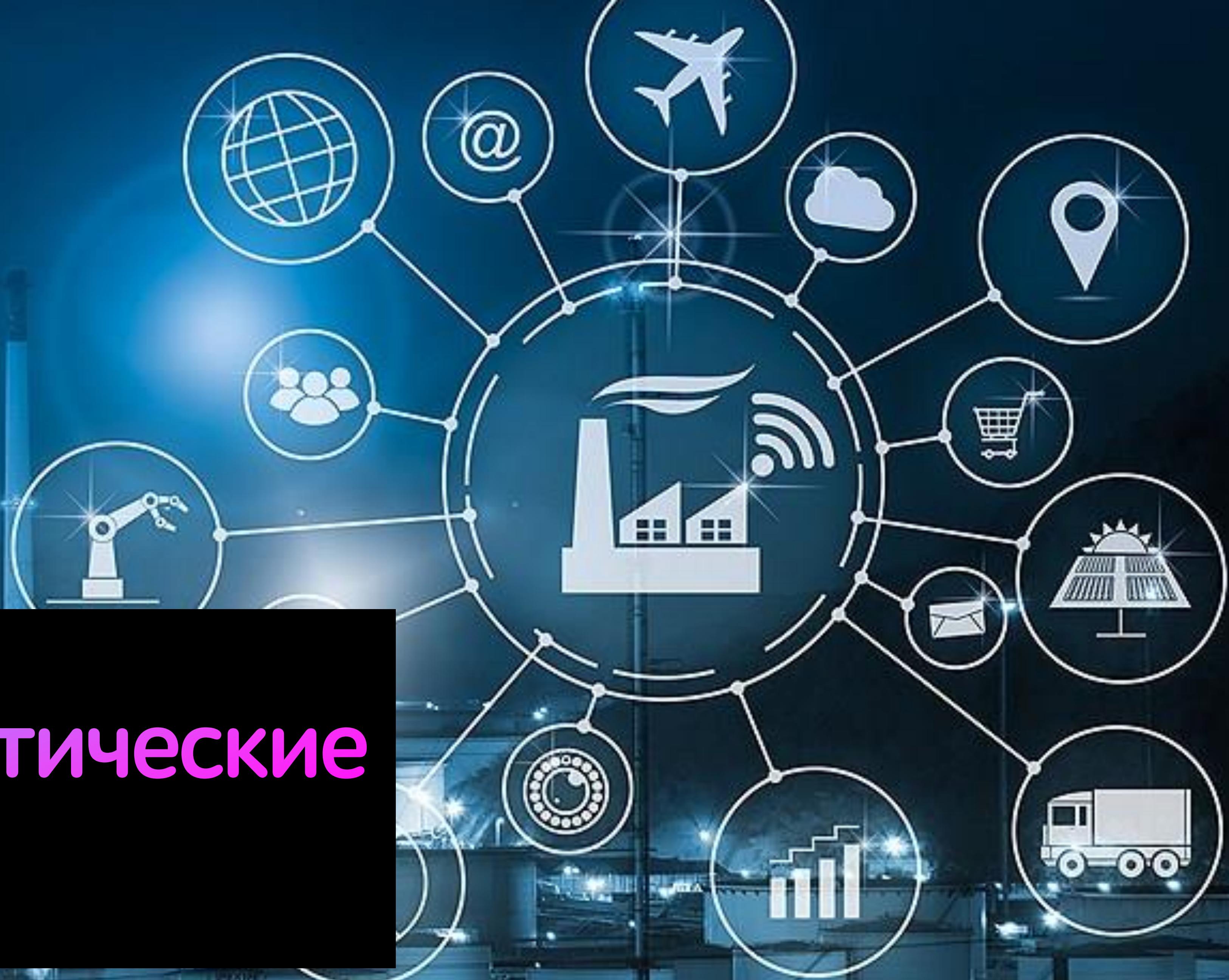
So far, Permanent Magnet (PM) clutches have been broadly used as torque transmission devices. With the aim of effective utilization of materials and energy in the manufacturing of PM clutches, design optimization has been widely applied. Generally, PM clutches are

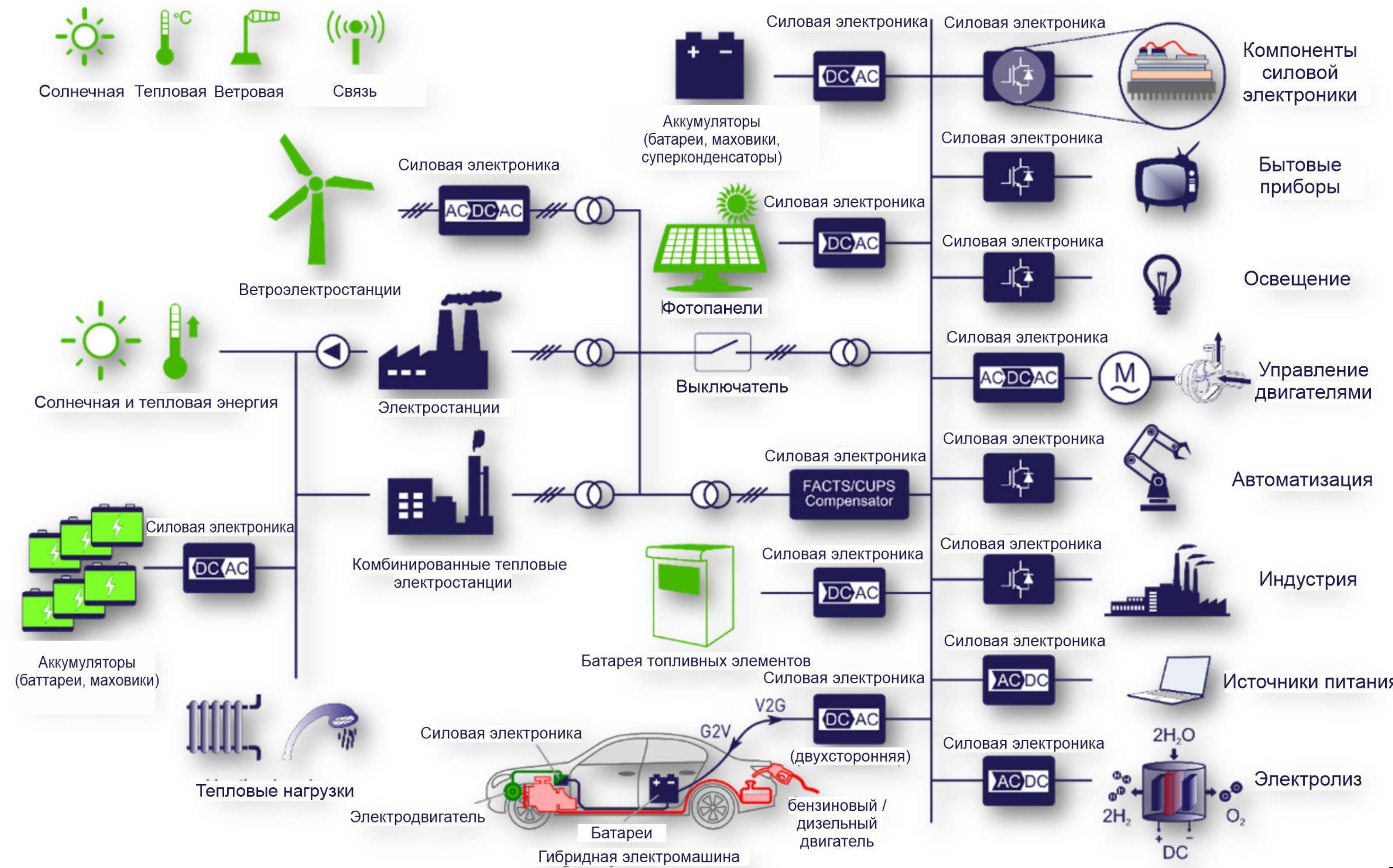


Andriushchenko, E. A., Kallaste, A., Belahcen, A., Heidari, H., Vaimann, T., & Rassõlkin, A. (2020). Design optimization of permanent magnet clutch. In Proceedings of the International Conference on Electrical Machines, ICEM 2020 (pp. 436-440). [9270726] (Proceedings (International Conference on Electrical Machines)). IEEE. <https://doi.org/10.1109/ICEM49940.2020.9270726>

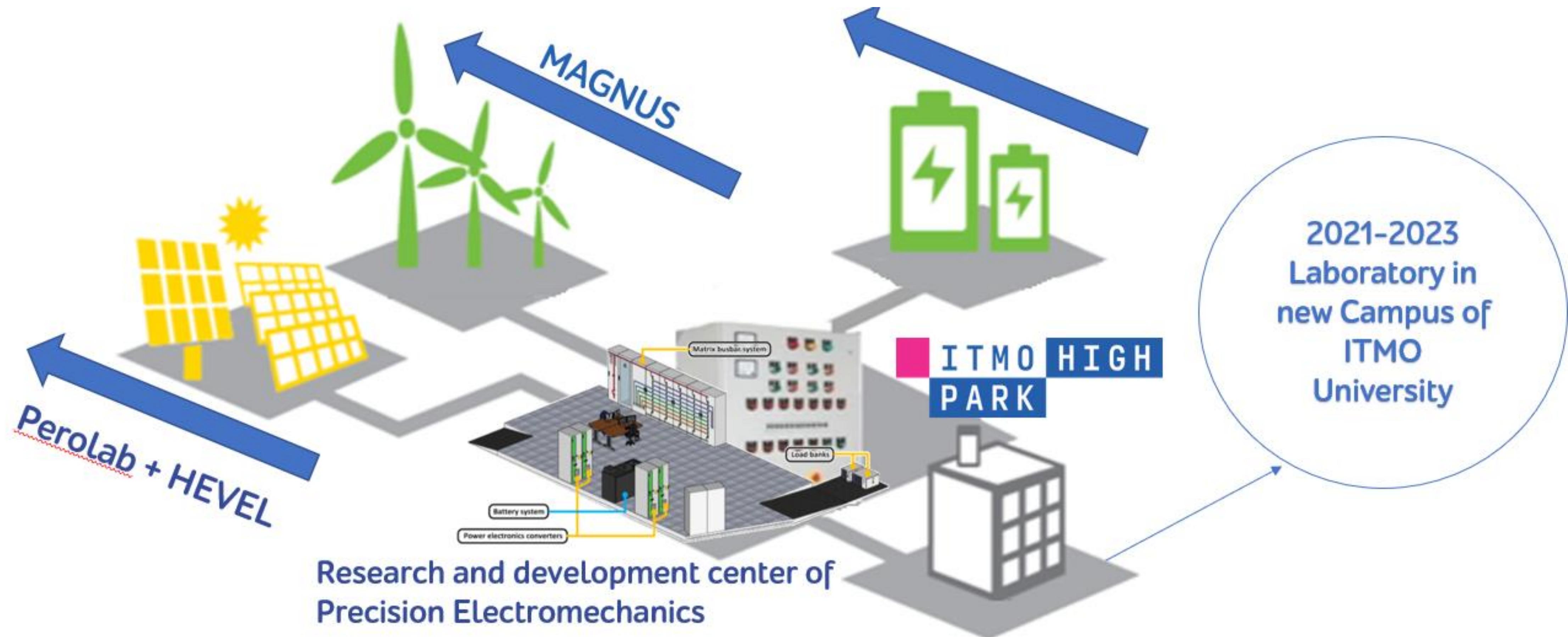
**TAL
TECH**

Электроэнергетические системы



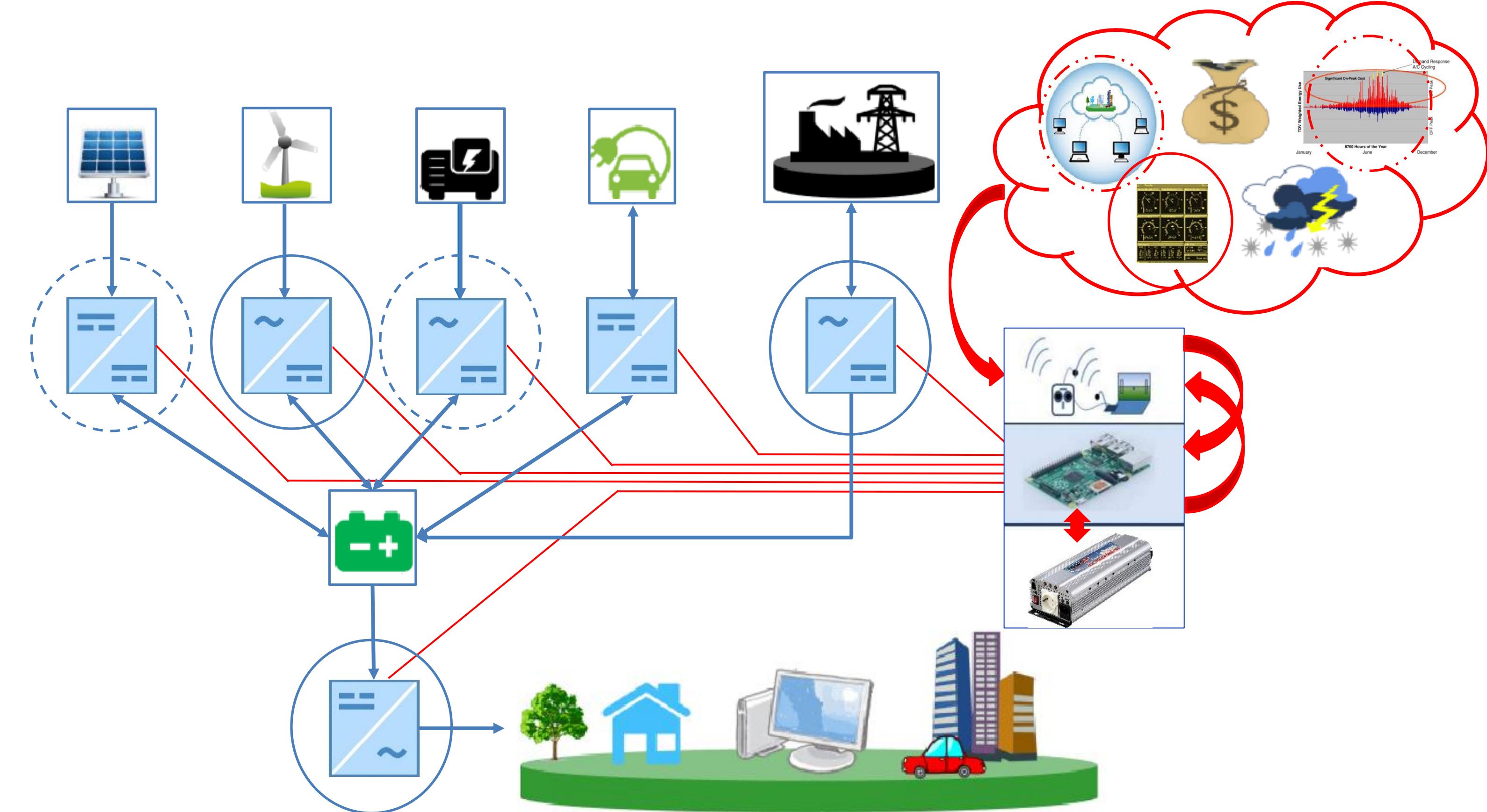


Проектирование современных энергетических систем

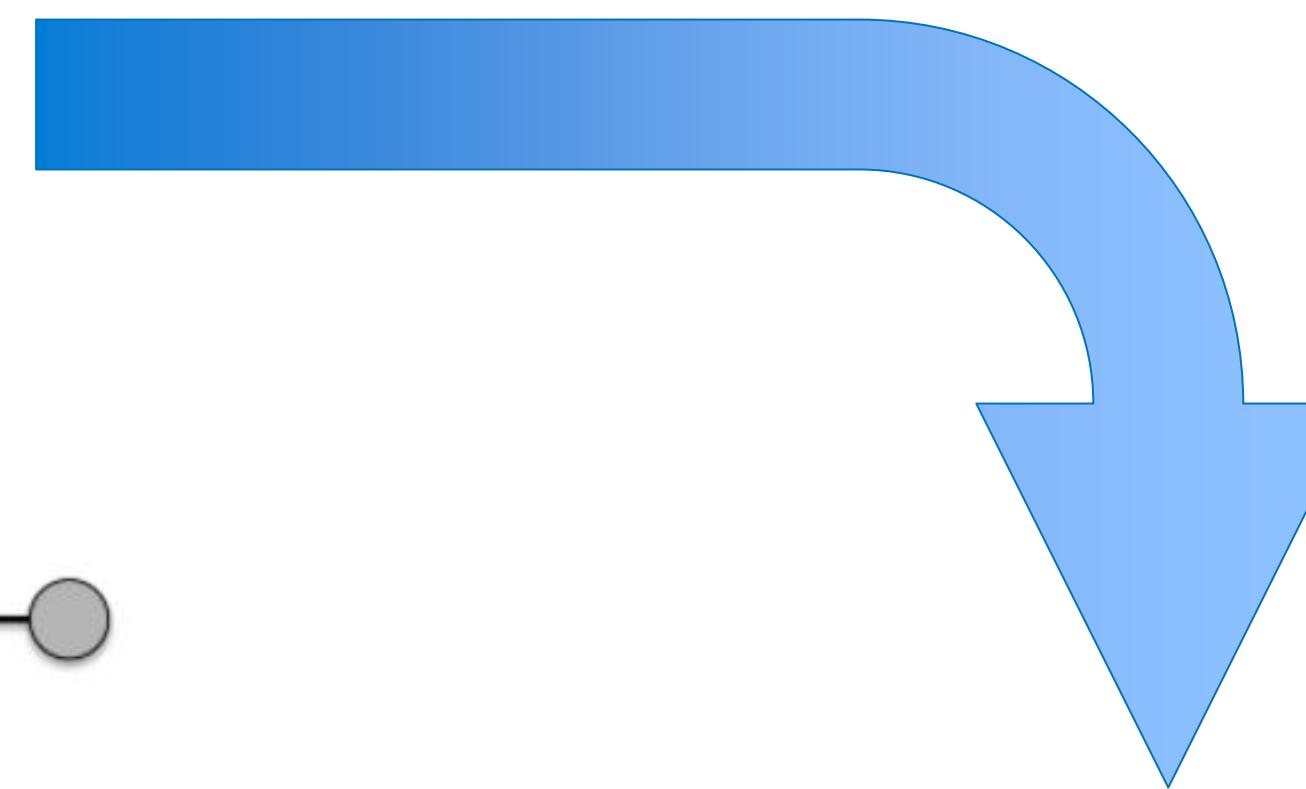
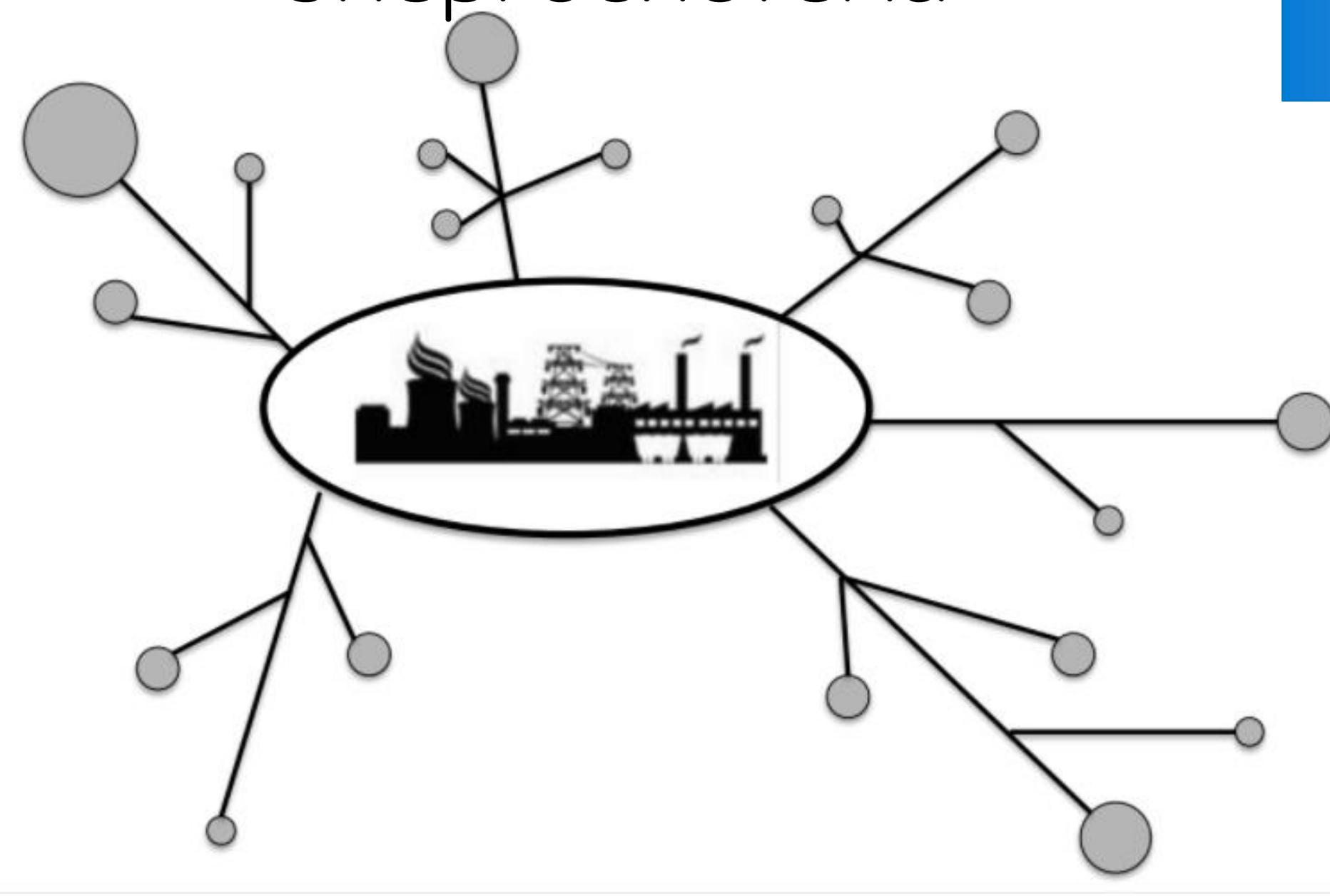


Проектирование современных энергетических систем

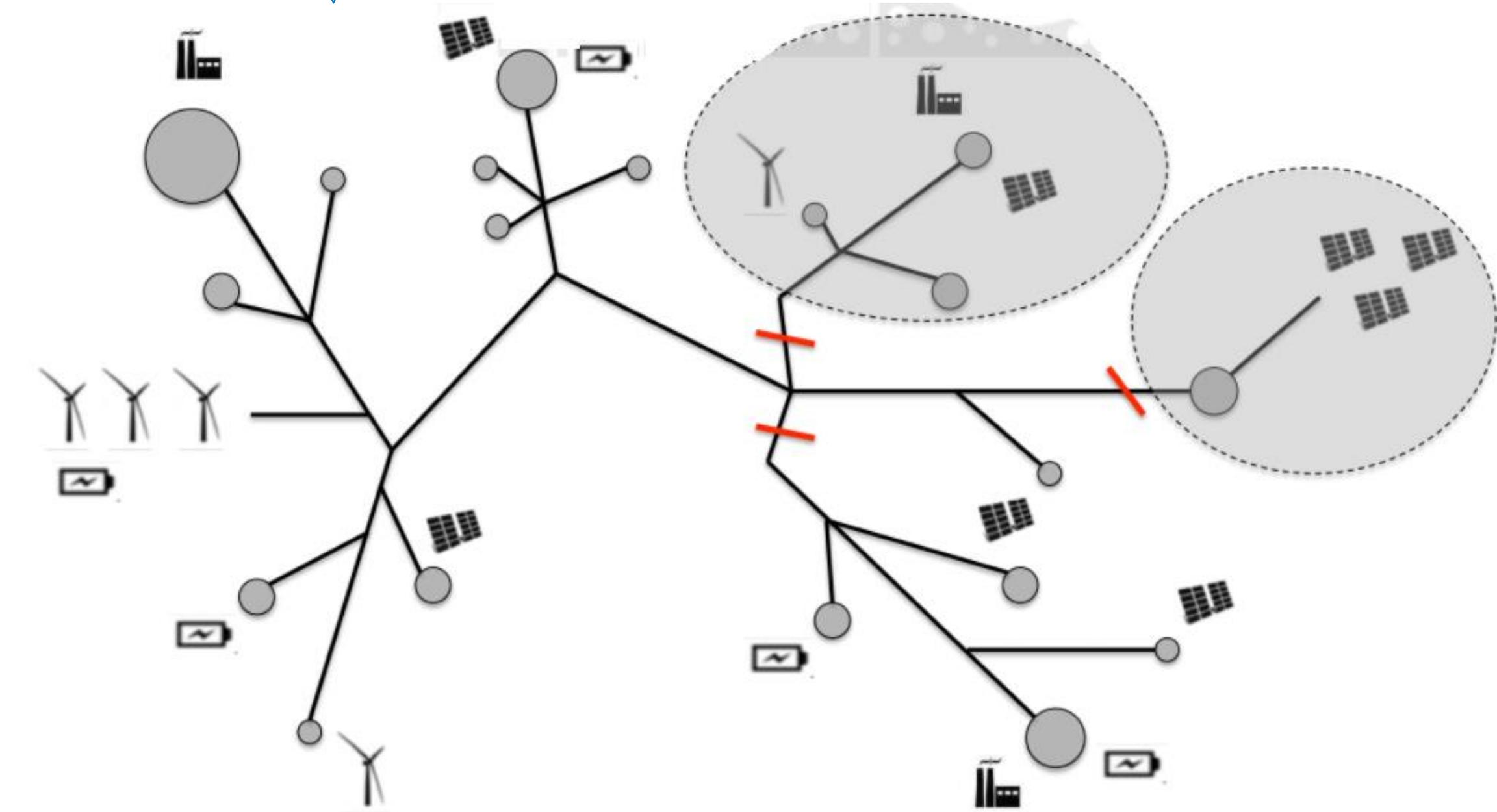
- Предотвращение сбоя в электроснабжении.
- Кастомизация параметров электроснабжения потребителей
- Управление спросом и поставка электроэнергии в сеть
- Интеграция распределенных энергетических ресурсов.



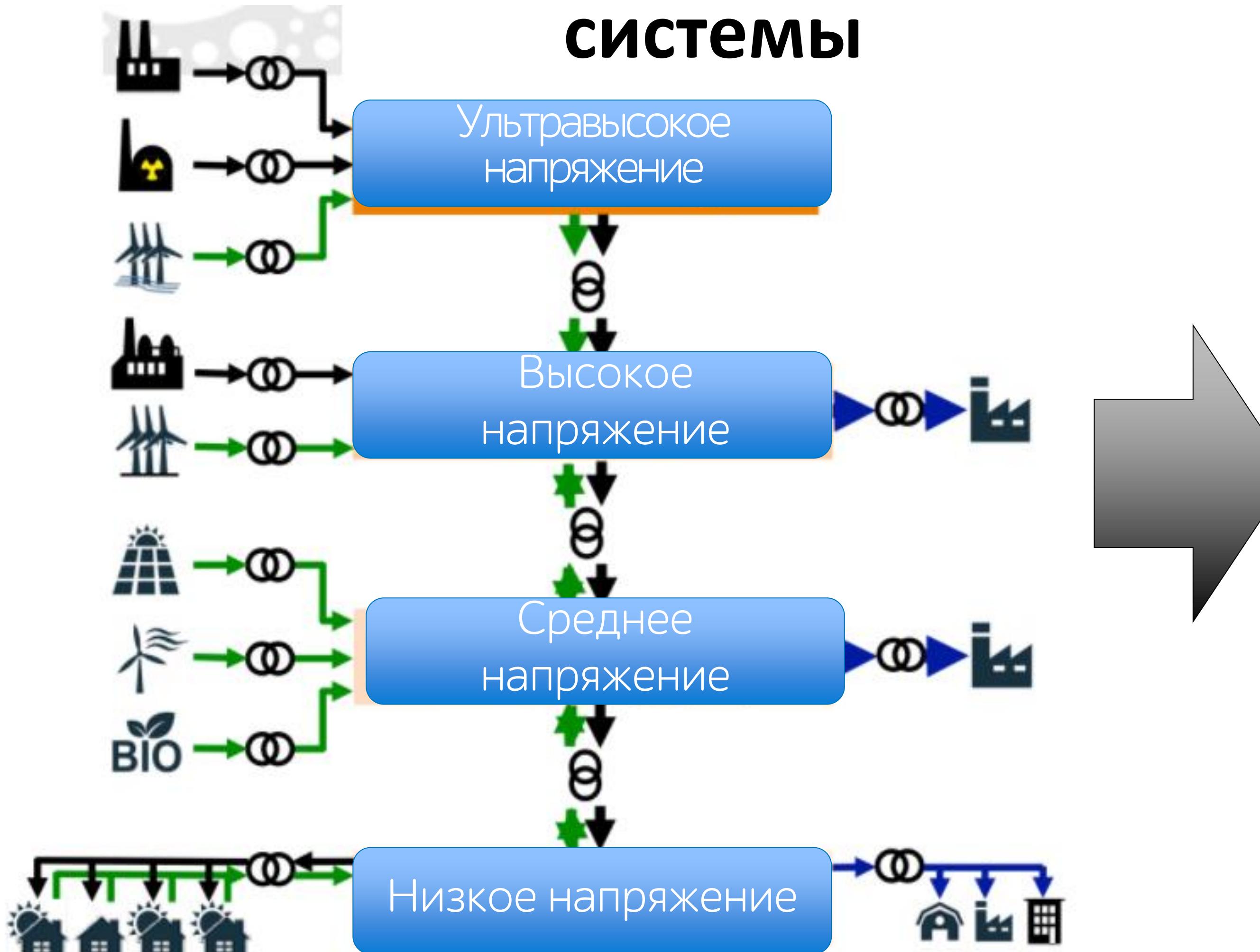
Традиционная
энергосистема



Распределенная
электроэнергетическая
система



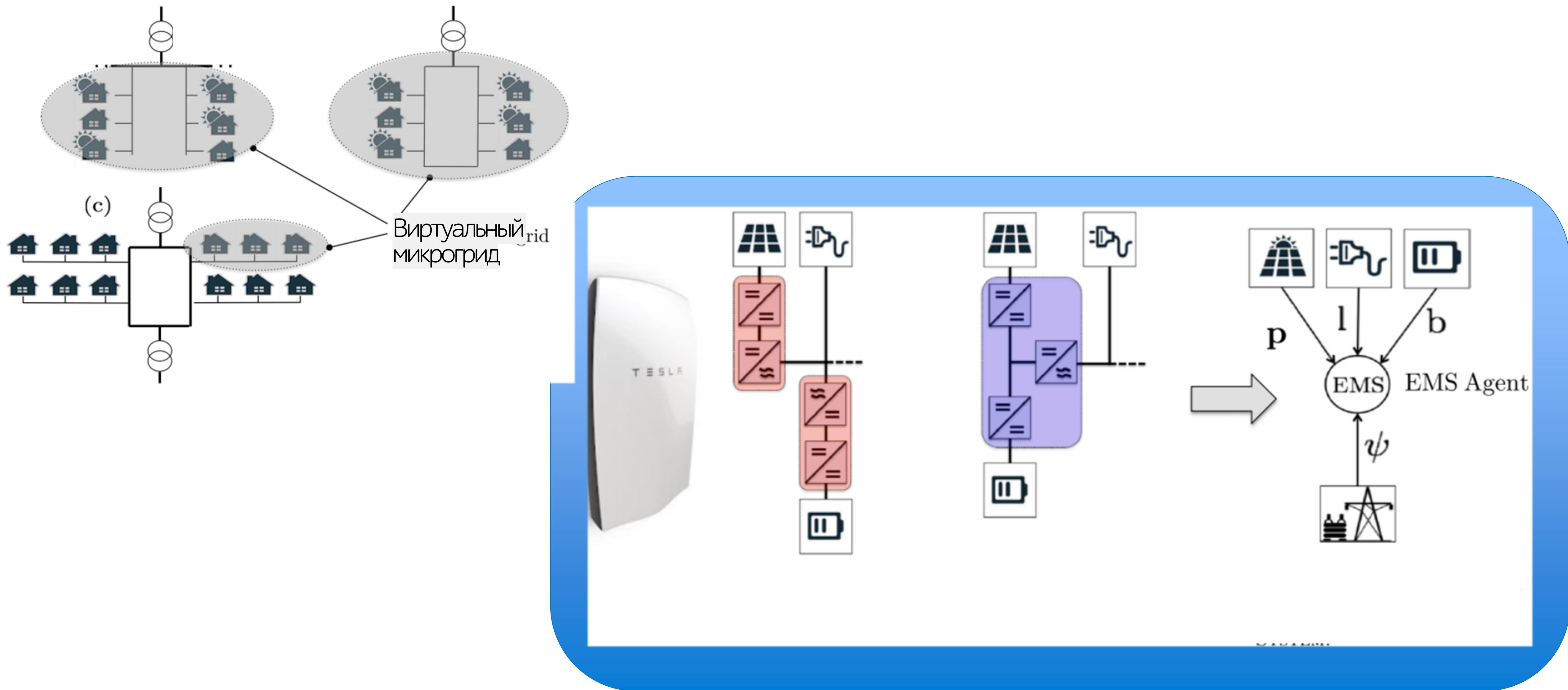
Распределенные электроэнергетические системы



Recent Facts about Photovoltaics in Germany, Harry Wirth, Fraunhofer ISE,
download from <https://www.ise.fraunhofer.de/en/publications/studies/recent-factsabout-pv-in-germany.html>, version of May 15, 2021

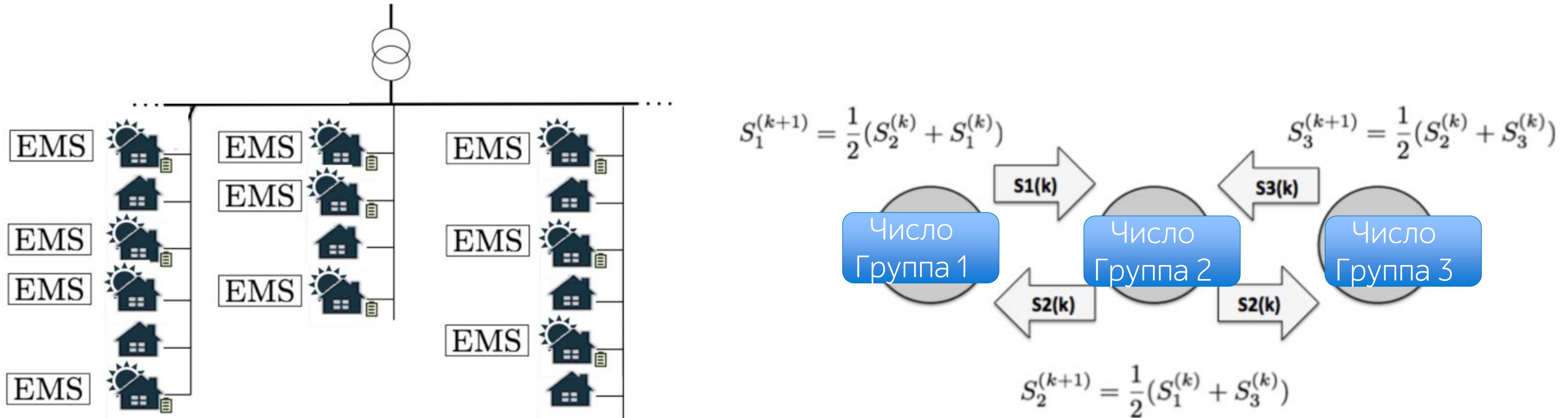
Фреймворк «Архитектура Интернета энергии. Версия 2.0»
(<https://drive.google.com/file/d/13JM0NIY4jUXOP6Mv4irjb2k77bK60p-Q/view>)

Распределенные электроэнергетические системы



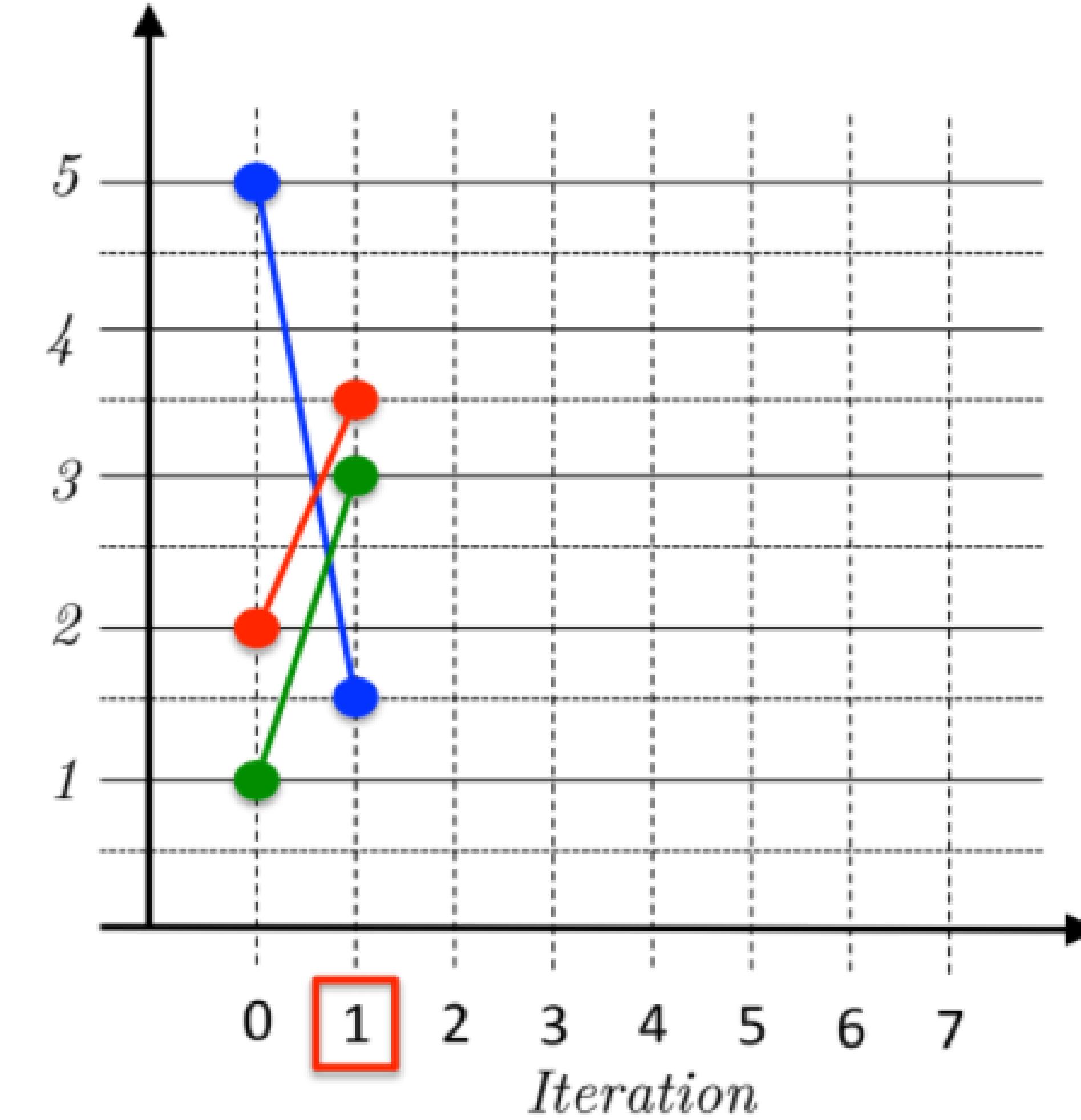
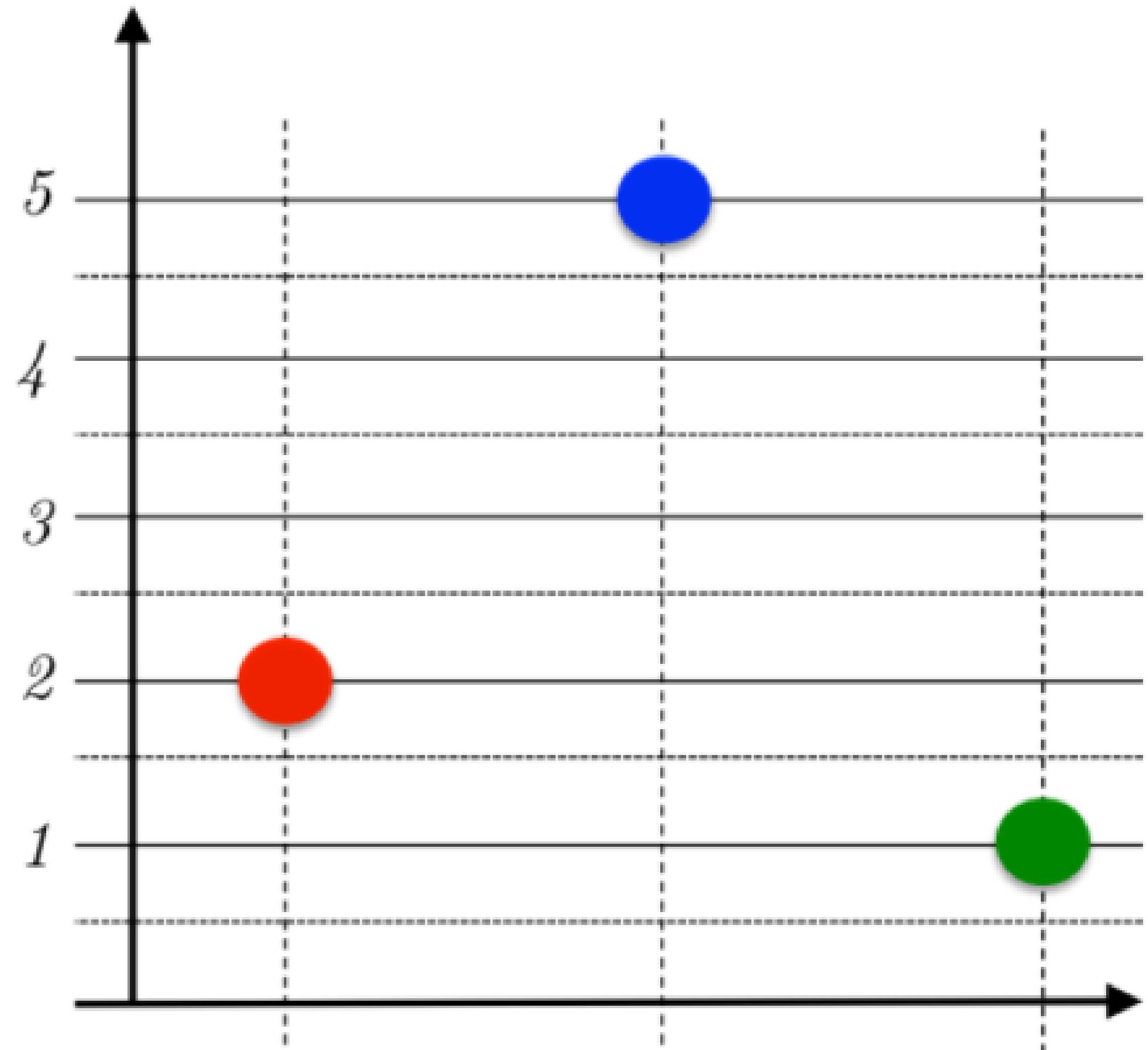
¹ Hollinger, R., Wille-Haussmann, B., Erge, T., Sönnichsen, J., Stillahn, T., and Kreifels, N. (2013). Kurzgutachten zur Abschätzung und einordnung energiewirtschaftlicher und anderer effekte bei förderung von objektgebundenen elektrochemischen speichern. Fraunhofer Institute for Solar Energy Systems, Freiburg, Germany.

Распределенные электроэнергетические системы

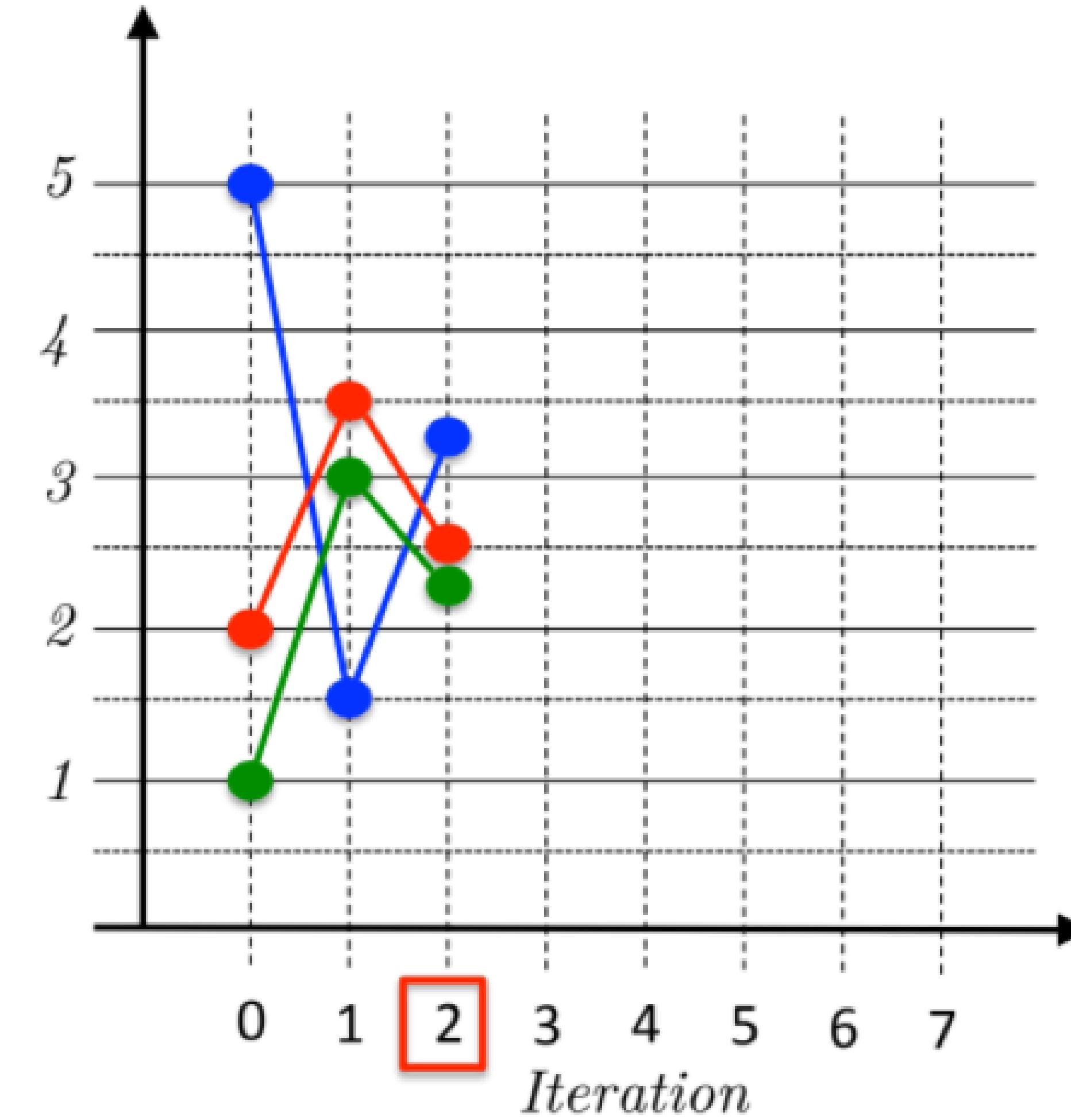
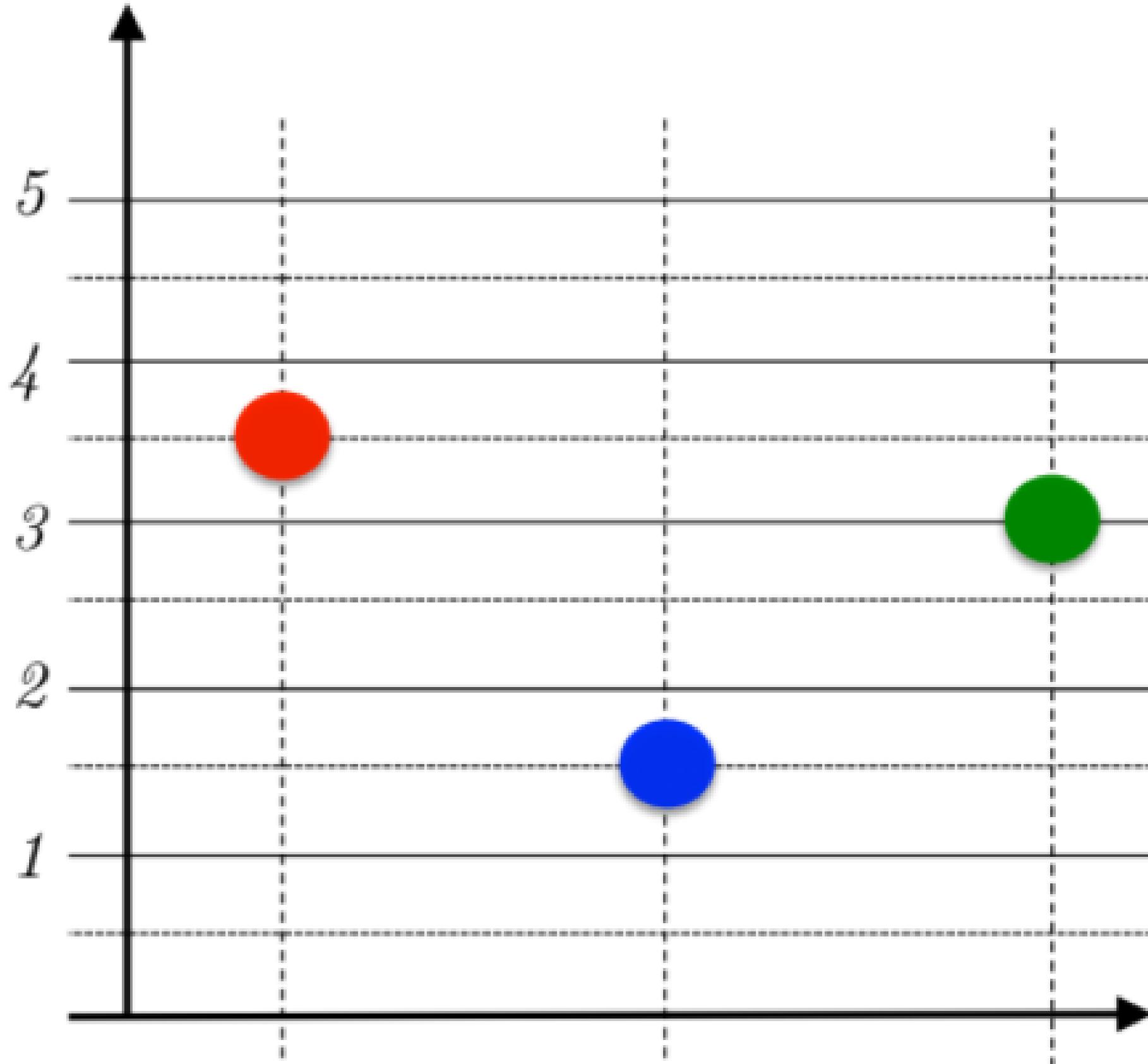


Алгоритм
консенсуса

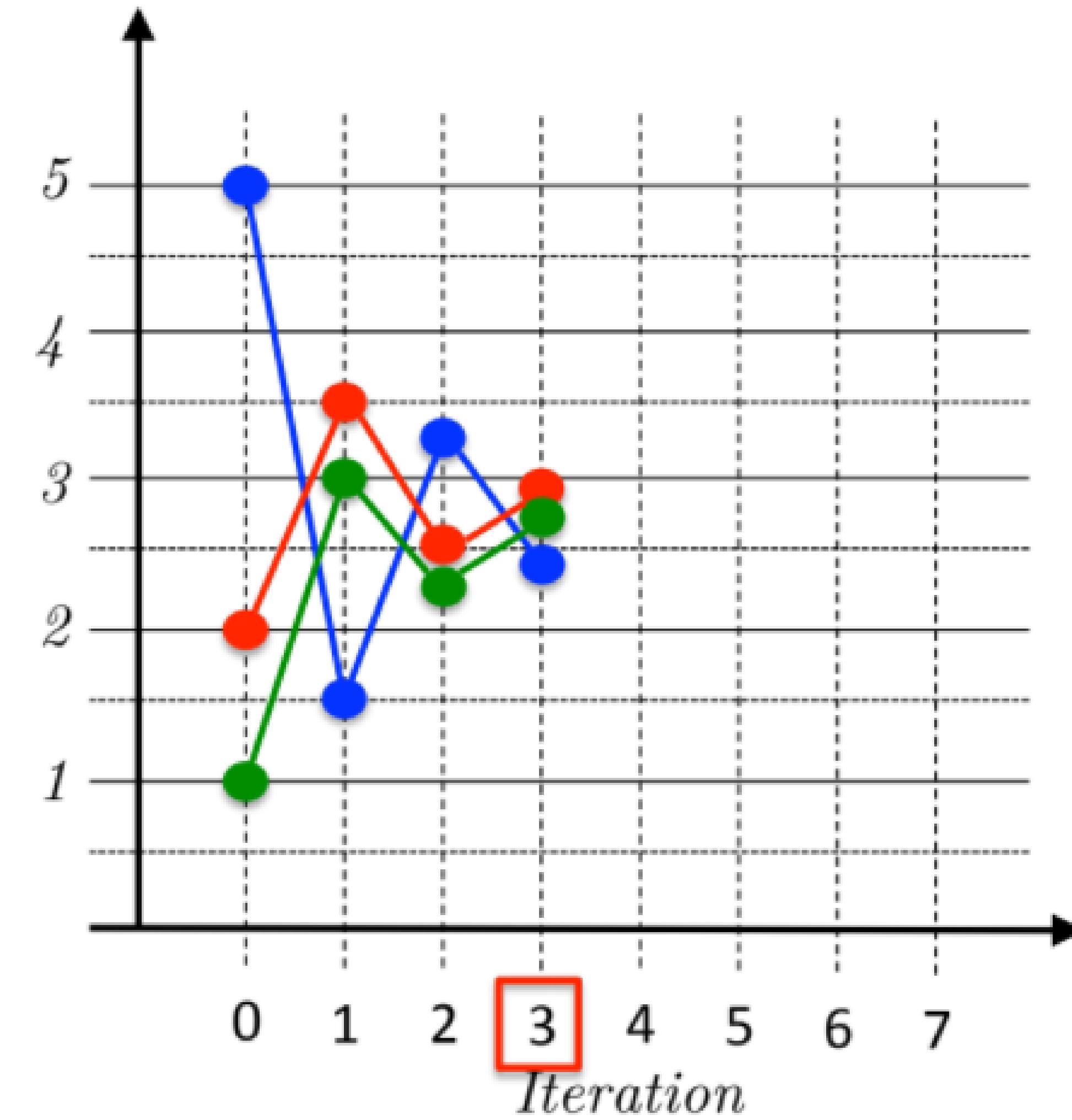
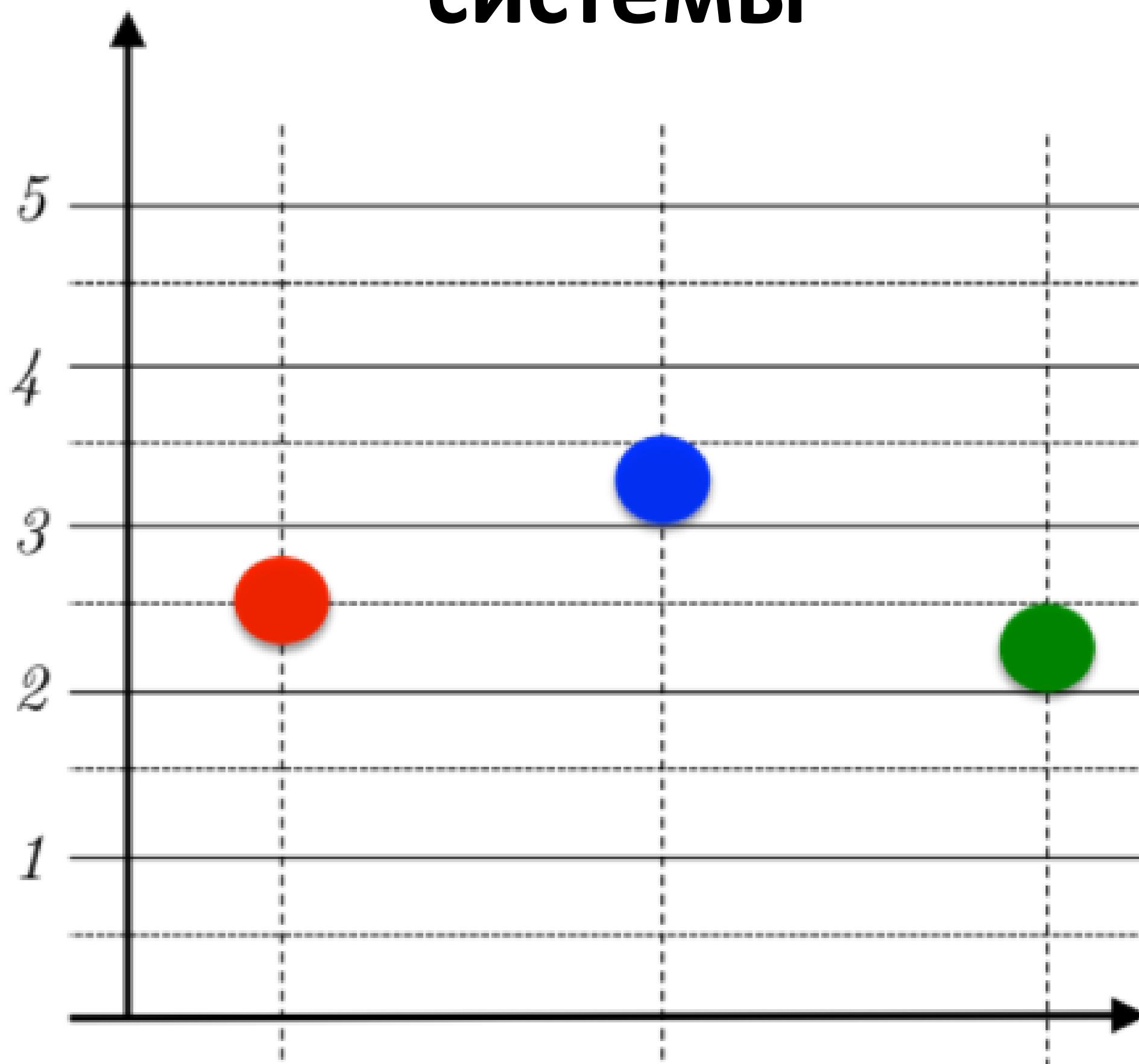
Распределенные электроэнергетические системы



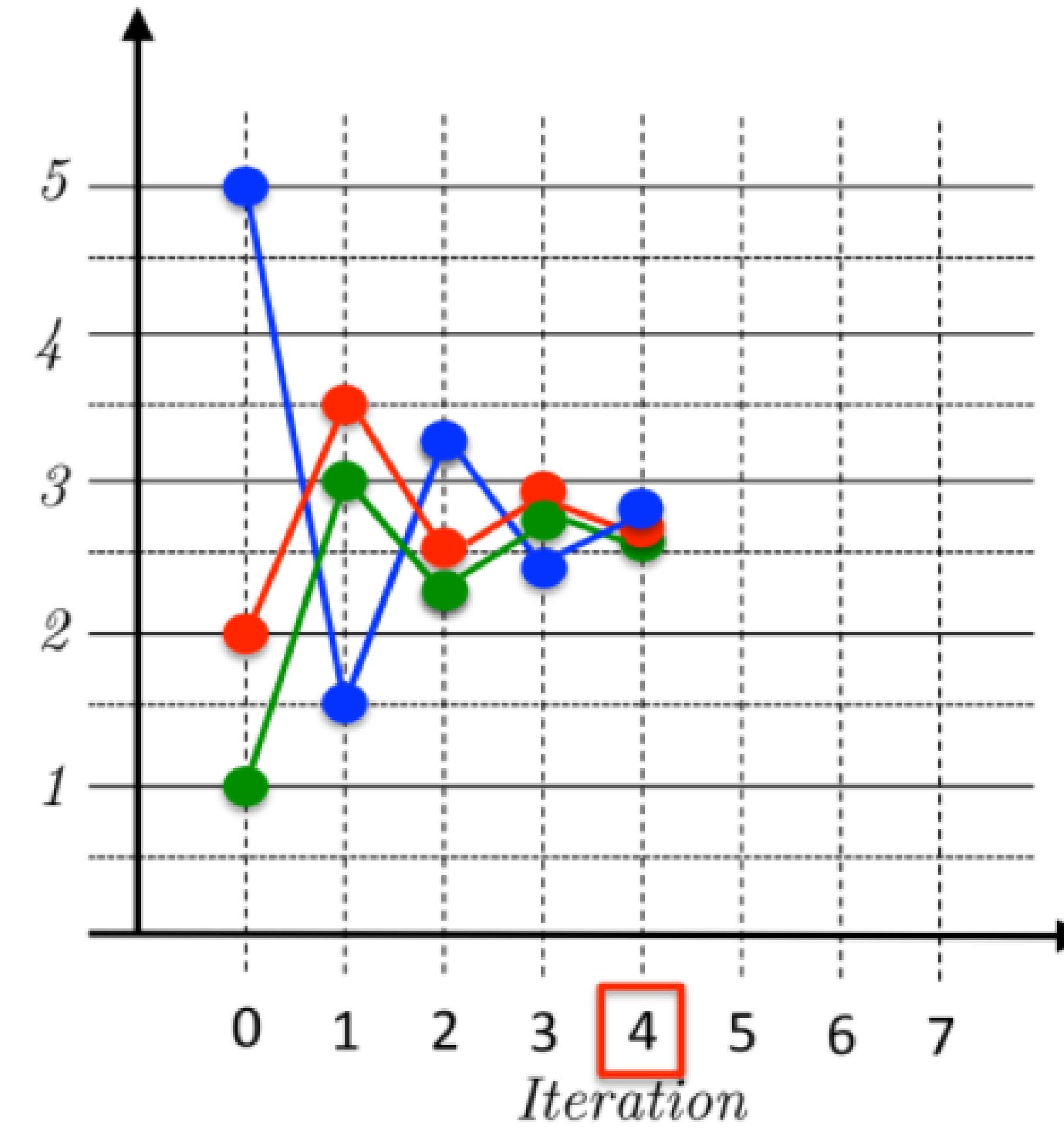
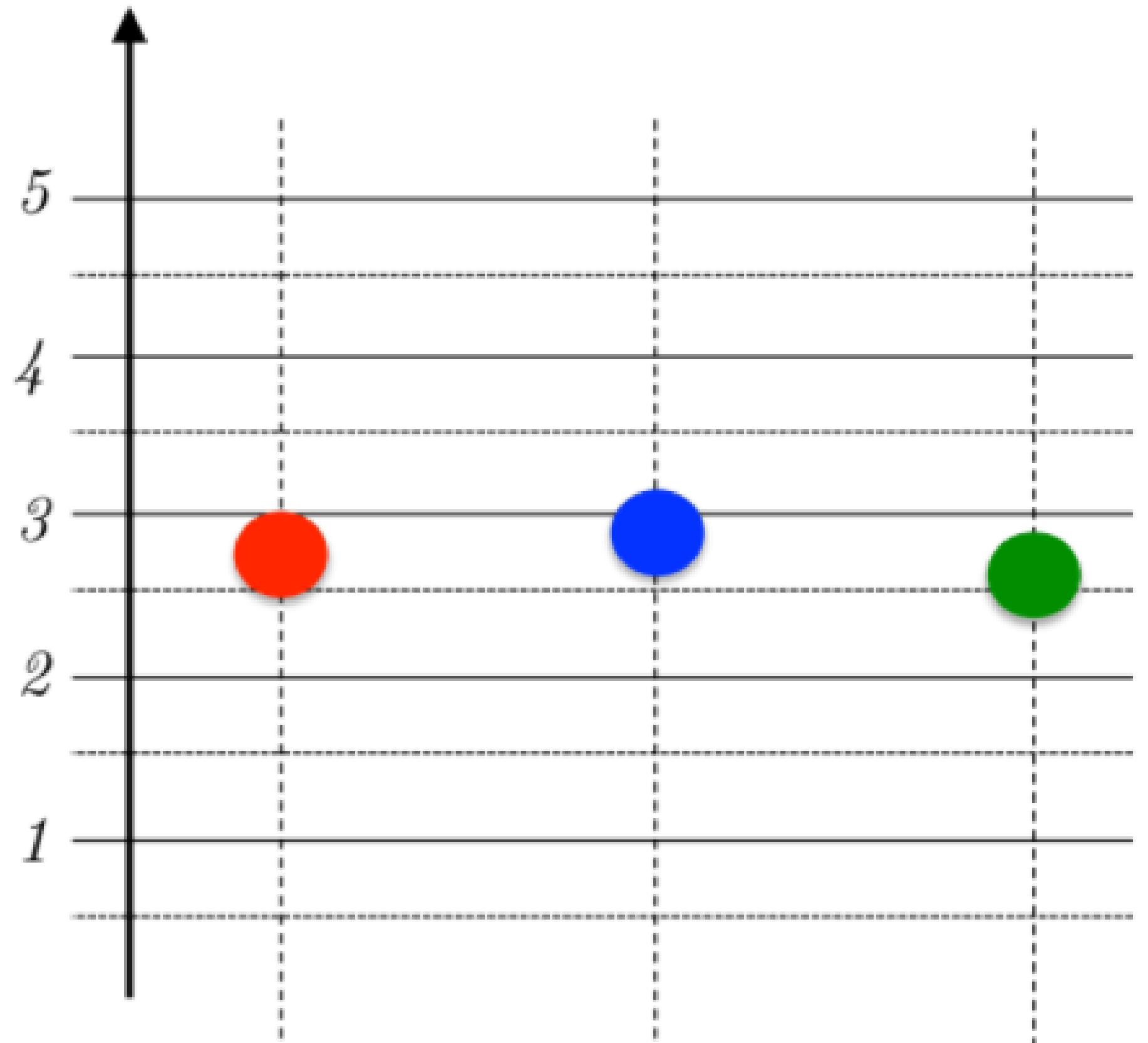
Распределенные электроэнергетические системы



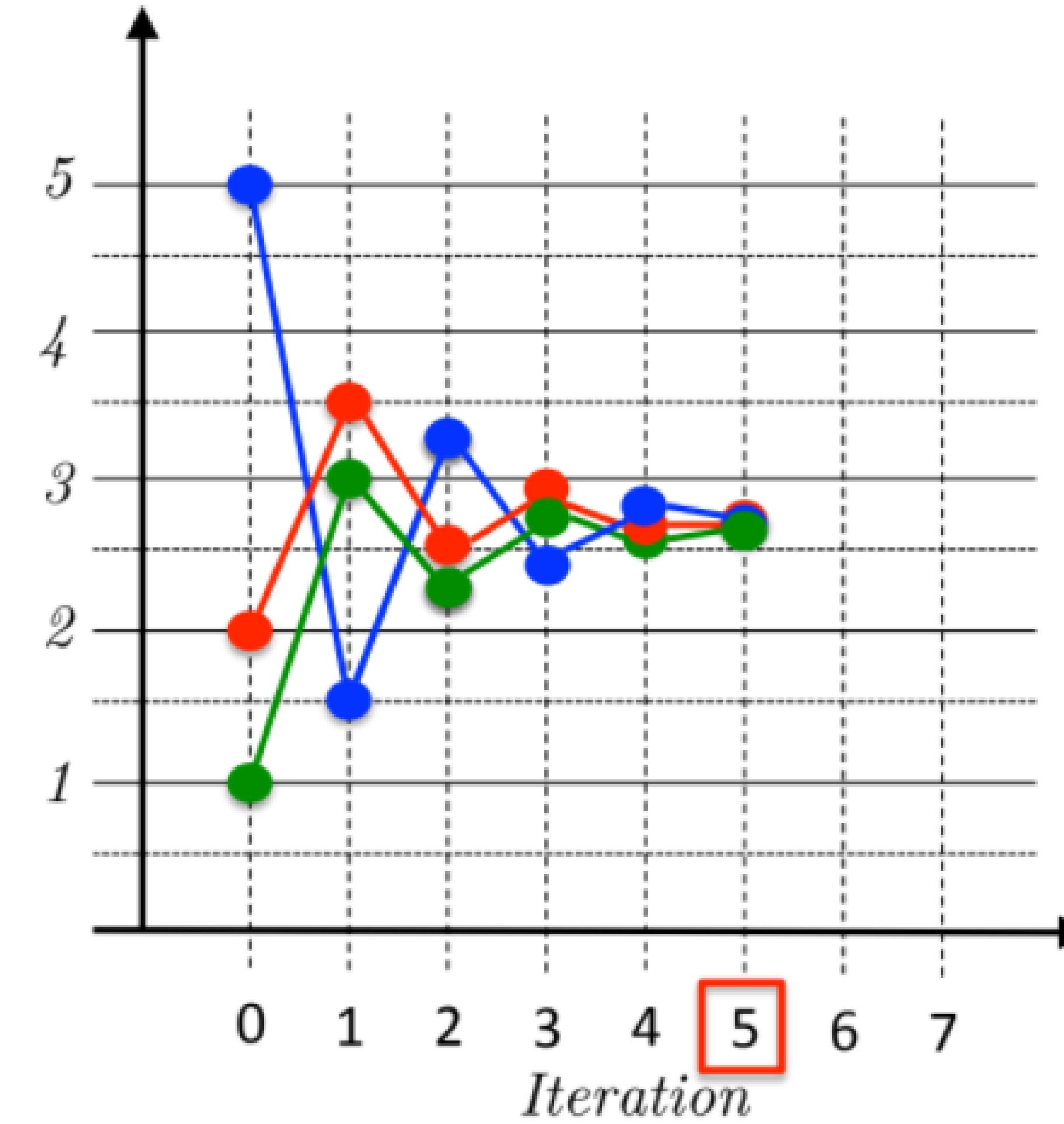
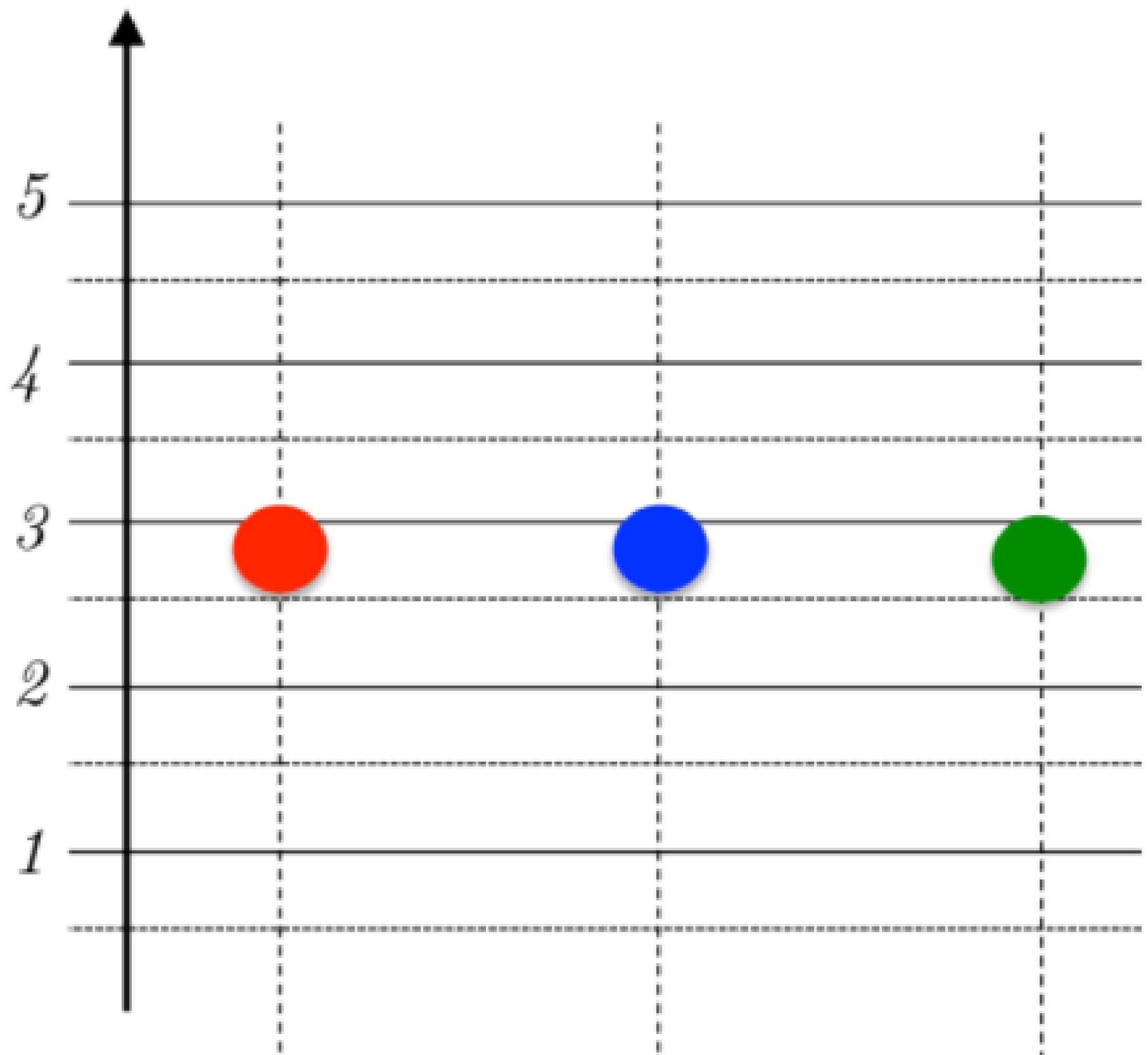
Распределенные электроэнергетические системы



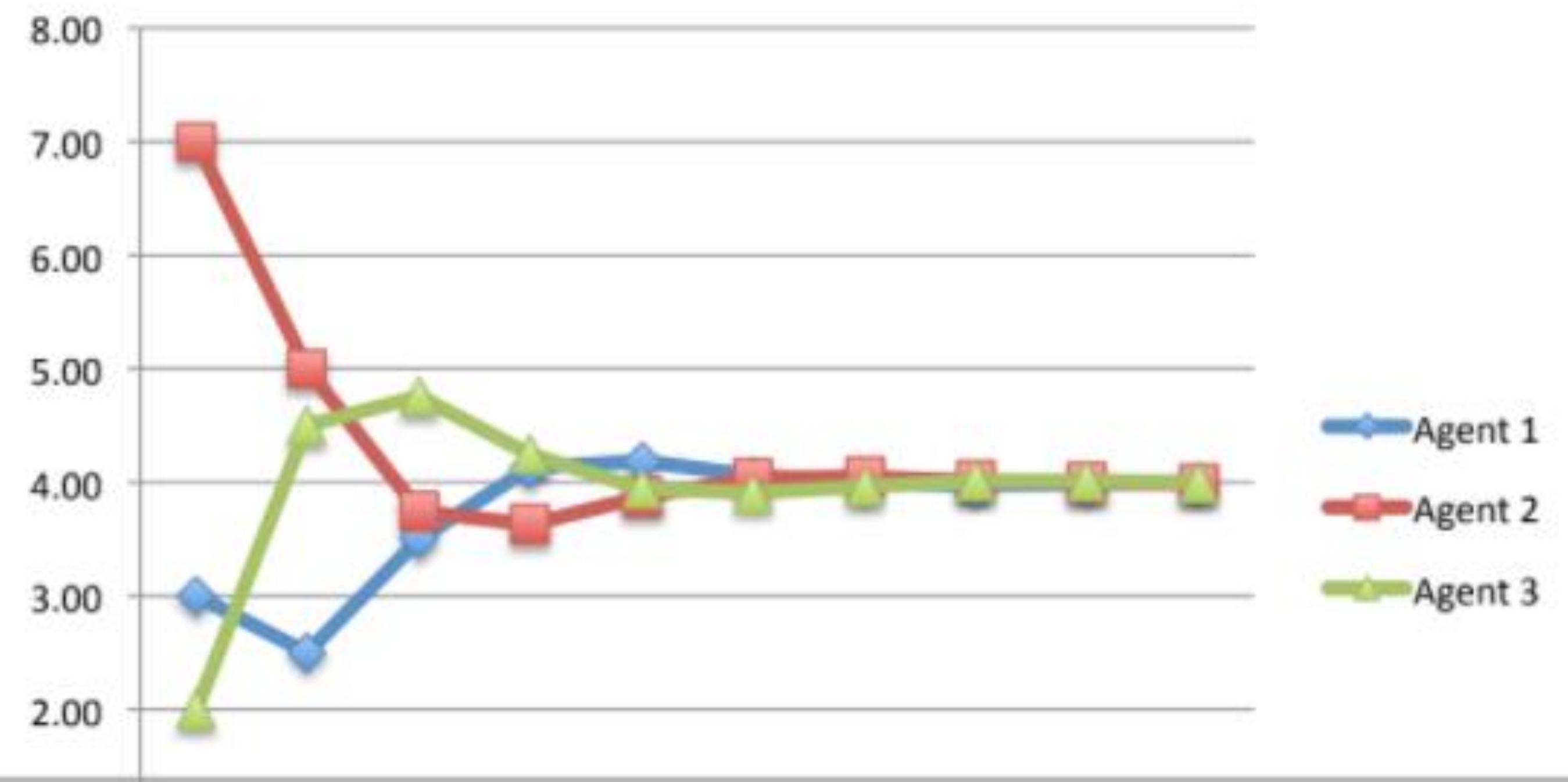
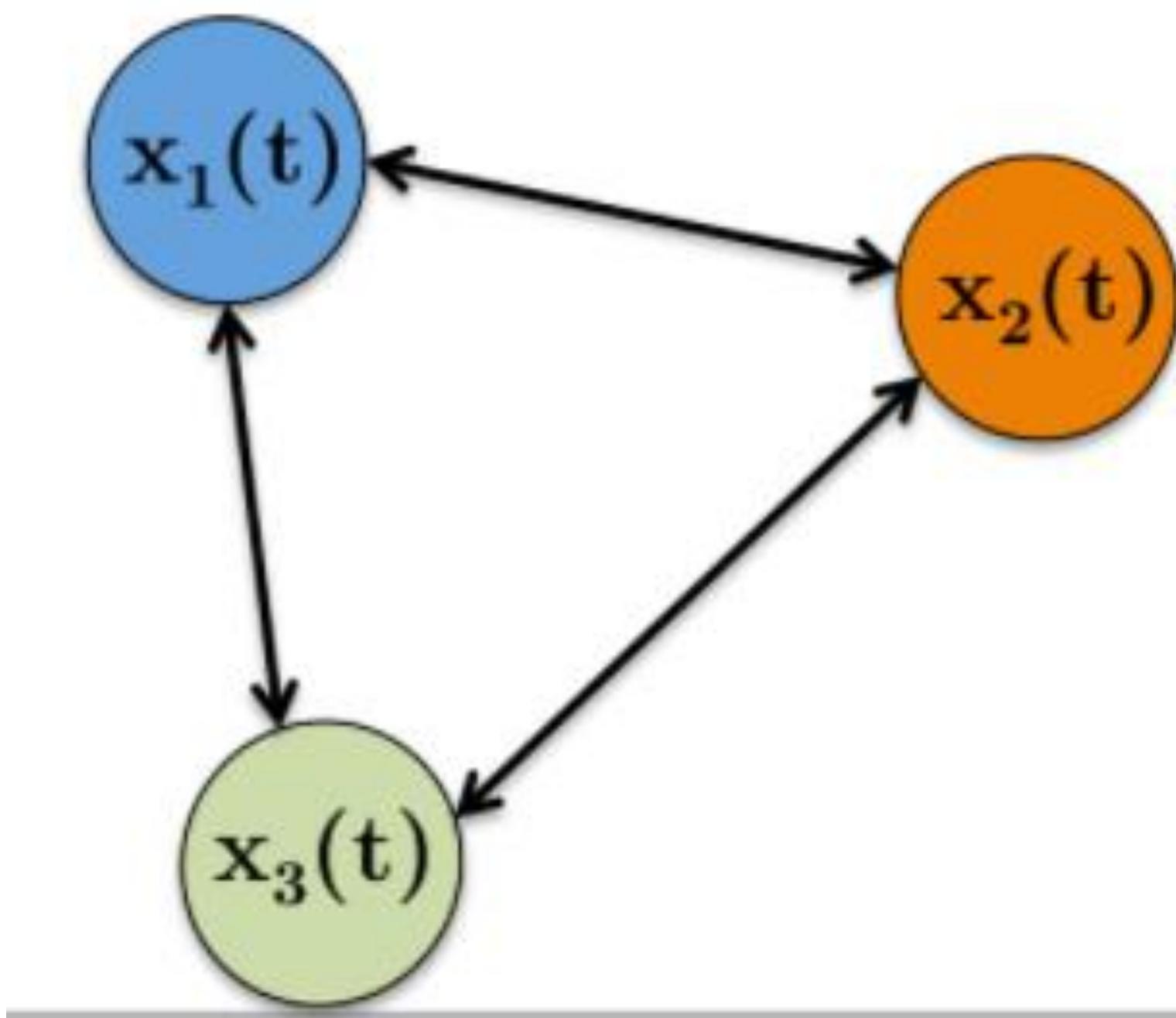
Распределенные электроэнергетические системы



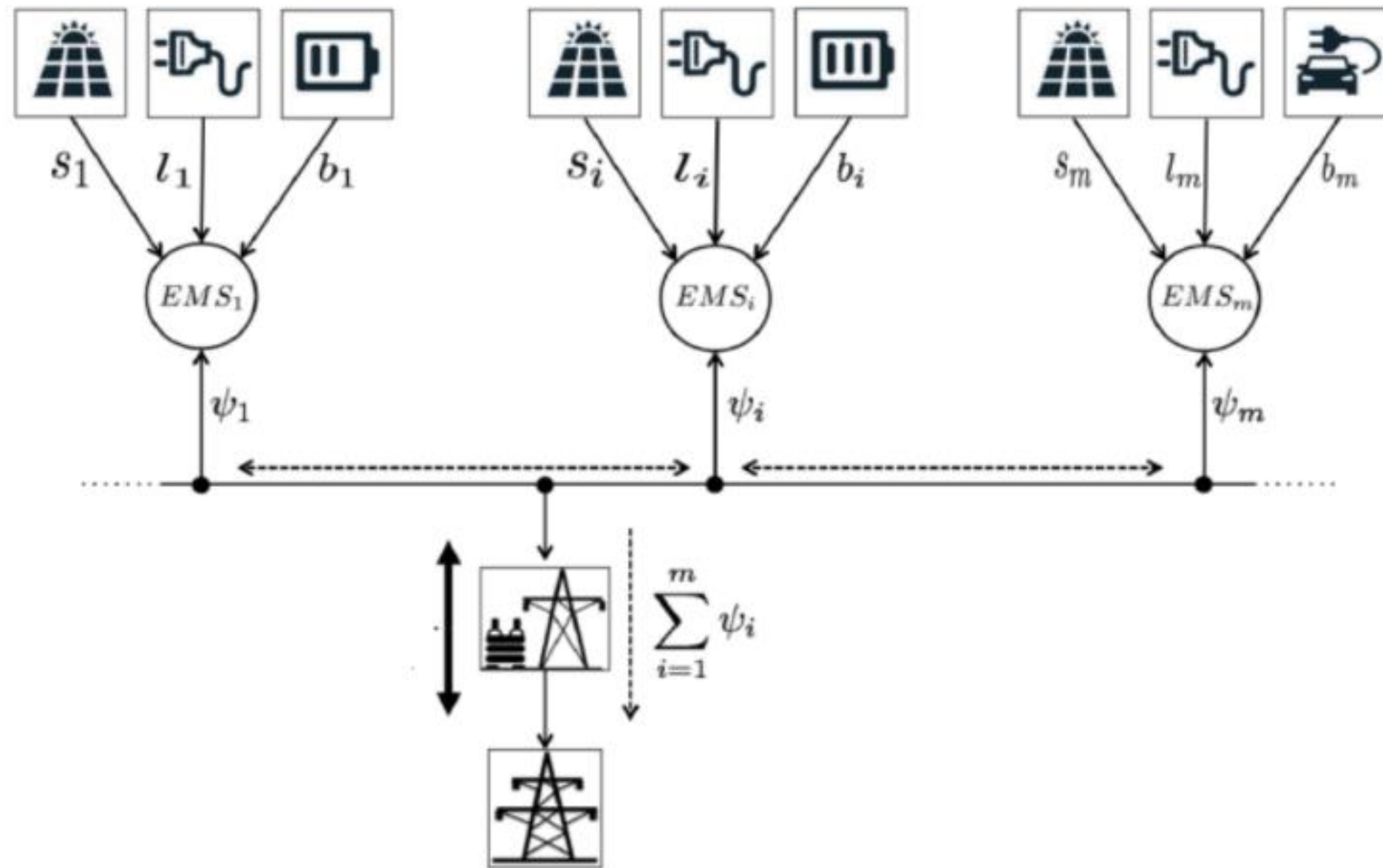
Распределенные электроэнергетические системы



Распределенные электроэнергетические системы

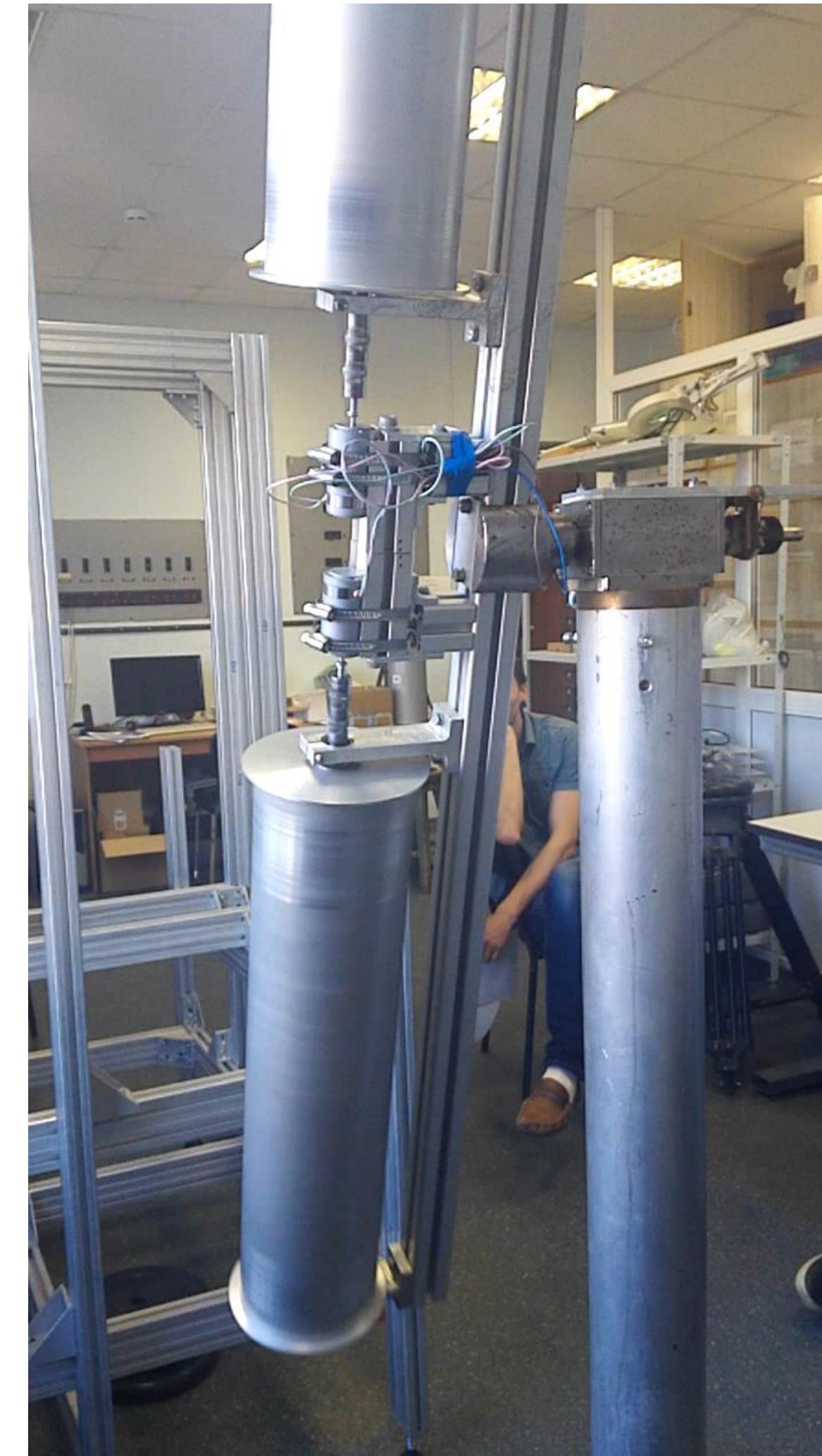
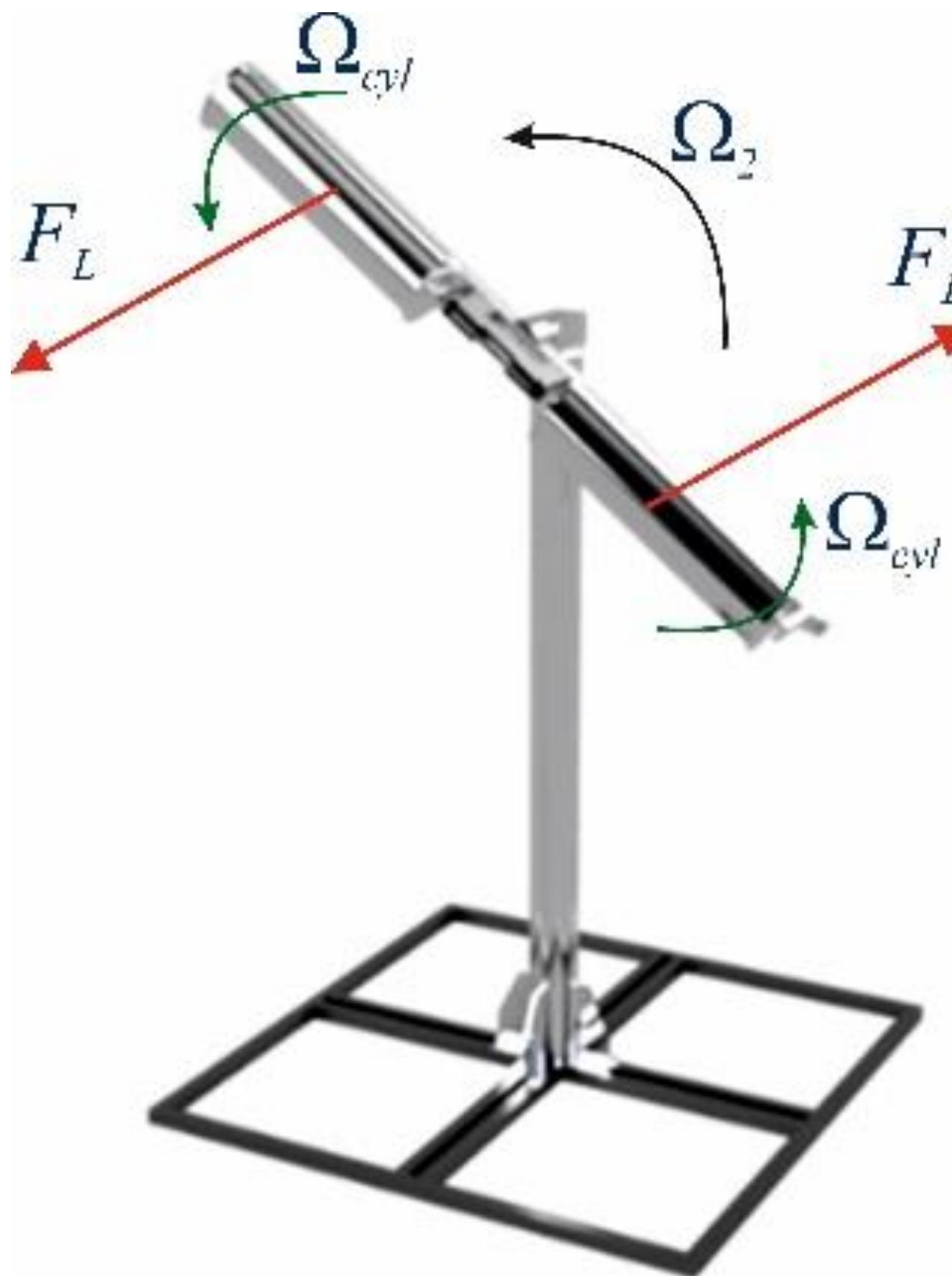


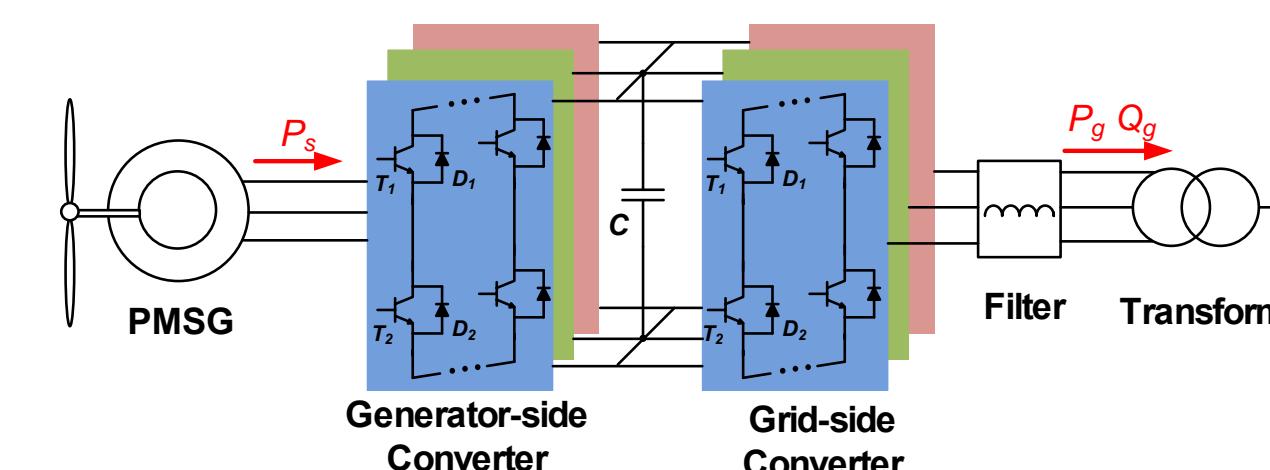
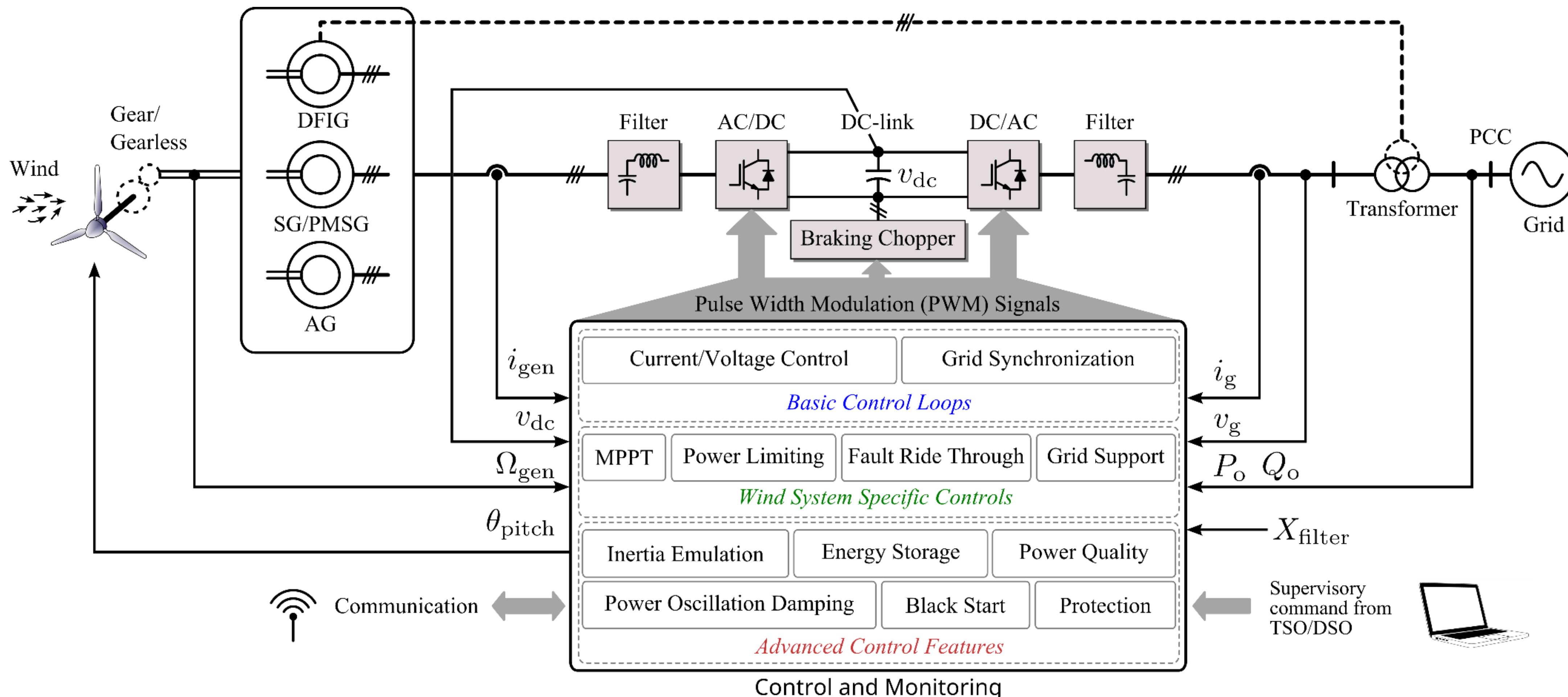
Распределенные электроэнергетические системы



Проектирование современных энергетических систем

Новые типы ветряных электростанций для частного сектора экономики





Frede Blaabjerg
Aalborg University

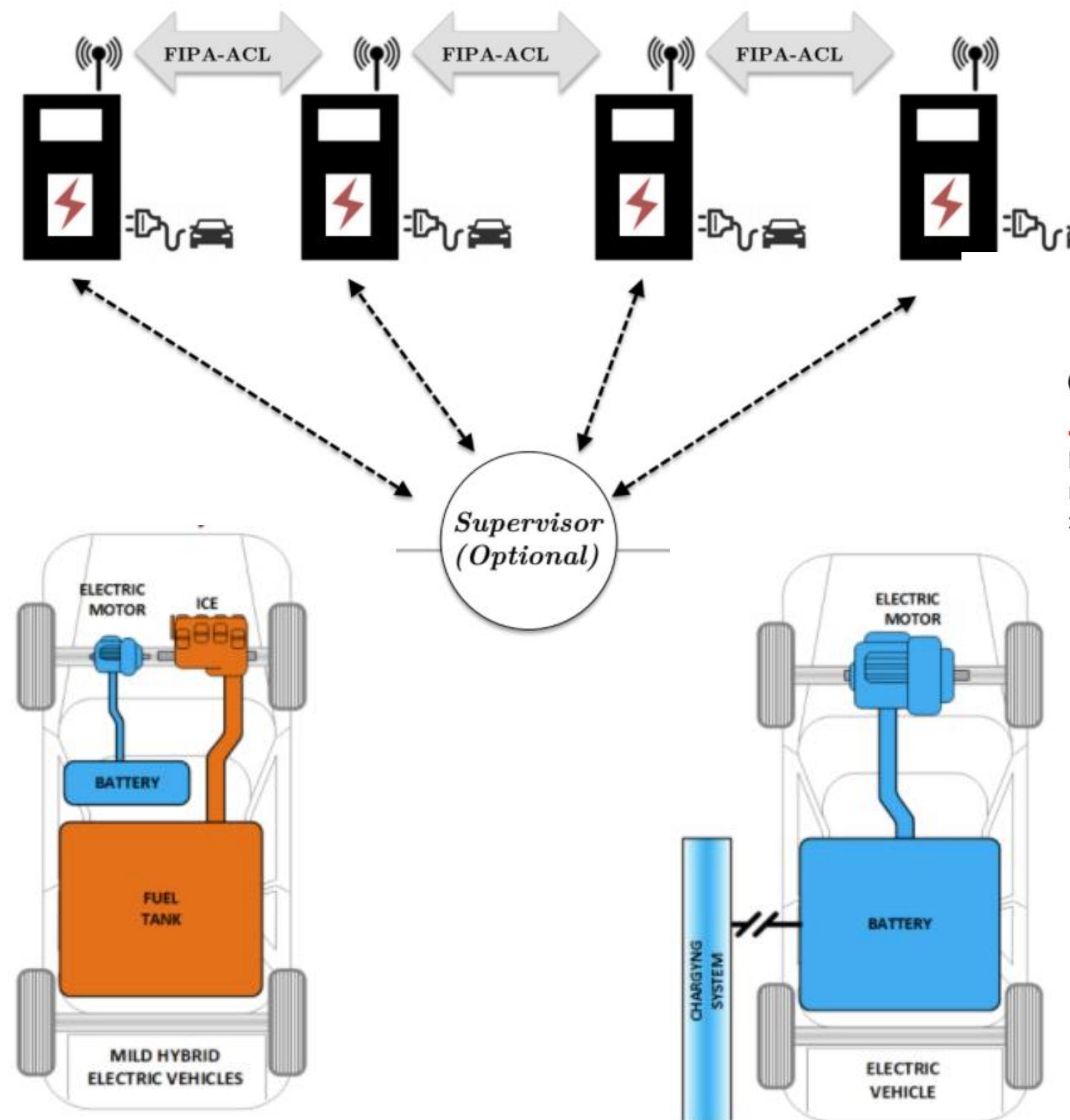
Проектирование современных энергетических систем



Электромобили

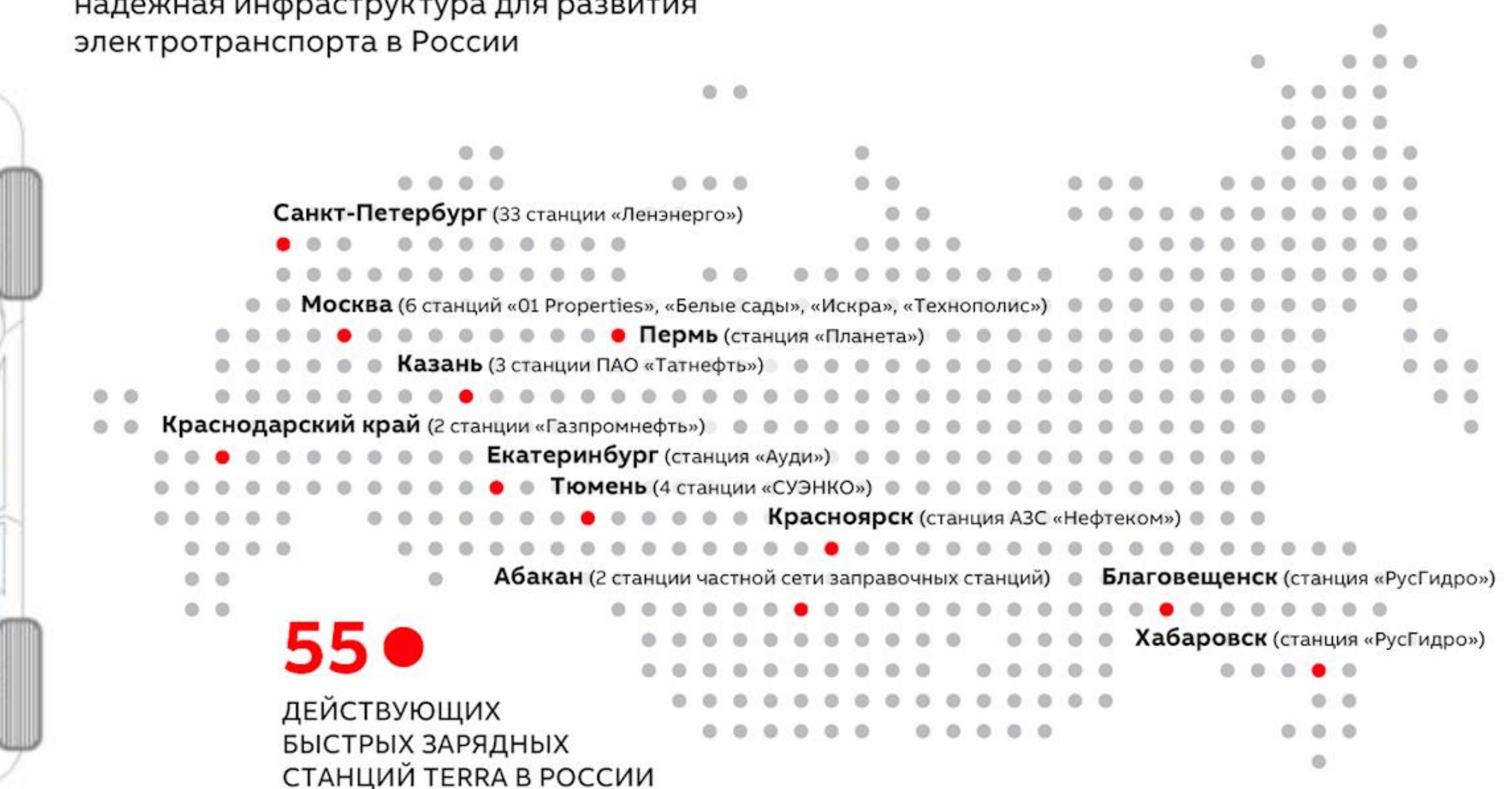


Электромобили



Станции быстрой зарядки Terra от ABB

Быстрые зарядные станции Terra от ABB – надёжная инфраструктура для развития электротранспорта в России



ABB

Travel Activity Based Stochastic Modelling of Load and Charging State of Electric Vehicles

Muhammad Naveed Iqbal ^{1,*}, Lauri Kütt ¹, Matti Lehtonen ², Robert John Millar ², Verner Püvi ², Anton Rassölkkin ¹ and Galina L. Demidova ³

¹ Department of Power Engineering and Mechatronics, Tallinn University of Technology, Ehitajate tee 5, 19086 Tallinn, Estonia; lauri.kutt@taltech.ee (L.K.); anton.rassolkkin@taltech.ee (A.R.)

² Department of Electrical Engineering and Automation, Aalto University, Maaratintie 8, 02150 Espoo, Finland; matti.lehtonen@aalto.fi (M.L.); john.millar@aalto.fi (R.J.M.); verner.puvi@aalto.fi (V.P.)

³ Faculty of Control Systems and Robotics, ITMO University, 197101 Saint Petersburg, Russia; demidova@itmo.ru

* Correspondence: miqbal@taltech.ee

Abstract: The uptake of electric vehicles (EV) is increasing every year and will eventually replace the traditional transport system in the near future. This imminent increase is urging stakeholders to plan up-gradation in the electric power system infrastructure. However, for efficient planning to support an additional load, an accurate assessment of the electric vehicle load and power quality indices is required. Although several EV models to estimate the charging profile and additional electrical load are available, but they are not capable of providing a high-resolution evaluation of charging current, especially at a higher frequency. This paper presents a probabilistic approach capable of estimating the time-dependent charging and harmonic currents for the future EV load. The model is based on the detailed travel activities of the existing car owners reported in the travel survey. The probability distribution functions of departure time, distance, arrival time, and time span are calculated. The charging profiles are based on the measurements of several EVs.



Citation: Iqbal, M.N.; Kütt, L.; Lehtonen, M.; Millar, R.J.; Püvi, V.; Rassölkkin, A.; Demidova, G.L. Travel Activity Based Stochastic Modelling of Load and Charging State of Electric Vehicles. *Sustainability* **2021**, *13*, 1550. <https://doi.org/10.3390/su13031550>

Academic Editor: Tomonobu Senju
Received: 22 December 2020

Accepted: 26 January 2021
Published: 2 February 2021

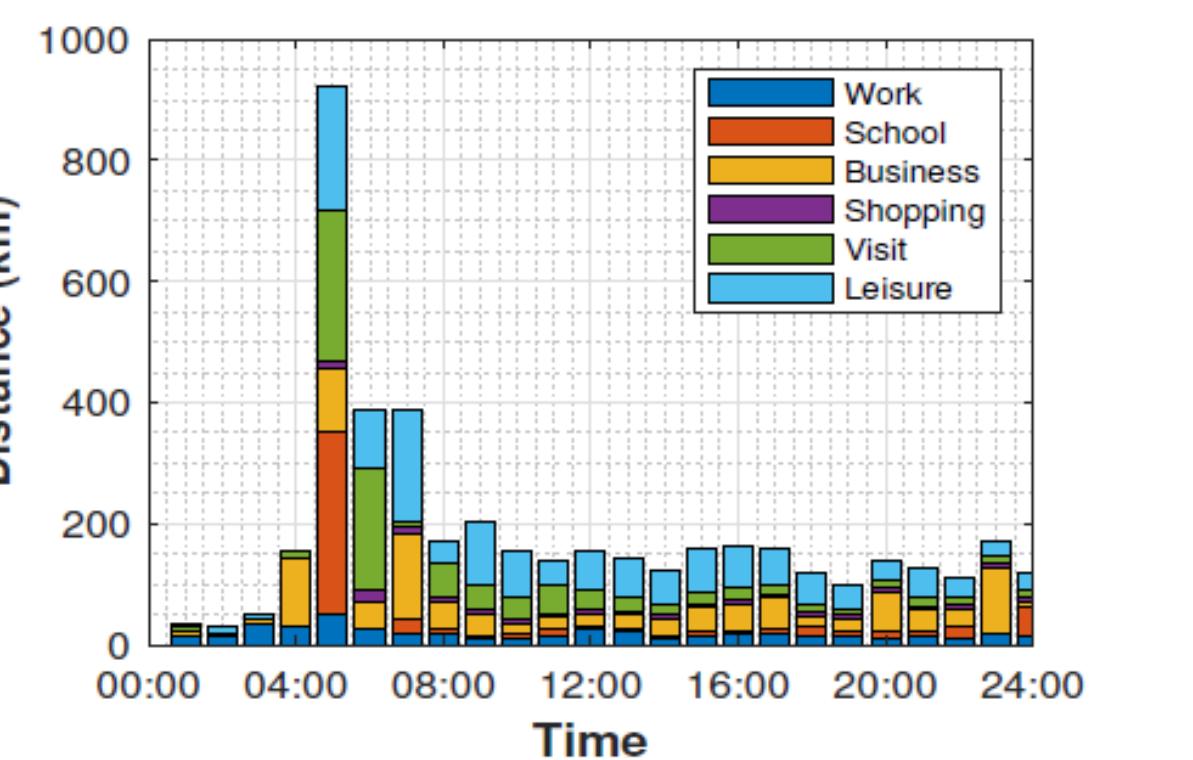
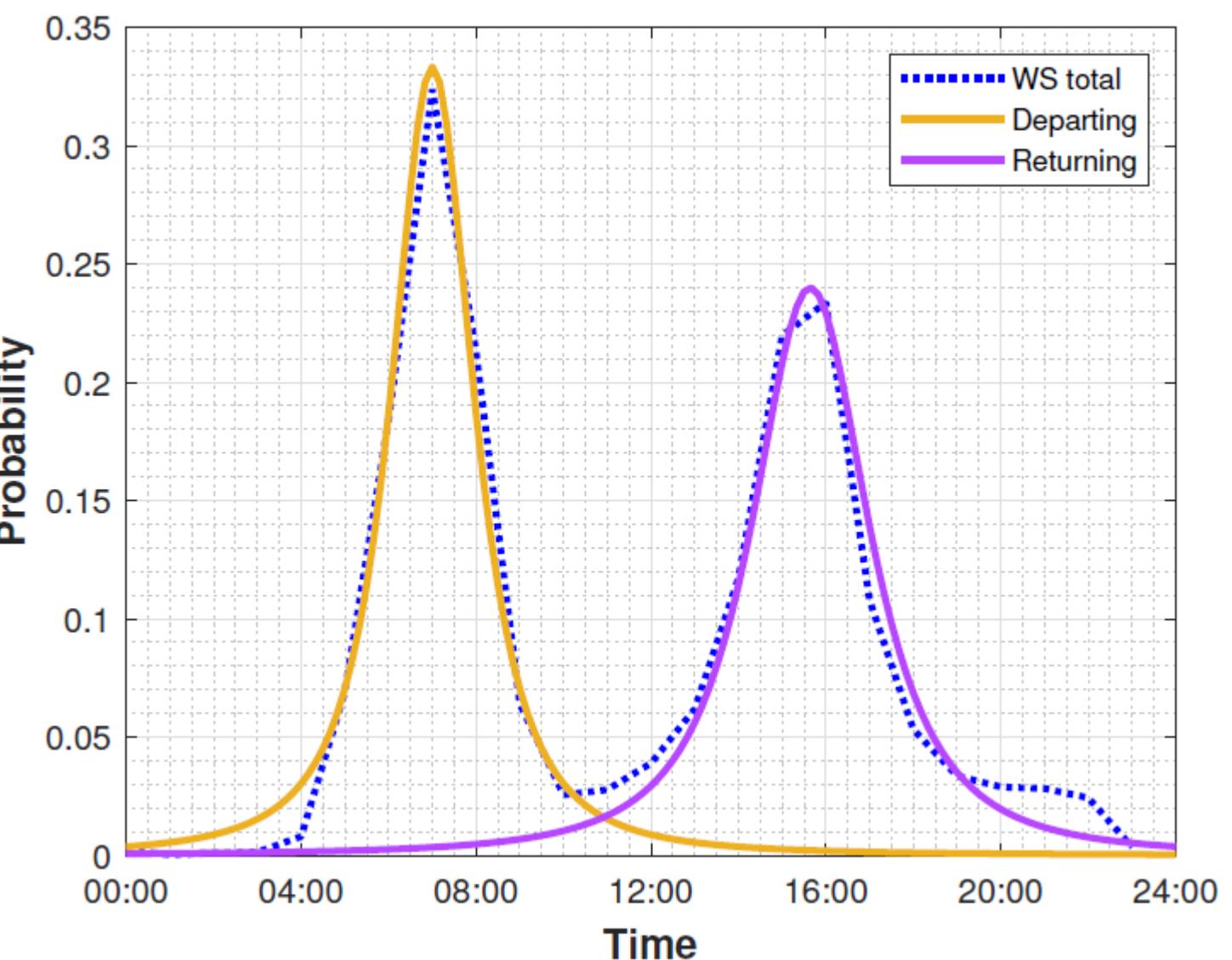
Publisher's Note: MDPI stays neutral with regard to jurisdictional claims in published maps and institutional affiliations.



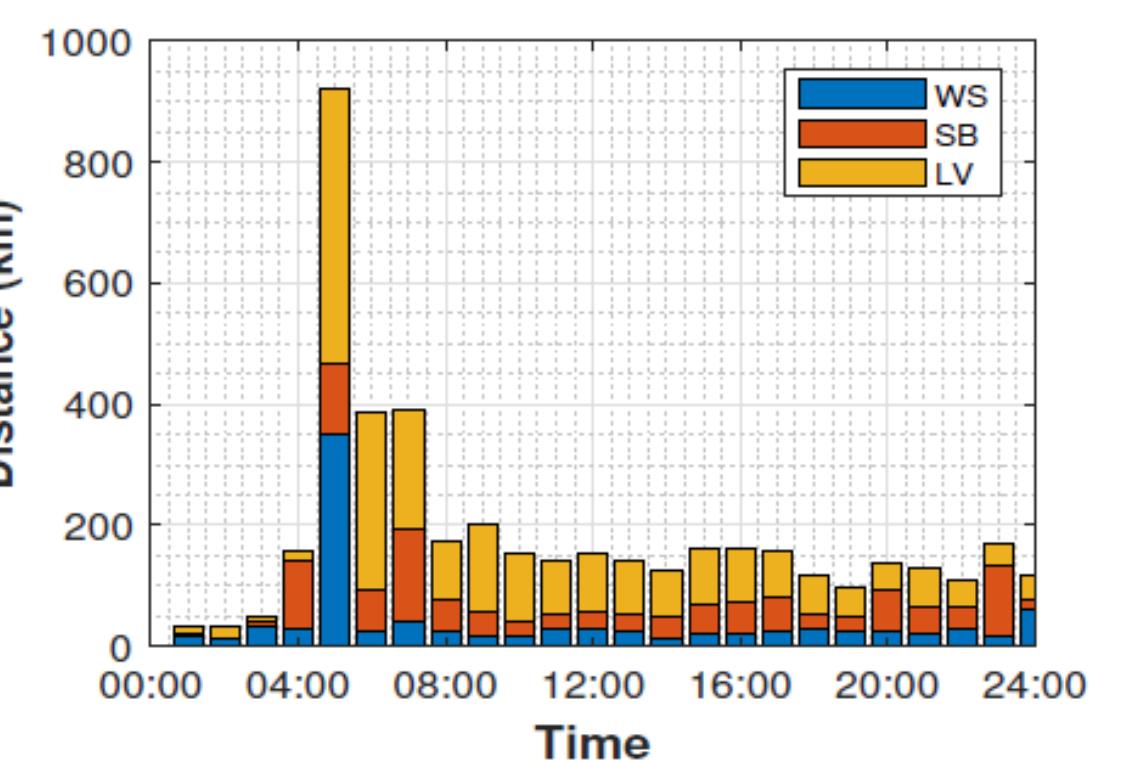
Copyright © 2021 by the authors. Licensee MDPI, Basel, Switzerland. This article is an open access article distributed under the terms and conditions of the Creative Commons Attribution (CC BY) license (<https://creativecommons.org/licenses/by/4.0/>).

The climate change and energy security concerns are pushing policy-making institutes towards setting strict targets towards reducing greenhouse gasses (GHG) emissions and dependency on fossil fuels. The transport sector consumes 58 % of the total oil, while 67% of fossil fuel is used to generate electricity [1]. Electric vehicles (EV) are promising an efficient replacement of the conventional transportation system. For a sustainable future with less dependency on fossil fuels and to meet the world's energy demand, the adoption of electric vehicles and renewable energy is essential. As EV's adoption is encouraged to meet energy security and climate-related targets, some challenges are also associated with their rapid integration. It would typically mean reinforcements to the existing grids to support the additional charging load. The EV charging is based on power electronic circuits that can compromise the network's sustainability by adding harmonic pollution. In planning such changes, the future load due to vehicle fleets would need to be known. A probabilistic EV usage model, based on the traffic surveys and the actual vehicle-driven data, can provide estimation of the EV charging load in the distribution grid.

Governments and automobile manufacturers are pushing towards developing efficient designs of electric vehicles. In 2017, electric vehicle's total stock increased to 3 million, including both battery electric vehicles (BEV) and plug-in hybrid electric vehicles (PHEV). This number is expected to surge up to 13 million by 2020 and 130 million by 2030 [2,3]. This growth is anticipated because of the improved life cycle of EVs and a decrease in the



(a)



(b)

Figure 3. Trip distance frequency per hour for different travel activities (a) From NTS survey (b) Data used in the model.

Iqbal, M.N.; Kütt, L.; Lehtonen, M.; Millar, R.J.; Püvi, V.; Rassölkkin, A.; Demidova, G.L. (2021). Travel activity based stochastic modelling of load and charging state of electric vehicles. *Sustainability*, *13* (3), 1–14. DOI: [10.3390/su13031550](https://doi.org/10.3390/su13031550).

**Интеллектуальное
управление**



**Интеллектуальное
управление**

Нечеткая логика

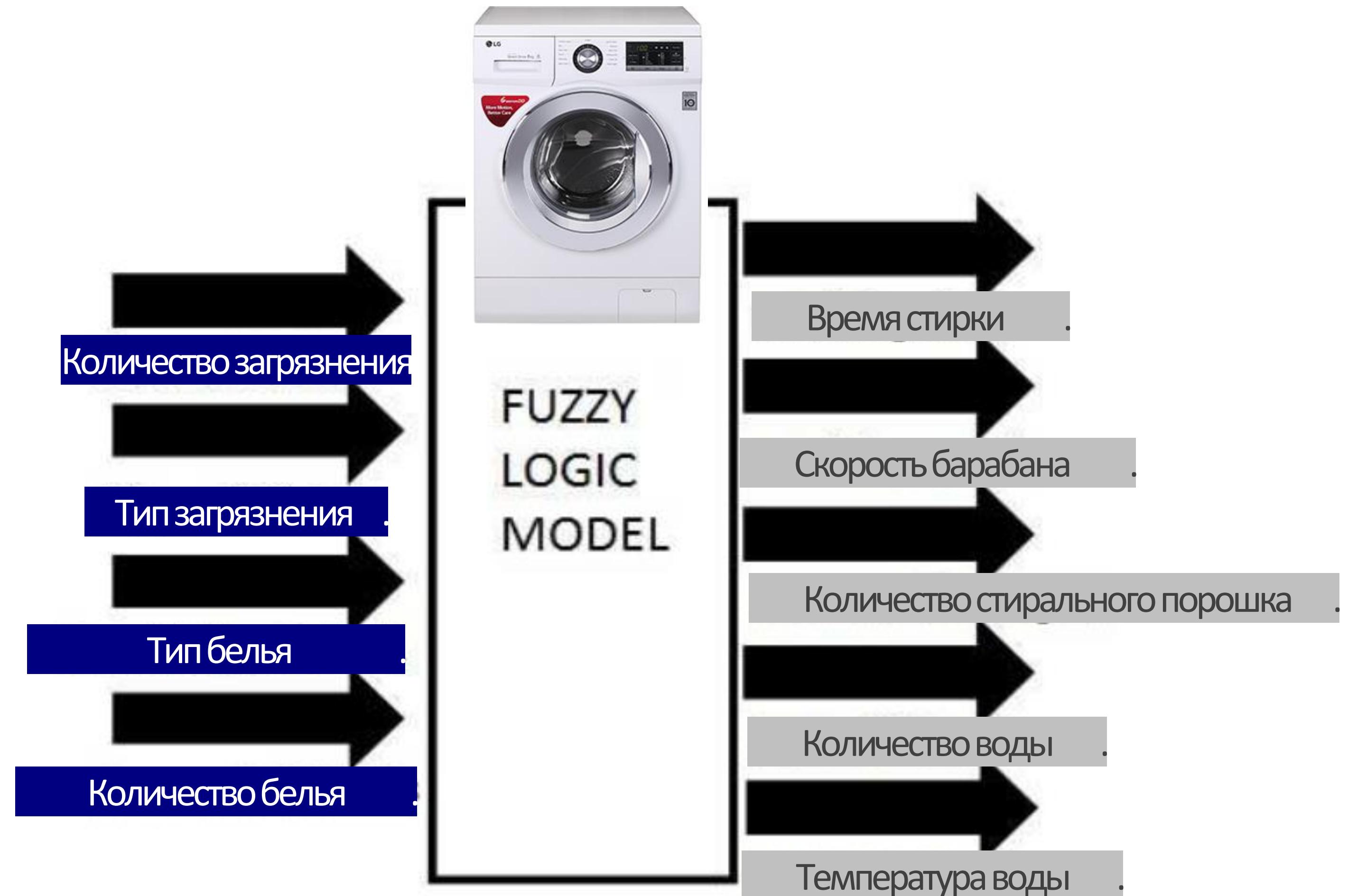
Нейронные сети

Машинное обучение

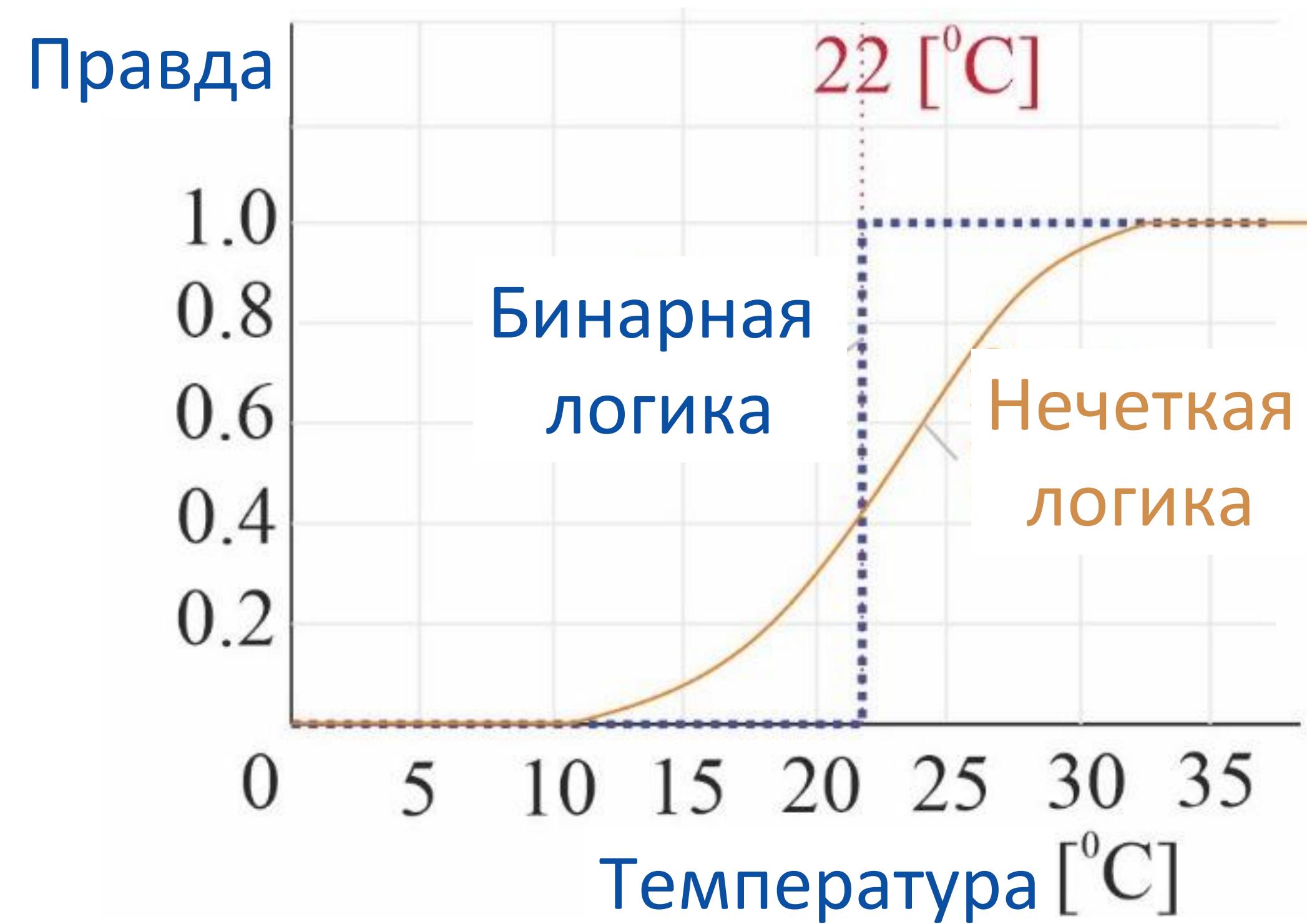
Нечеткая логика



Нечеткая логика



Нечеткая логика

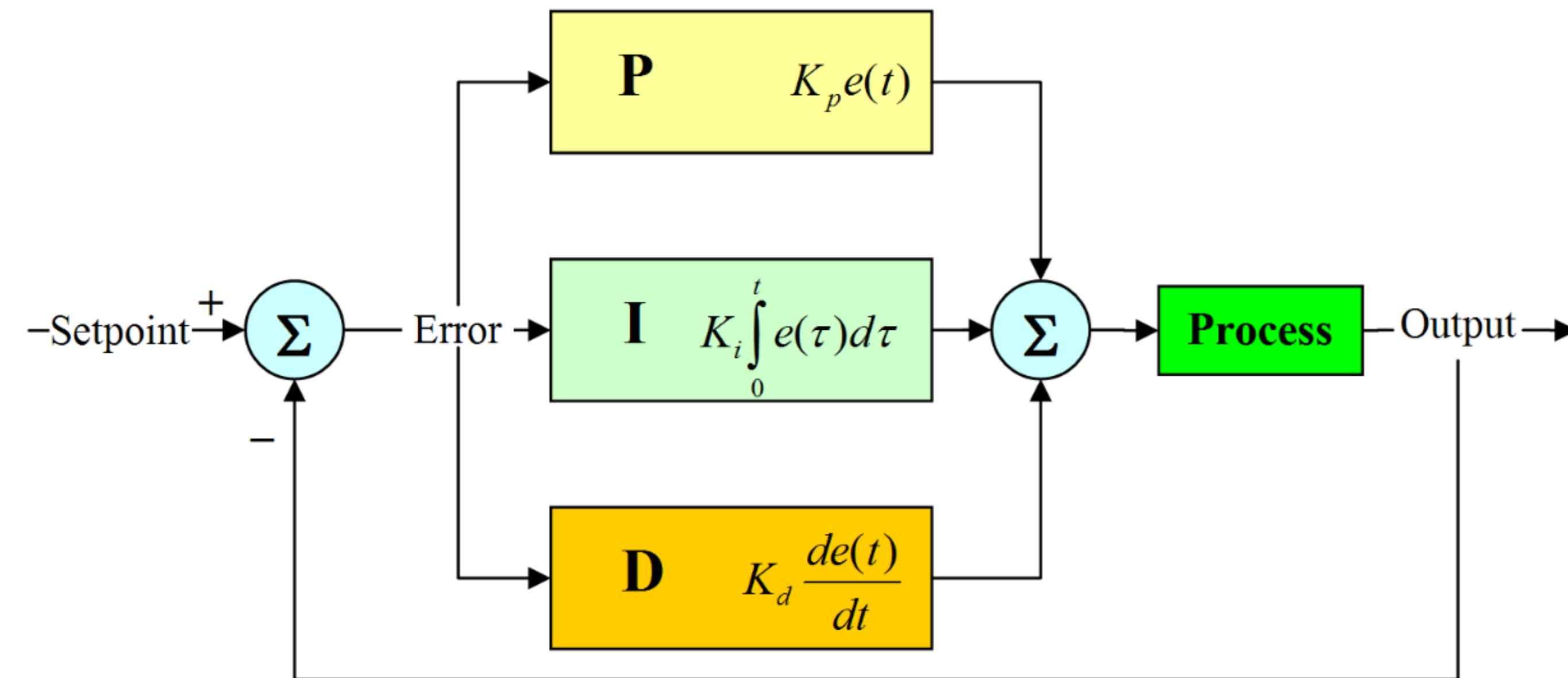


- ✓ Нечеткое управление использует предложения в форме правил для управления процессом.
- ✓ Контроллер может принимать множество входных данных, а преимуществом нечеткого управления является возможность включения экспертных знаний.
- ✓ Интерфейс контроллера представляет собой «естественный язык», и это отличает нечеткое управление от других методов управления.
- ✓ Обычно это нелинейный регулятор.



Lotfi Askar Zadeh Ebrahim Mamdani Michio Sugeno Tomohiro Takagi

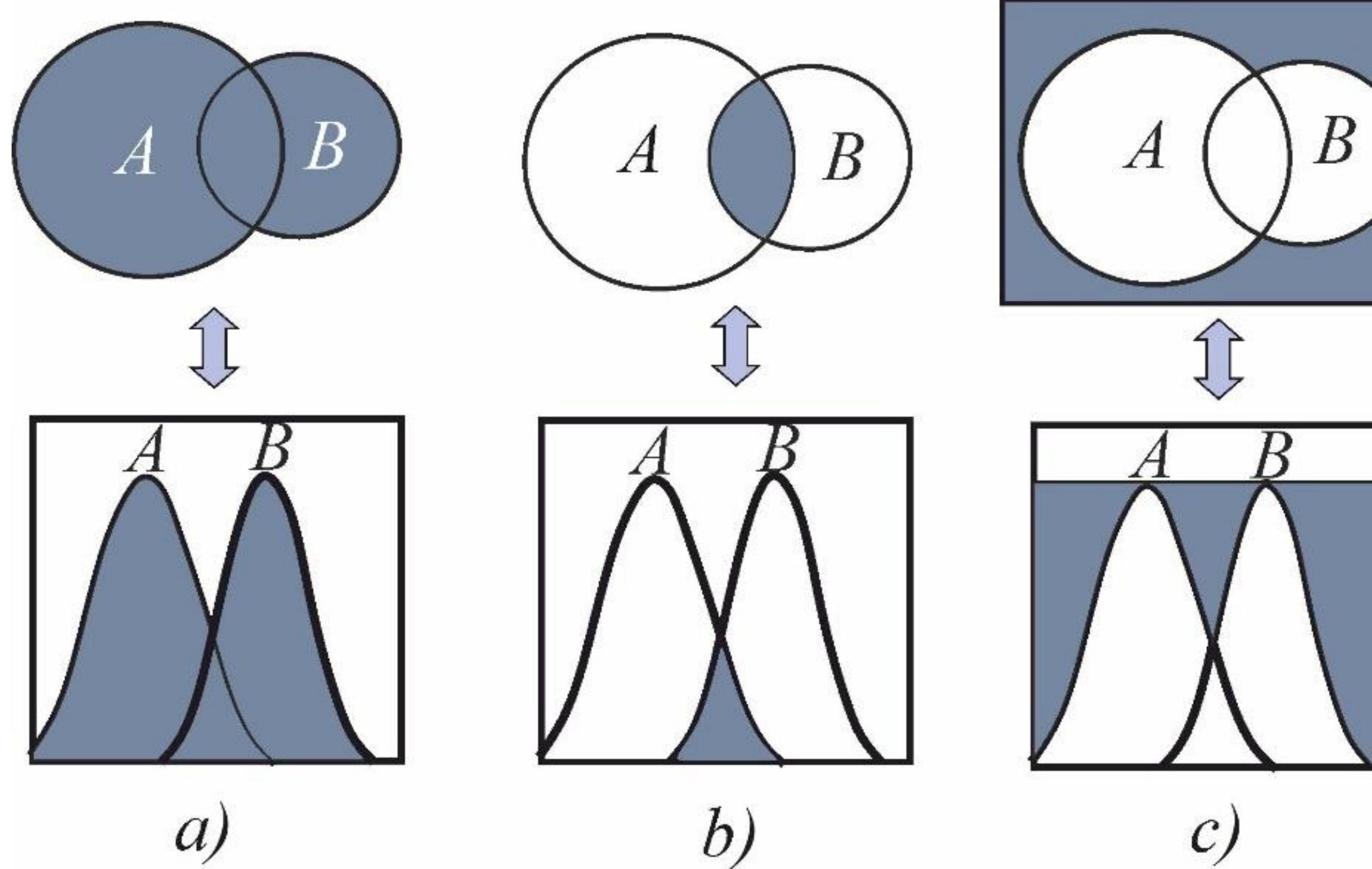
Нечеткая логика



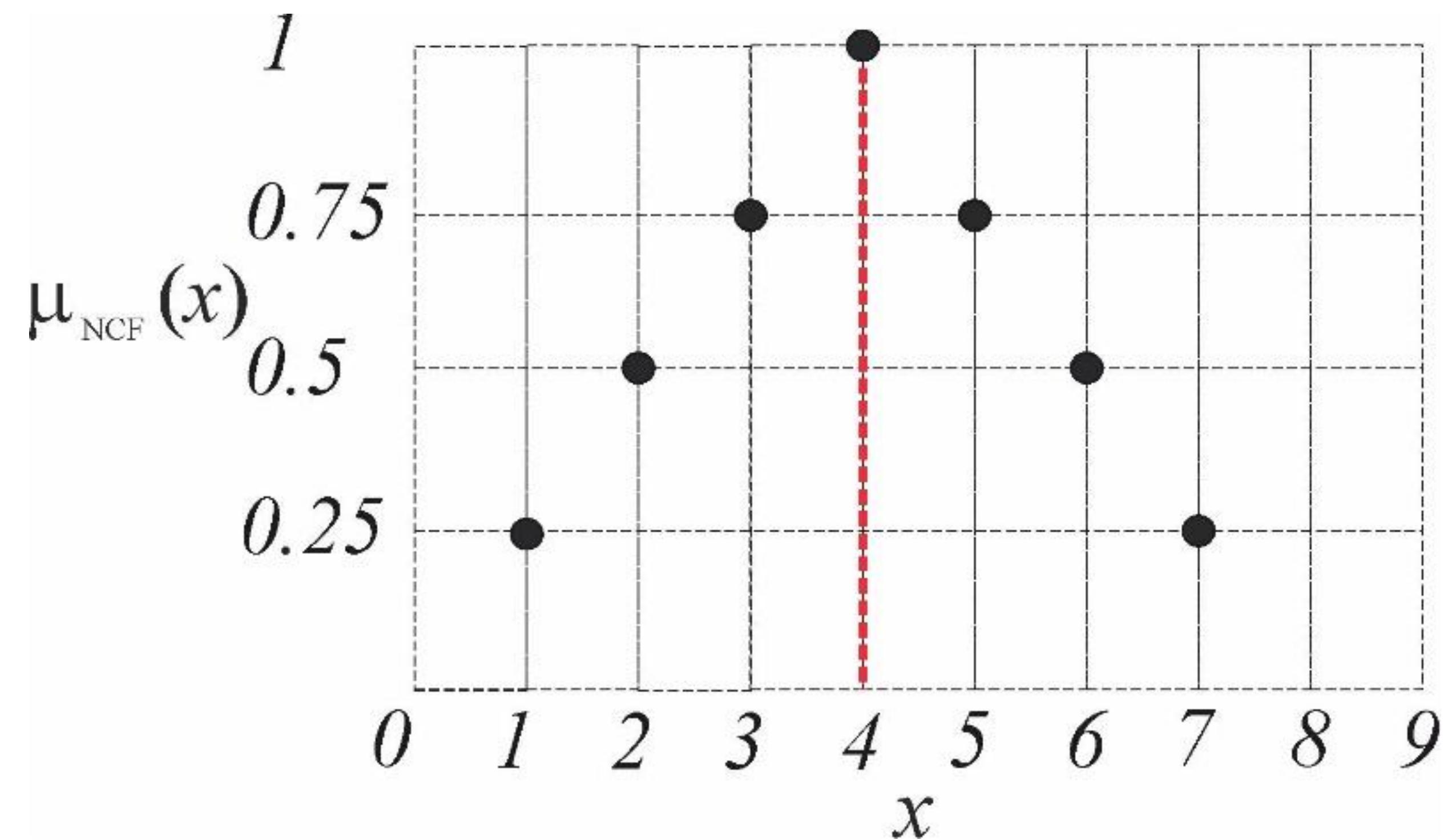
Нечеткая логика



Базовые операции – логические операции

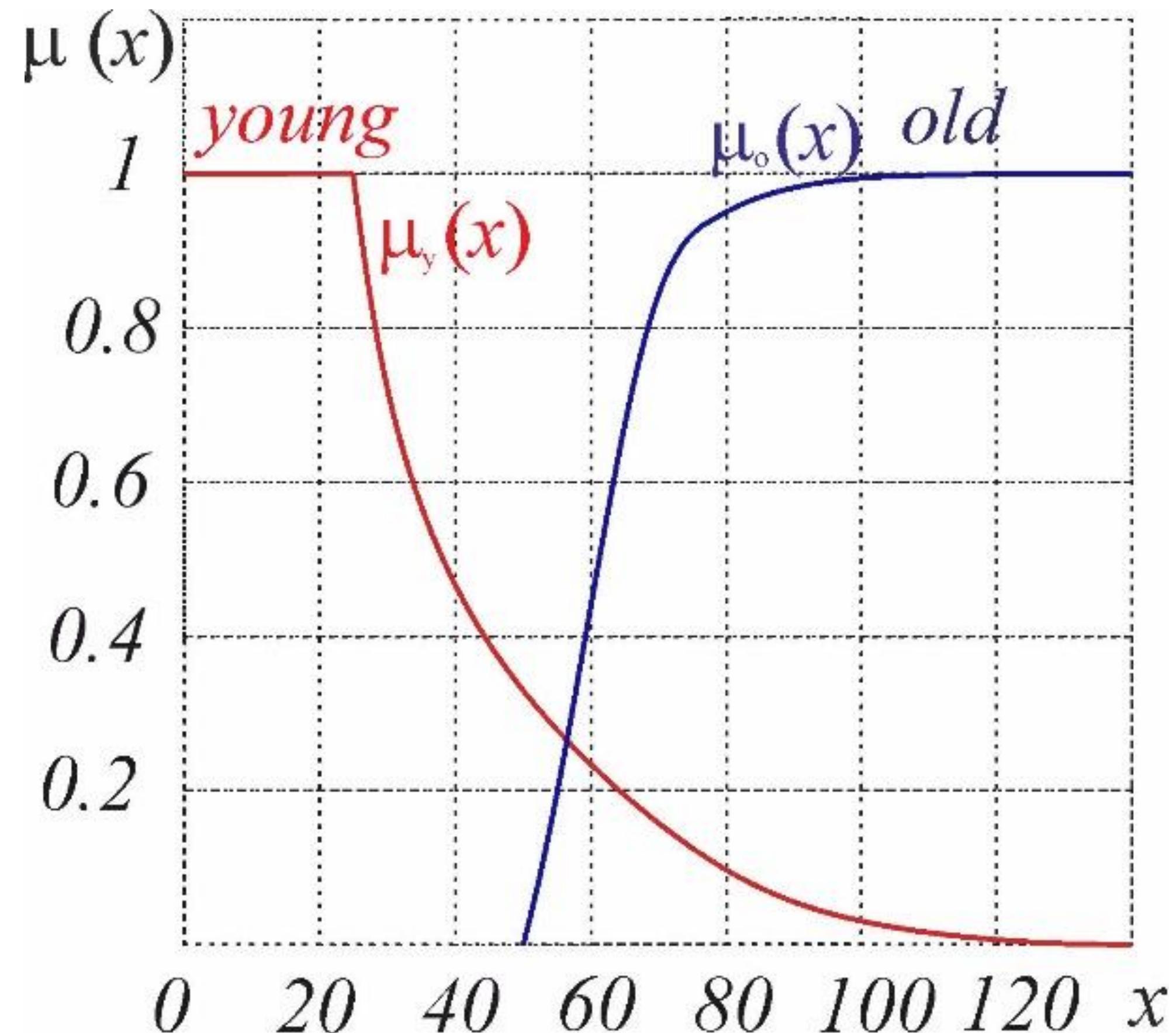


Функции принадлежности



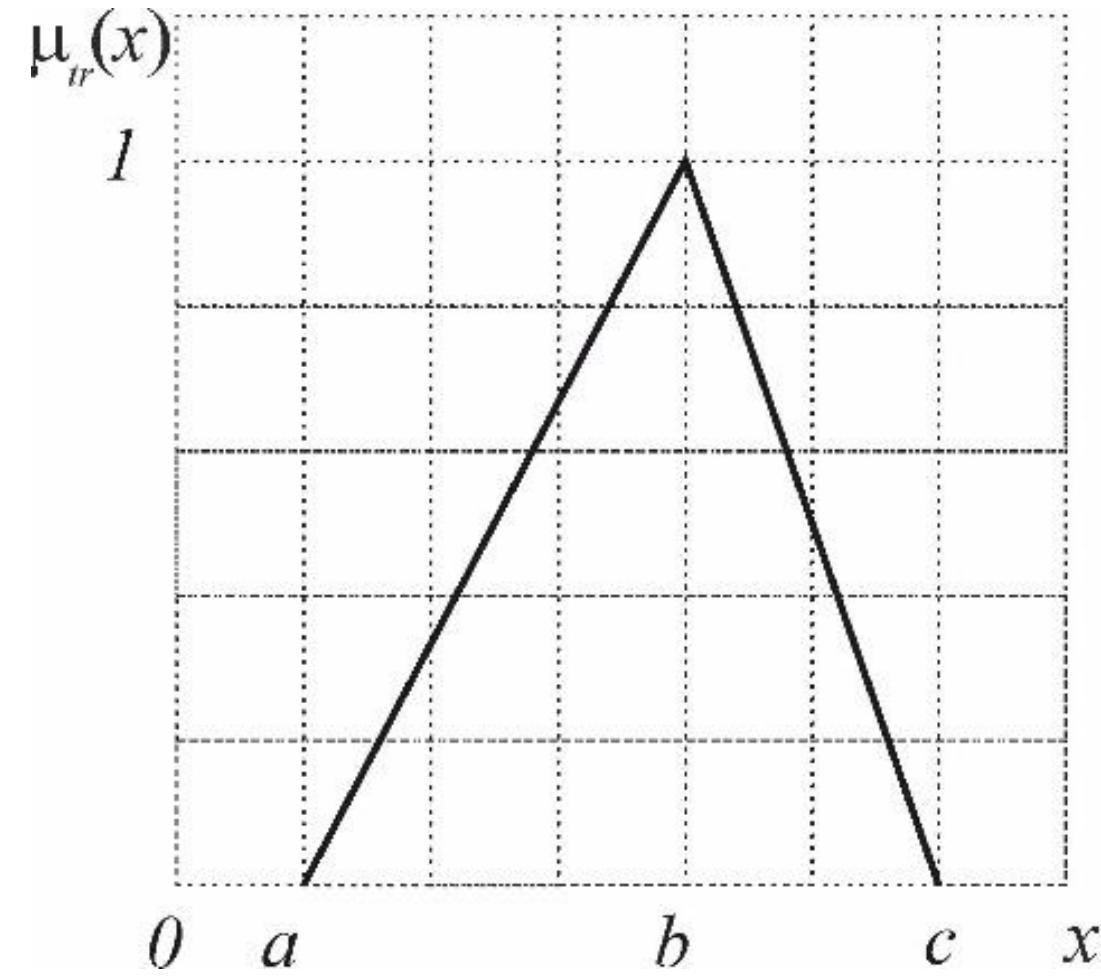
$$A = \sum_U \mu_{NCF}(x) / x$$

Функции принадлежности



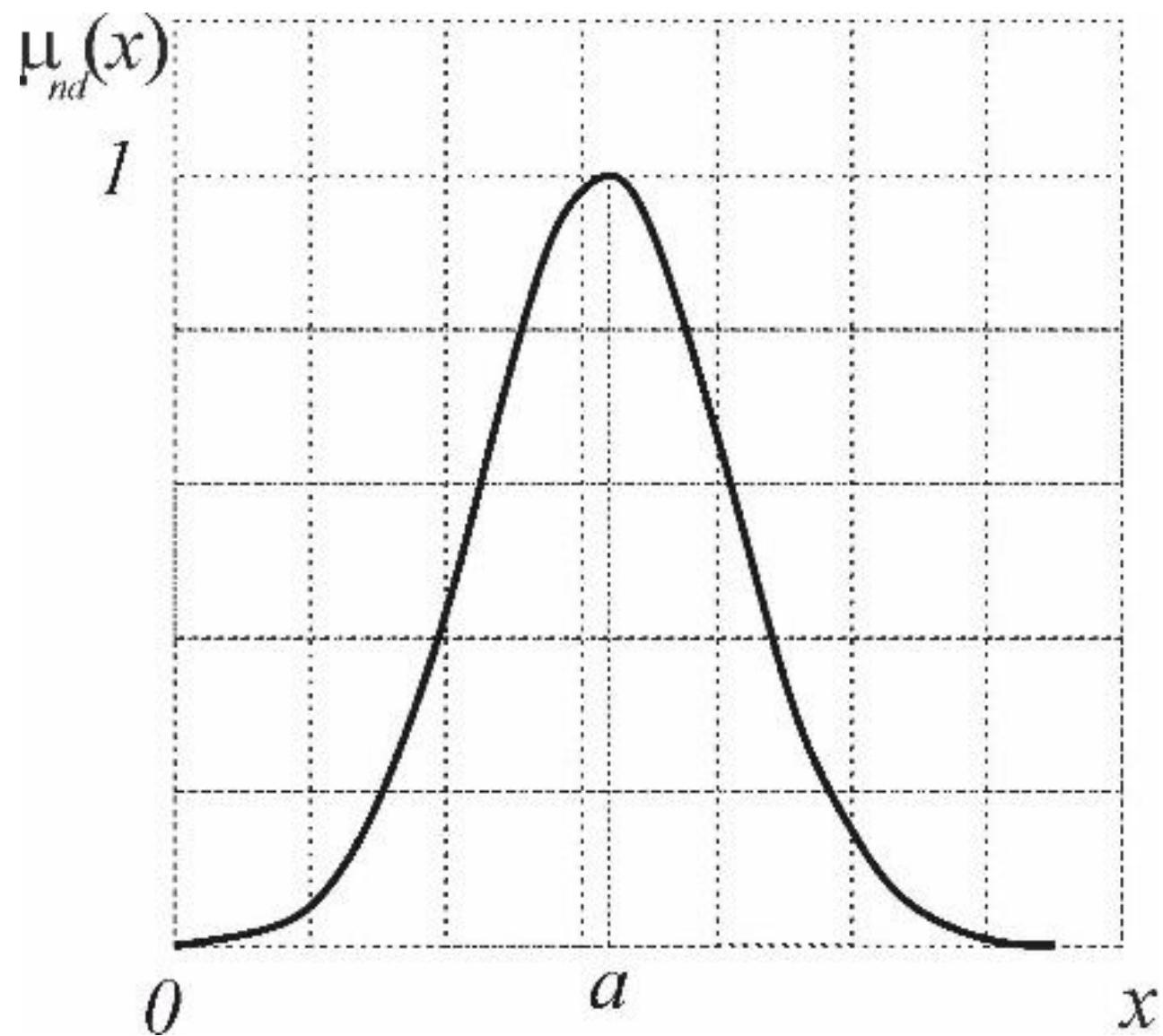
$$A = \int_U \mu(x) / x$$

Функции принадлежности



треугольная

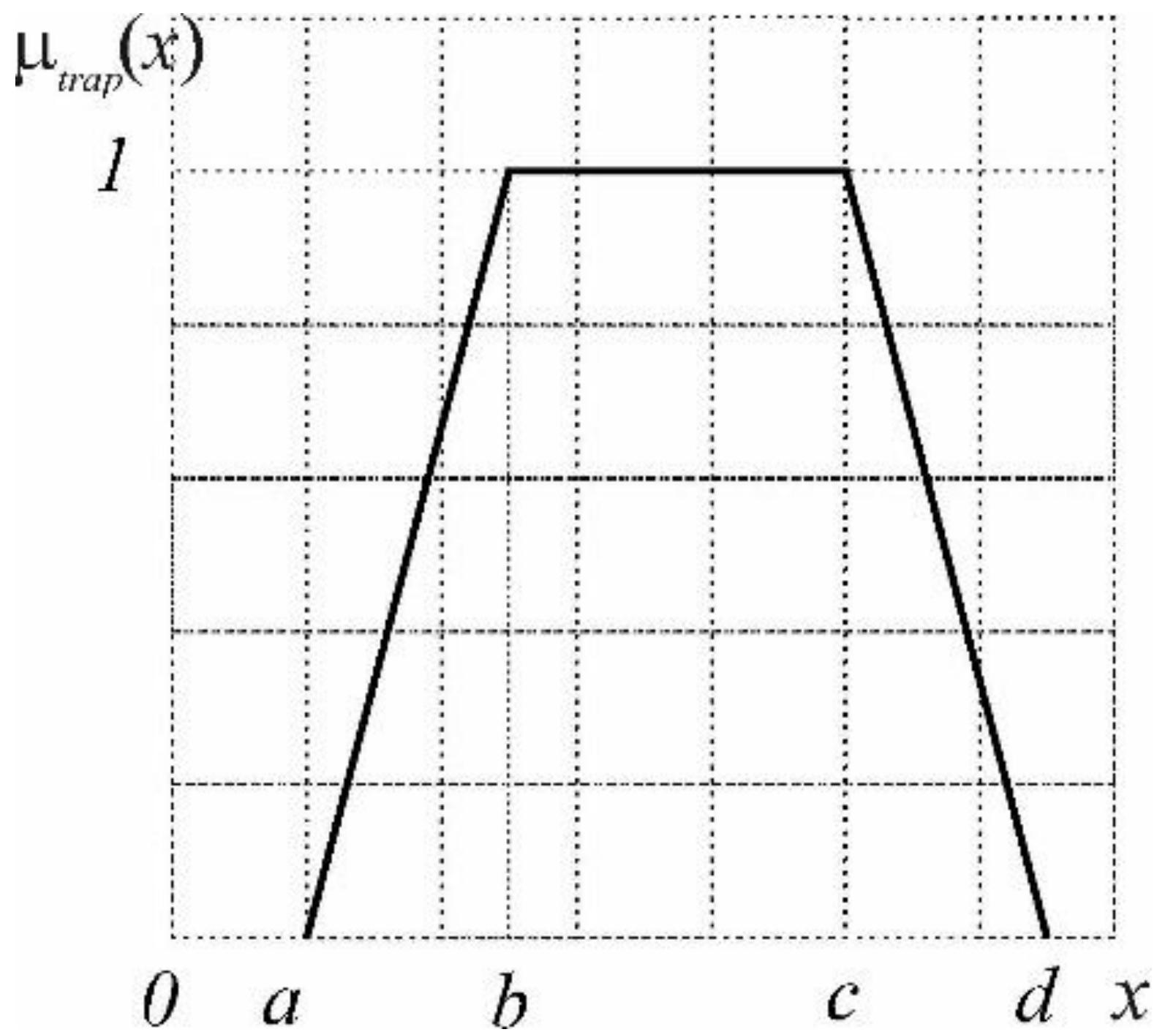
$$\mu_{tr}(x) = \begin{cases} \frac{x-a}{b-a}, & a \leq x < b; \\ \frac{c-x}{c-b}, & b < x \leq c; \\ 0, & x < a \text{ or } x > c. \end{cases}$$



$$\mu_{nd}(x) = e^{-\left(\frac{x-a}{b}\right)^2}, \quad b > 0$$

Нормального распределения

Функции принадлежности

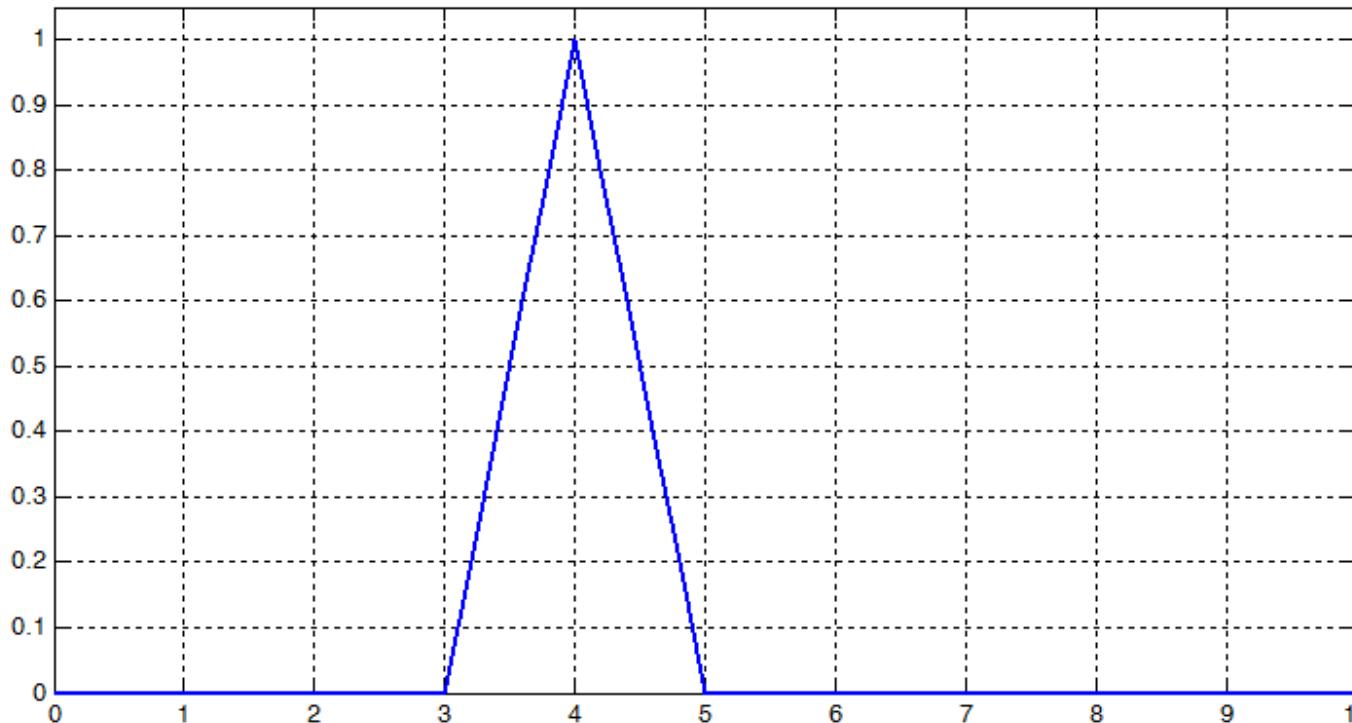


$$\mu_{trap}(x) = \begin{cases} 0, & x < a; \\ \frac{x-a}{b-a}, & a \leq x < b; \\ 1, & b < x \leq c; \\ \frac{d-x}{d-b}, & c < x \leq d; \\ 0, & x > d. \end{cases}$$

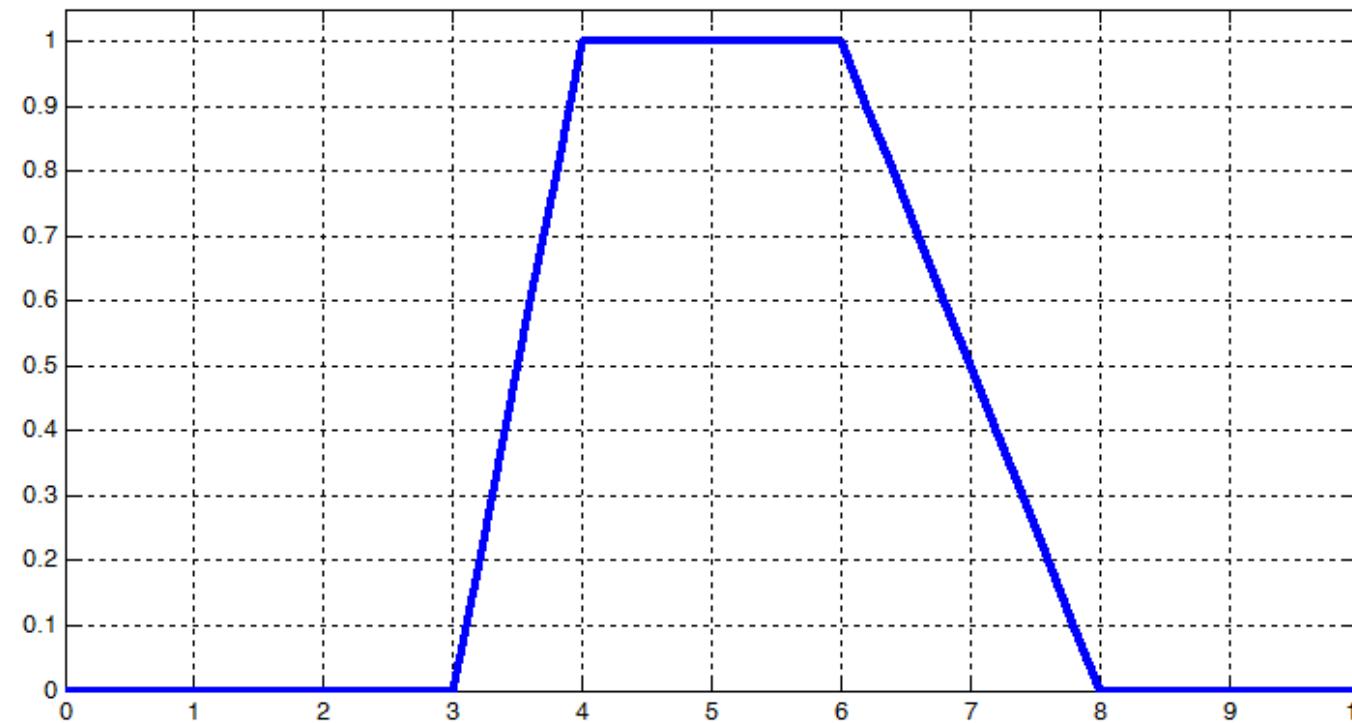
Трапецидальная

Функции принадлежности

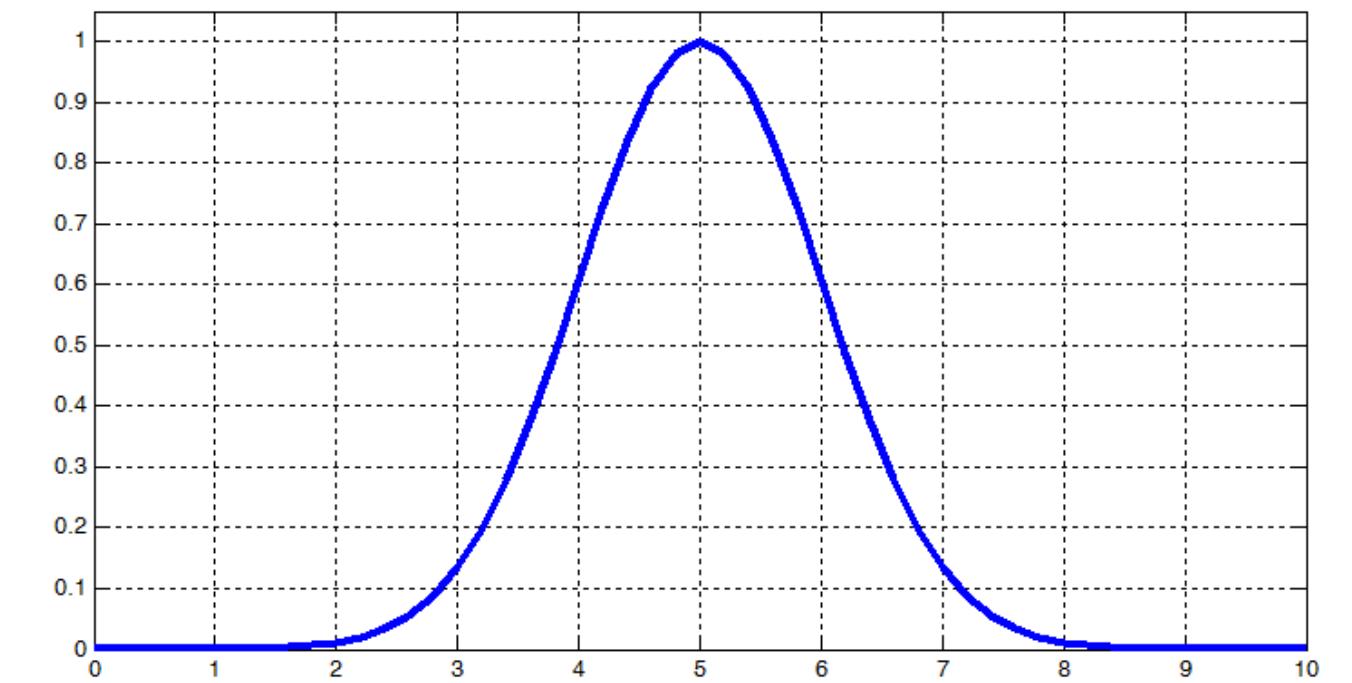
```
>> x = (0:0.2:10);  
>> y = trimf(x, [3 4 5]);  
>> plot(x, y);
```



```
>> y = trapmf(x, [3 4 6 8]);  
>> plot(x, y)
```

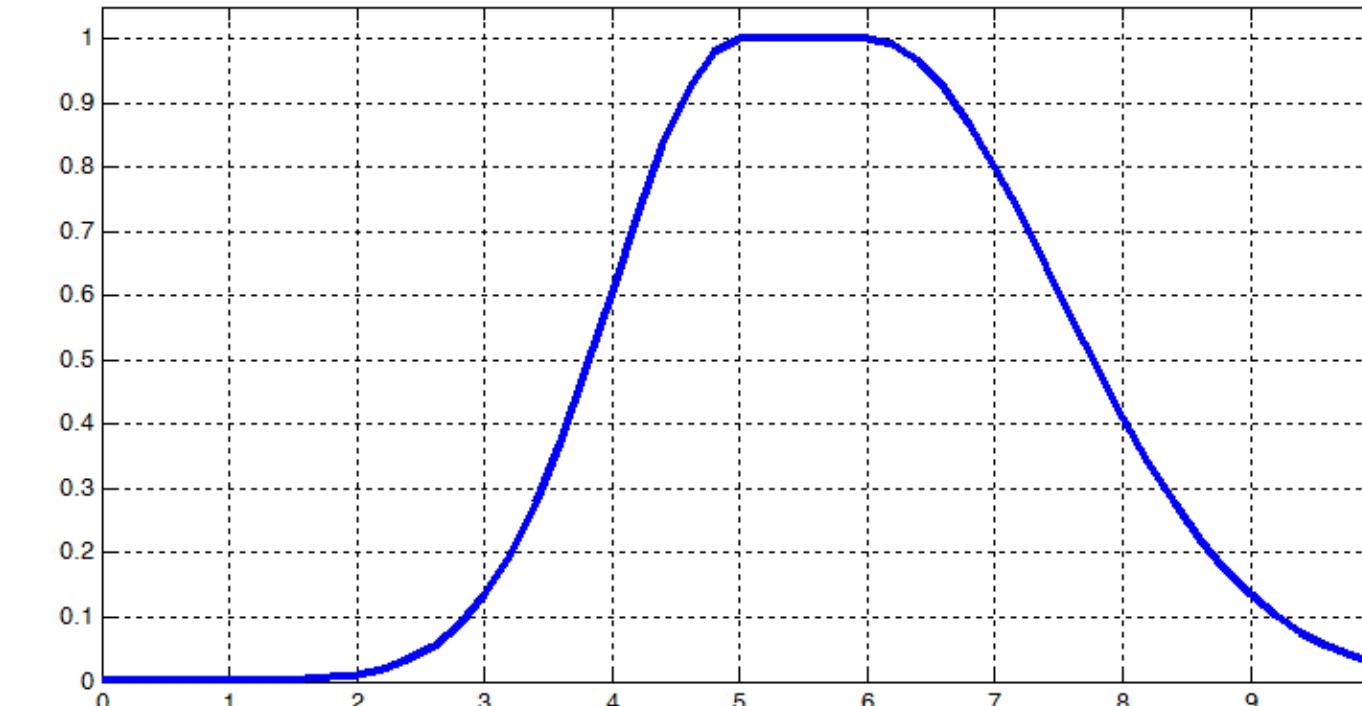


```
>> y = gaussmf(x, [1 5]);  
>> plot(x, y)
```

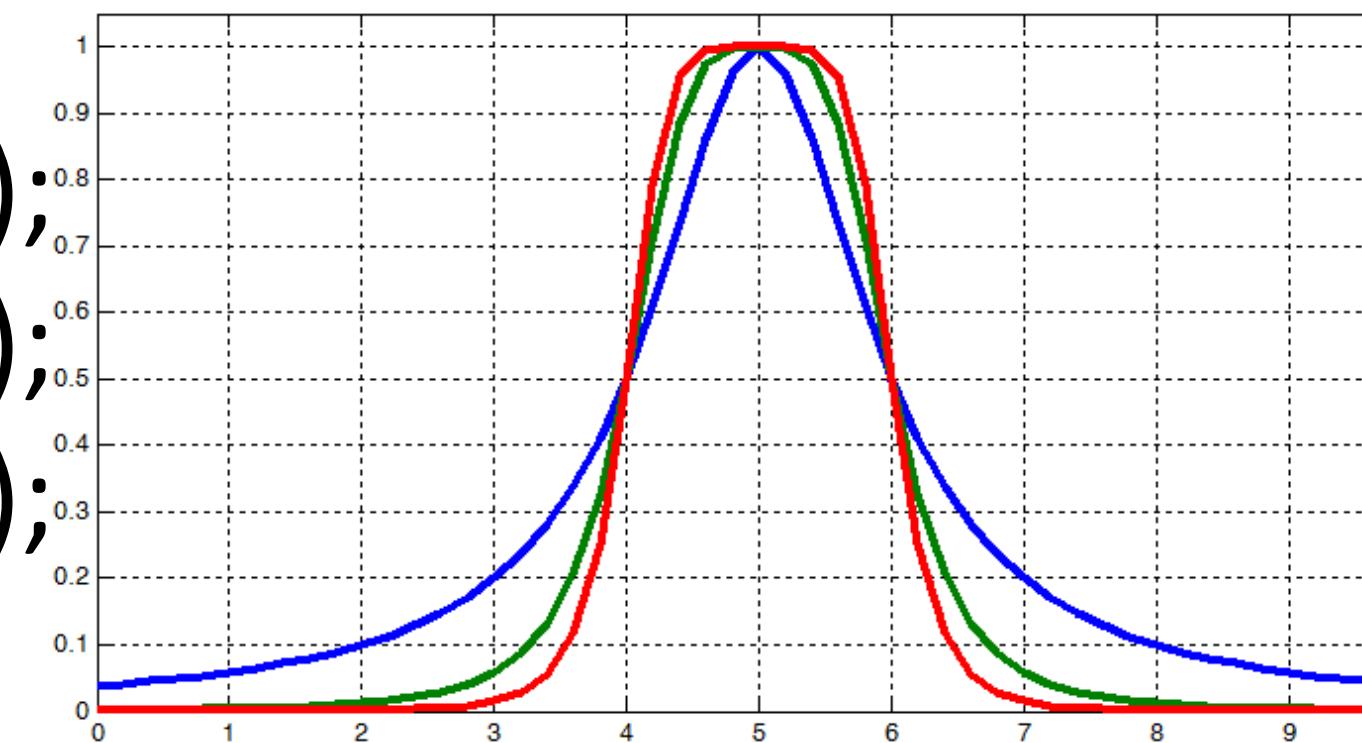


Функции принадлежности

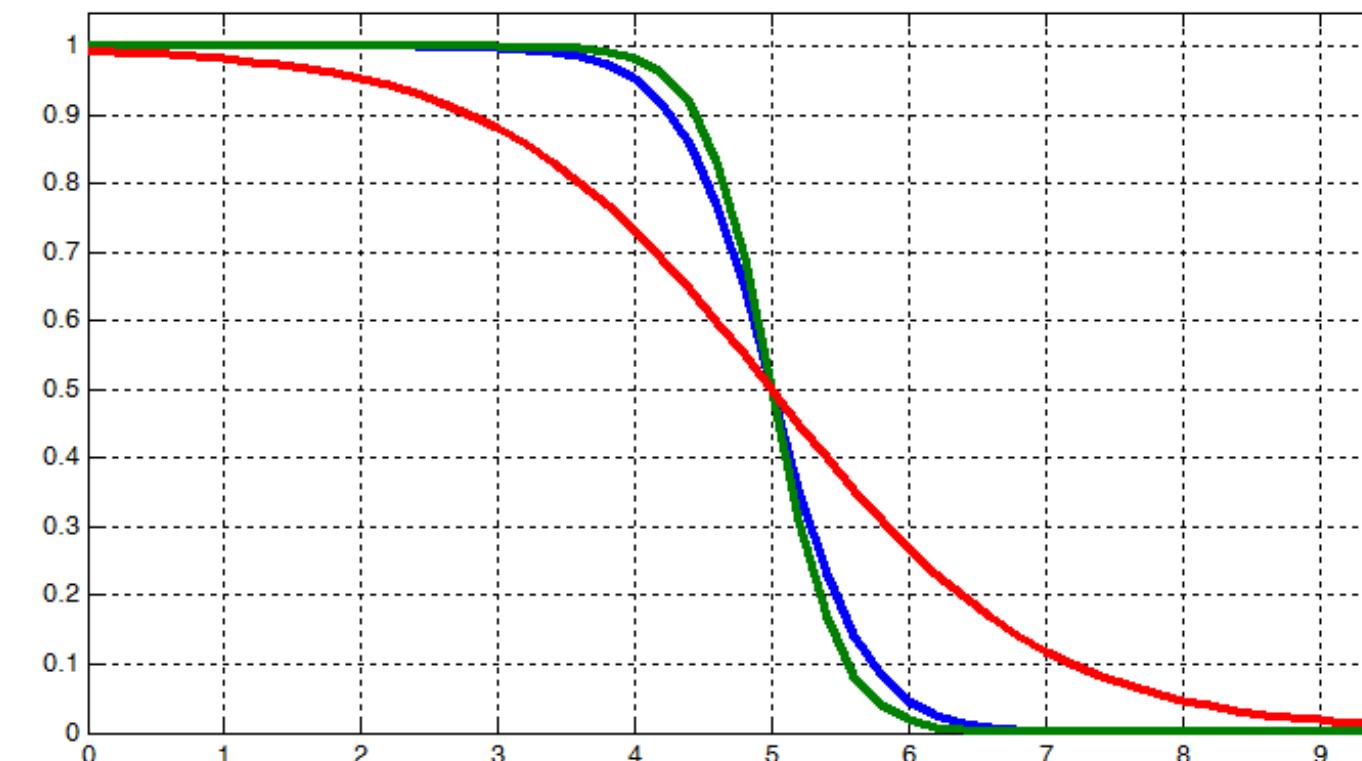
```
>> y = gauss2mf(x, [1 5 1.5 6]);  
>> plot(x, y);
```



```
>> y1 = gbellmf(x, [1 1 5]);  
>> y2 = gbellmf(x, [1 2 5]);  
>> y3 = gbellmf(x, [1 3 5]);  
>> plot(x,y1,x,y2,x,y3);
```

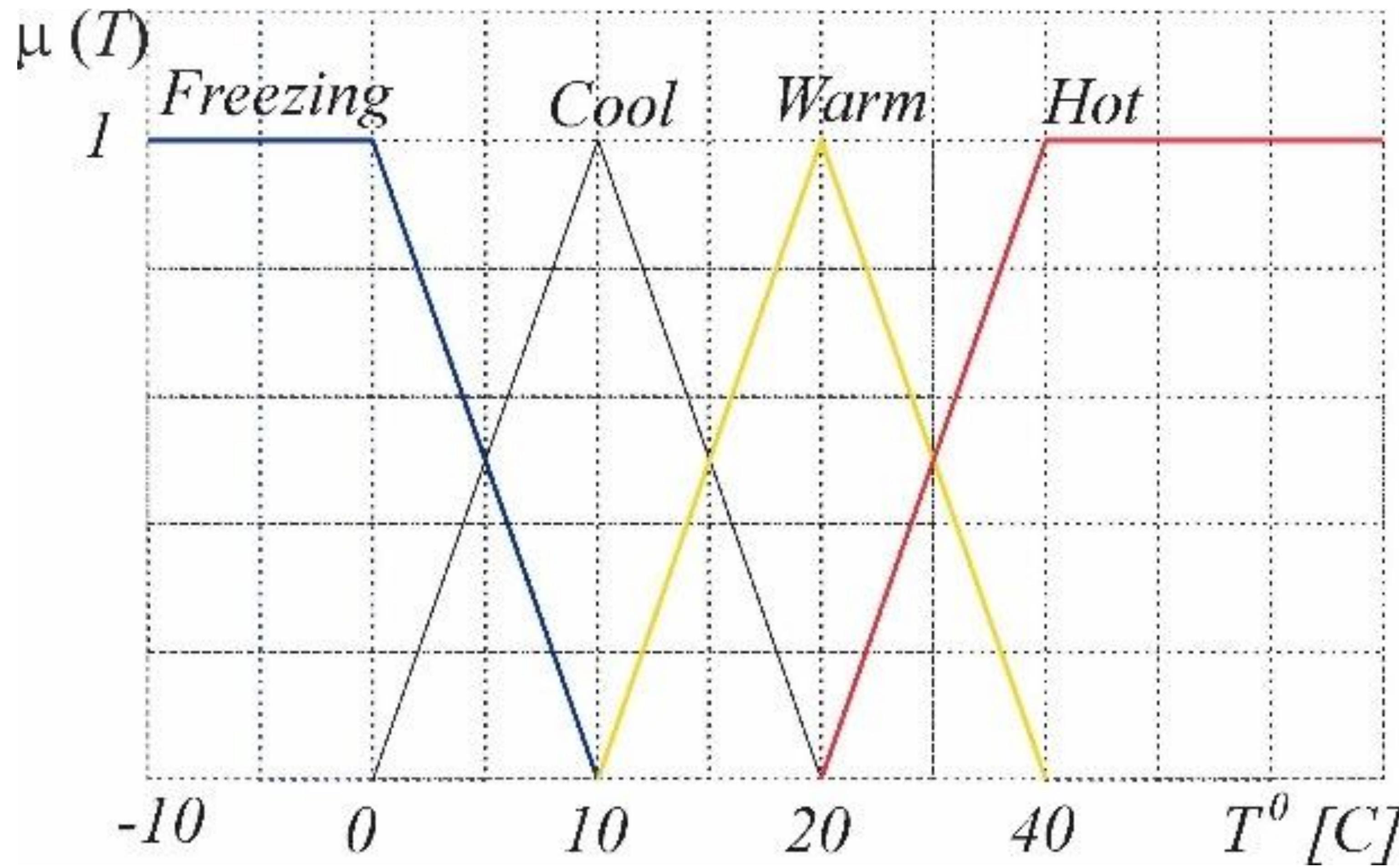


```
>> y1 = sigmf(x, [-3 5]);  
>> y2 = sigmf(x, [-4 5]);  
>> y3 = sigmf(x, [-1 5]);  
>> plot(x,y1,x,y2,x,y3)
```

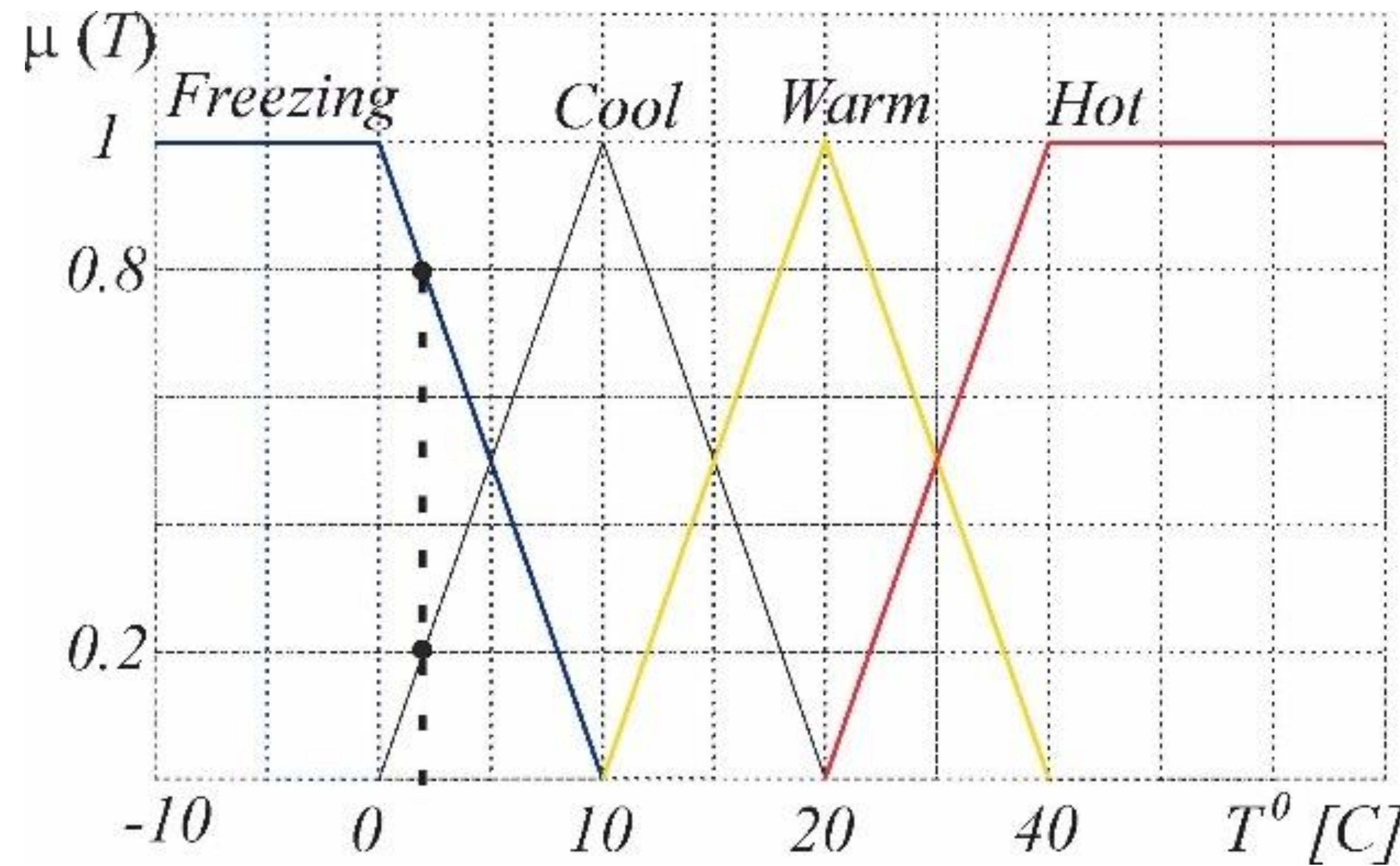


- Нечеткие лингвистические переменные используются для представления качеств, охватывающих определенный спектр.
- Температура: {**Freezing**, **Cool**, **Warm**, **Hot**}
- Функции принадлежности
- Вопрос: Какая температура?
- Ответ: Тепло.
- Вопрос: Сколько это – тепло?

Лингвистические переменные



Лингвистические переменные



20% Cool и 80% Freezing

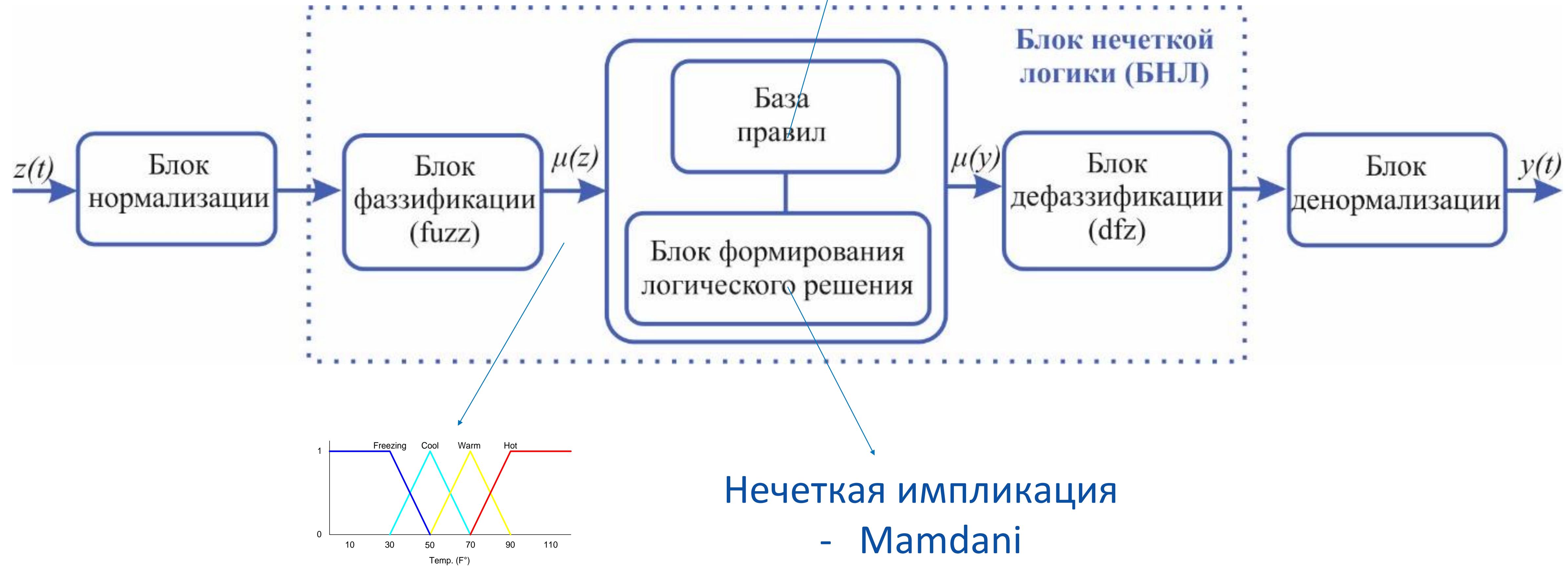
Нечеткие регуляторы строятся на основе правил типа «ЕСЛИ – ТО»:

If x is A then y is B

Здесь A и B нечеткие множества – определенных во множествах X и Y , соответственно – определенные как малый, средний, большой

‘ x is A ’ условие
‘ y is B ’ следствие.

«IF холодно THEN включить обогреватель»



Нечеткая импликация

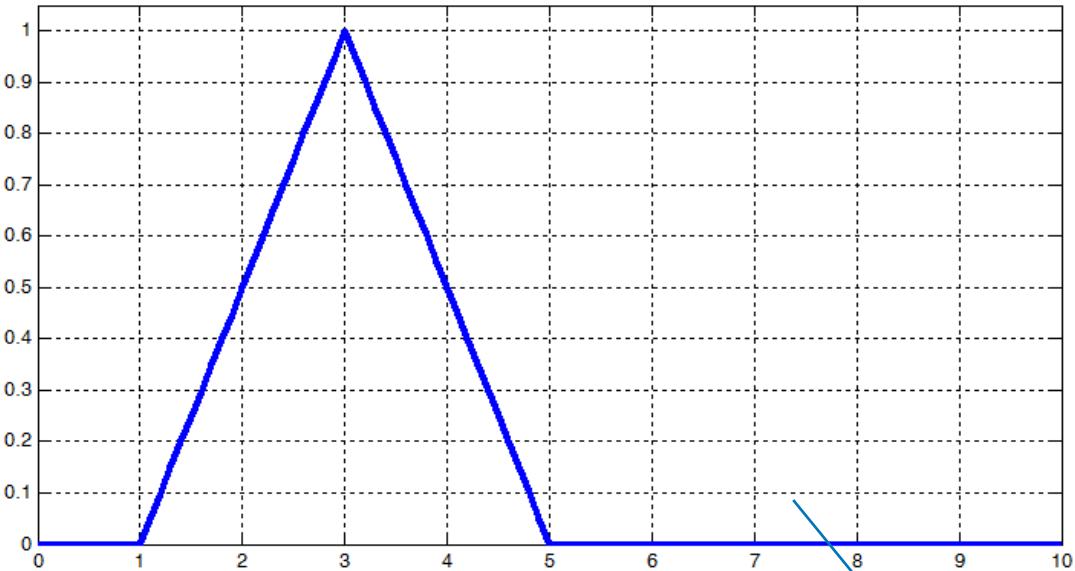
- Mamdani
- Sugeno....

Нечеткая импликация и блок формирования логического решения

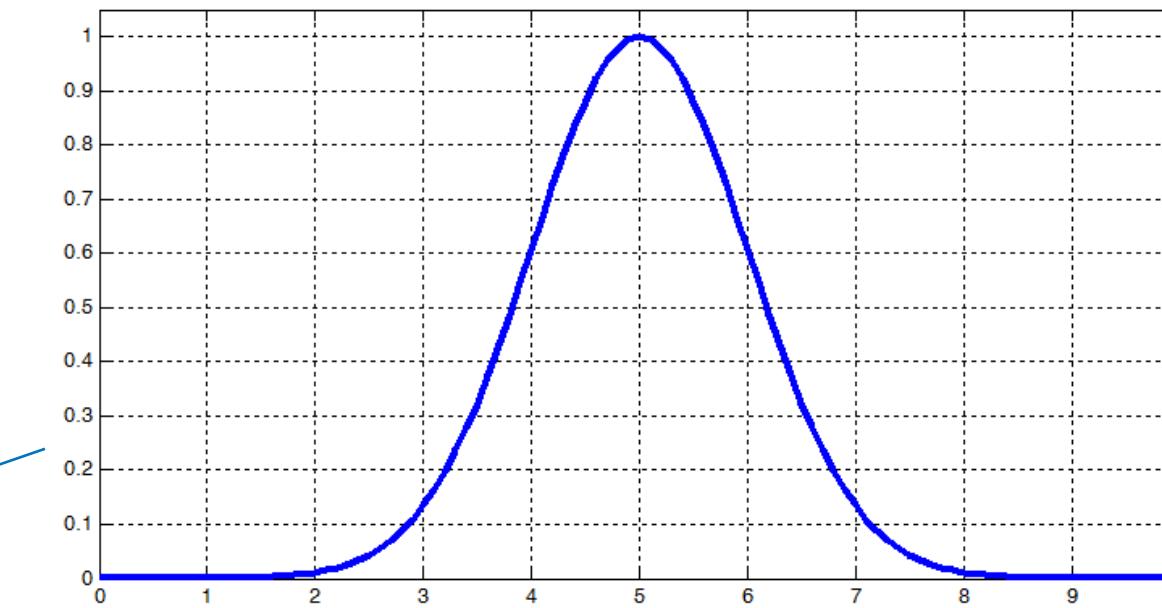
№ _п	Импликация	Формула
1	Mamdani	$I(A, B) = \min(A, B)$
2	Larsen	$I(A, B) = A \cdot B$
3	Yager	$I(A, B) = B^A$
4	Kleene-Dienes	$I(A, B) = \max(1 - A, B)$
5	Gaines	$I(A, B) = \begin{cases} 1, & A \leq B \\ 0, & A > B \end{cases}$
6	Goguen	$I(A, B) = \begin{cases} 1, & A = 0 \\ \min\left(\frac{B}{A}, 1\right), & A \neq 0 \end{cases}$

Нечеткая импликация

```
>> x = (0:0.1:10);  
>> y = trimf(x, [1 3 5]);  
>> plot(x, y);
```

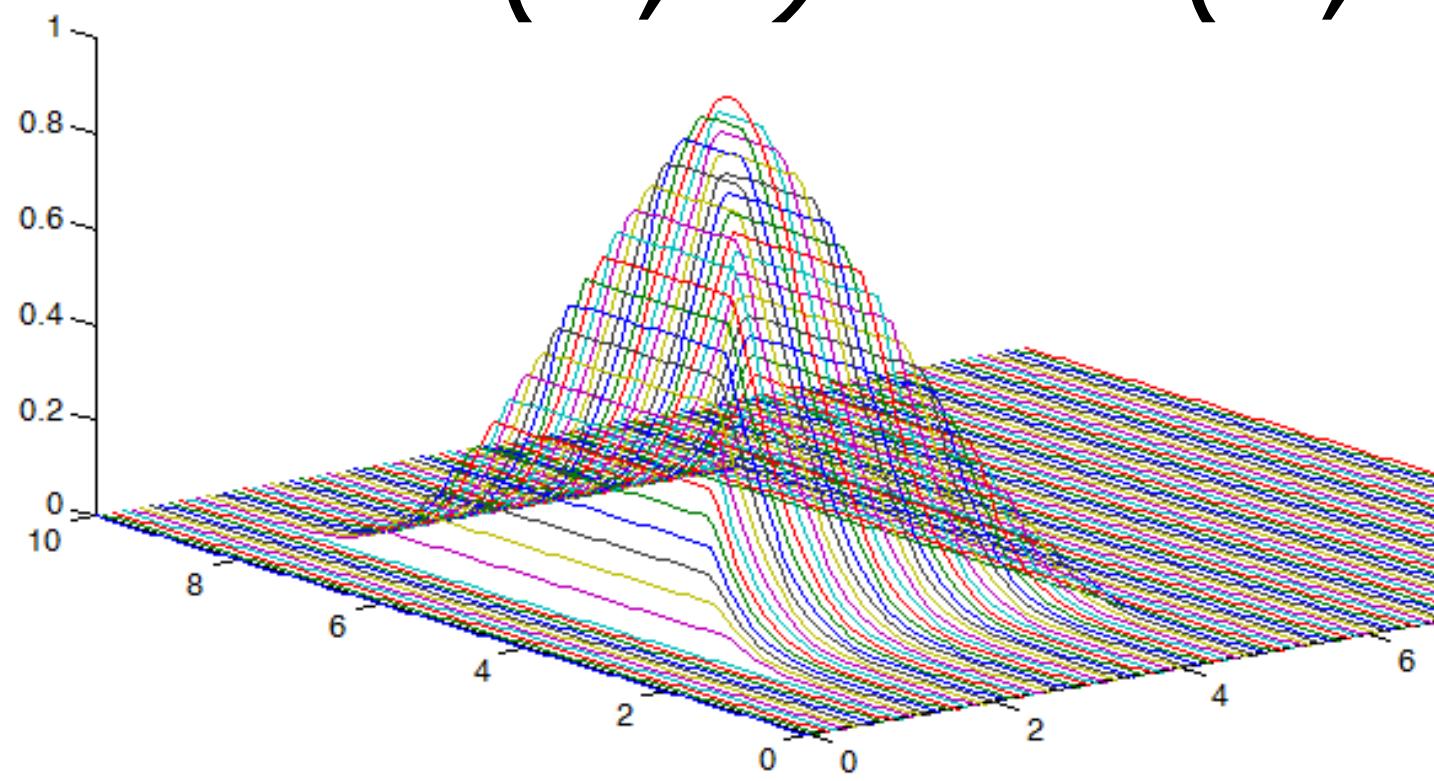


```
>> x = (0:0.1:10);  
>> y = gaussmf(x, [1 5]);  
>> plot(x, y);
```

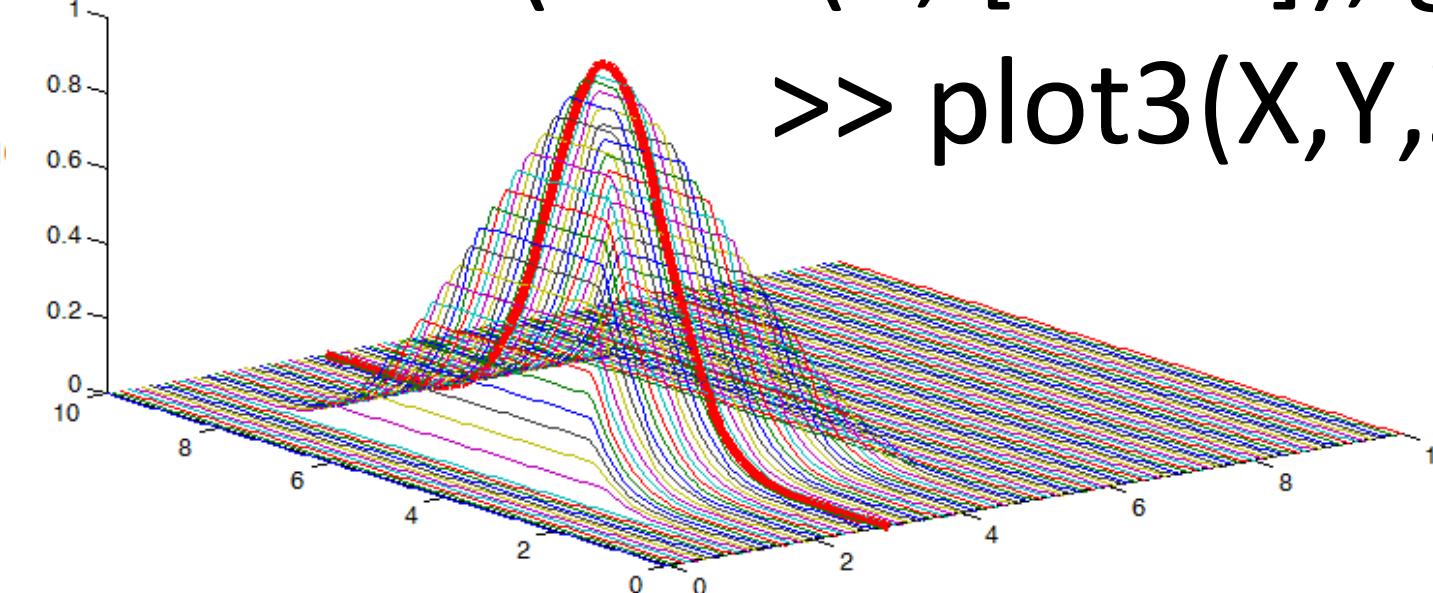


Mamdani Algorithm
If A then B

$$I(A, B) = \min(A, B)$$



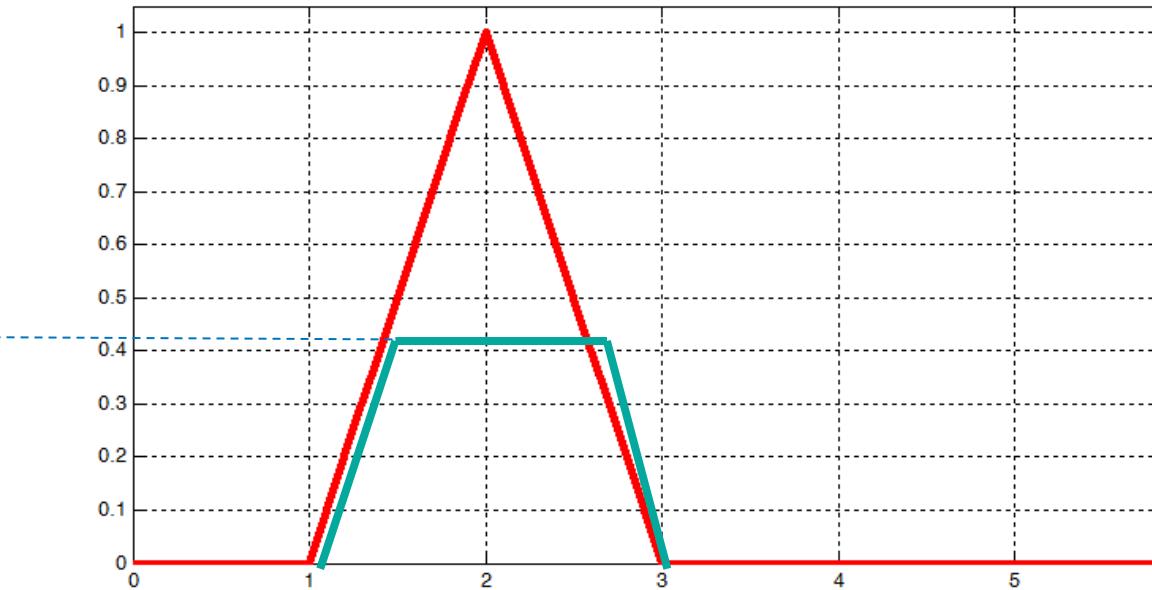
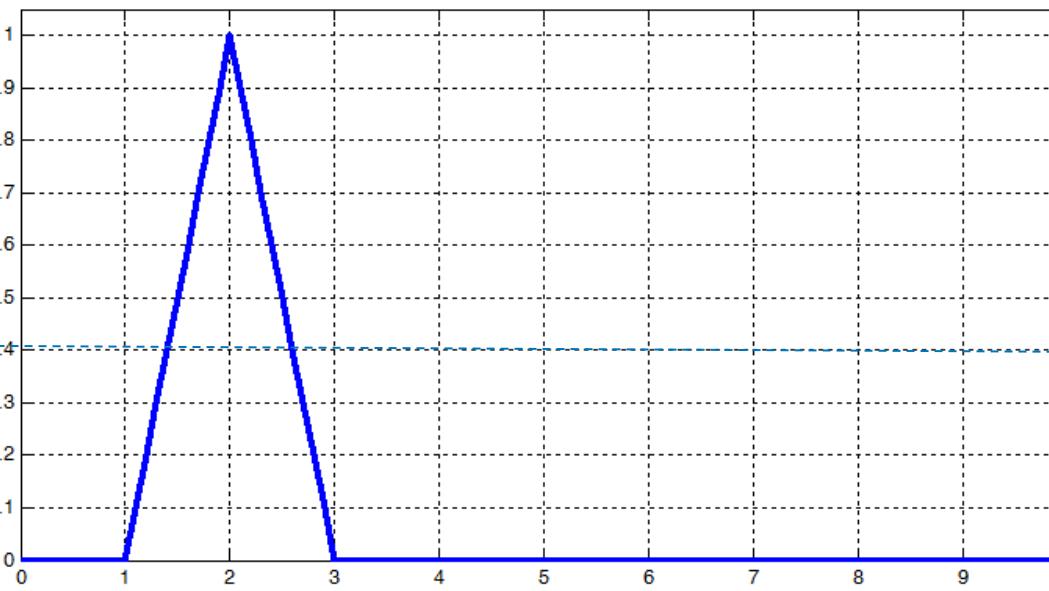
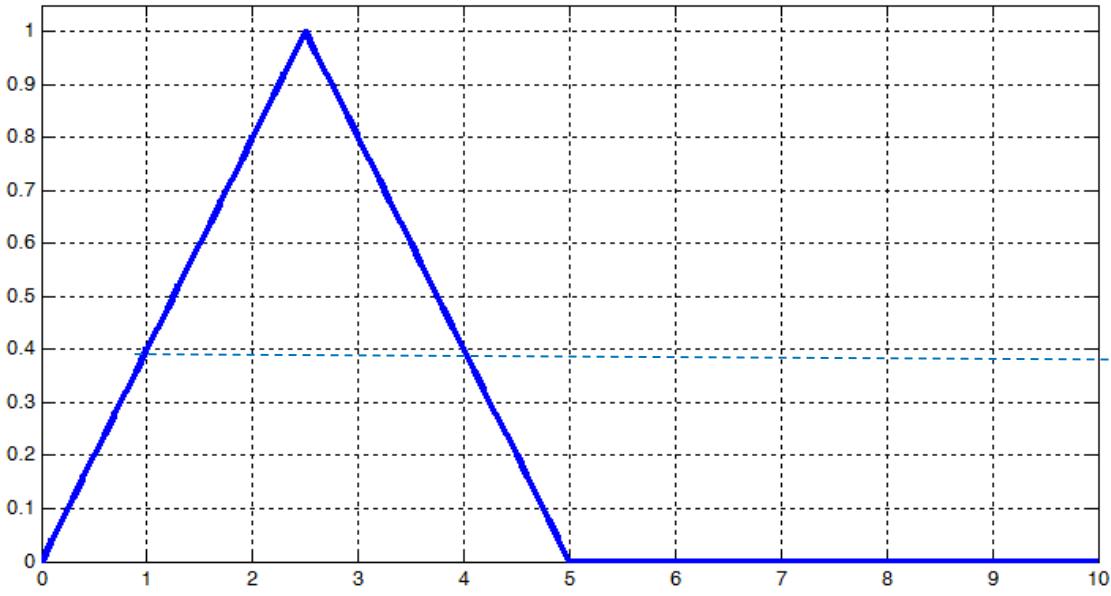
```
>> x1 = (0:0.1:10);  
>> x2 = (0:0.1:10);  
>> [X, Y] = meshgrid(x1, x2);  
>> Z = min(trimf(X, [1 3 5]), gaussmf(Y, [1 5]));  
>> plot3(X, Y, Z)
```



Нечеткая импликация

Mamdani Algorithm

If A then B

$$I(A,B) = \min(A,B)$$


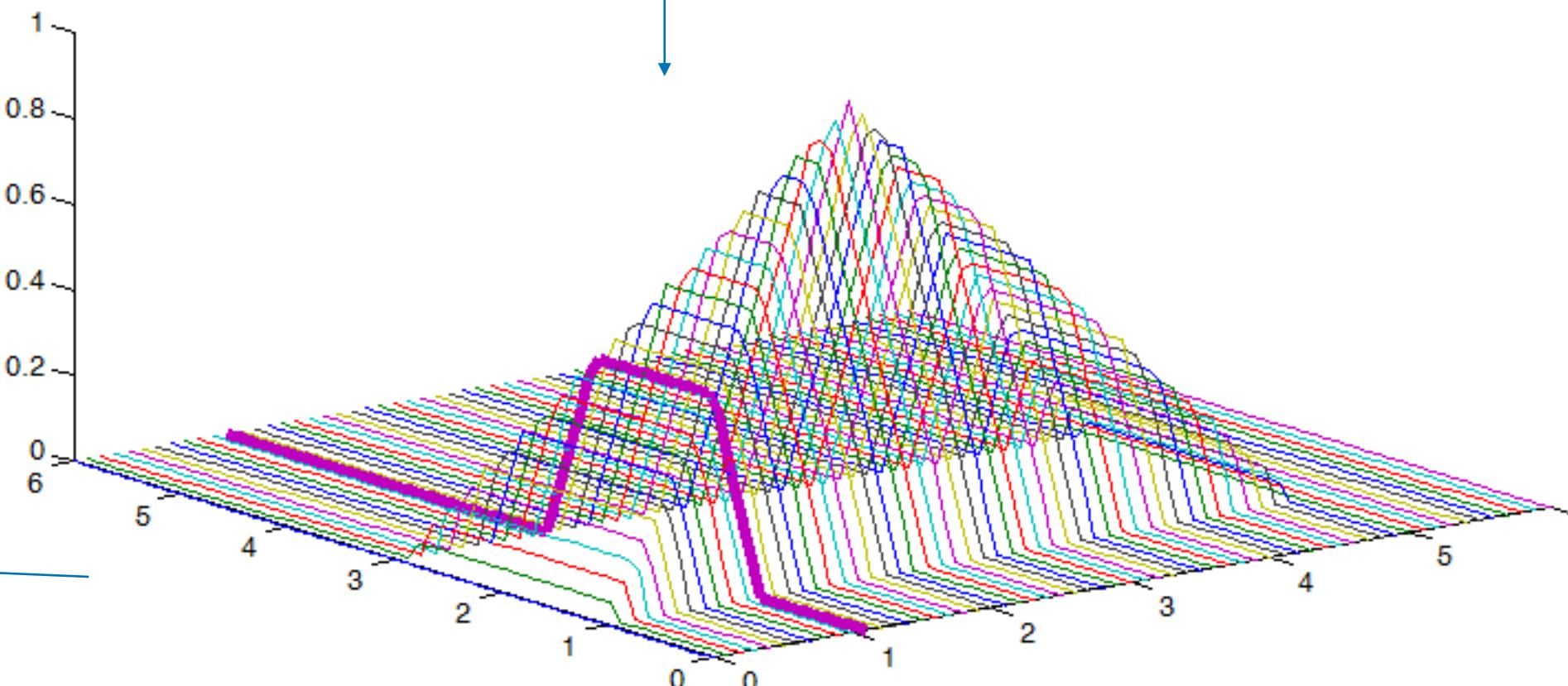
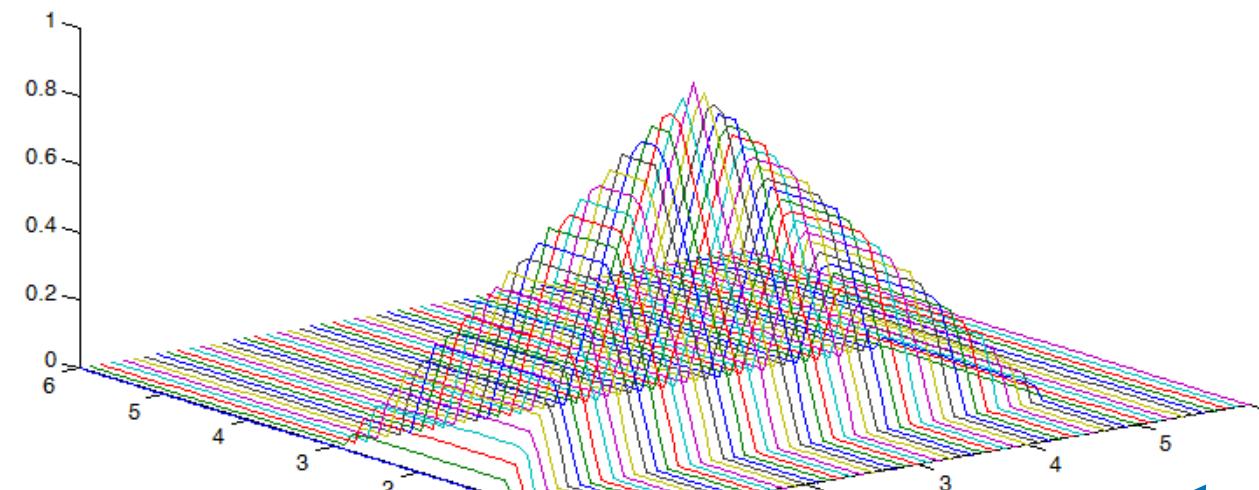
```
>> x = (0:0.1:10);
```

```
>> y = trimf(x, [0 2.5 5]);  
>> plot(x, y);
```

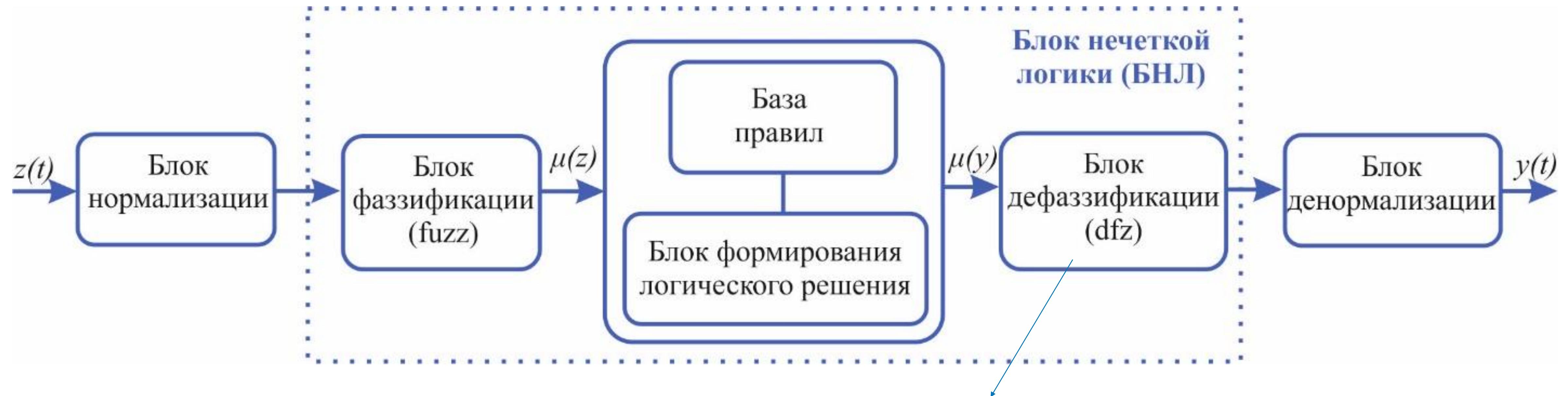
```
>> x = (0:0.1:10);
```

```
>> y = trimf(x, [1 2 3]);  
>> plot(x, y);
```

```
>> x2 = (0:0.1:6);  
>> x1 = (0:0.1:6);  
>> [X, Y] = meshgrid(x1, x2);  
>> Z = min(trimf(X,[0 2.5 5]),trimf(Y,[1 2 3]));  
>> plot3(X,Y,Z)
```



Нечеткая логика



Centre of gravity (cog)
Center of Area (coa)
Mean of maximum (mom)
Indexed defuzzification methods (idfz)

Дефазификация

Centre of gravity (cog)

$$z_{cog}(B) = \frac{\int \mu_B(z) \cdot z dz}{\int \mu_B(z) dz} - \text{continuous}$$

$$z_{cog}(B) = \frac{\sum_{i=1}^N \mu_B(z_i) \cdot z_i}{\sum_{i=1}^N \mu_B(z_i)} - \text{discrete}$$

$$z_{jcog}(B) = \frac{\int \mu_B(z_1 \dots z_n) \cdot z_j dz_1 \dots dz_n}{\int \mu_B(z_1 \dots z_n) dz_1 \dots dz_n} - n\text{-continuous}$$

Center of Area (coa)

$$z_{1coa}(B) = \int_{\inf z_2}^{\sup z_2} \int_{\inf z_1}^{\sup z_1} \mu_B(z_1, z_2) dz_1 dz_2 = \int_{\inf z_2}^{\sup z_2} \int_{z_{1coa}(B)}^{\sup z_1} \mu_B(z_1, z_2) dz_1 dz_2,$$

$$z_{2coa}(B) = \int_{\inf z_2}^{z_{2coa}(B)} \int_{\inf z_1}^{\sup z_1} \mu_B(z_1, z_2) dz_1 dz_2 = \int_{z_{2coa}(B)}^{\sup z_2} \int_{\inf z_2}^{\sup z_1} \mu_B(z_1, z_2) dz_1 dz_2.$$

defuzzification

Mean of maximum (mom)

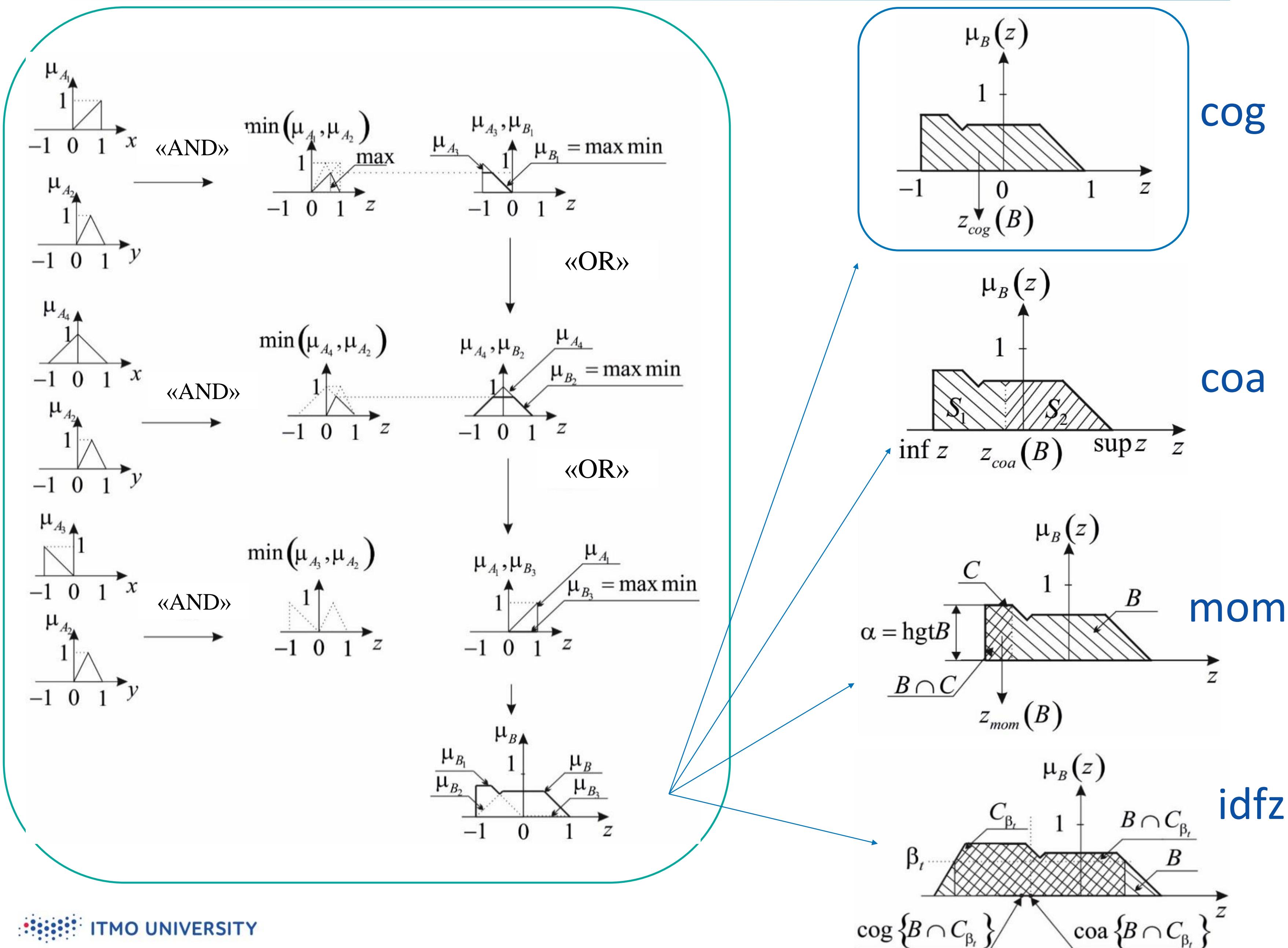
$$z_{mom}(B) = \text{cog}\{B \cap C\}, \quad C = \alpha - \text{cut}B|_{\alpha=\text{hgt}B}$$

Indexed defuzzification methods (idfz)

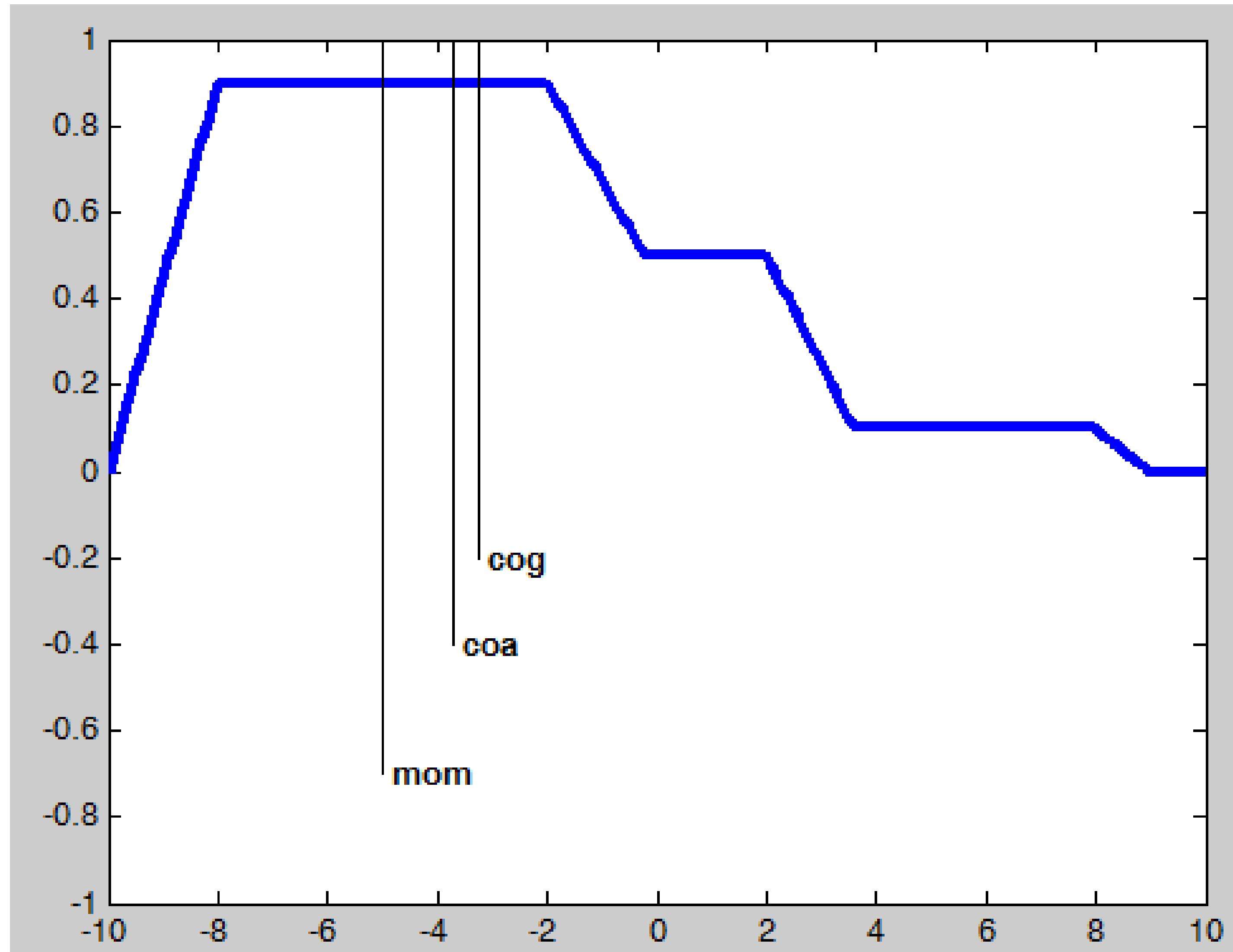
$$z_{idfz}(B, \beta_t) = \text{cog}\{B \cap C_{\beta_t}\}, \quad C_{\beta_t} = \alpha - \text{cut}B|_{\alpha=\beta_t}$$

$$z_{idfz}(B, \beta_t) = \text{coa}\{B \cap C_{\beta_t}\}, \quad C_{\beta_t} = \alpha - \text{cut}B|_{\alpha=\beta_t}$$

Дефазификация



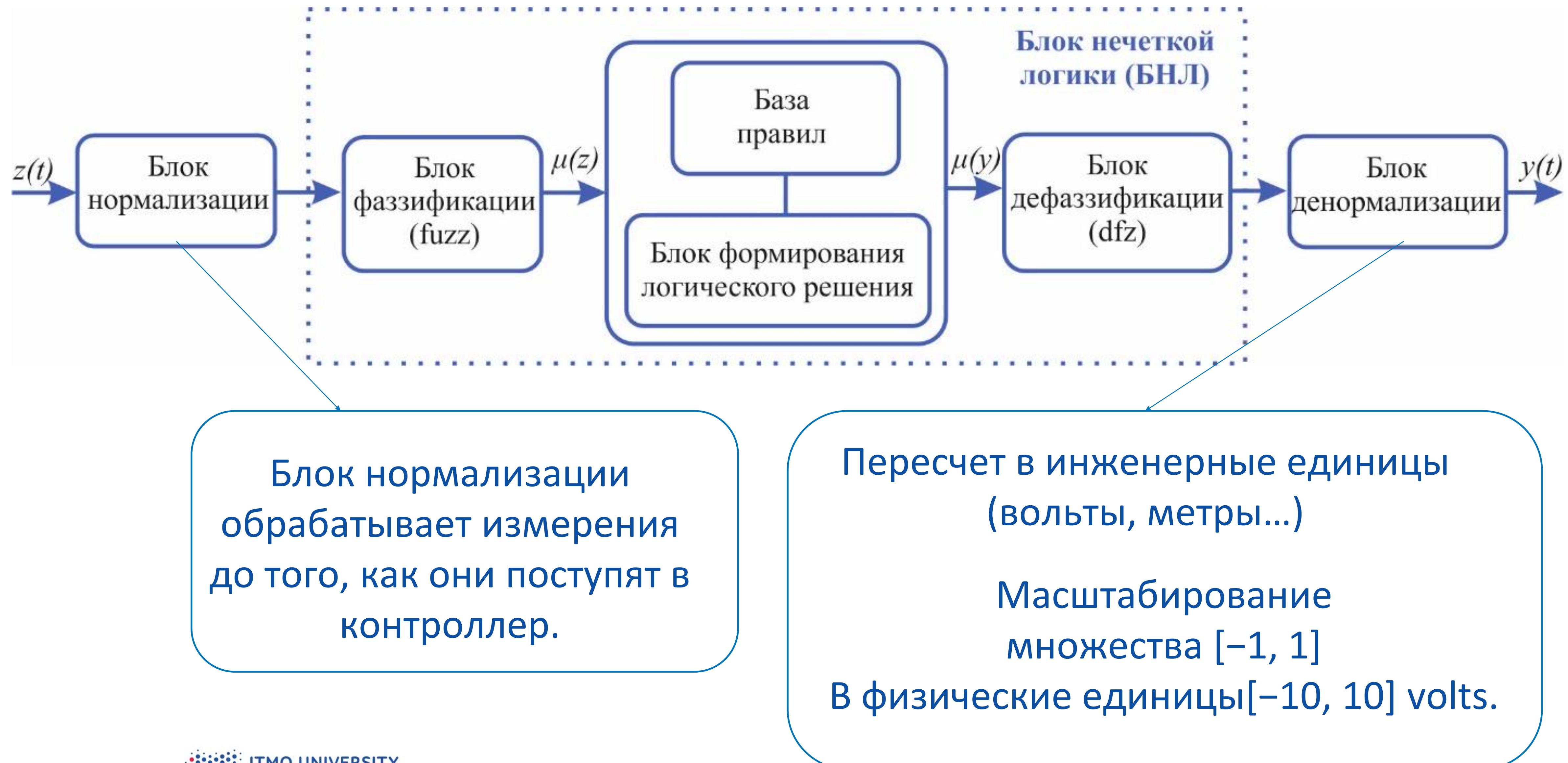
Дефазификация



Использование разных методов дефазификации при решении задачи «примерно 5»

Название метода		$dfzB$	$Idfz (B, \beta=0,5)$
Centre of gravity (cog)	continuous	$4\frac{4}{9}$	$4\frac{4}{29}$
	discrete	$4\frac{4}{9}$	3
Center of Area (coa)		$4\frac{1}{2}$	$4\frac{1}{16}$
Mean of maximum (mom)		$3\frac{1}{2}$	$3\frac{1}{2}$

Нечеткая логика



Нечеткие правила

Ошибка – $e(t)$

Изменение ошибки – de/dt

Управление – $u(t)$

if-then формат

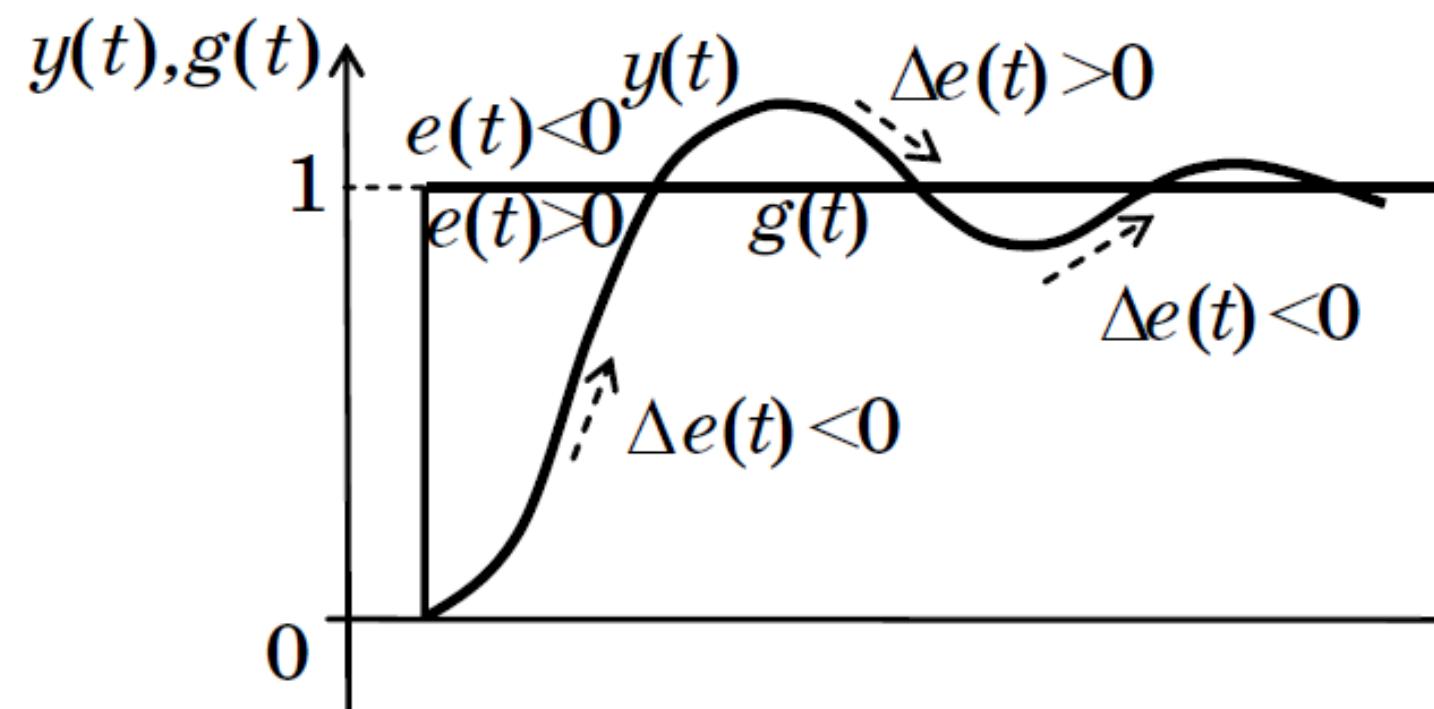
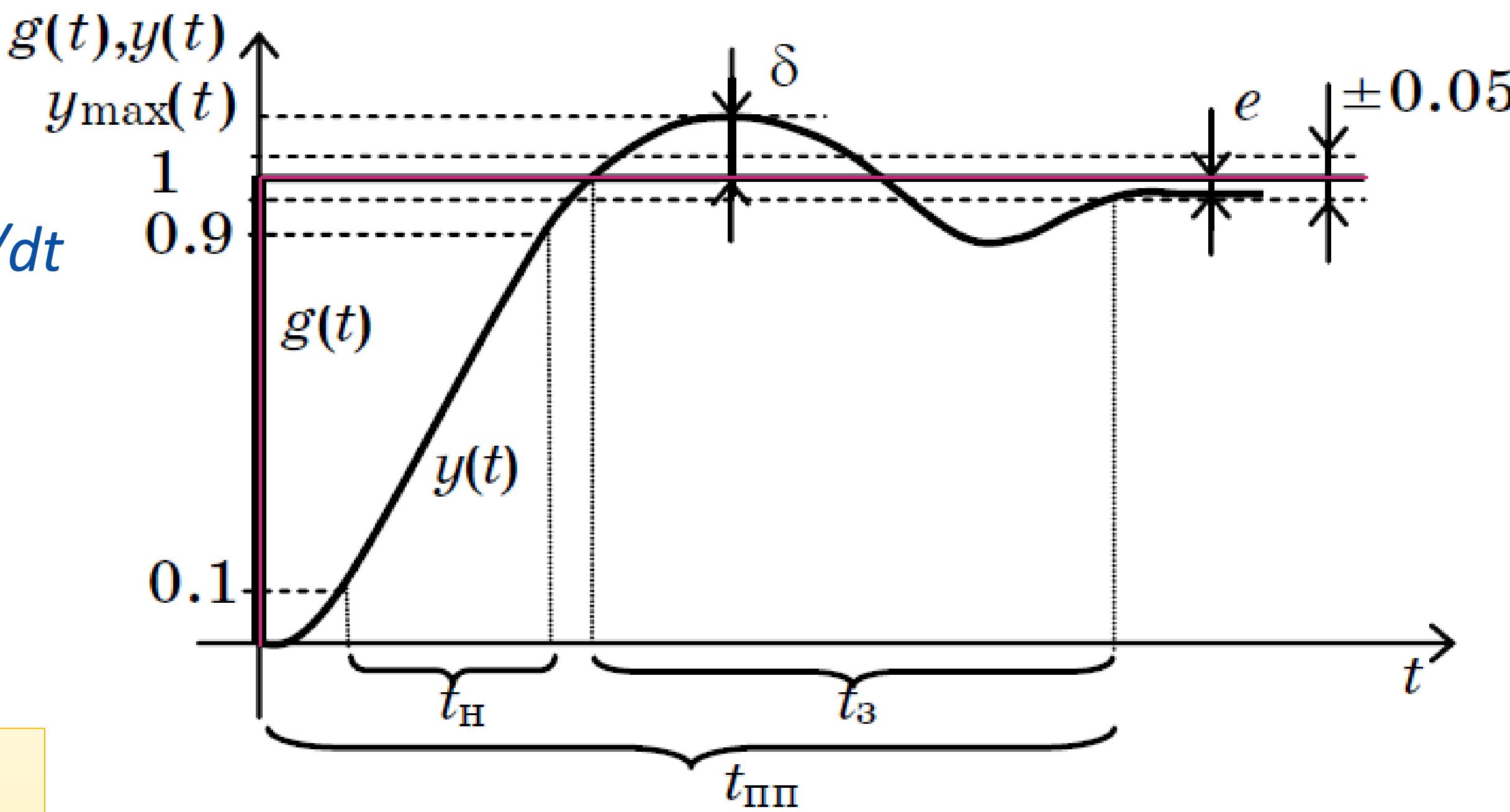
Ошибка. Изменение ошибки, управление :

negative big - NB

negative – N

positive – P

positive big - PB

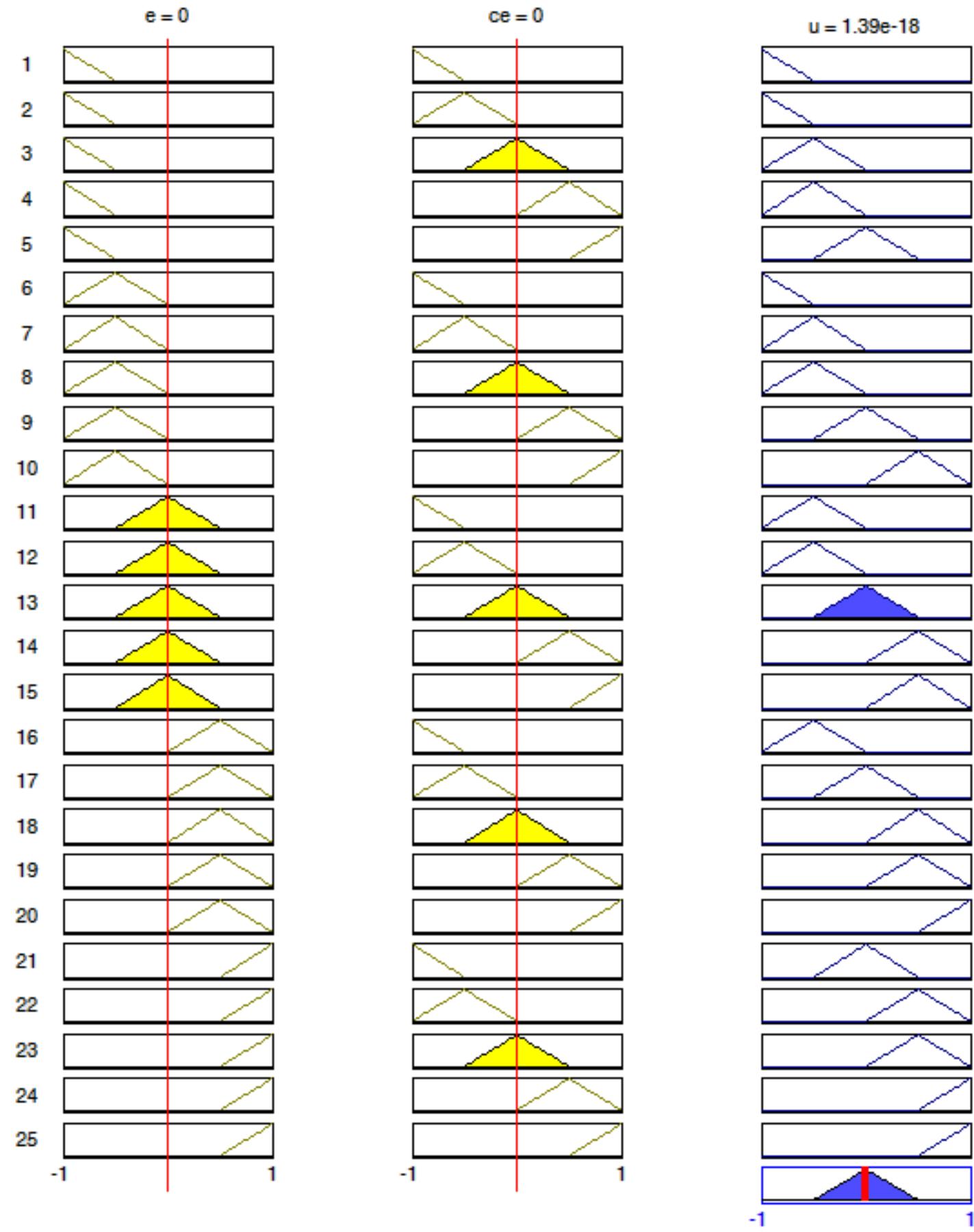


Example:

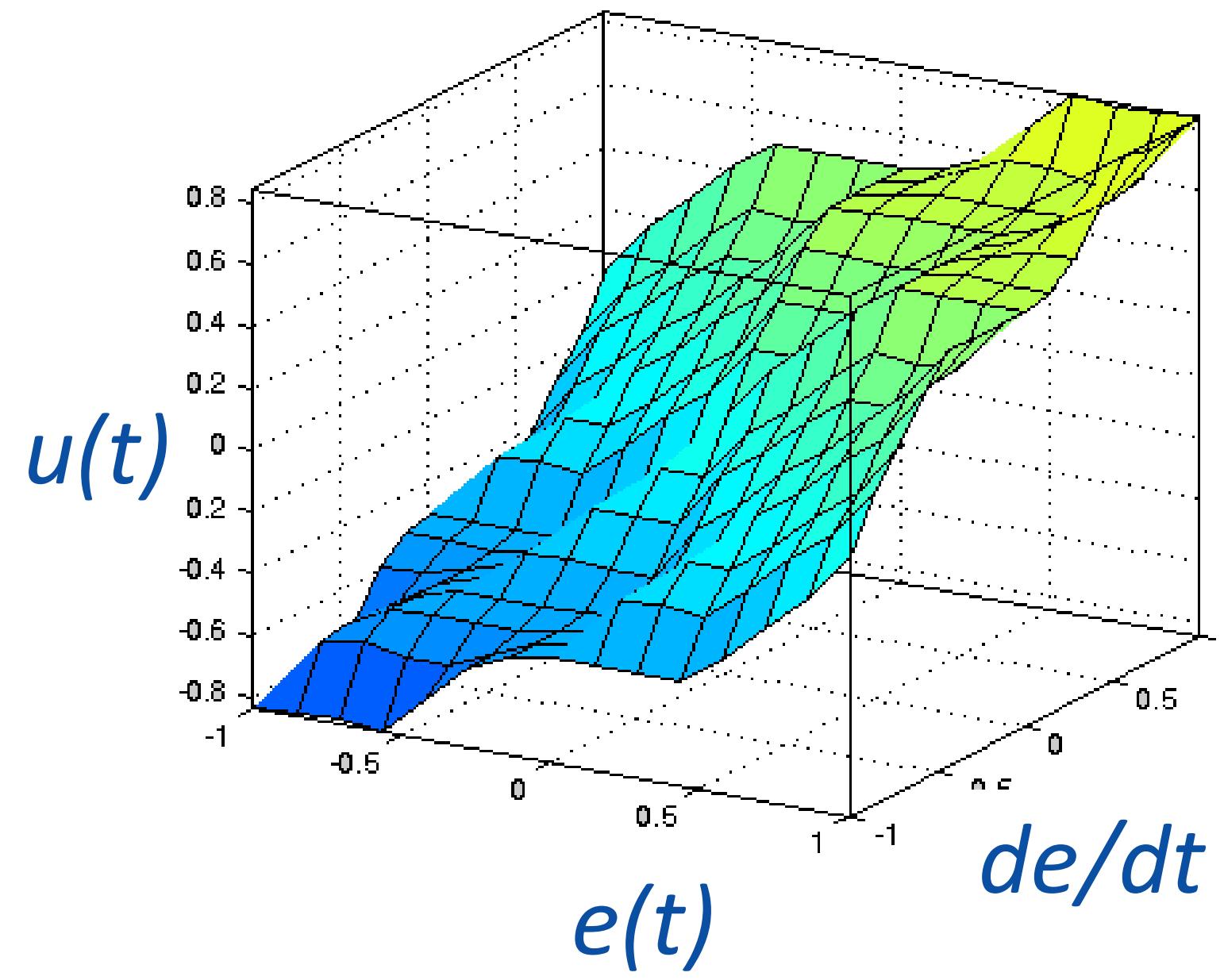
If ошибка Big Neg и изменение ошибки Big Neg
then управление Big Neg

....

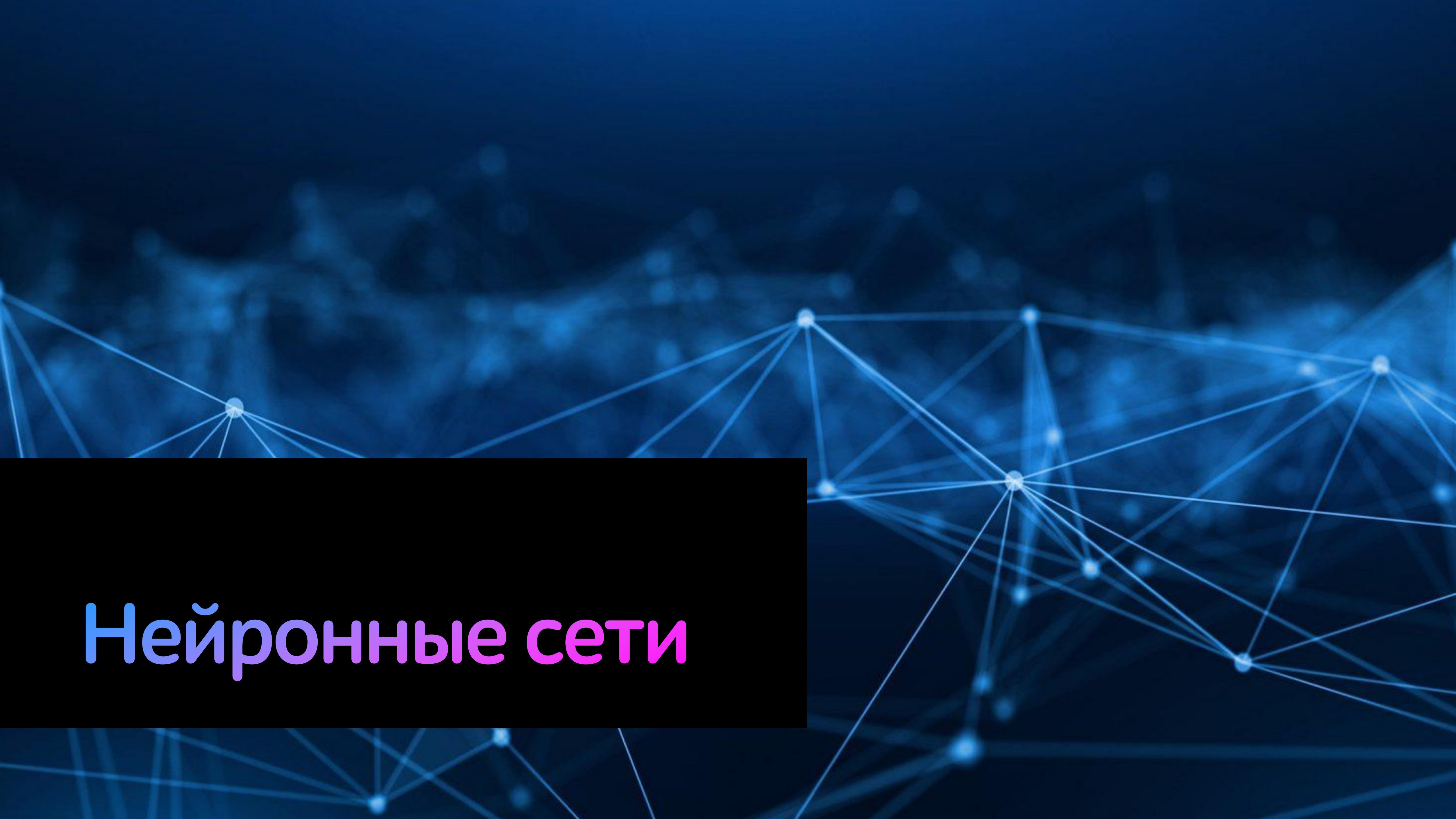
Нечеткие правила



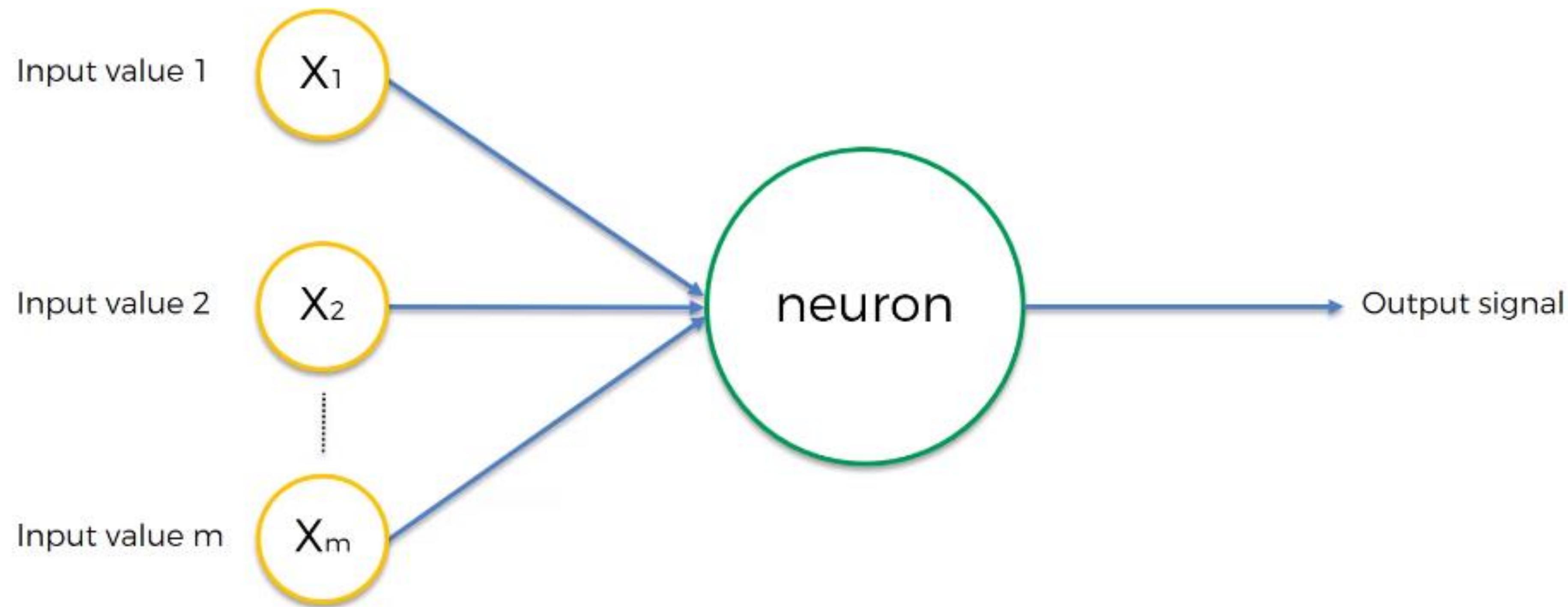
$\mu_{\Delta e}$	BN	N	Z	P	BP
μ_e	BN	BN	N	N	Z
BN	BN	BN	N	N	Z
N	BN	N	N	Z	P
Z	N	N	Z	P	P
P	N	Z	P	P	BP
BP	Z	P	P	BP	BP



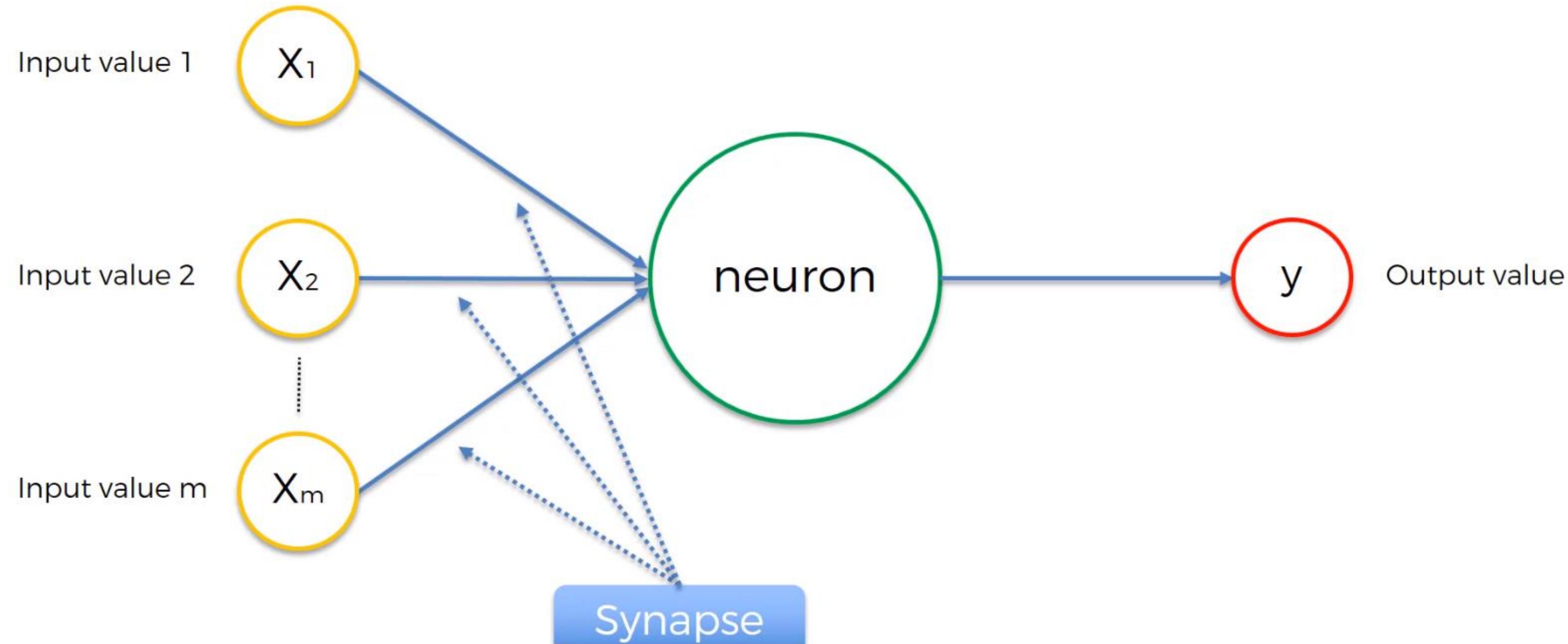
Нейронные сети



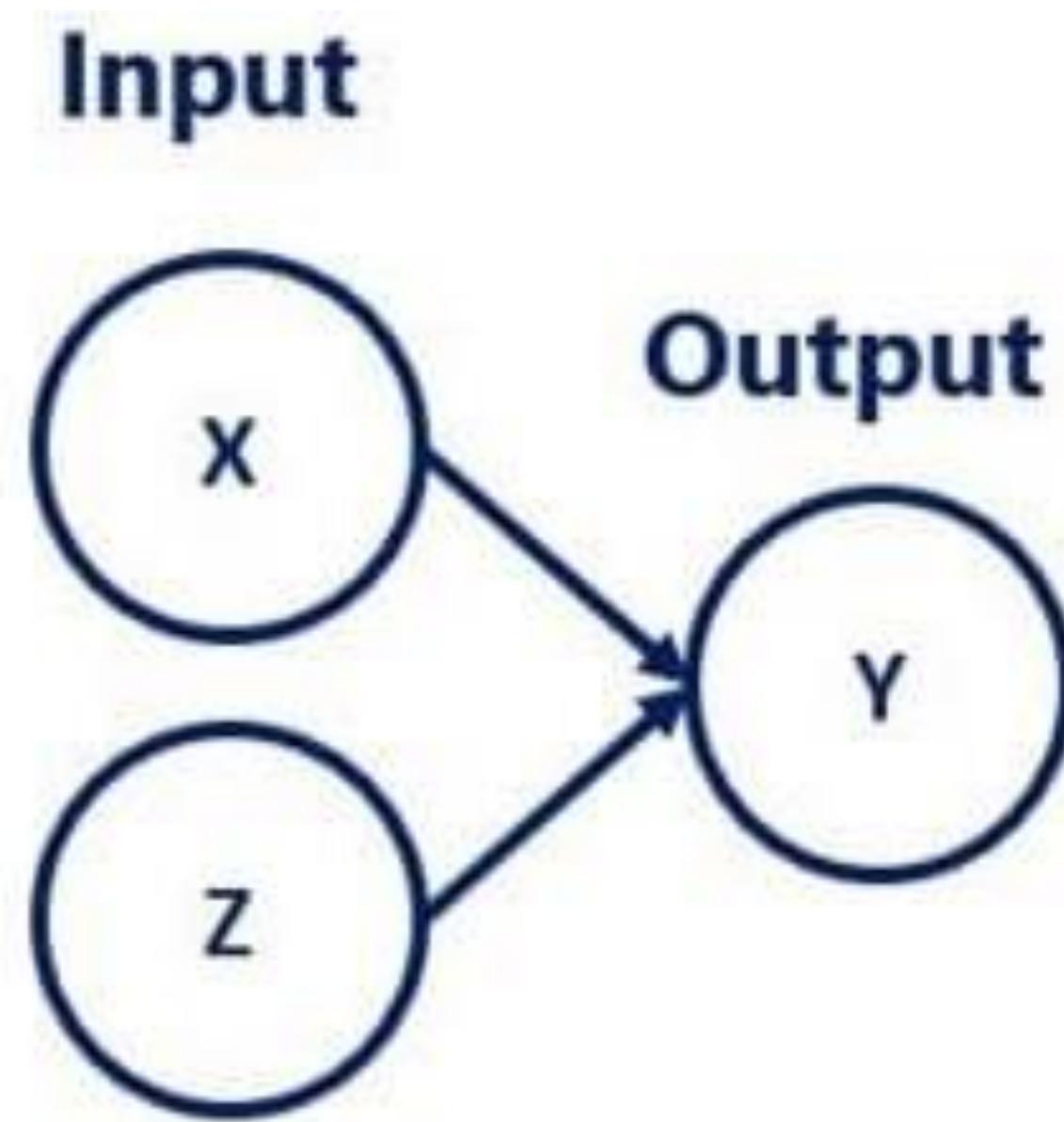
Нейрон



Нейрон



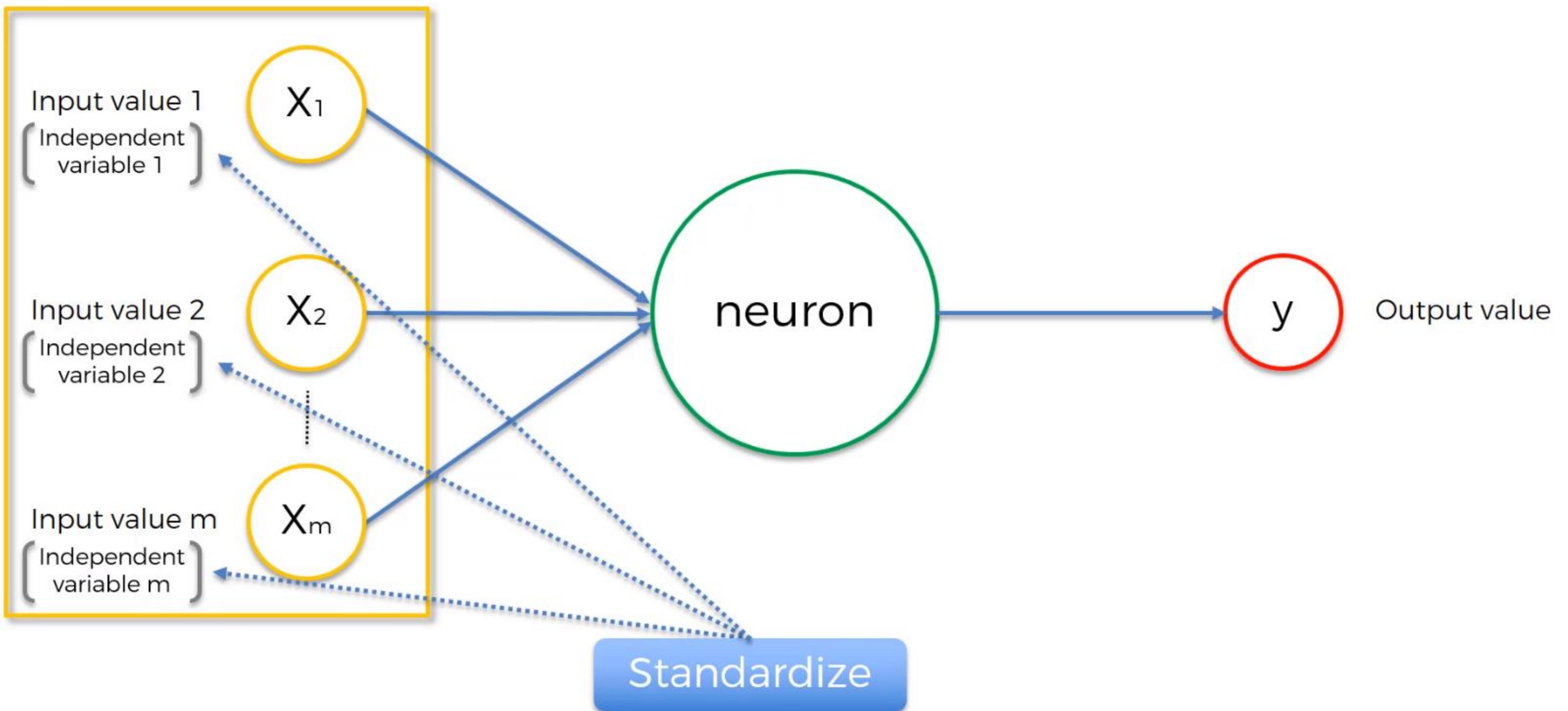
Нейрон



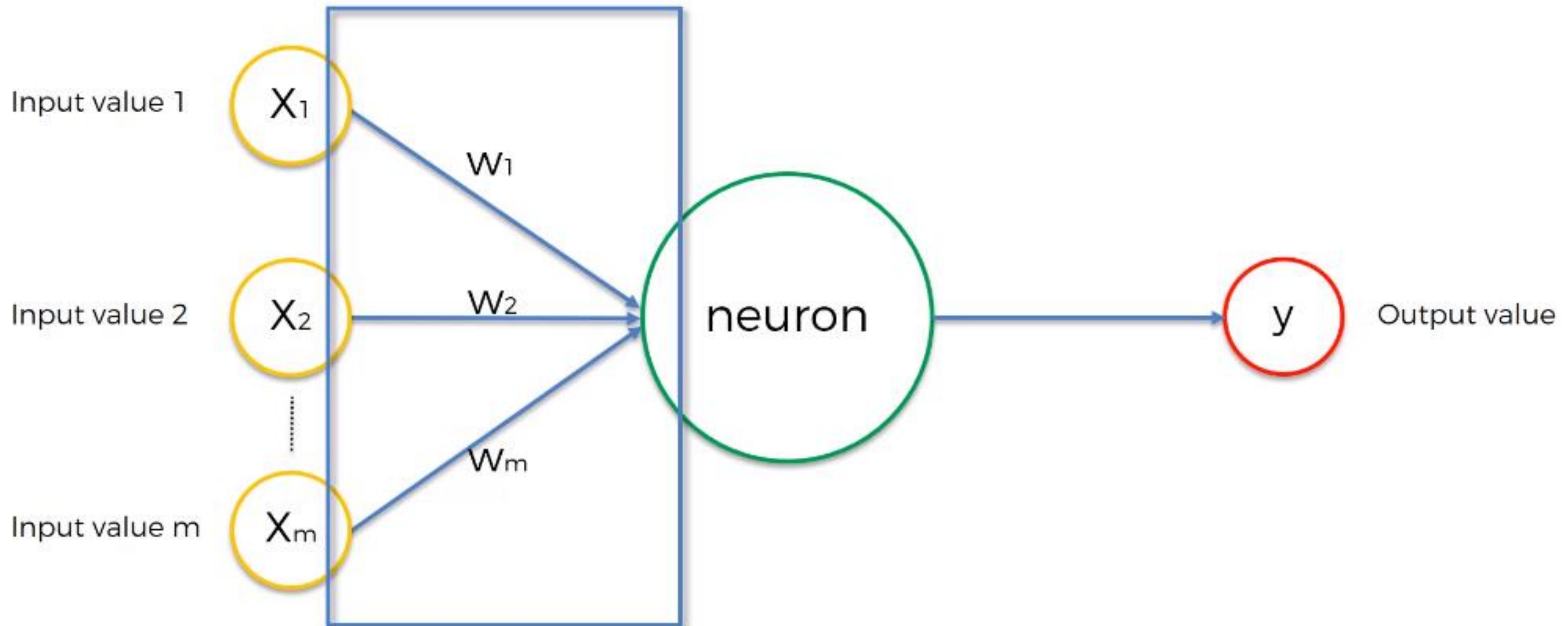
Linear model

$$\sum_i (y_i - t_i)^2$$

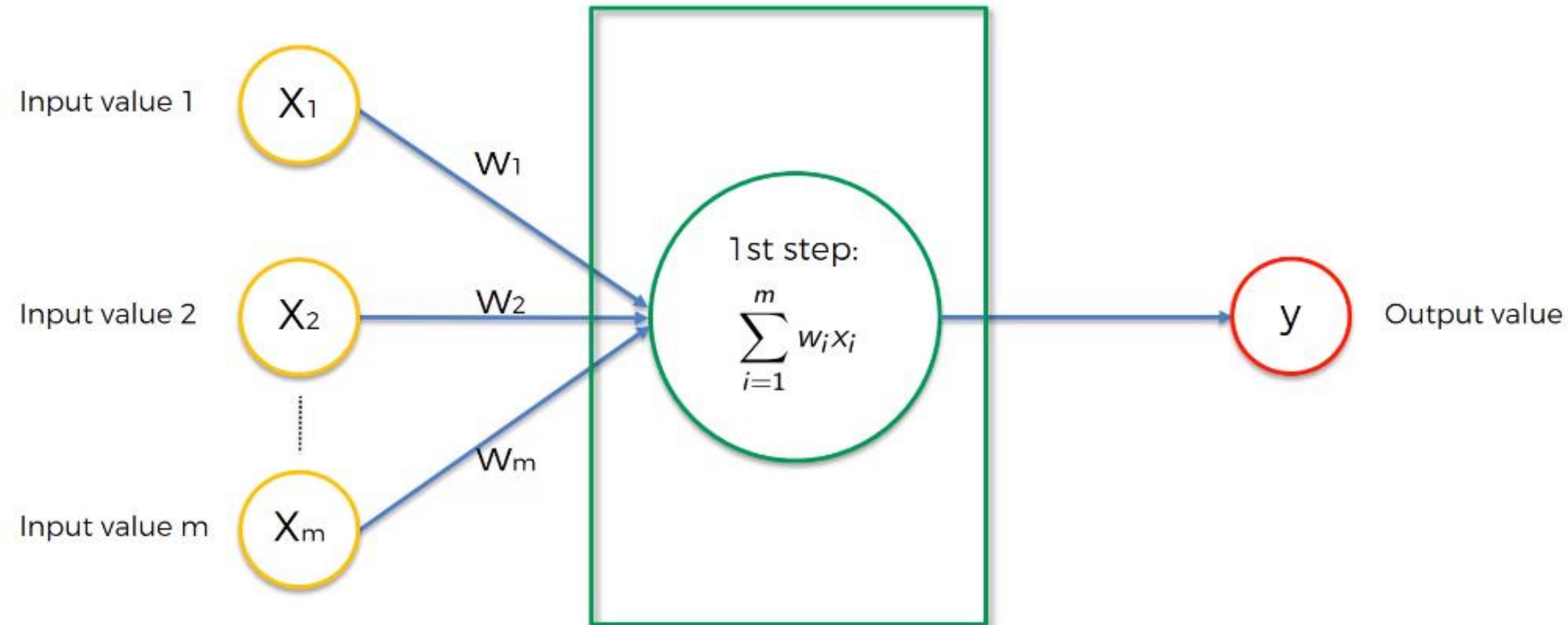
Нейрон



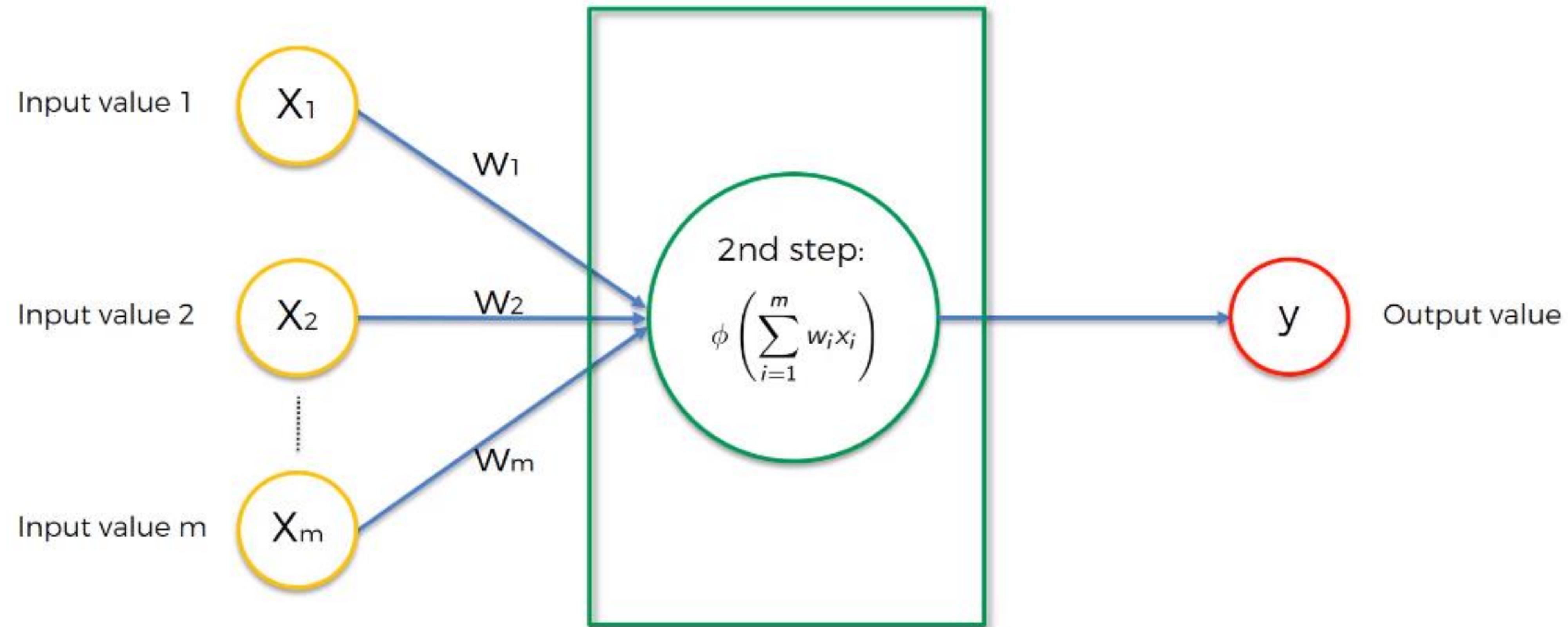
Нейрон



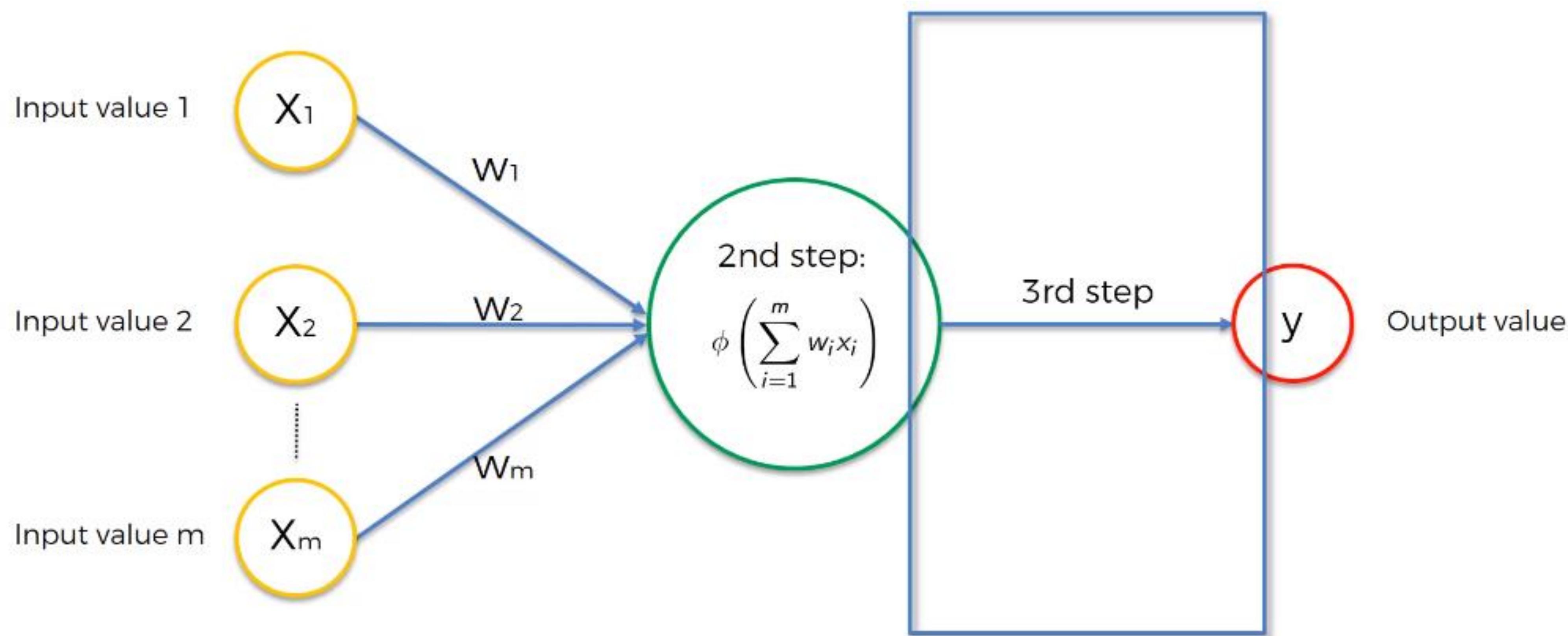
Нейрон



Нейрон



Нейрон



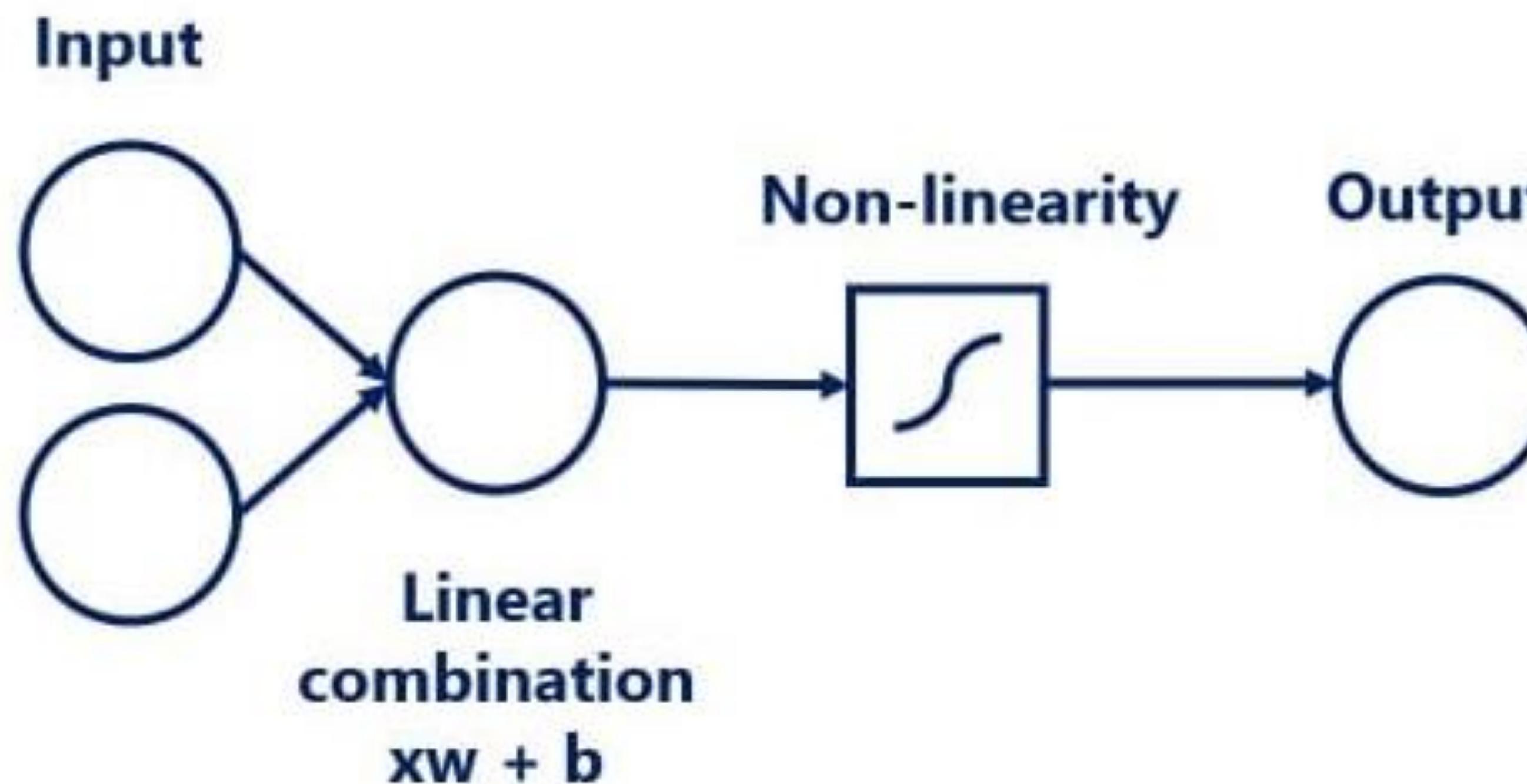
The Activation Function

Нейрон

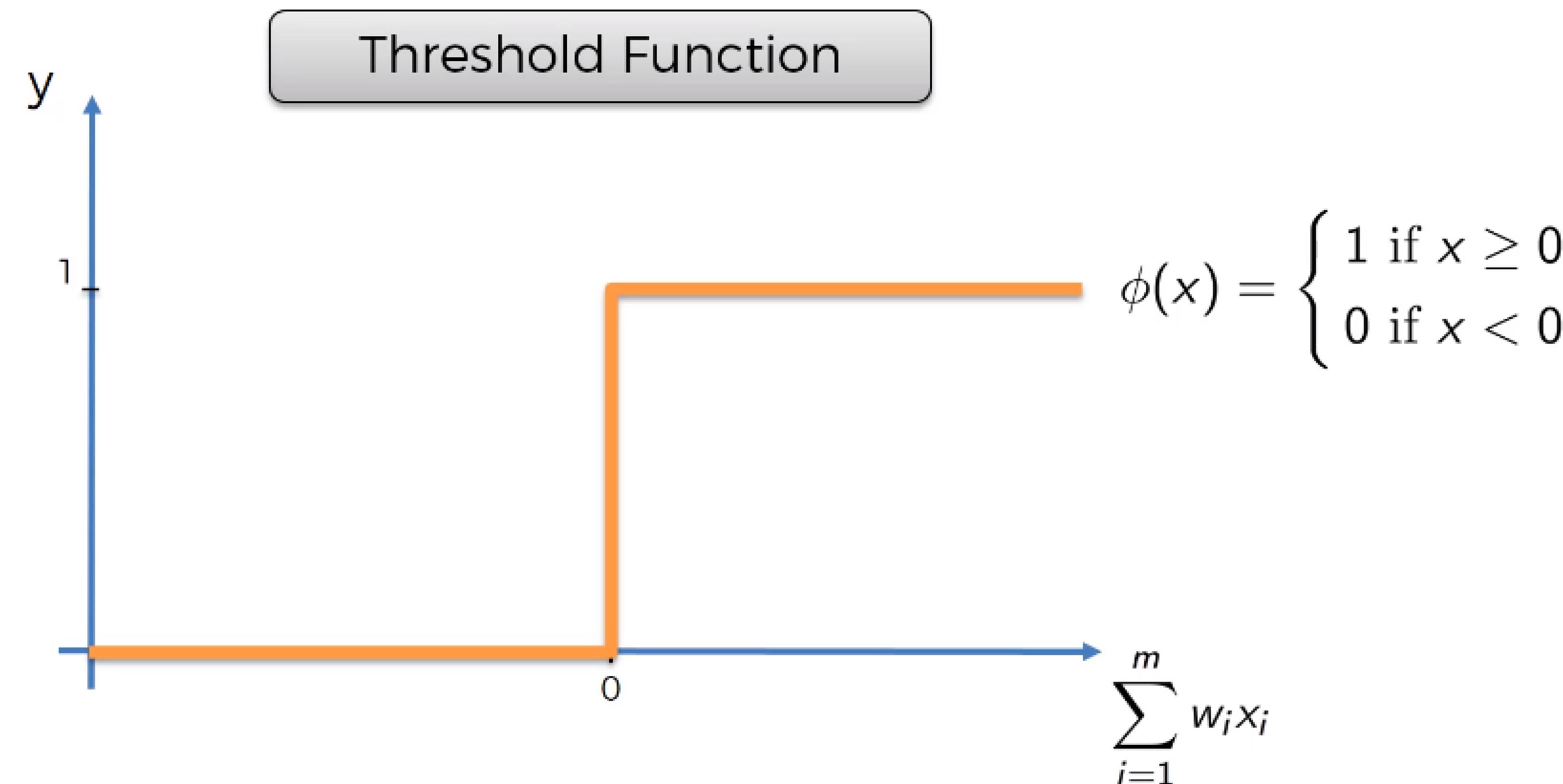
Linear

+

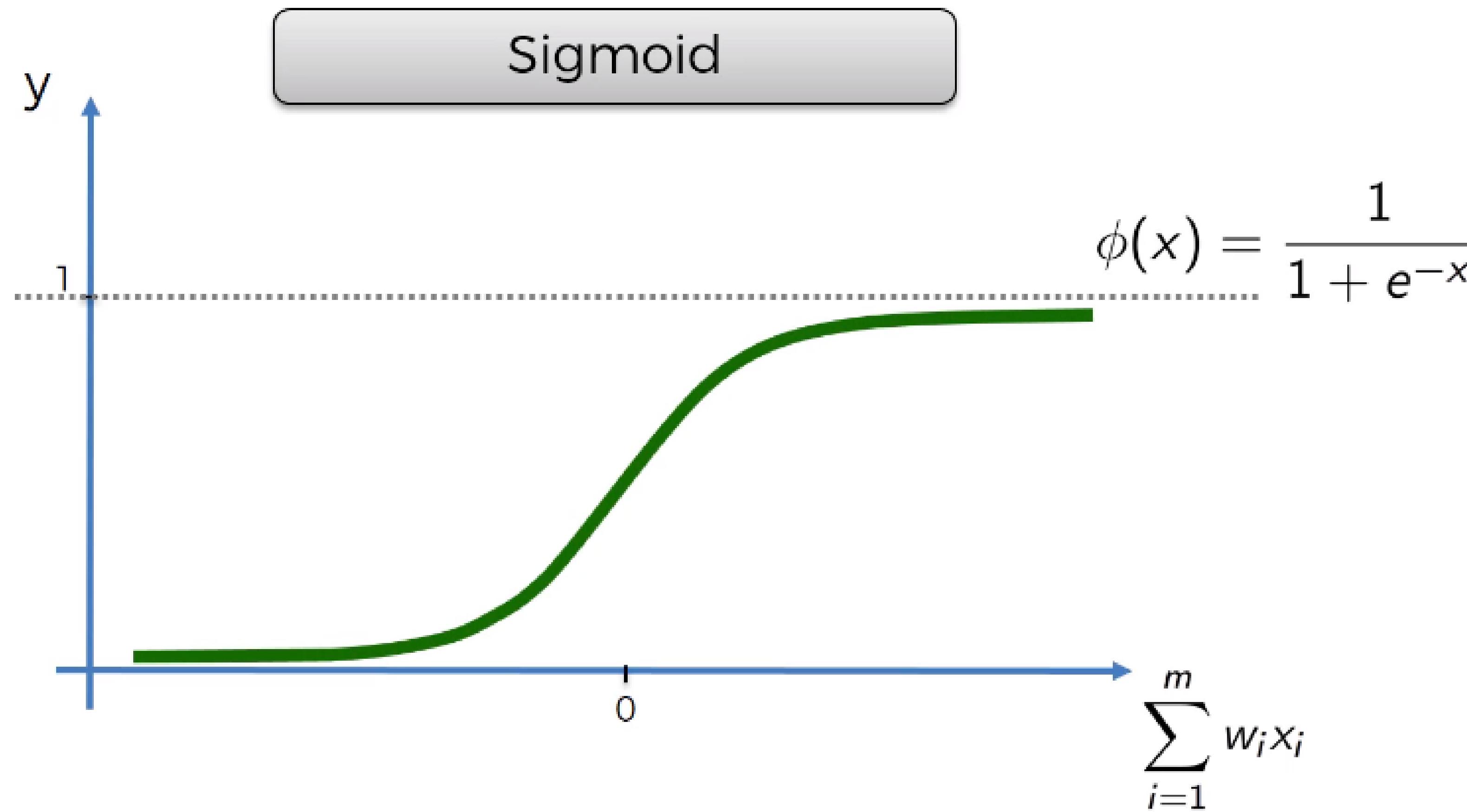
Non-linear



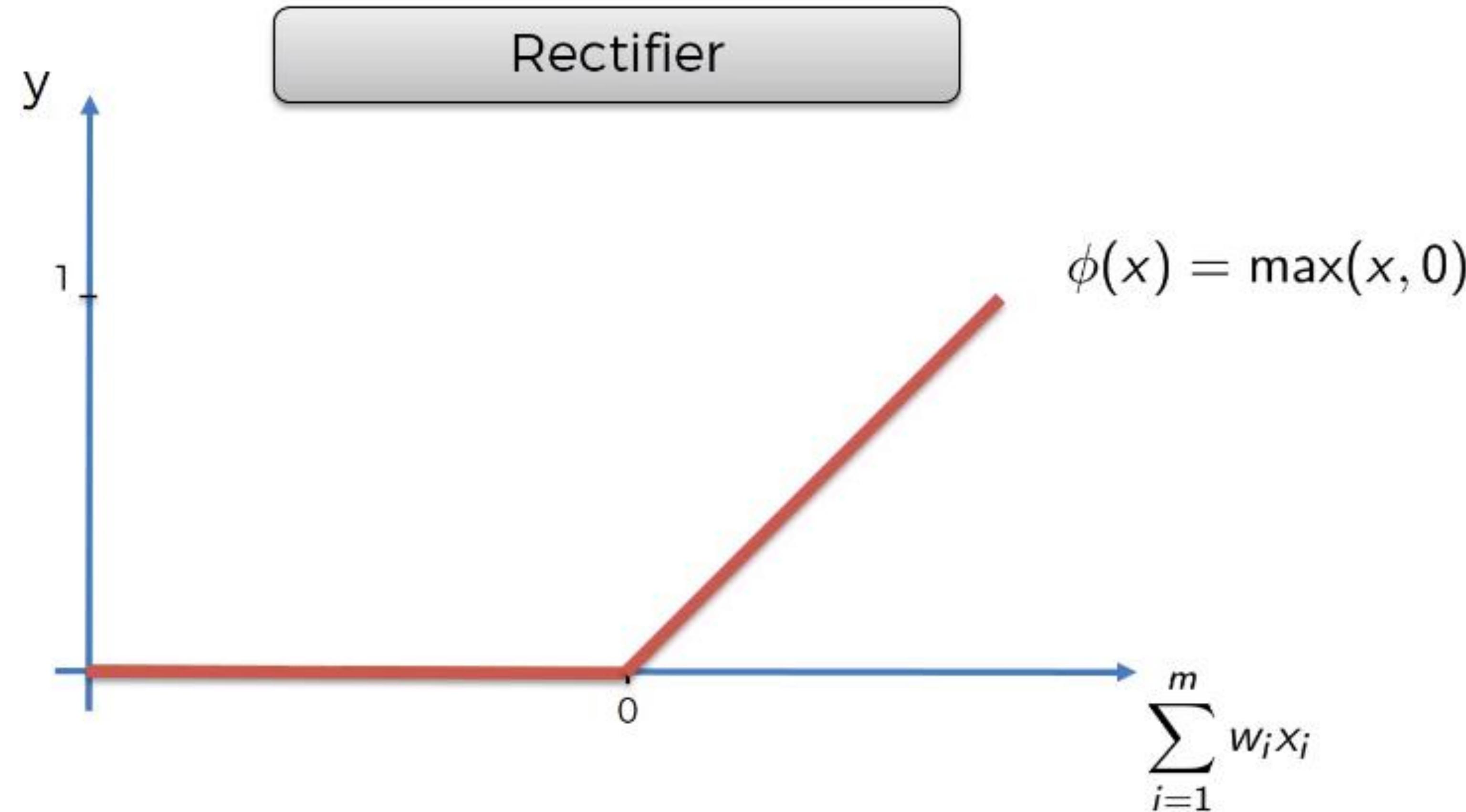
Функция активации



Функция активации

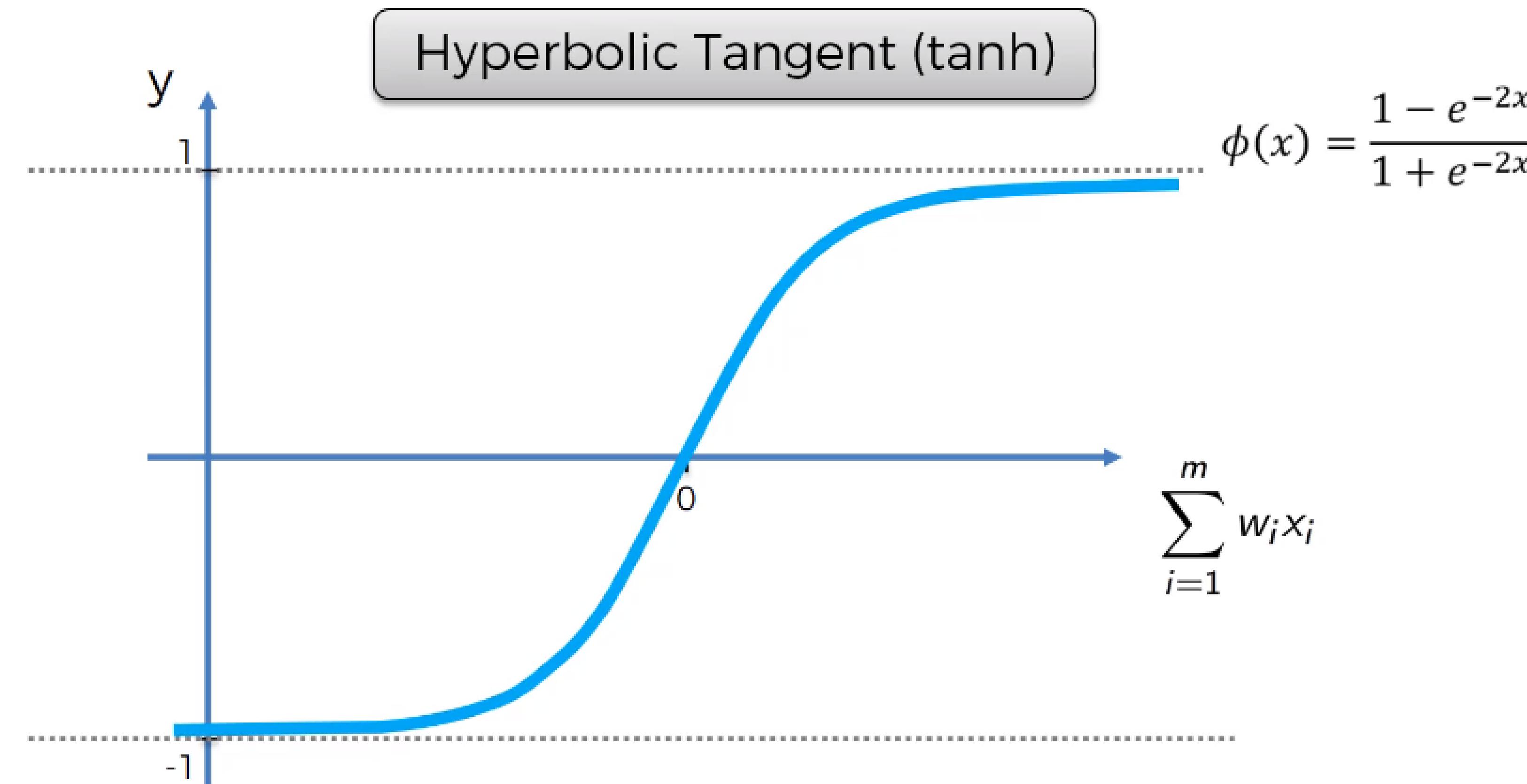


Функция активации



paper

Функция активации



Функция активации

Common activation functions

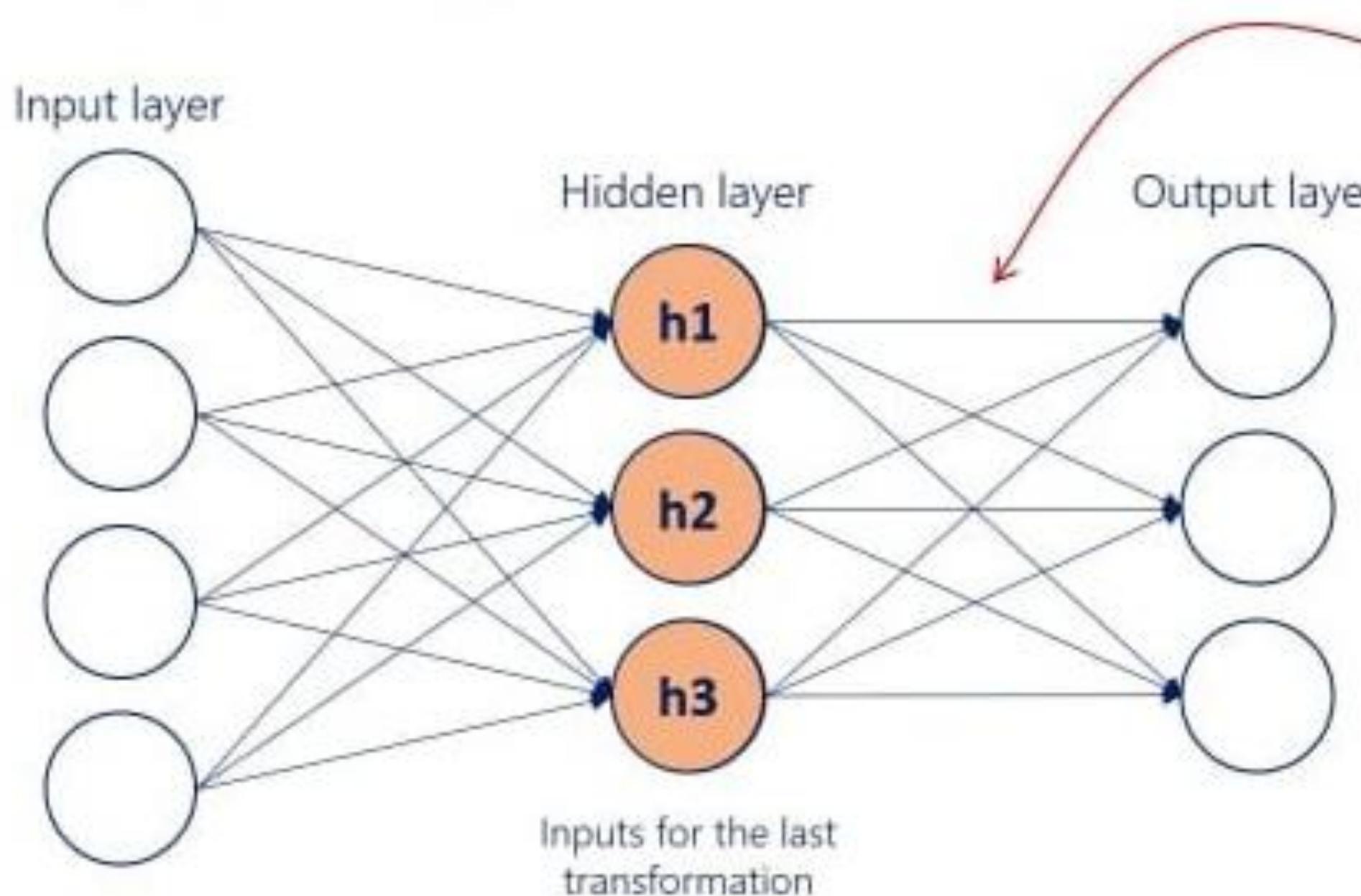
Name	Formula	Derivative	Graph	Range
sigmoid (logistic function)	$\sigma(a) = \frac{1}{1+e^{-a}}$	$\frac{\partial \sigma(a)}{\partial a} = \sigma(a)(1 - \sigma(a))$		(0, 1)
TanH (hyperbolic tangent)	$\tanh(a) = \frac{e^a - e^{-a}}{e^a + e^{-a}}$	$\frac{\partial \tanh(a)}{\partial a} = \frac{4}{(e^a + e^{-a})^2}$		(-1, 1)
ReLU (rectified linear unit)	$\text{relu}(a) = \max(0, a)$	$\frac{\partial \text{relu}(a)}{\partial a} = \begin{cases} 0, & \text{if } a \leq 0 \\ 1, & \text{if } a > 0 \end{cases}$		(0, ∞)
softmax	$\sigma_i(\mathbf{a}) = \frac{e^{a_i}}{\sum_j e^{a_j}}$	$\frac{\partial \sigma_i(\mathbf{a})}{\partial a_j} = \sigma_i(\mathbf{a}) (\delta_{ij} - \sigma_j(\mathbf{a}))$ Where δ_{ij} is 1 if $i=j$, 0 otherwise	different every time	(0, 1)

Функция активации

Softmax

$$a = xw + b$$

Linear combination



$$y = \text{softmax}(\mathbf{a})$$

Activation

$$\mathbf{a}_h = h\mathbf{w} + \mathbf{b}$$

$$\mathbf{a} = [-0.21, 0.47, 1.72]$$

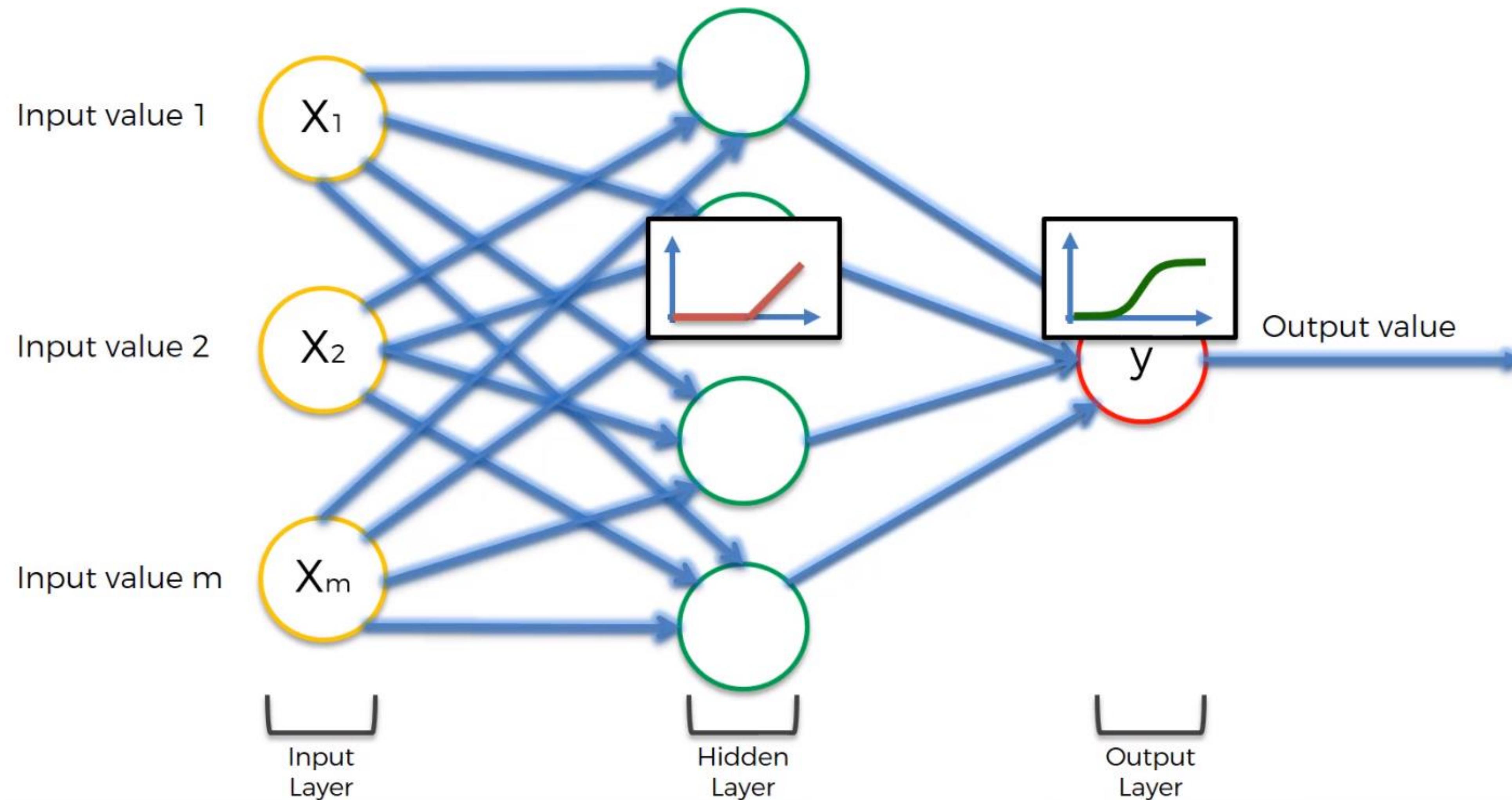
$$\text{softmax}(\mathbf{a}) = \frac{e^{a_i}}{\sum_j e^{a_j}}$$

$$\sum_j e^{a_j} = e^{-0.21} + e^{0.47} + e^{1.72} = 8$$

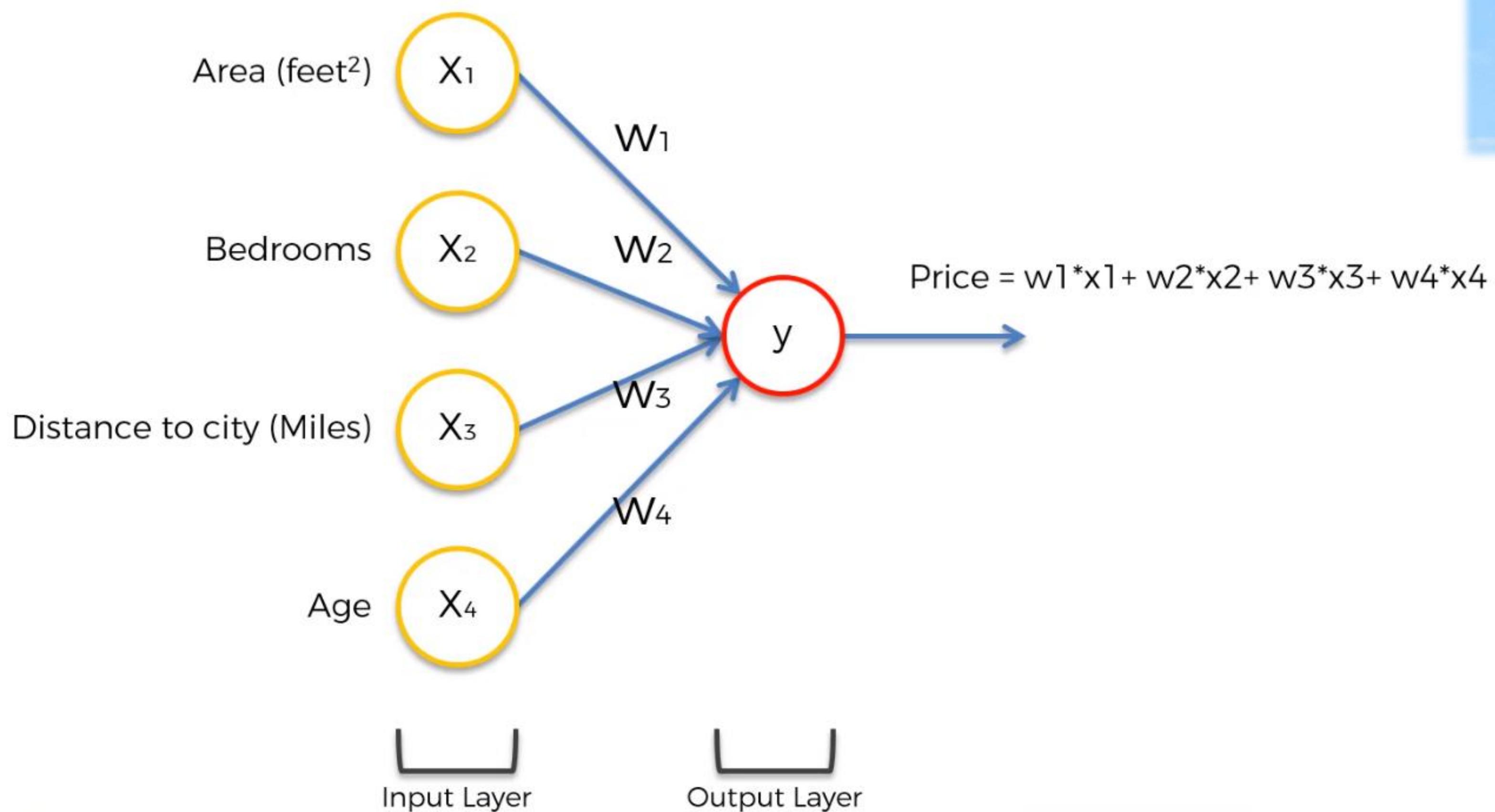
$$\text{softmax}(\mathbf{a}) = \left[\frac{e^{-0.21}}{8}, \frac{e^{0.47}}{8}, \frac{e^{1.72}}{8} \right]$$

$$y = [0.1, 0.2, 0.7]$$

Функция активации



Нейронные сети



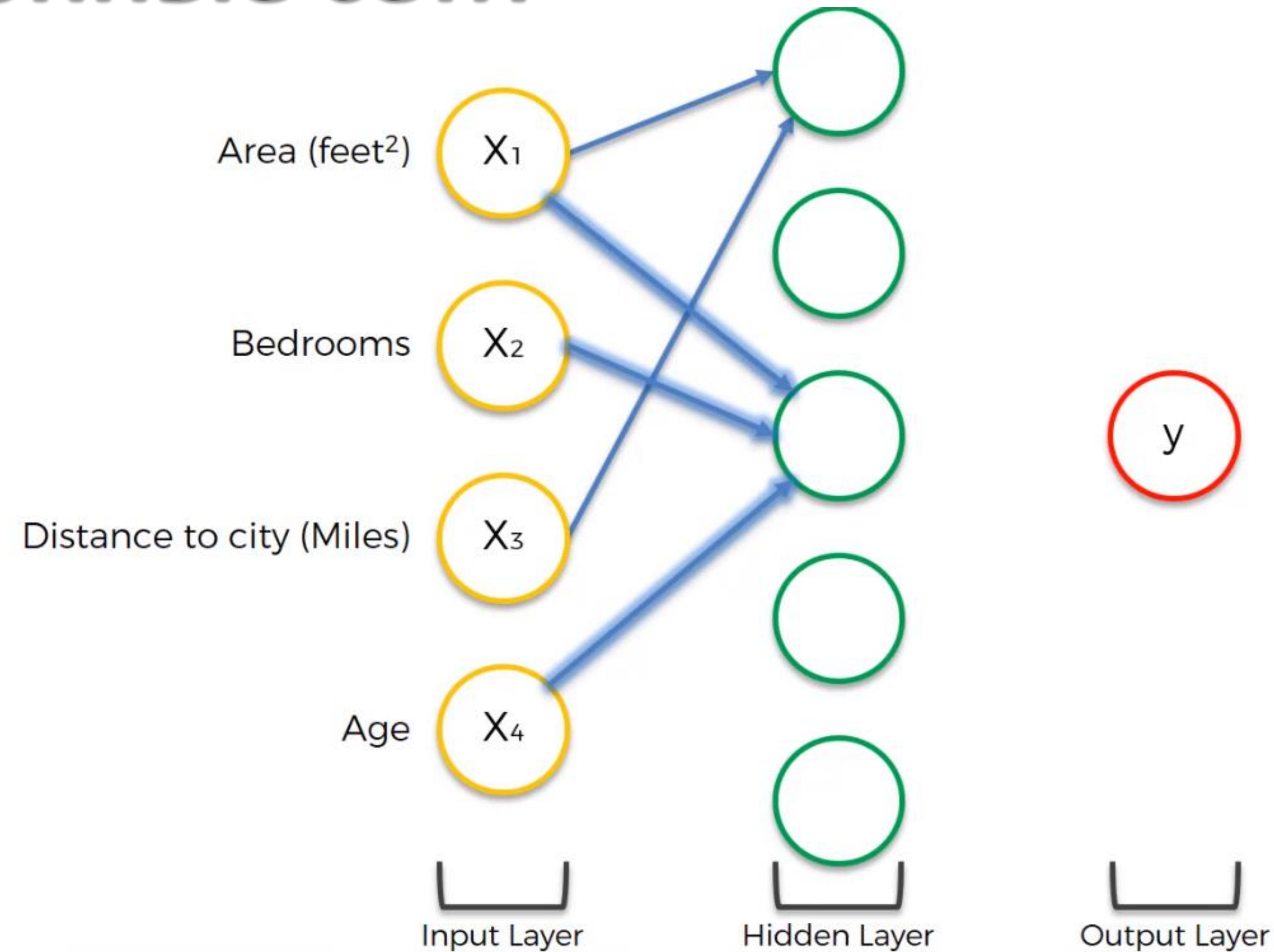
Нейронные сети



Нейронные сети



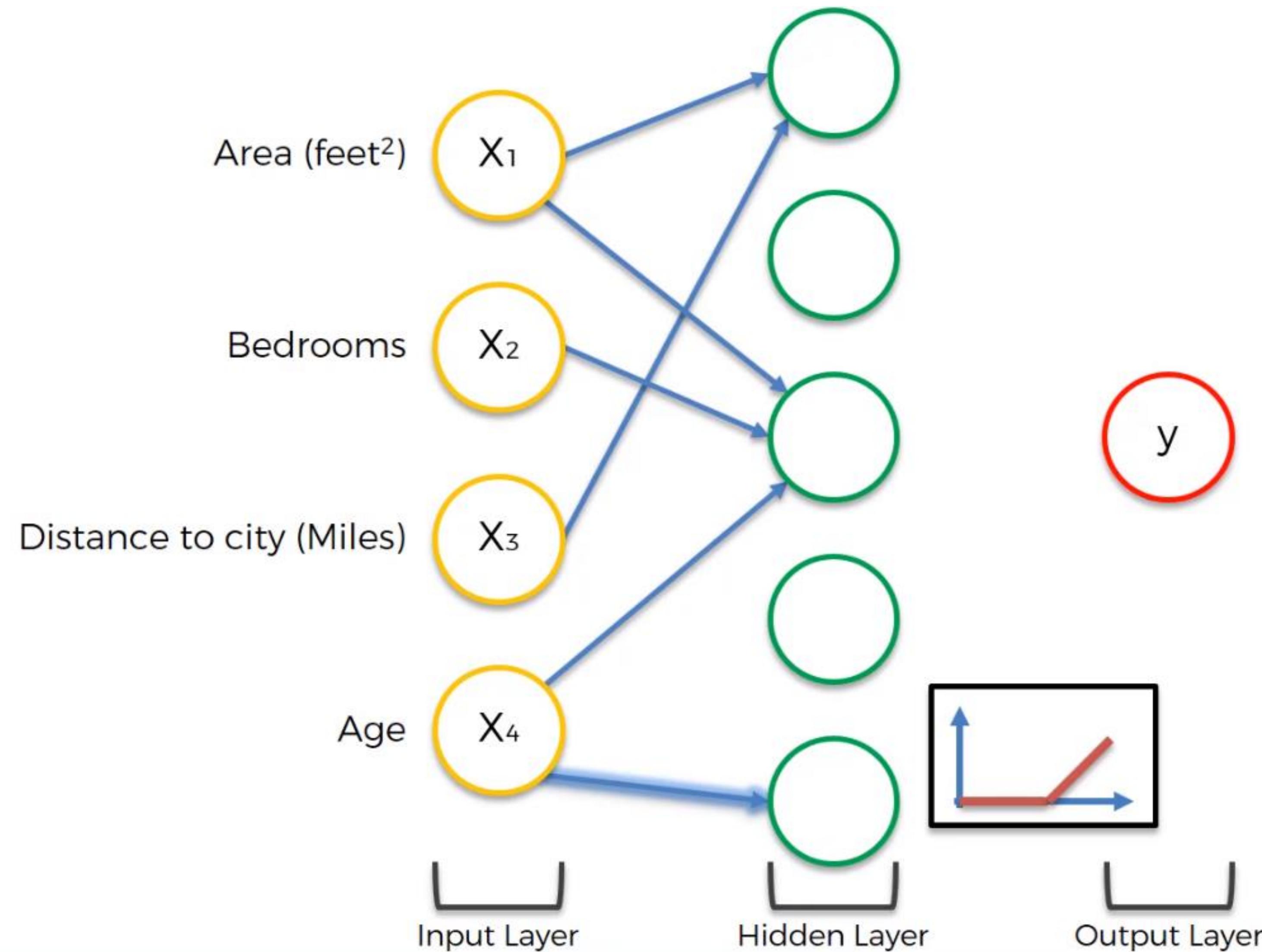
Нейронные сети



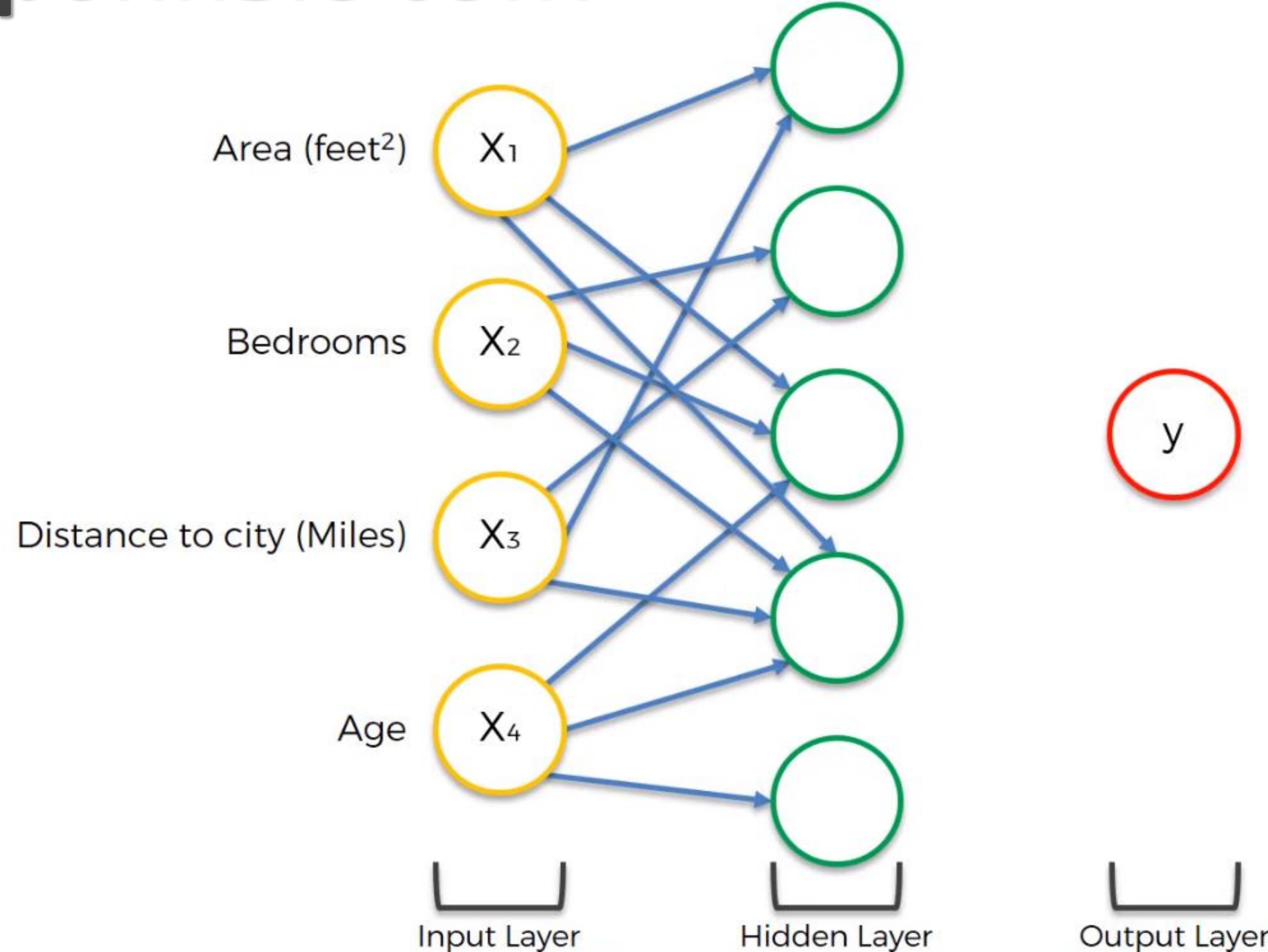
Нейронные сети



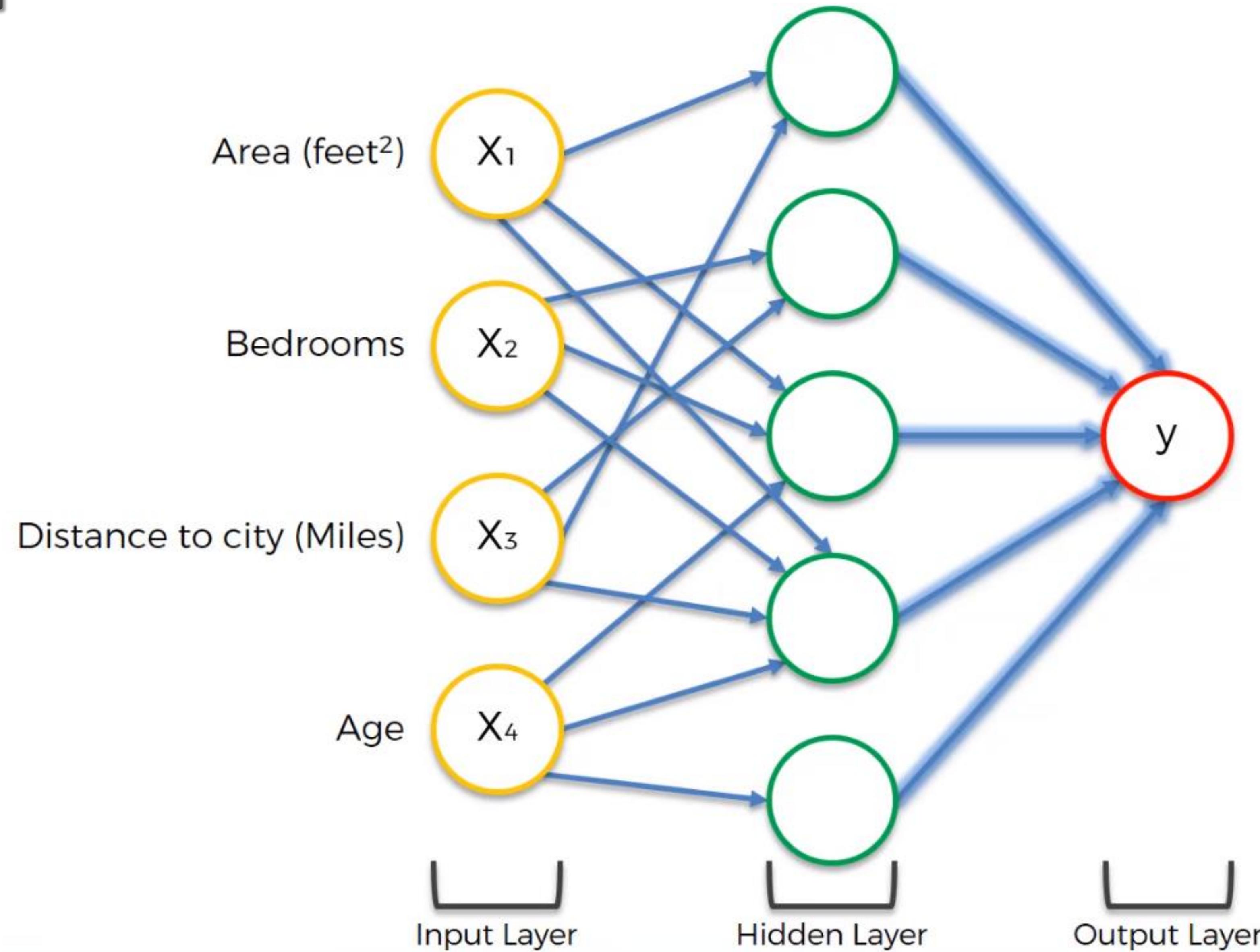
Нейронные сети



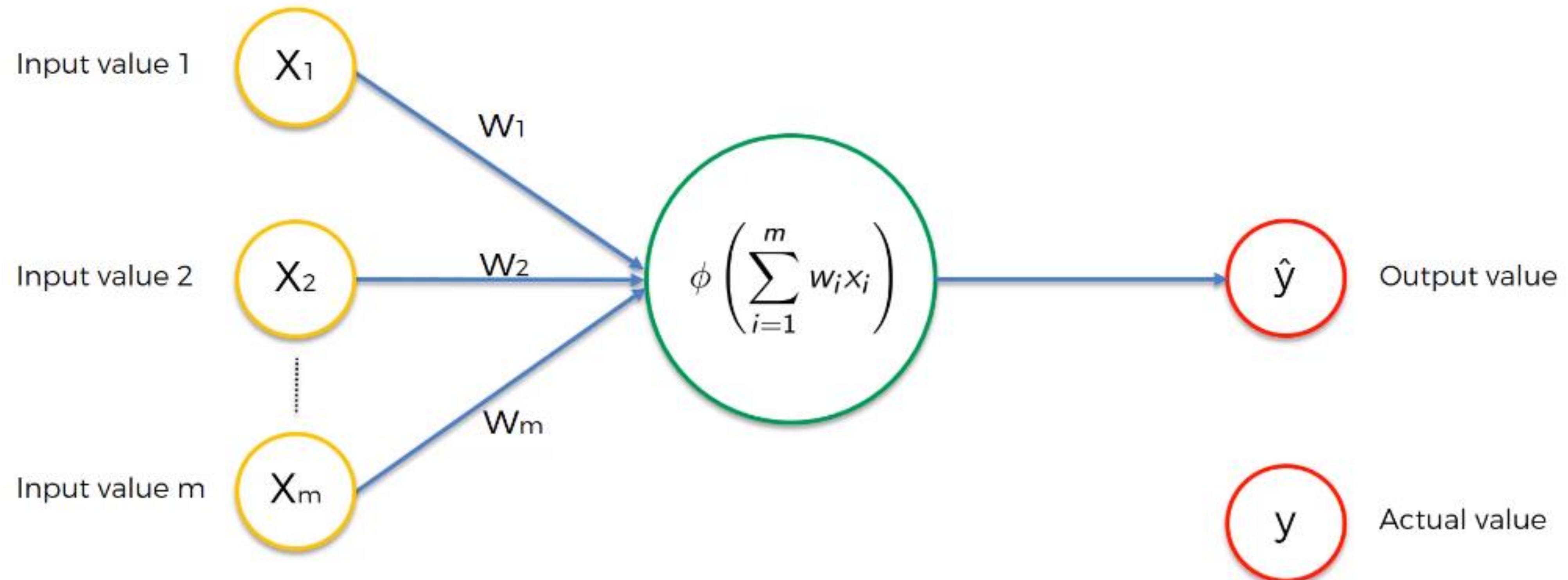
Нейронные сети



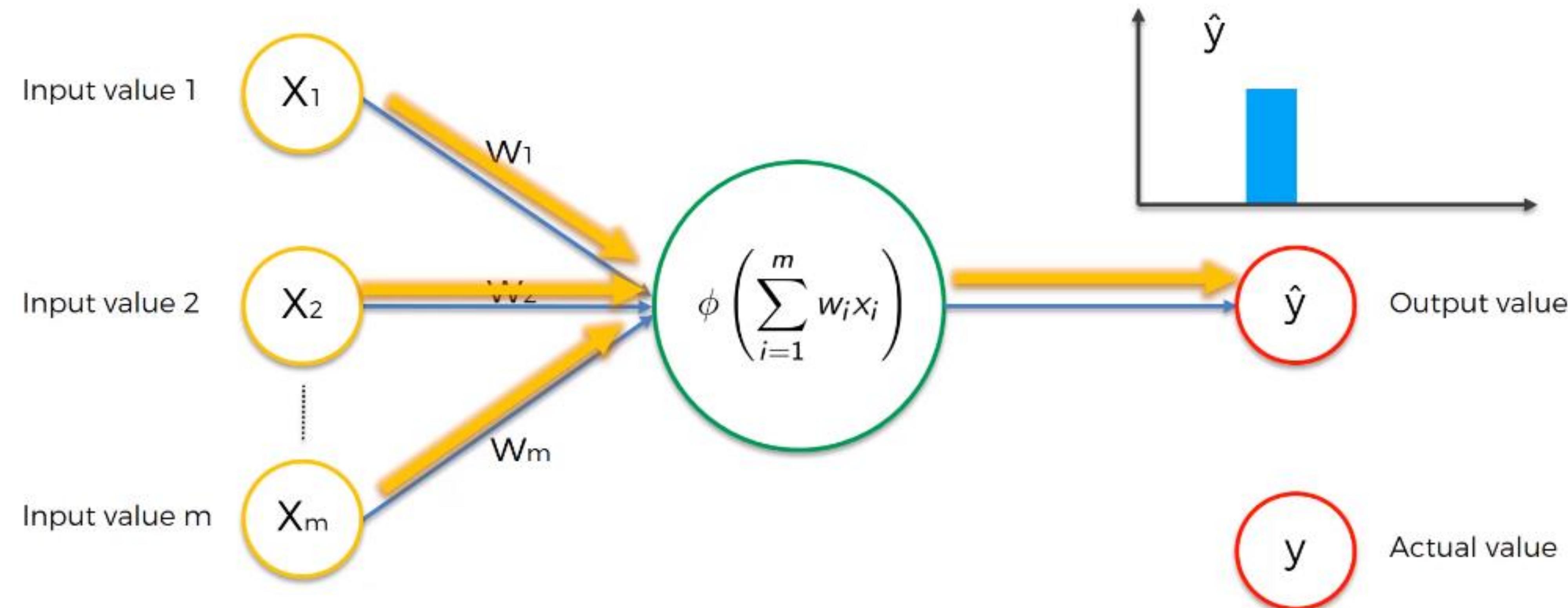
Нейронные сети



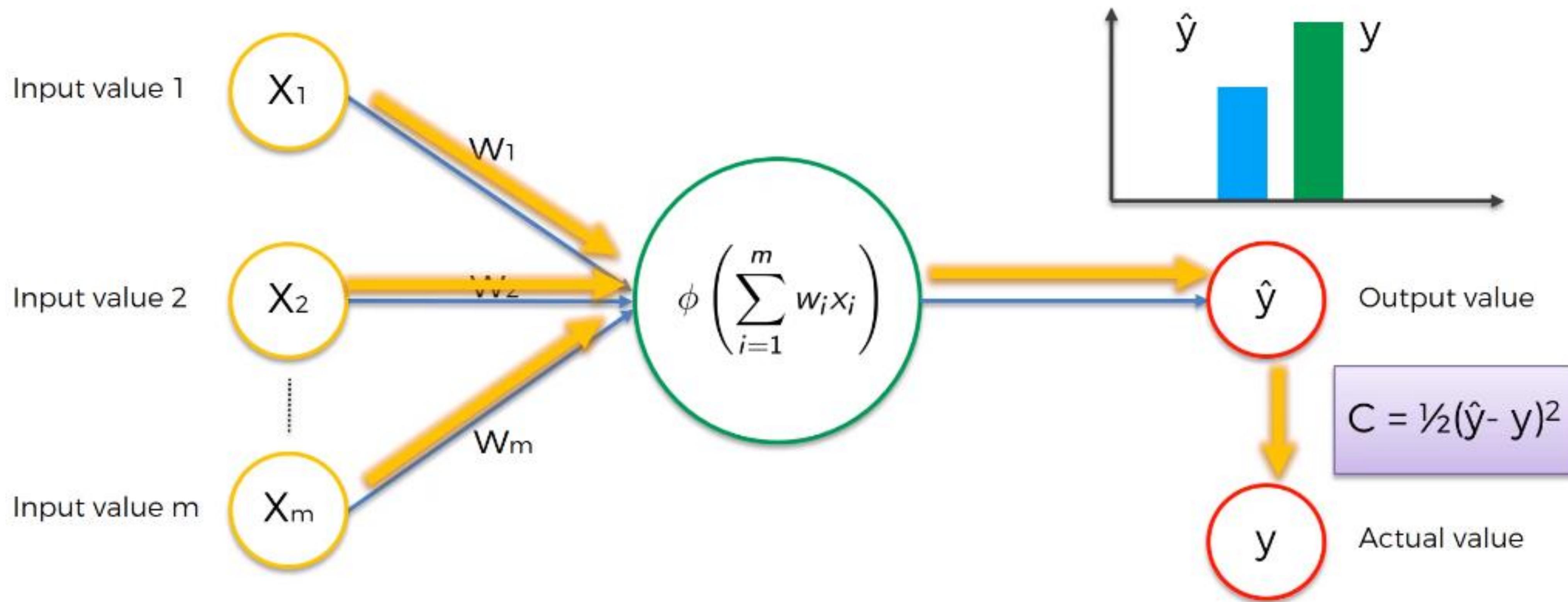
Нейронные сети



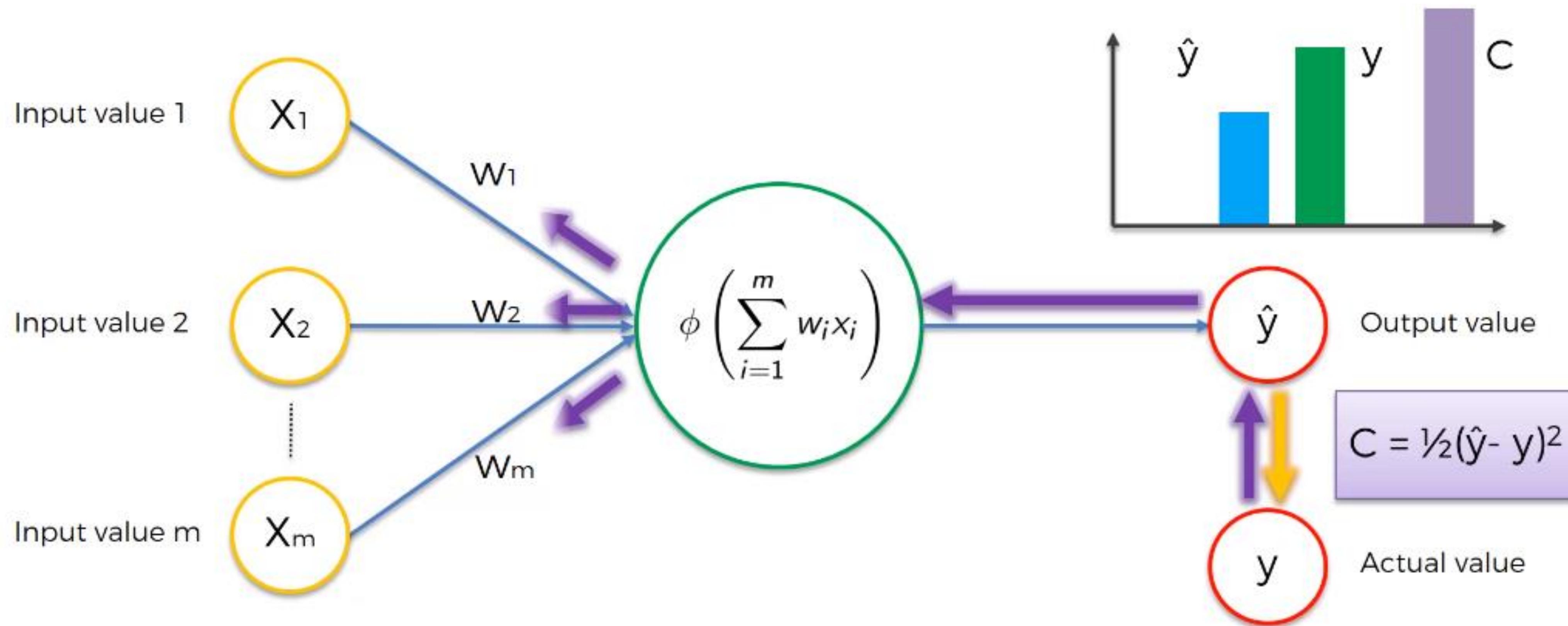
Нейронные сети



Нейронные сети

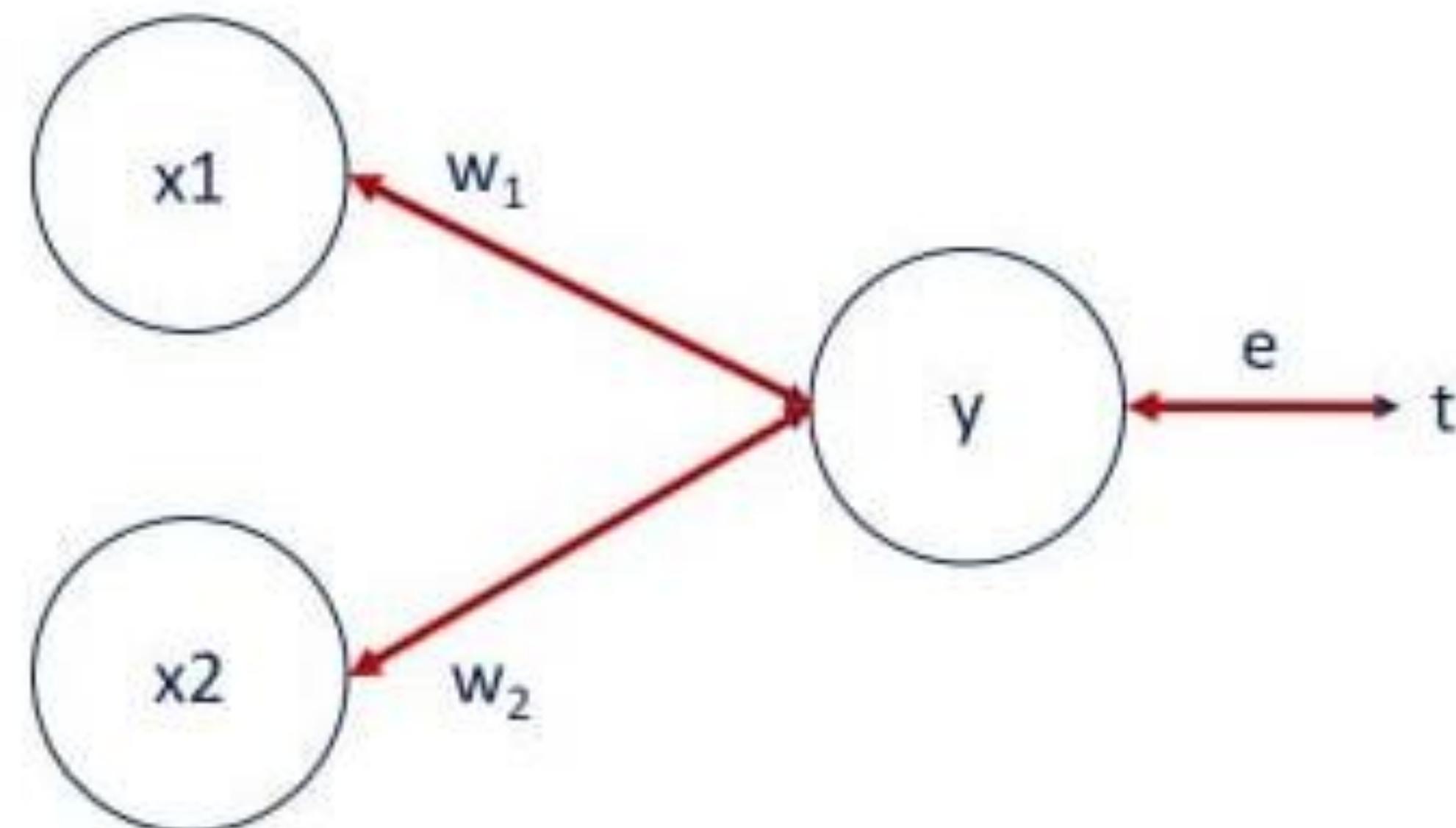


Нейронные сети



Нейронные сети

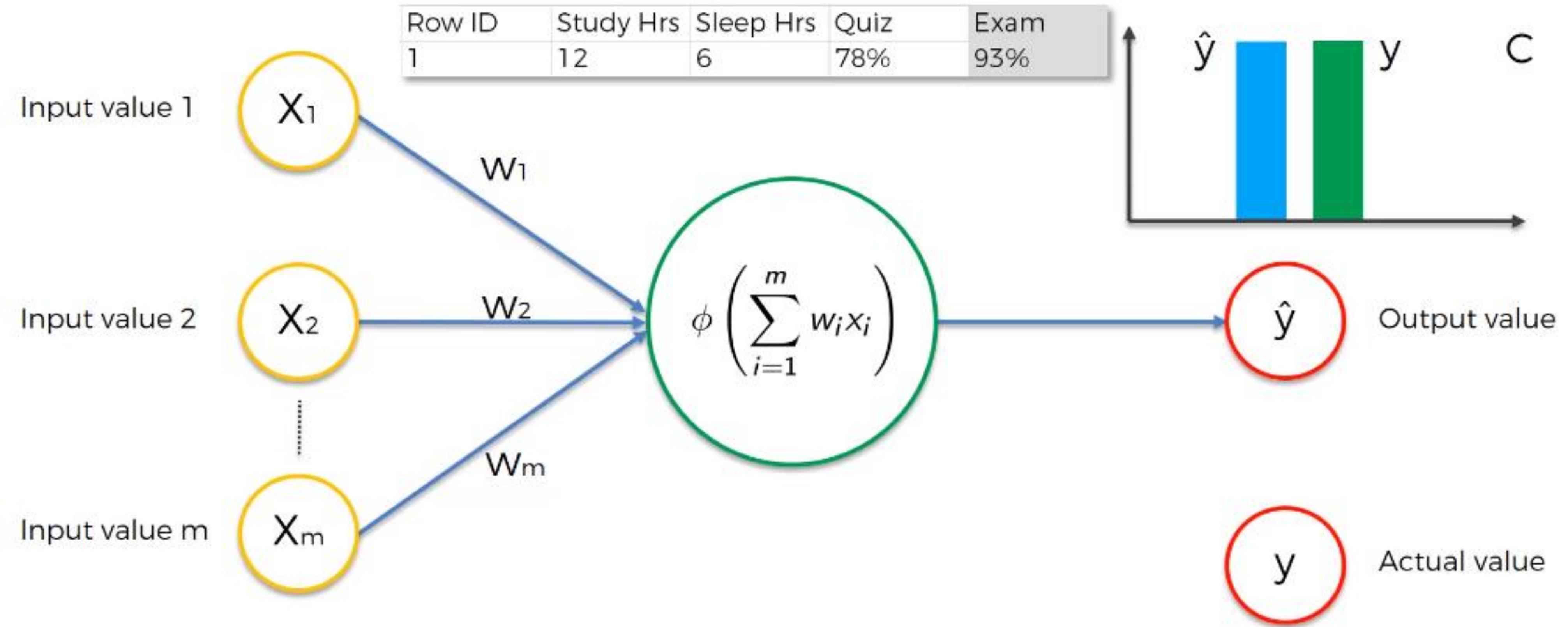
Backpropagation



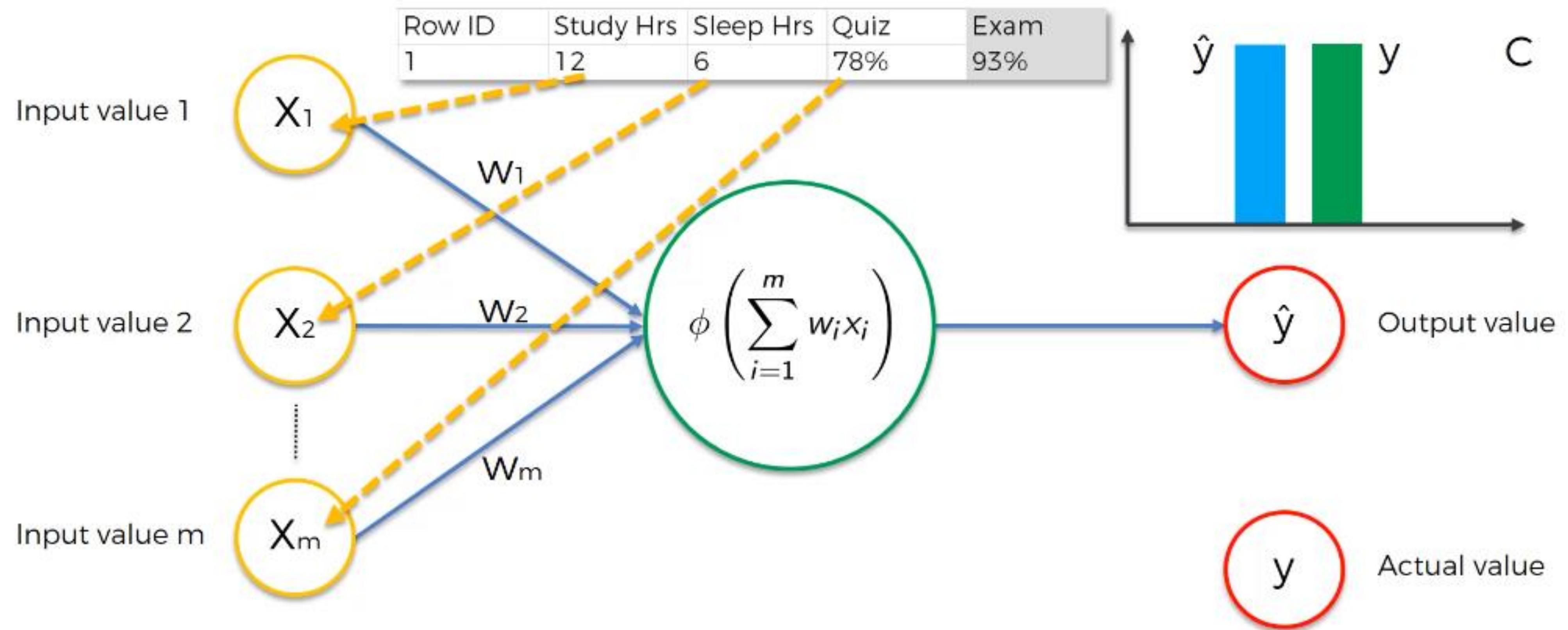
$$\mathbf{w}_{i+1} = \mathbf{w}_i - \eta \sum_i \mathbf{x}_i e_i$$

$$\mathbf{b}_{i+1} = \mathbf{b}_i - \eta \sum_i e_i$$

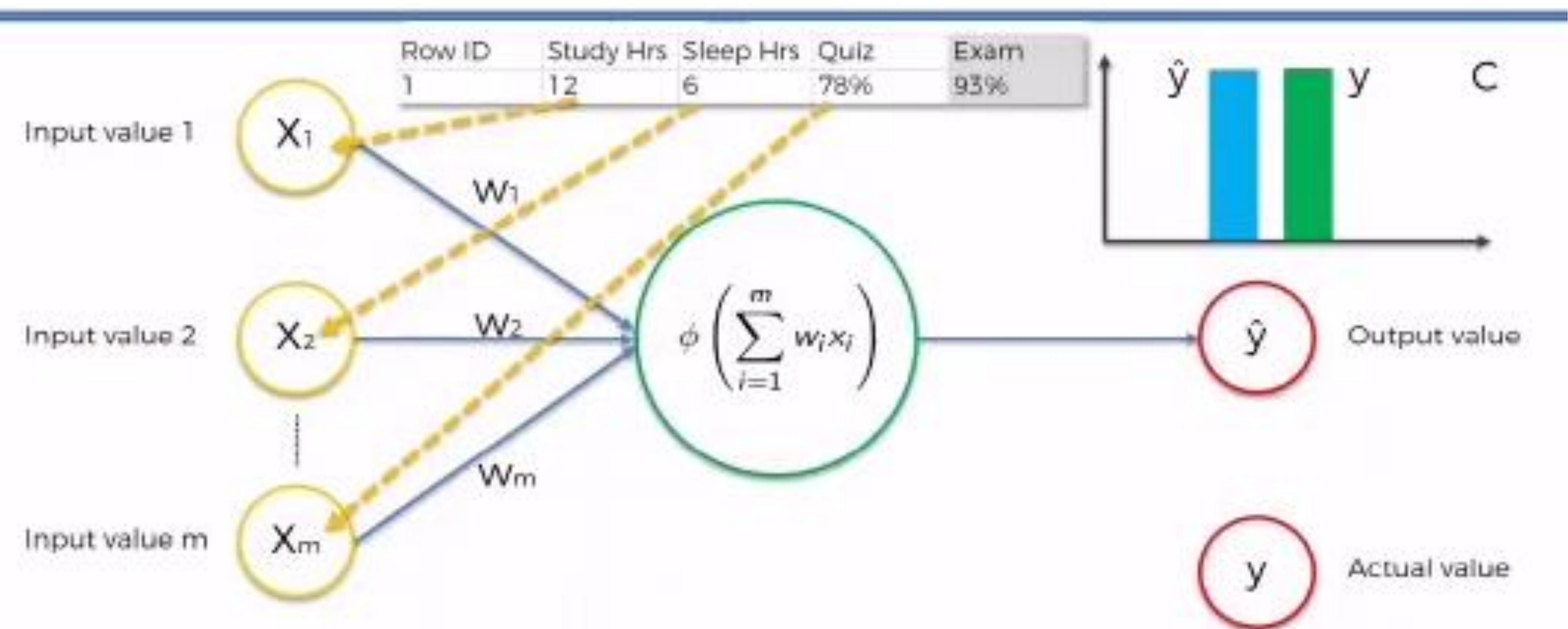
Нейронные сети



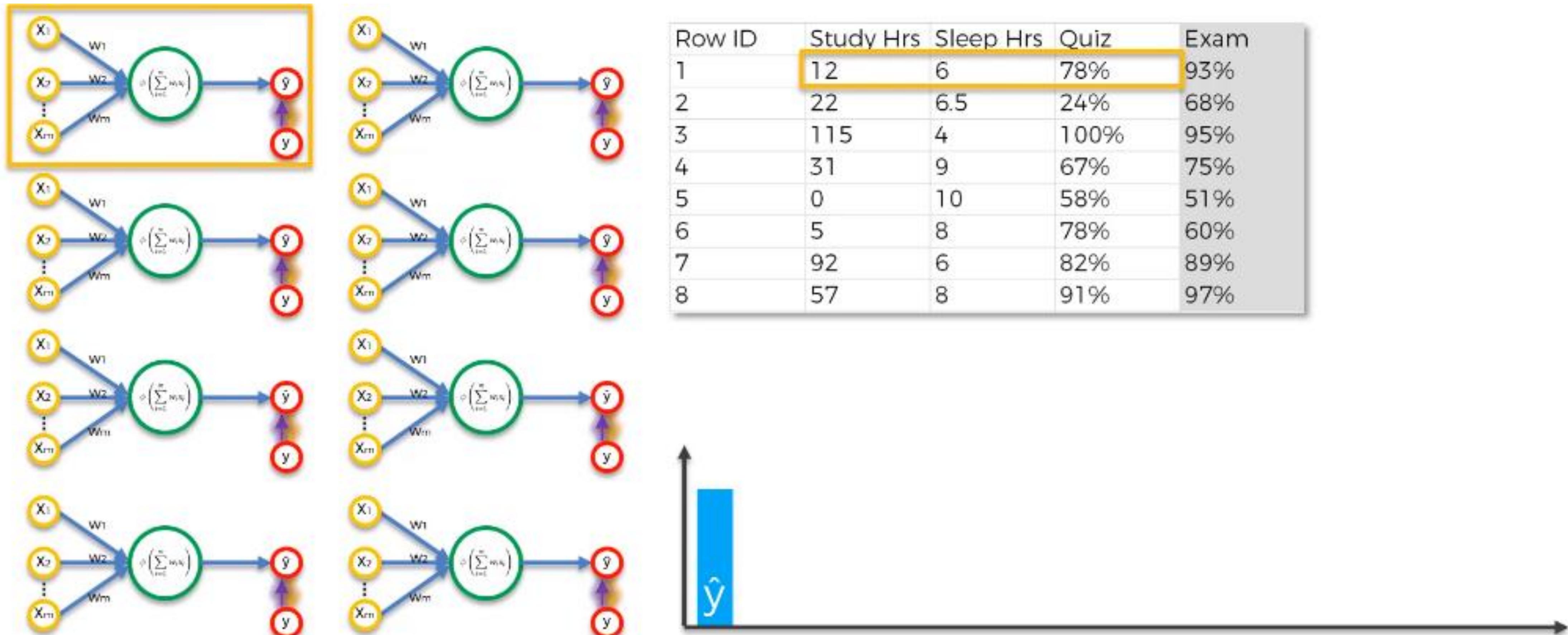
Нейронные сети



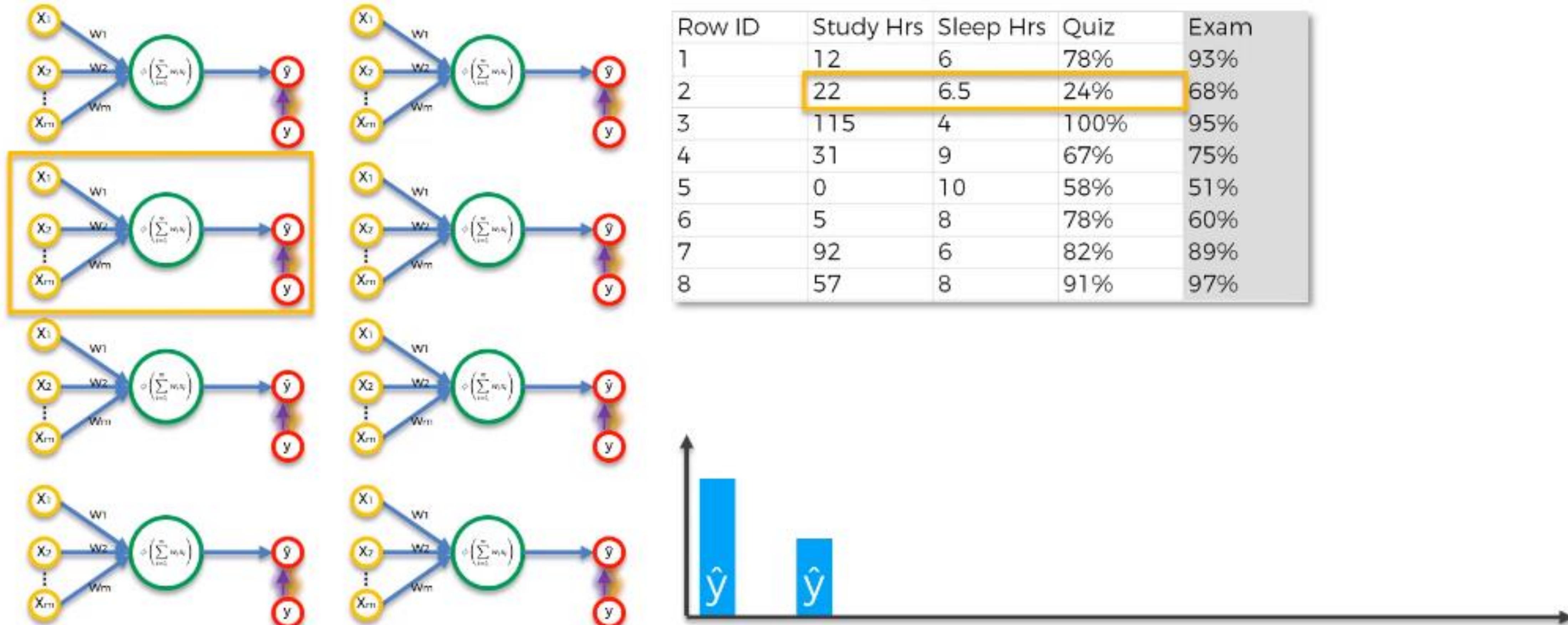
Нейронные сети



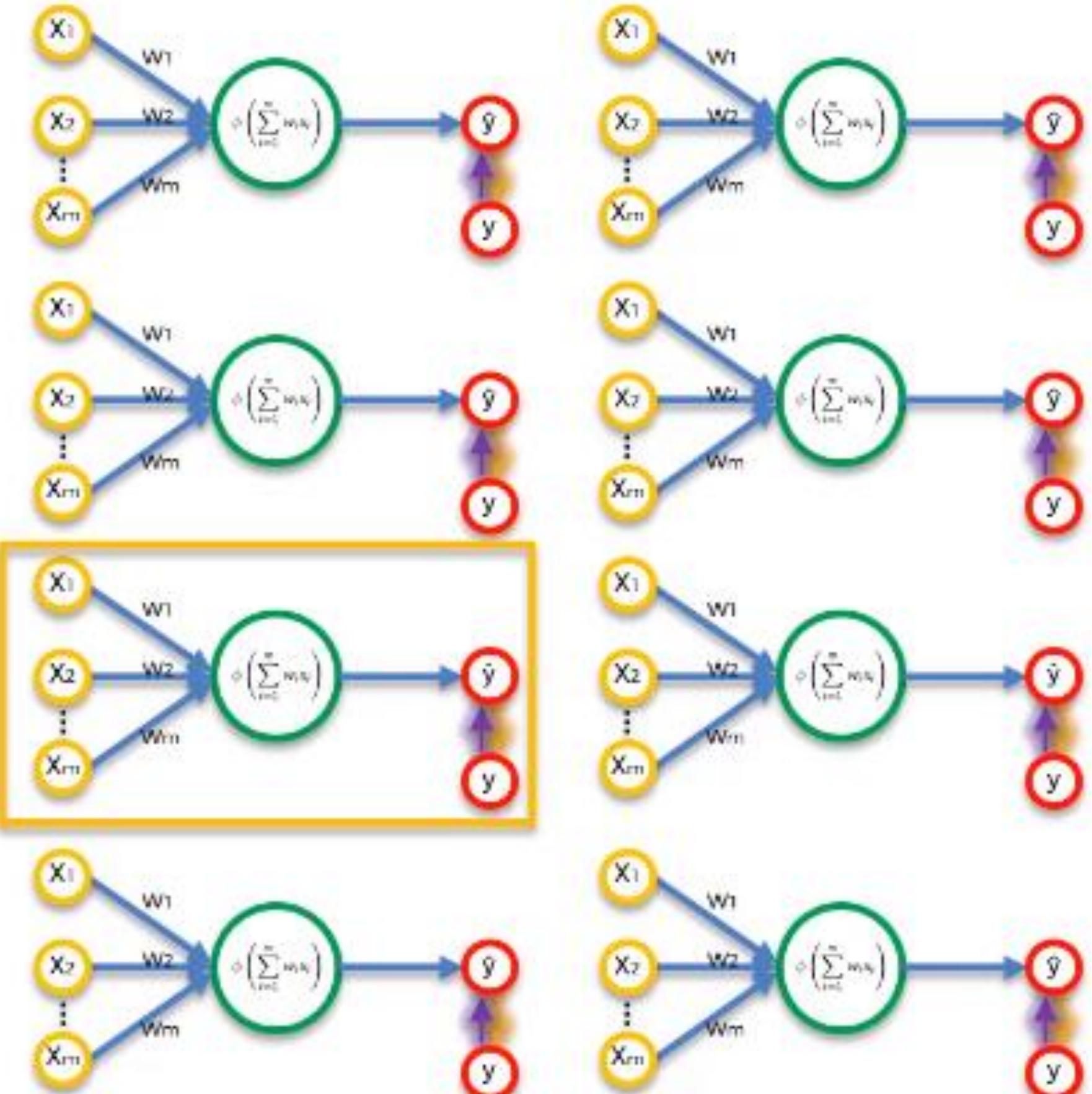
Нейронные сети



Нейронные сети



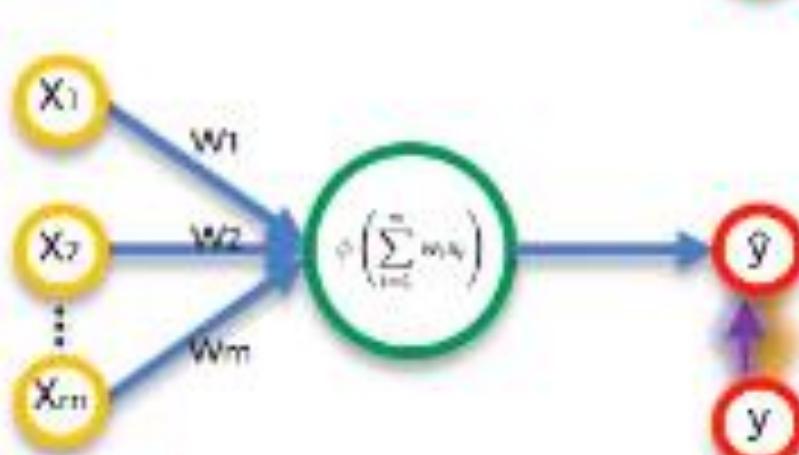
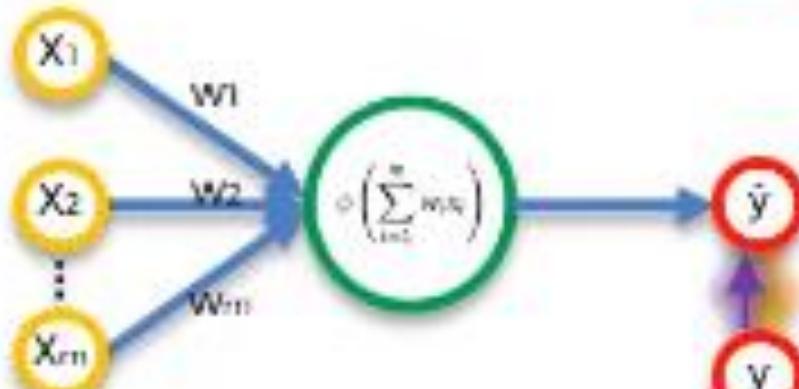
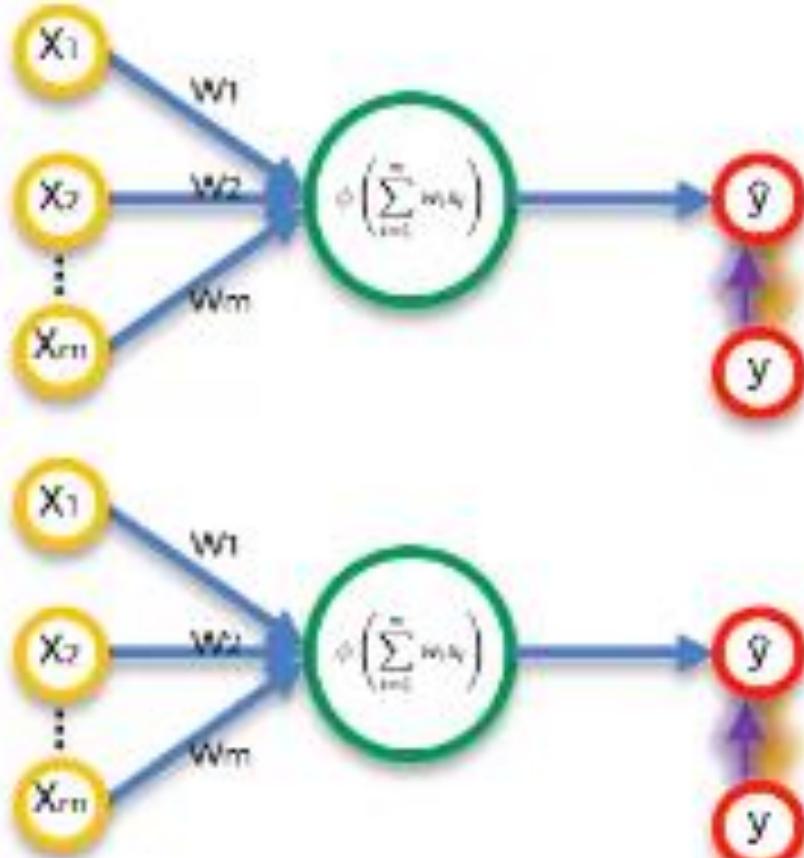
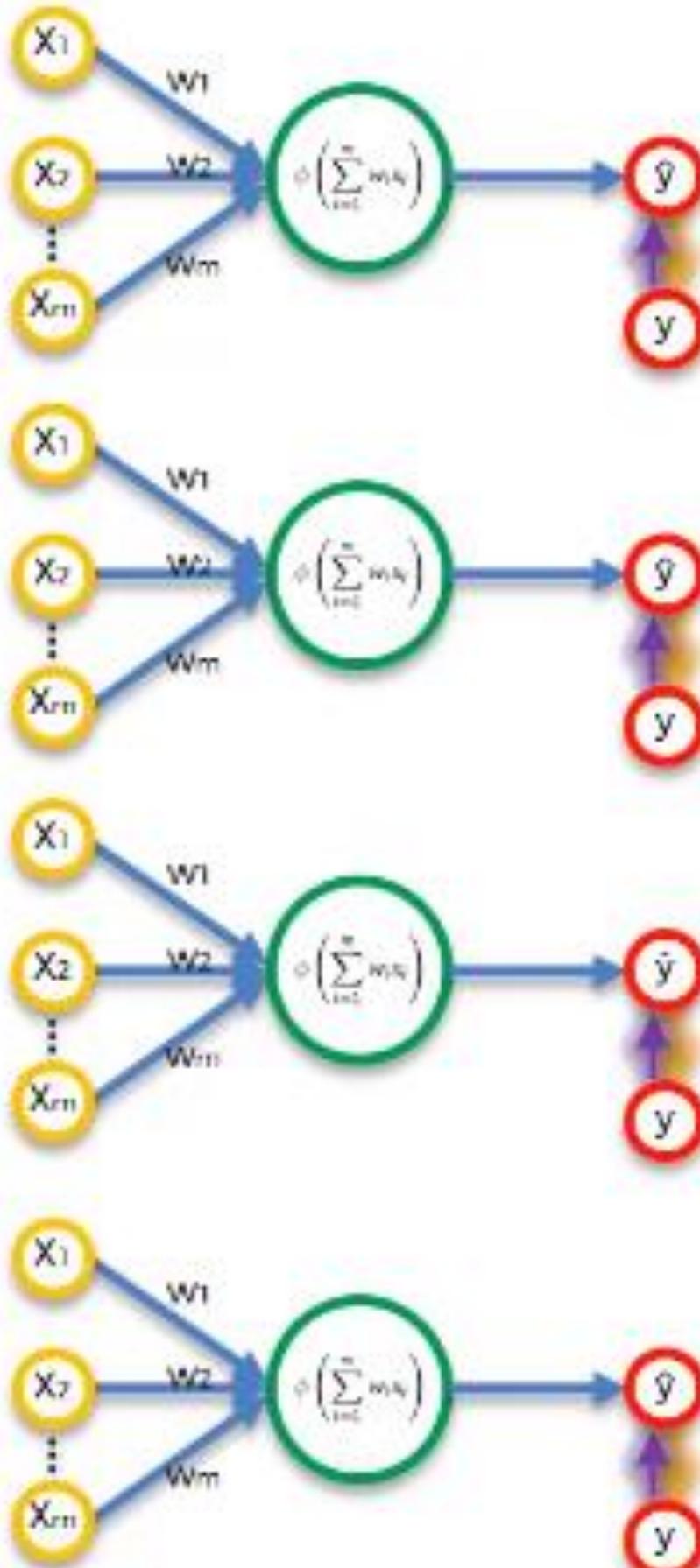
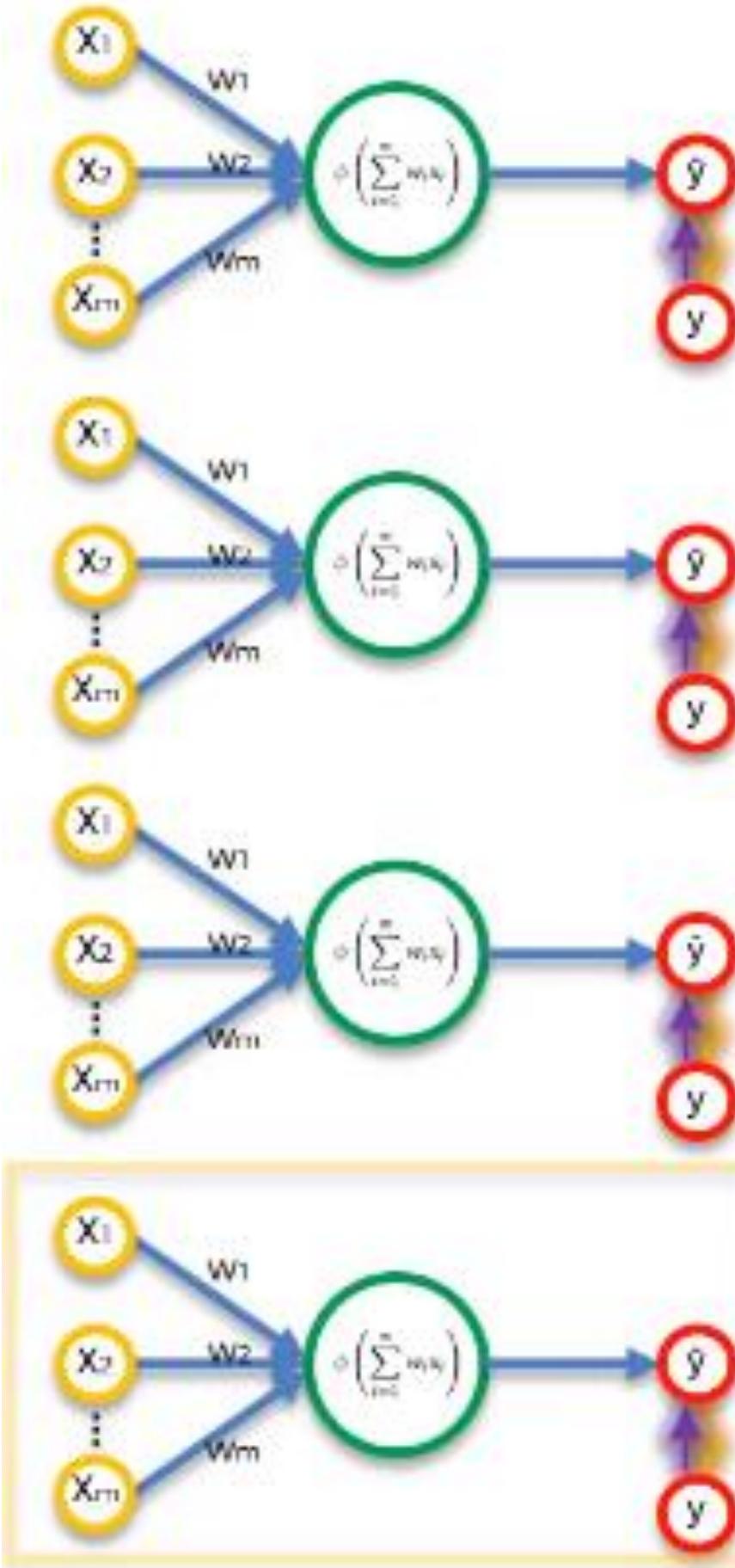
Нейронные сети



Row ID	Study Hrs	Sleep Hrs	Quiz	Exam
1	12	6	78%	93%
2	22	6.5	24%	68%
3	115	4	100%	95%
4	31	9	67%	75%
5	0	10	58%	51%
6	5	8	78%	60%
7	92	6	82%	89%
8	57	8	91%	97%



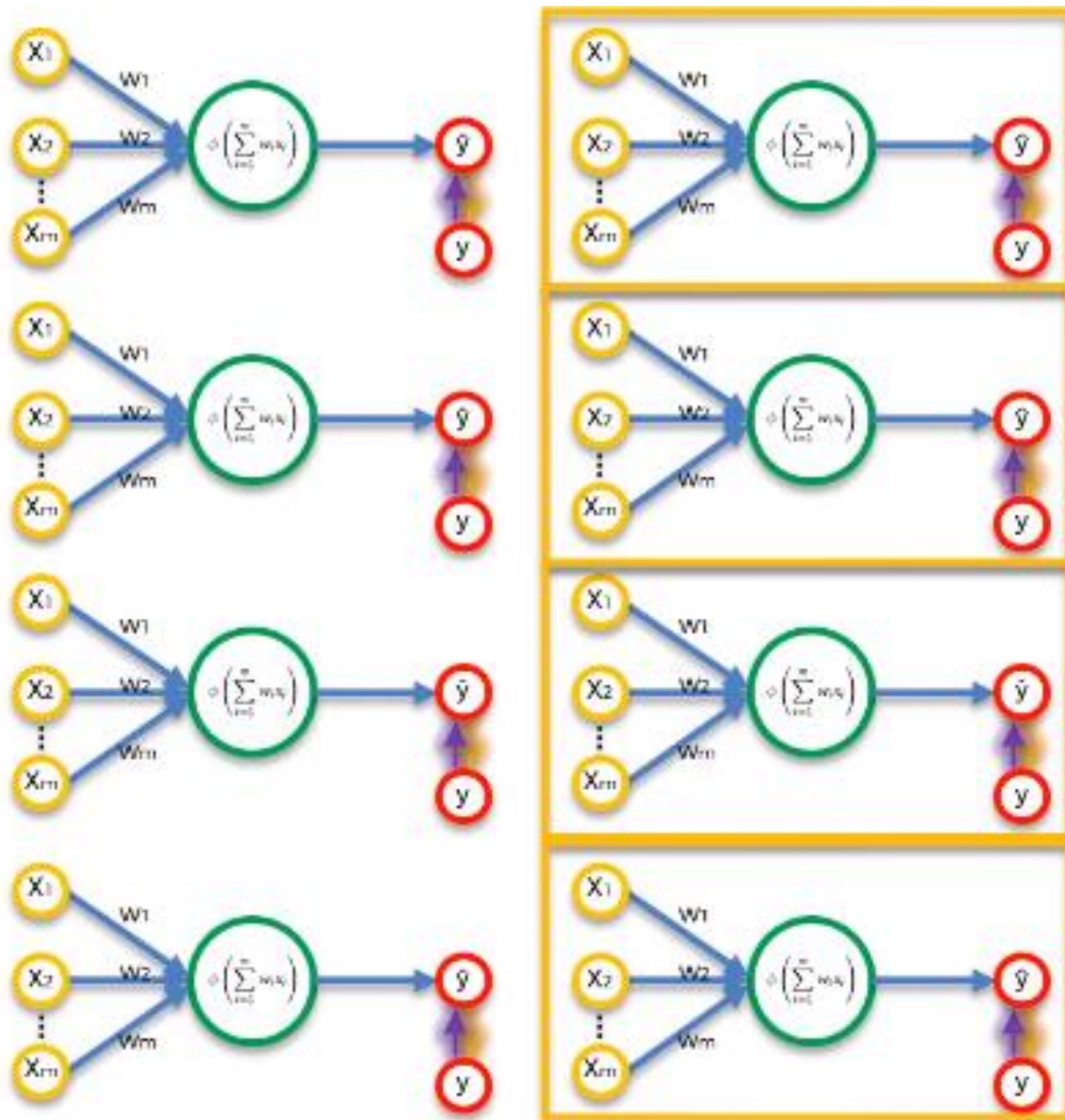
Нейронные сети



Row ID	Study Hrs	Sleep Hrs	Quiz	Exam
1	12	6	78%	93%
2	22	6.5	24%	68%
3	115	4	100%	95%
4	31	9	67%	75%
5	0	10	58%	51%
6	5	8	78%	60%
7	92	6	82%	89%
8	57	8	91%	97%



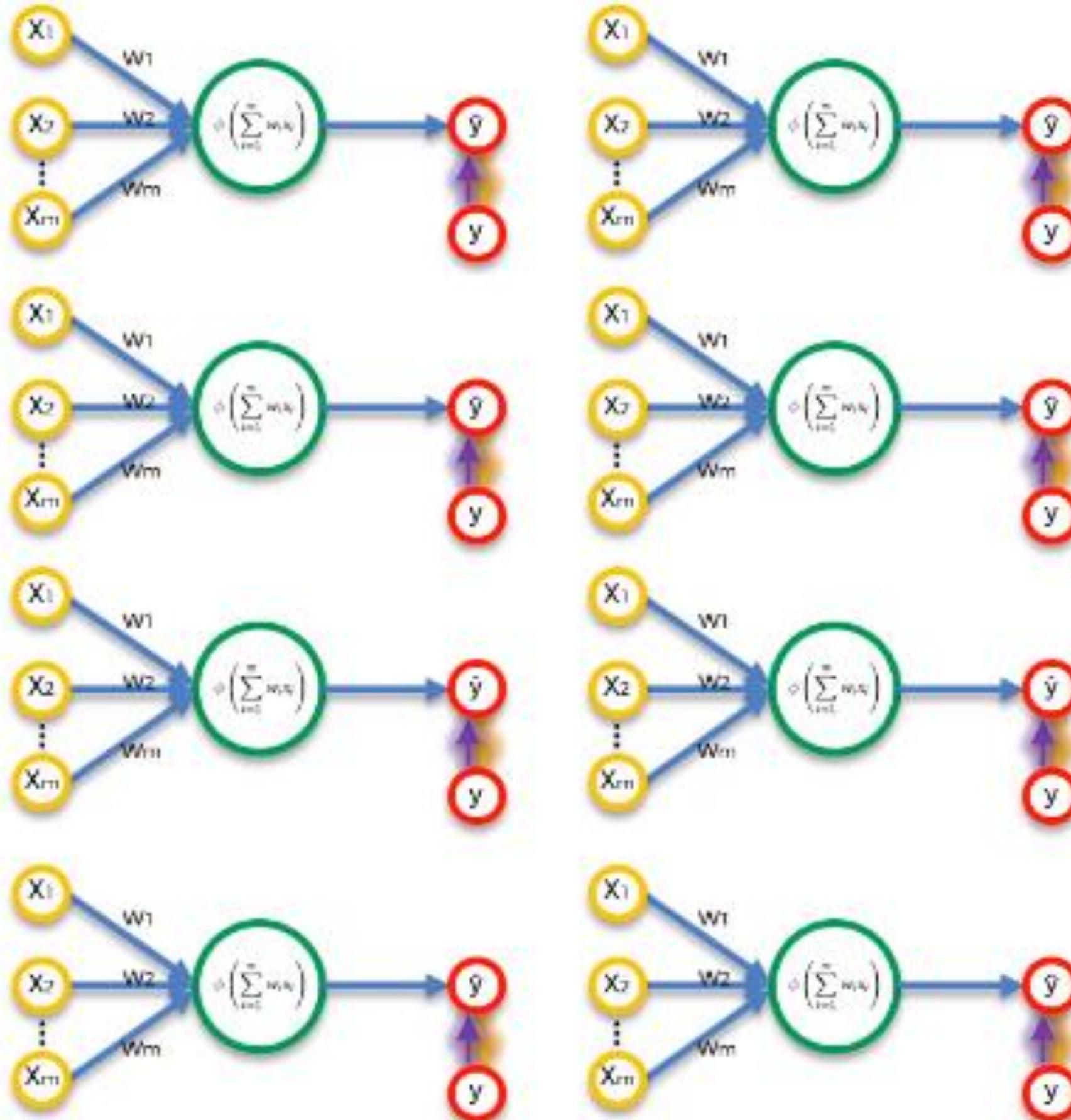
Нейронные сети



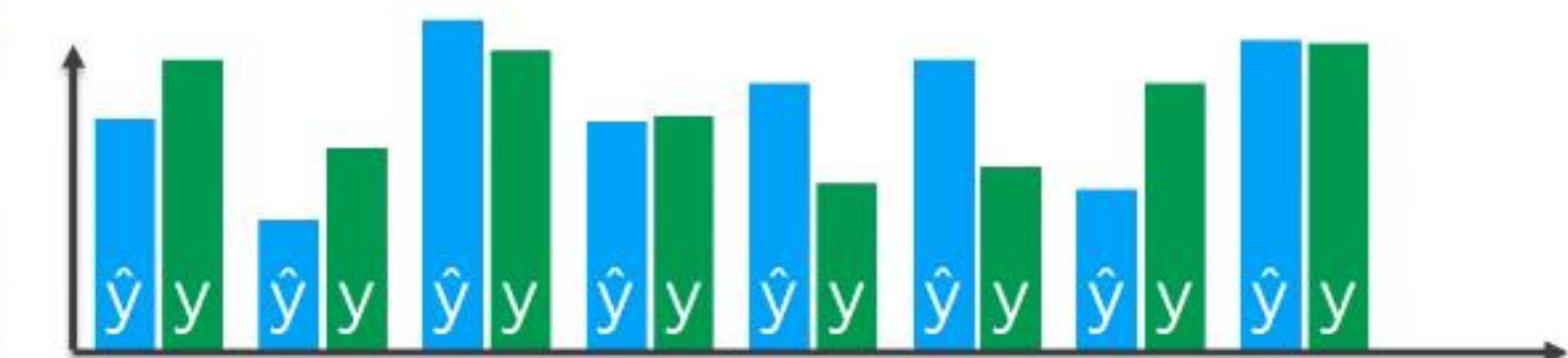
Row ID	Study Hrs	Sleep Hrs	Quiz	Exam
1	12	6	78%	93%
2	22	6.5	24%	68%
3	115	4	100%	95%
4	31	9	67%	75%
5	0	10	58%	51%
6	5	8	78%	60%
7	92	6	82%	89%
8	57	8	91%	97%



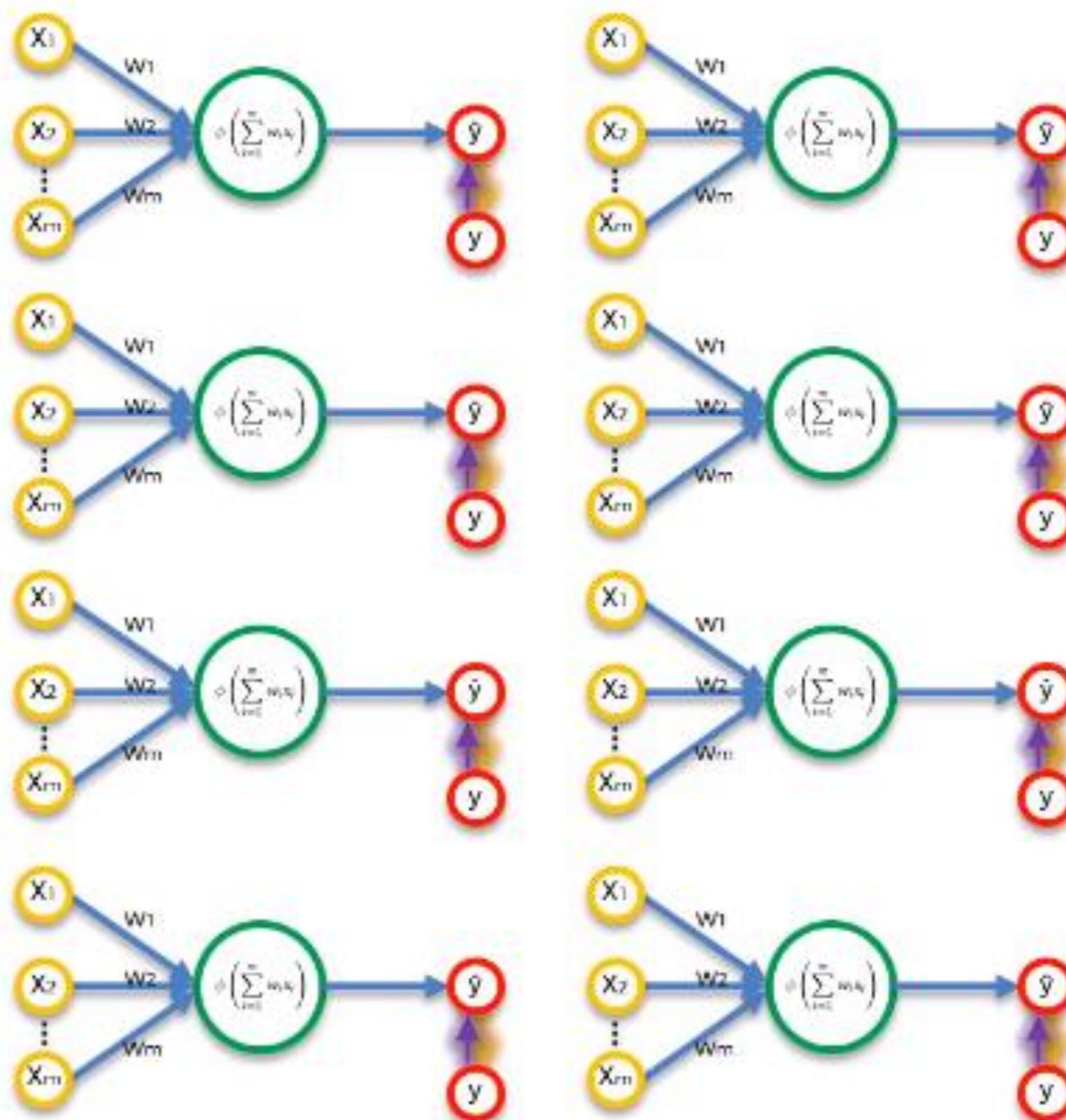
Нейронные сети



Row ID	Study Hrs	Sleep Hrs	Quiz	Exam
1	12	6	78%	93%
2	22	6.5	24%	68%
3	115	4	100%	95%
4	31	9	67%	75%
5	0	10	58%	51%
6	5	8	78%	60%
7	92	6	82%	89%
8	57	8	91%	97%



Нейронные сети

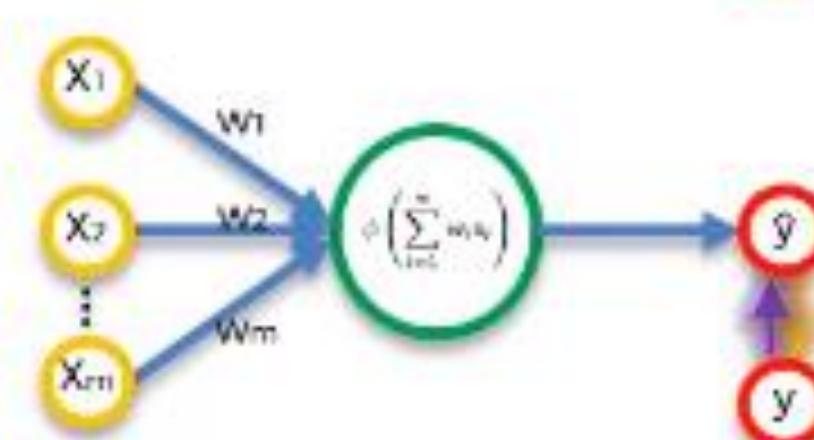
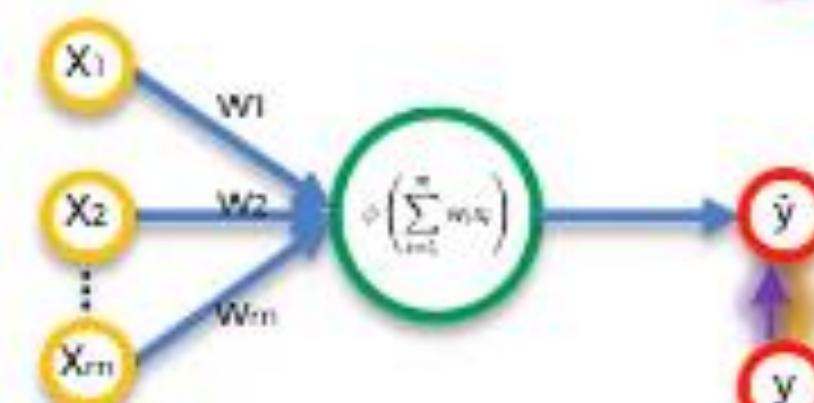
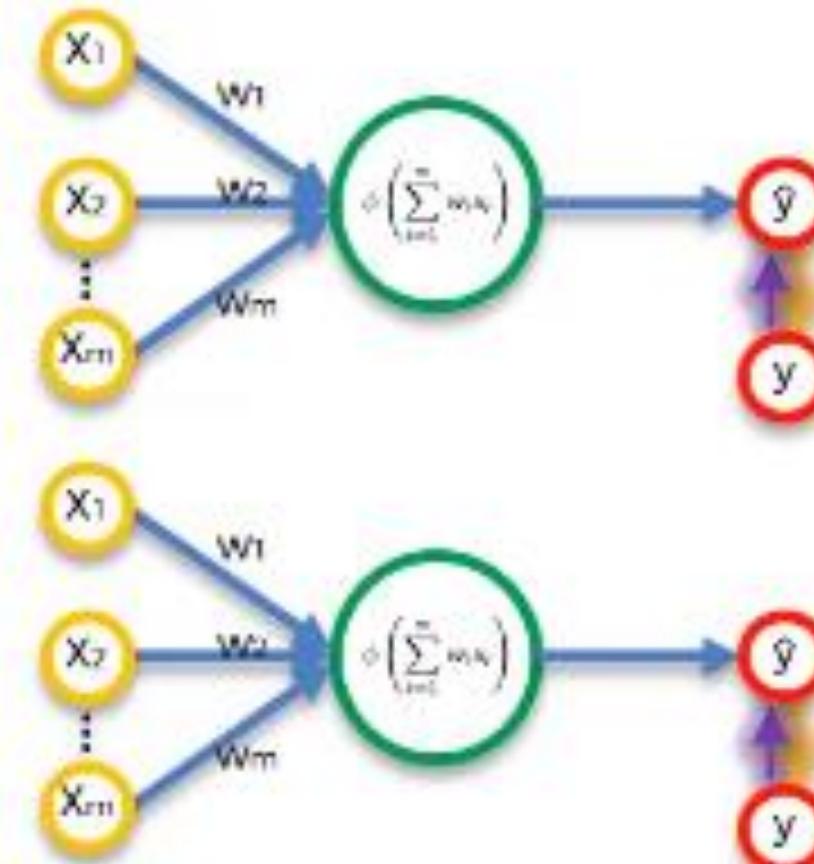
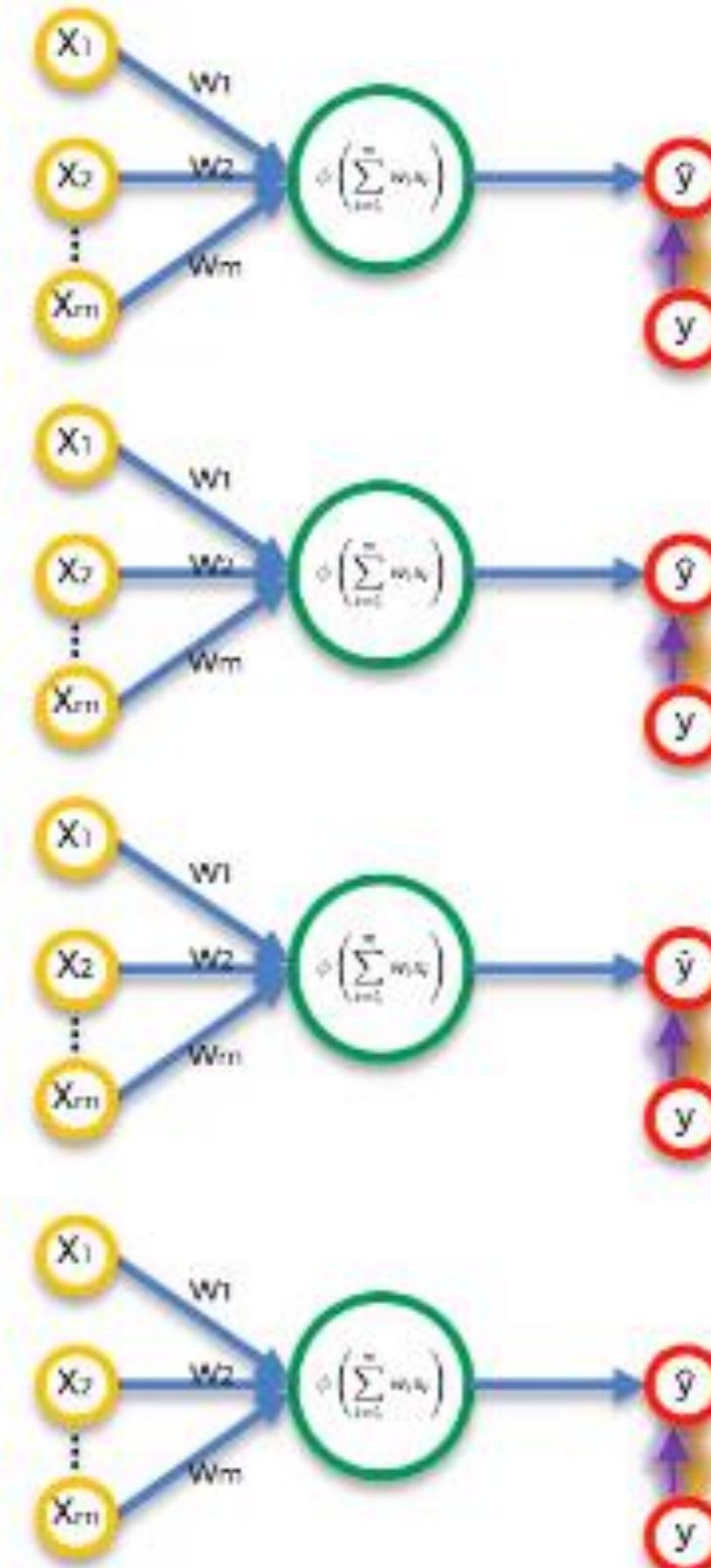
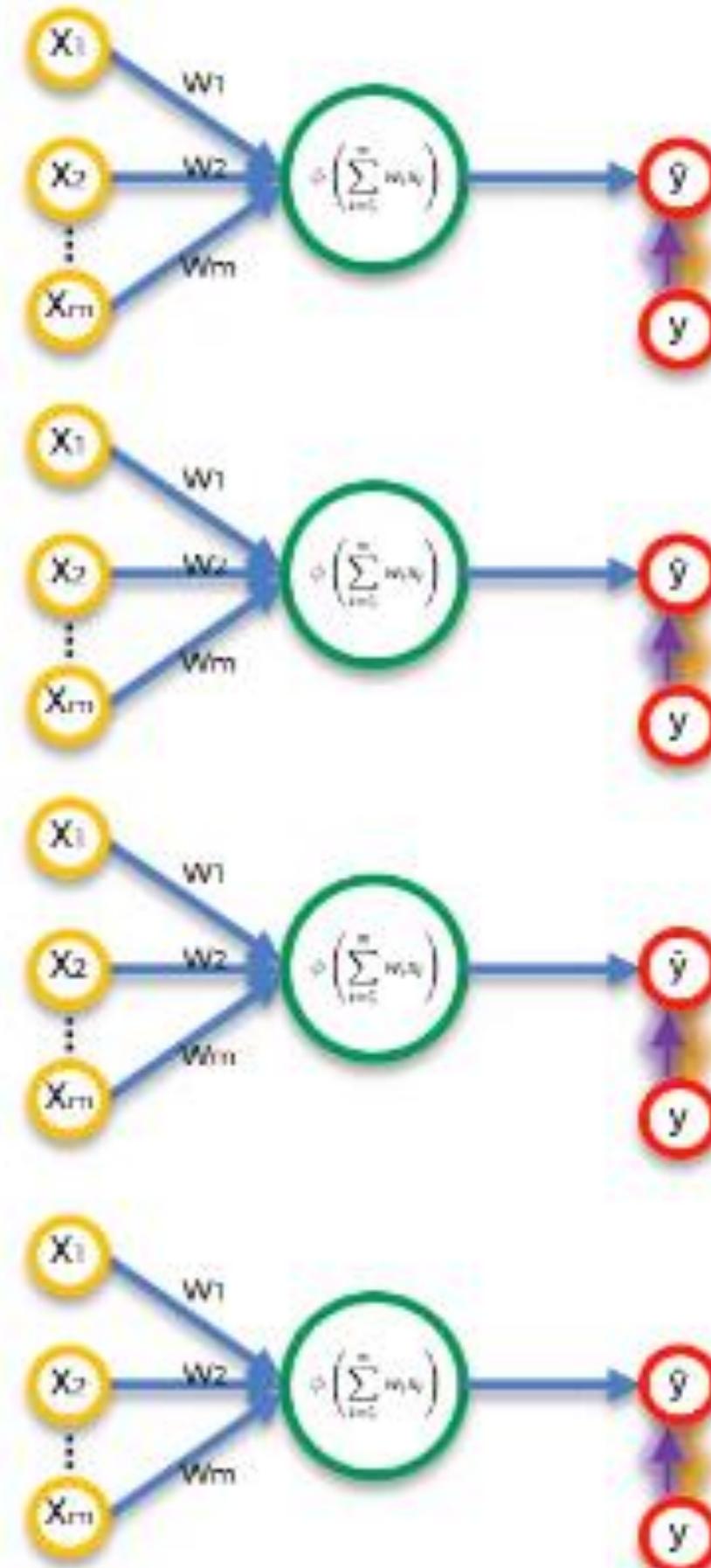


Row ID	Study Hrs	Sleep Hrs	Quiz	Exam
1	12	6	78%	93%
2	22	6.5	24%	68%
3	115	4	100%	95%
4	31	9	67%	75%
5	0	10	58%	51%
6	5	8	78%	60%
7	92	6	82%	89%
8	57	8	91%	97%

$$C = \sum \frac{1}{2}(\hat{y} - y)^2$$



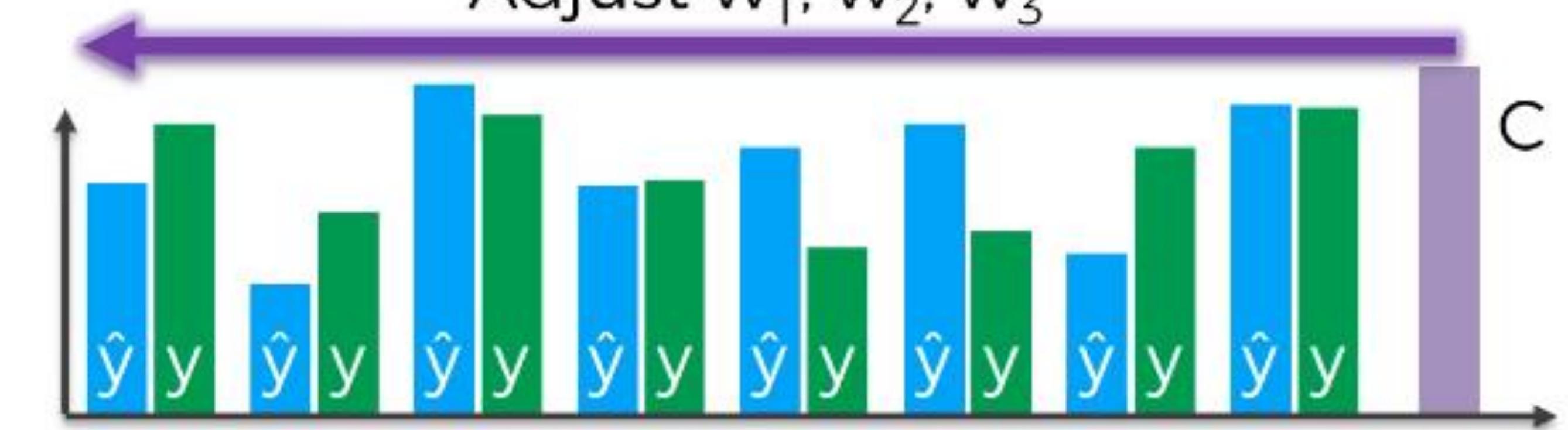
Нейронные сети



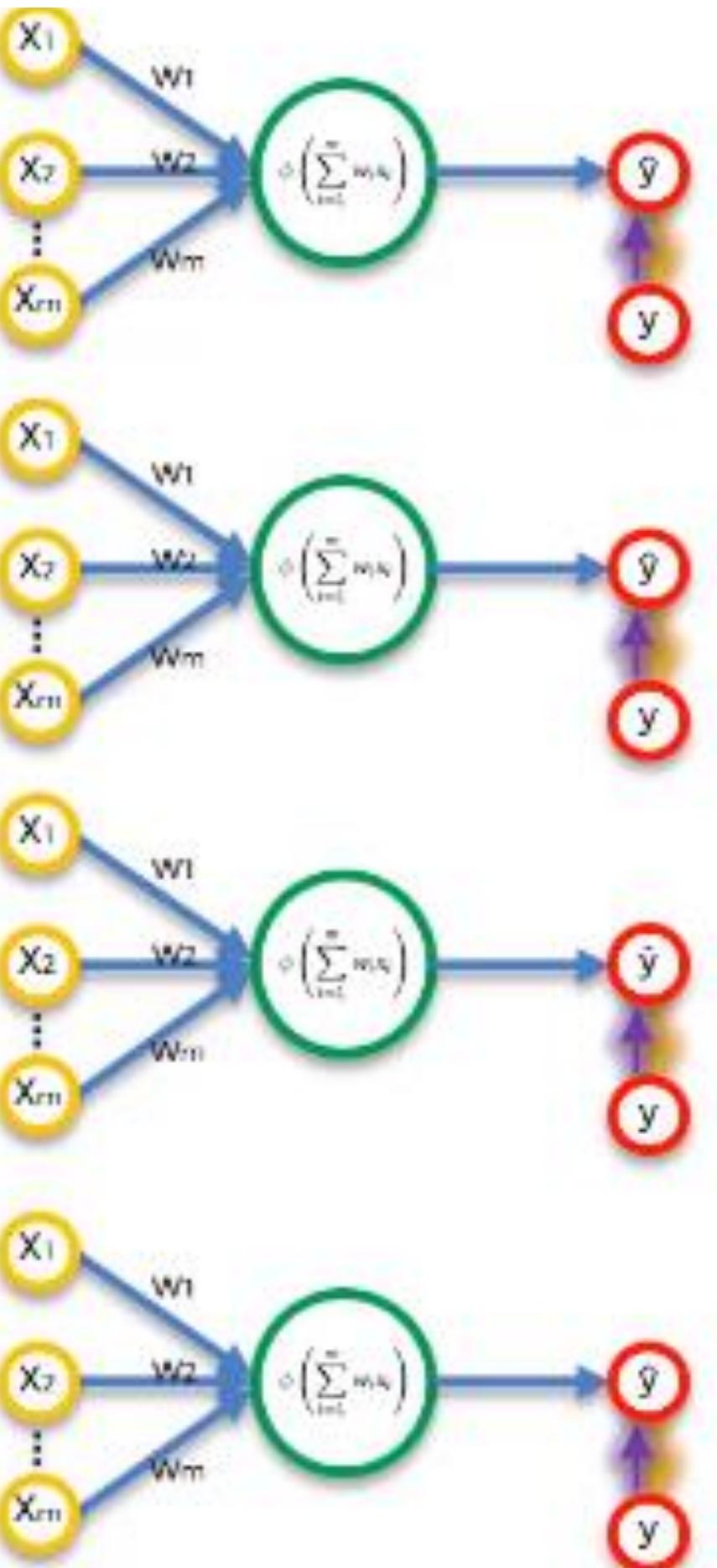
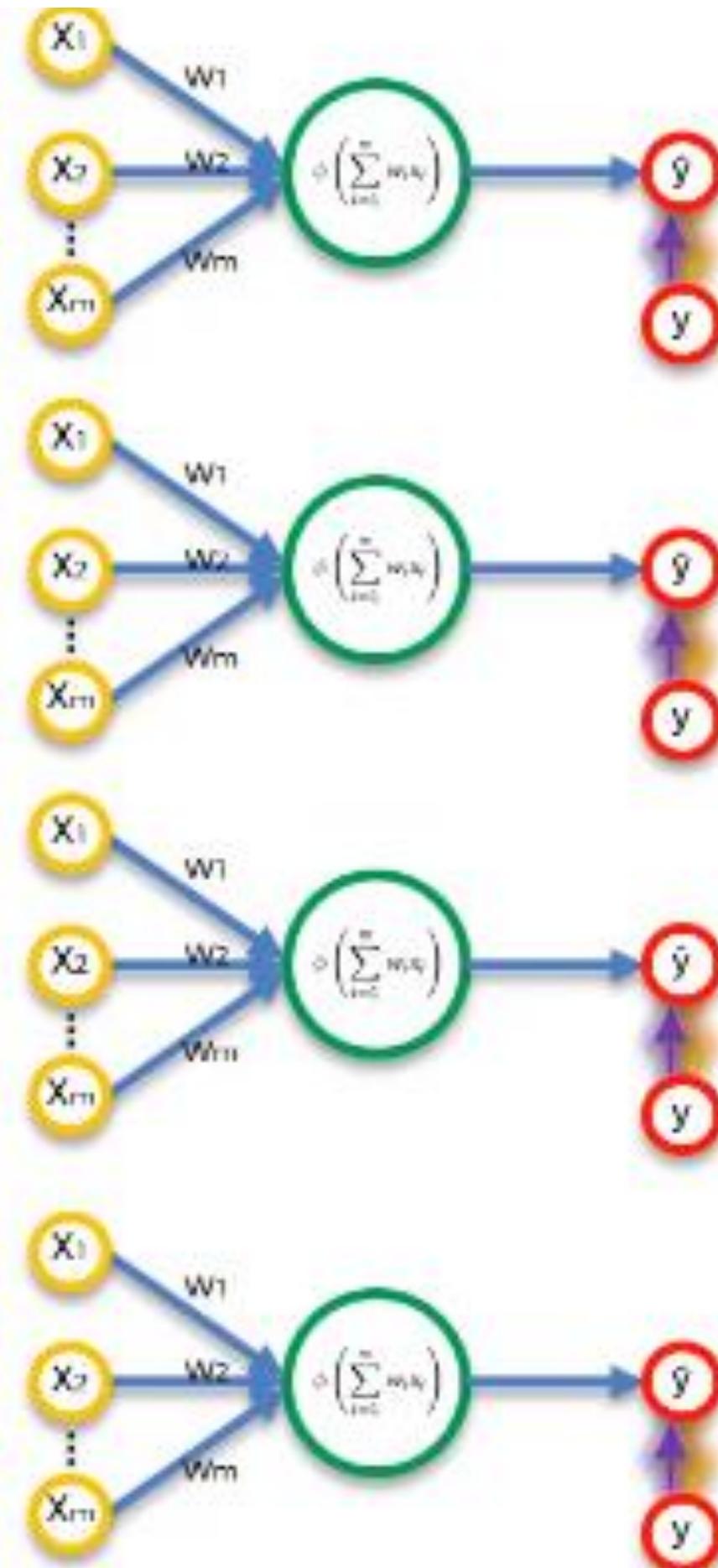
Row ID	Study Hrs	Sleep Hrs	Quiz	Exam
1	12	6	78%	93%
2	22	6.5	24%	68%
3	115	4	100%	95%
4	31	9	67%	75%
5	0	10	58%	51%
6	5	8	78%	60%
7	92	6	82%	89%
8	57	8	91%	97%

$$C = \sum \frac{1}{2}(\hat{y} - y)^2$$

Adjust w_1, w_2, w_3

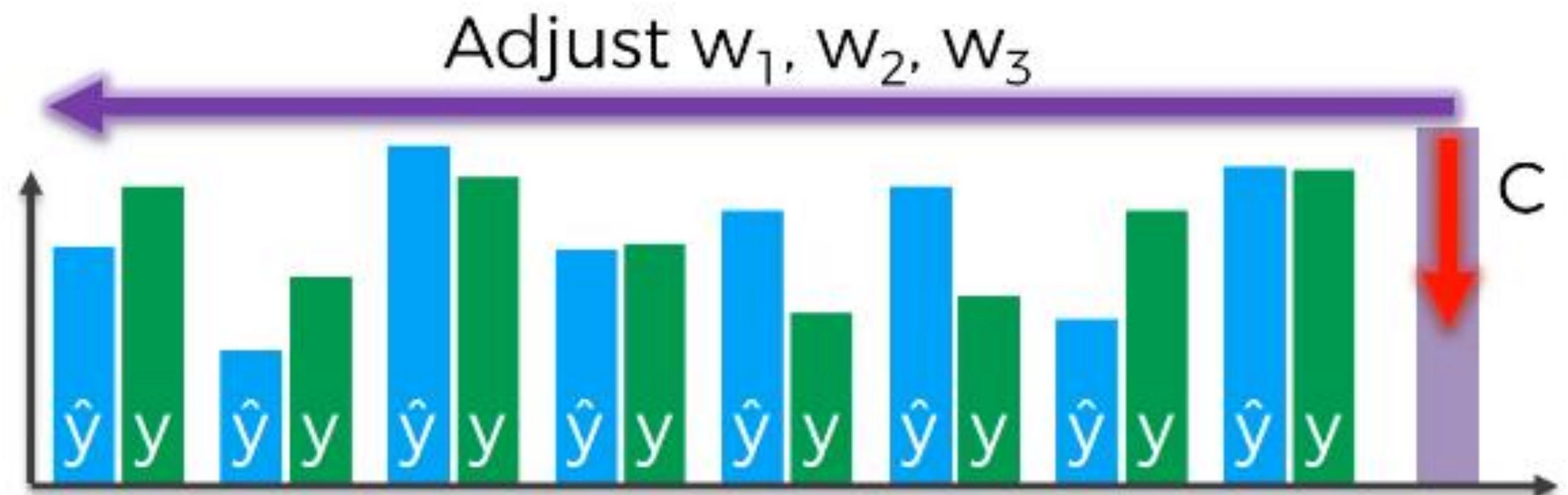


Нейронные сети



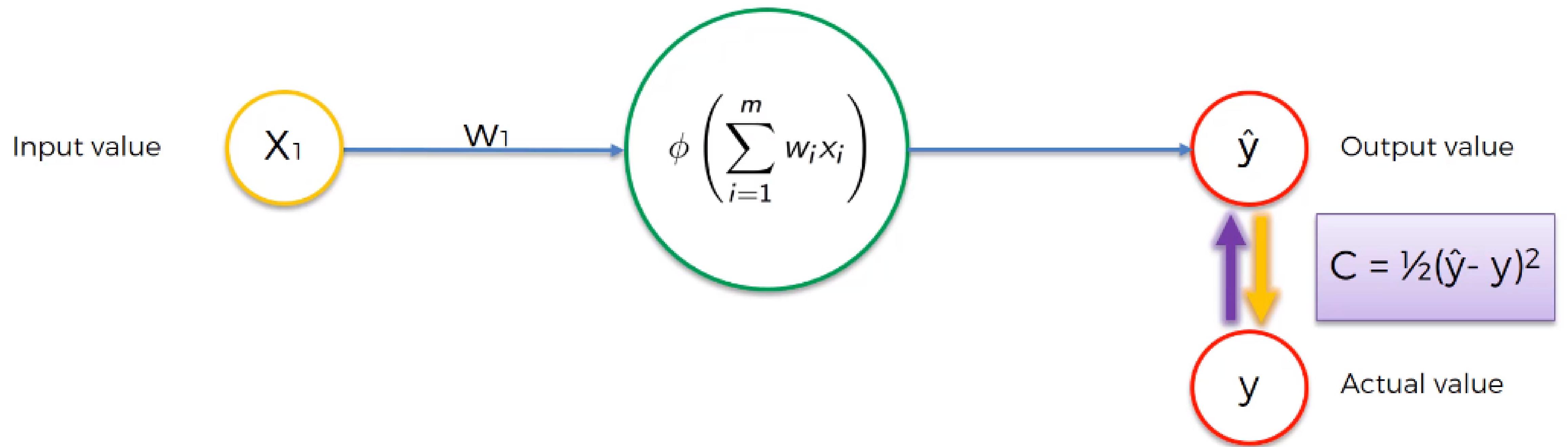
Row ID	Study Hrs	Sleep Hrs	Quiz	Exam
1	12	6	78%	93%
2	22	6.5	24%	68%
3	115	4	100%	95%
4	31	9	67%	75%
5	0	10	58%	51%
6	5	8	78%	60%
7	92	6	82%	89%
8	57	8	91%	97%

$$C = \sum \frac{1}{2}(\hat{y} - y)^2$$

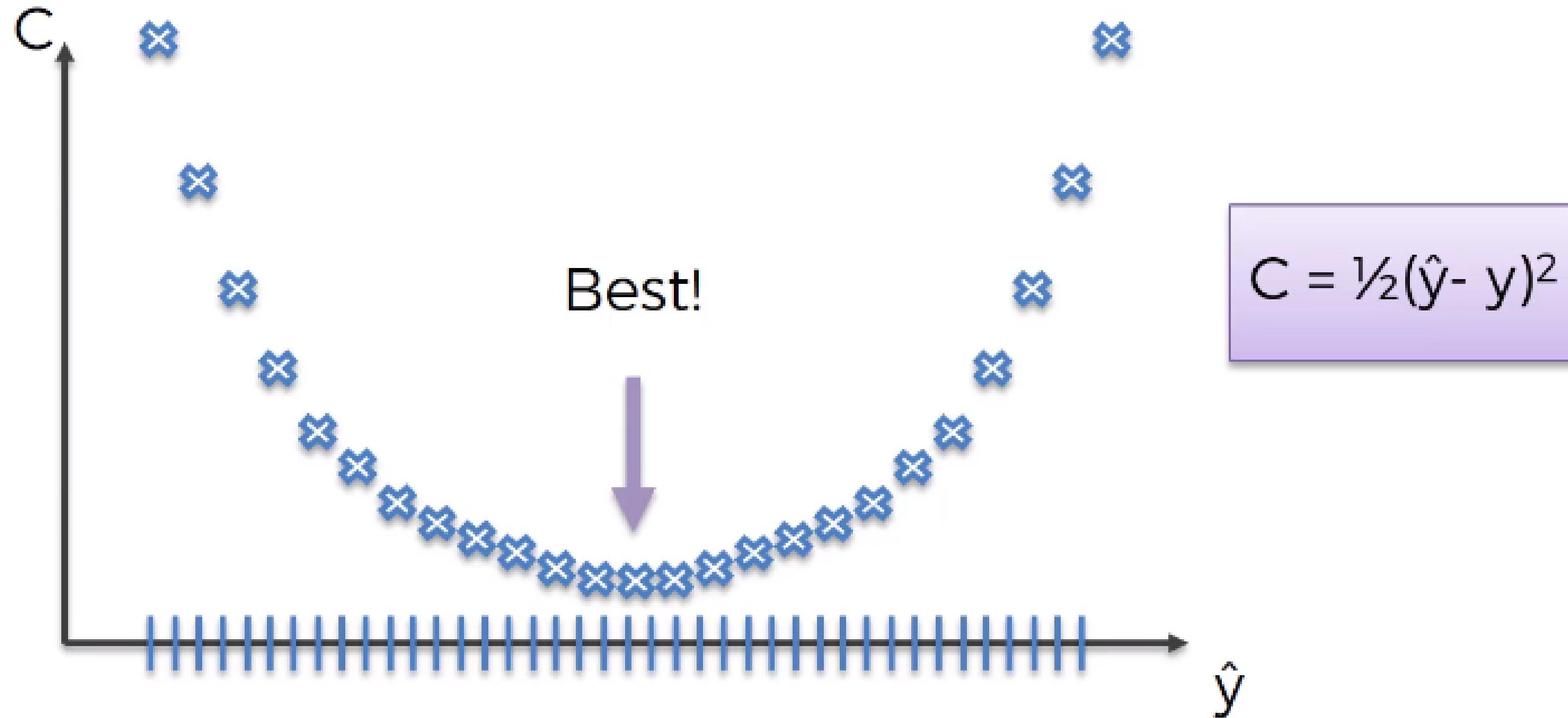


<https://stats.stackexchange.com/questions/154879/a-list-of-cost-functions-used-in-neural-networks-alongside->

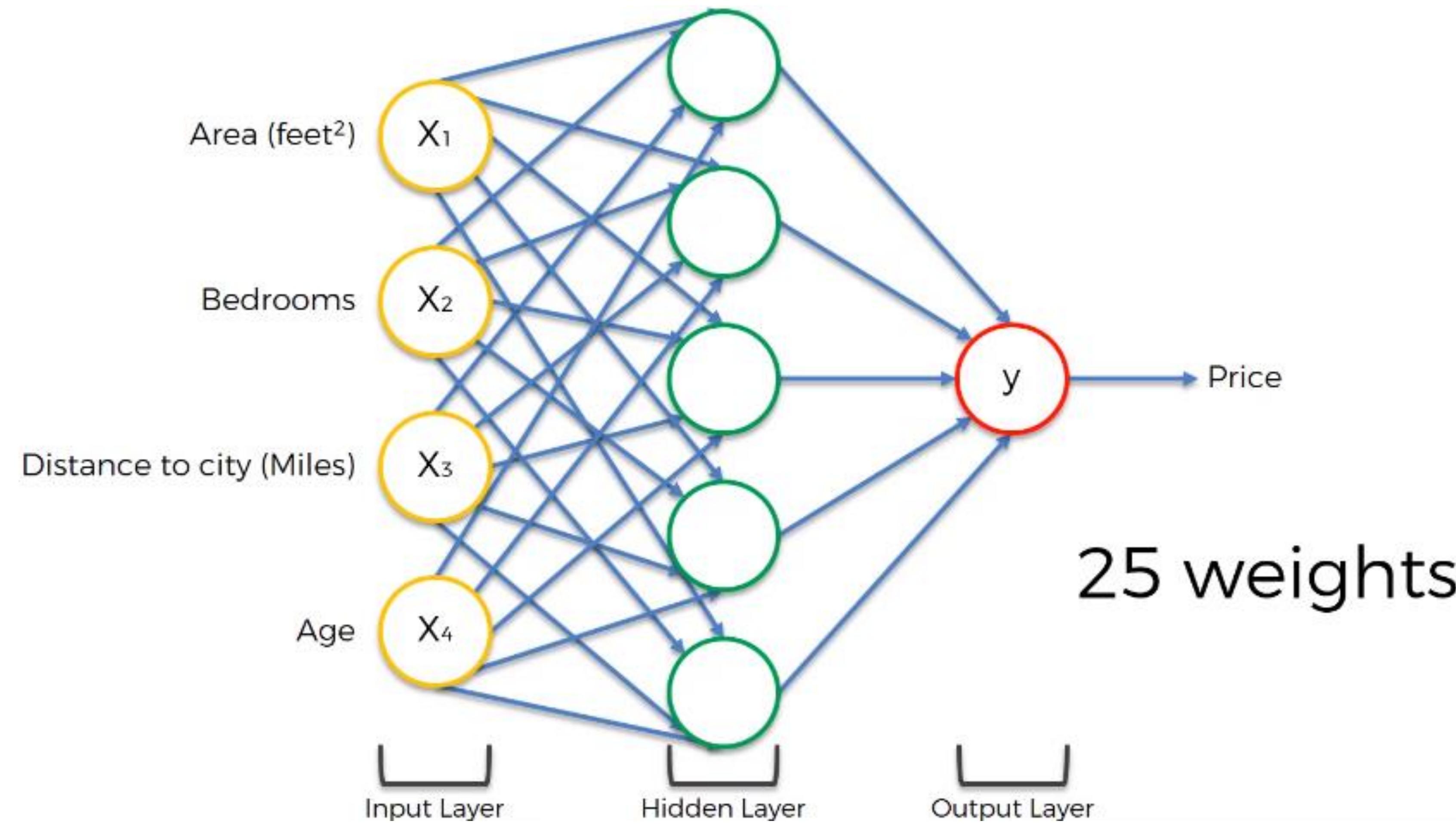
Градиентный спуск



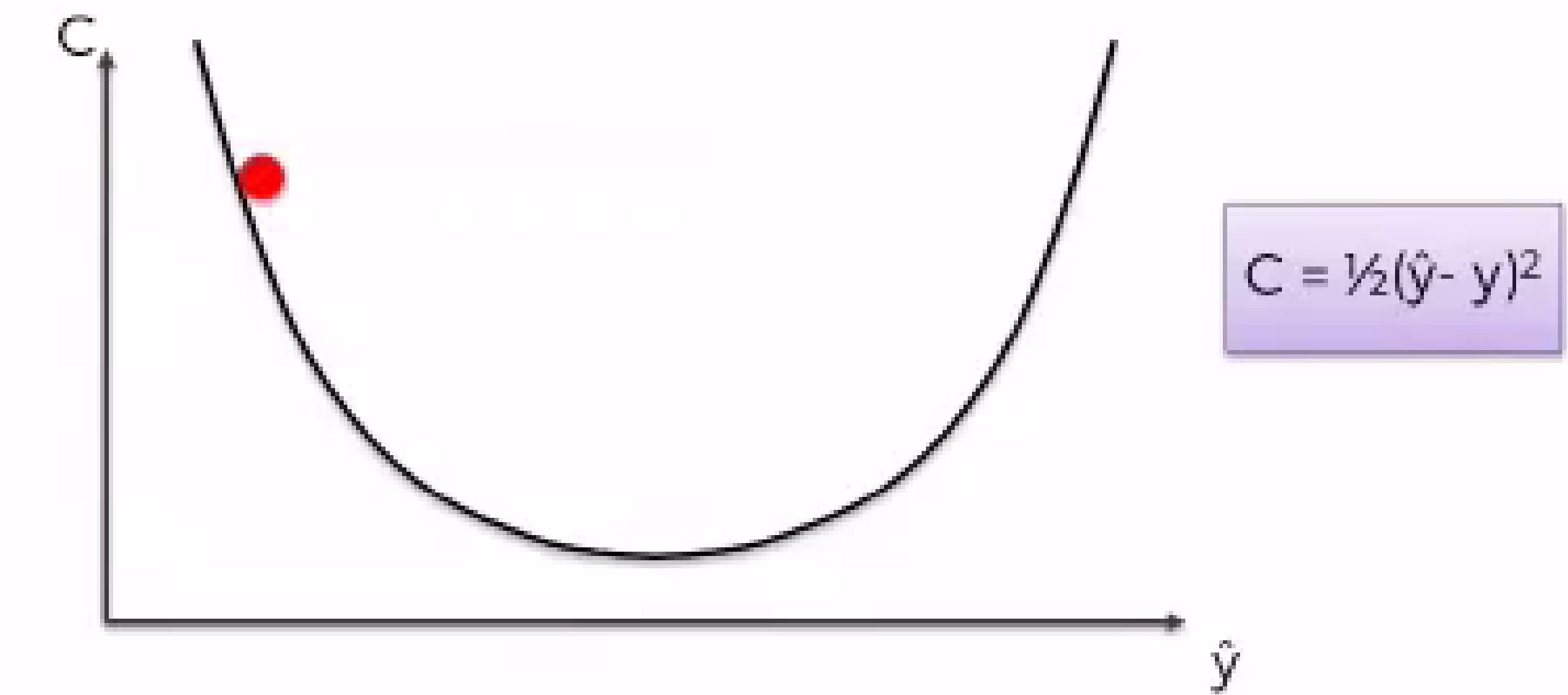
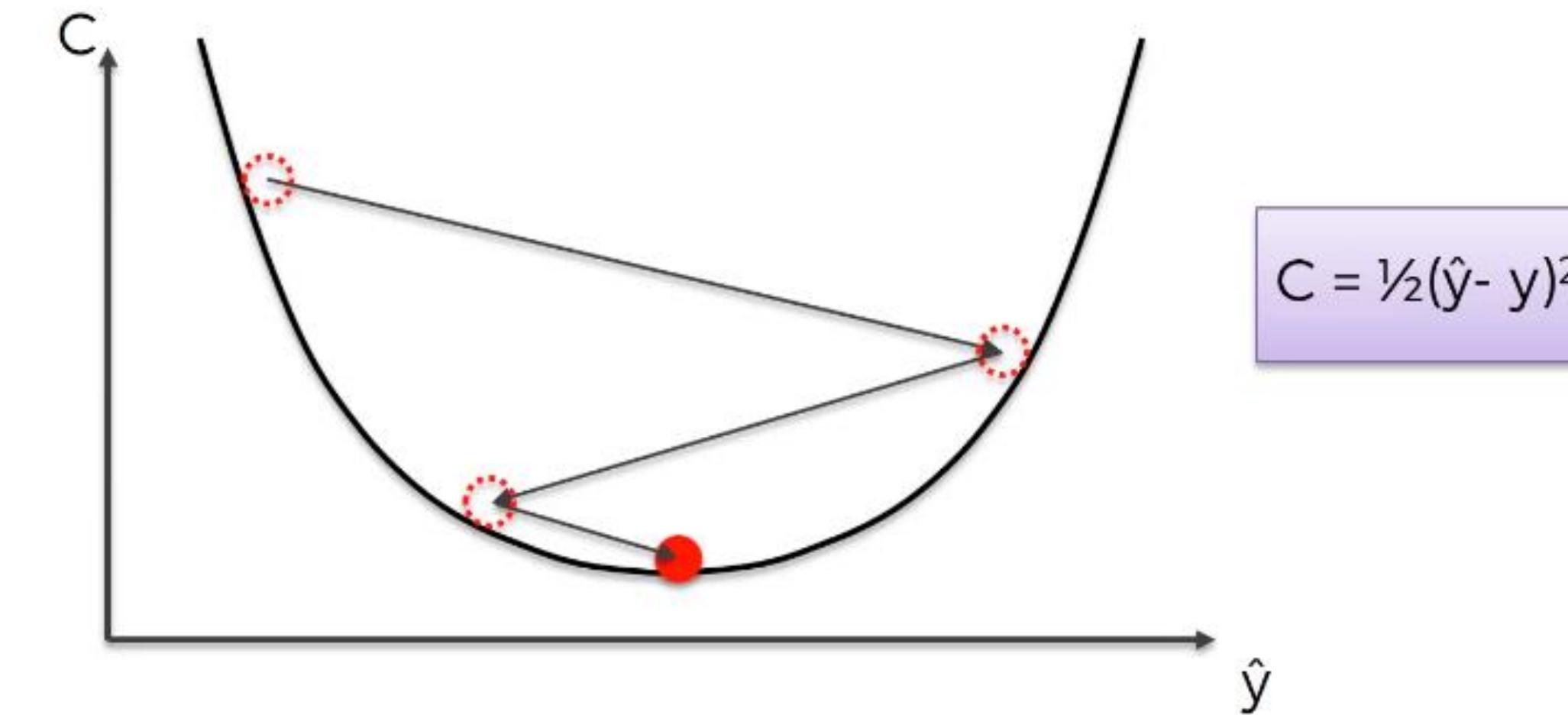
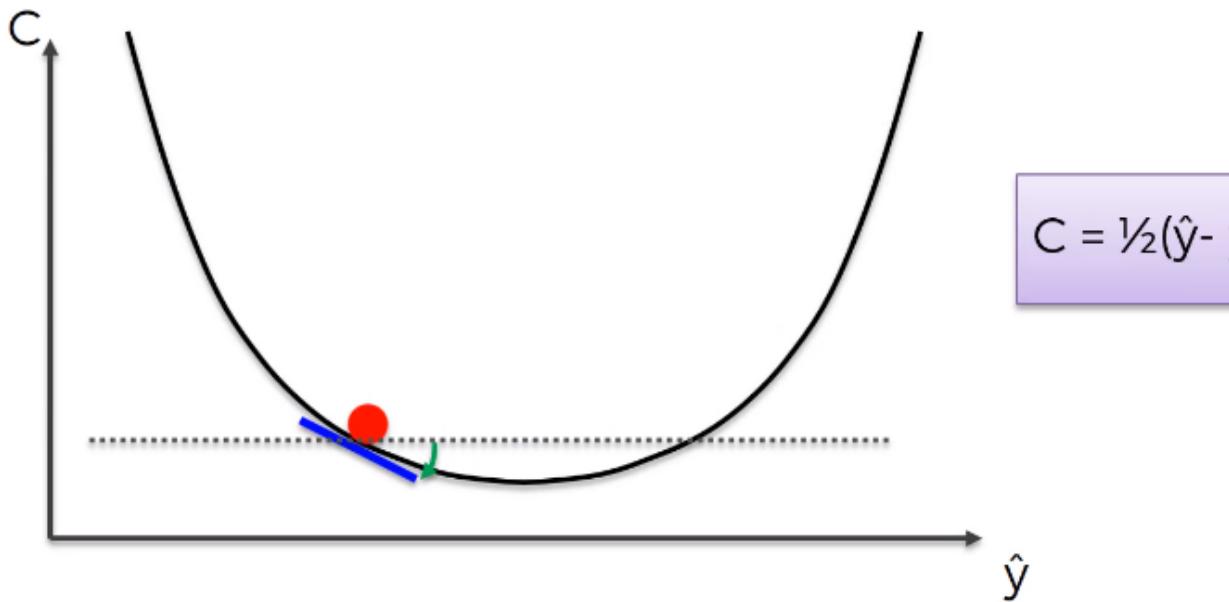
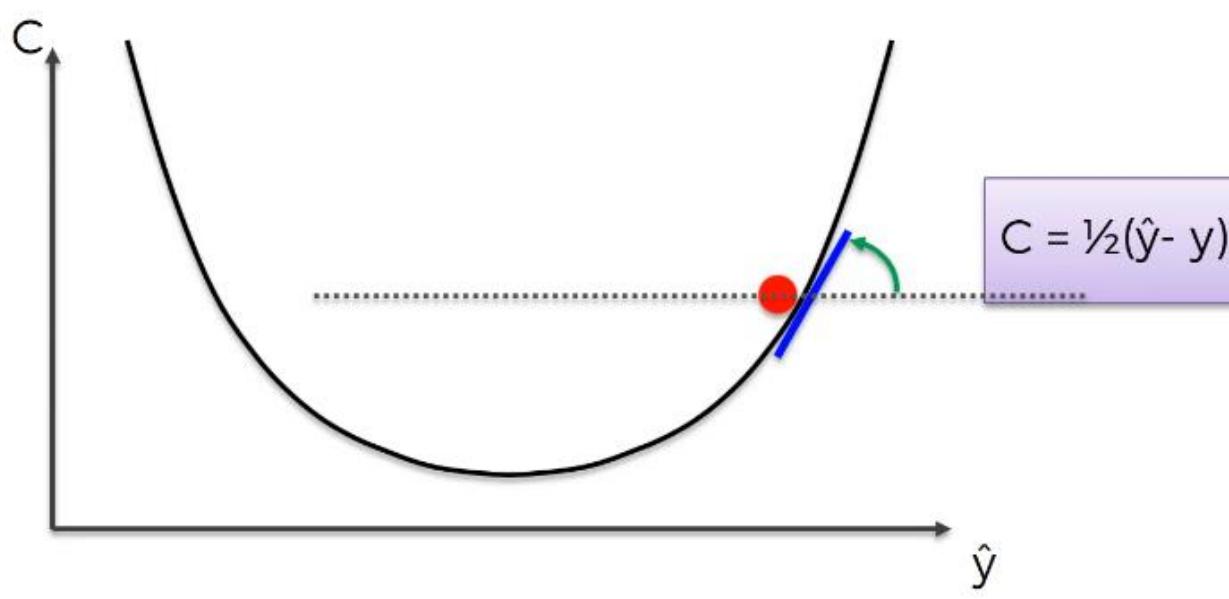
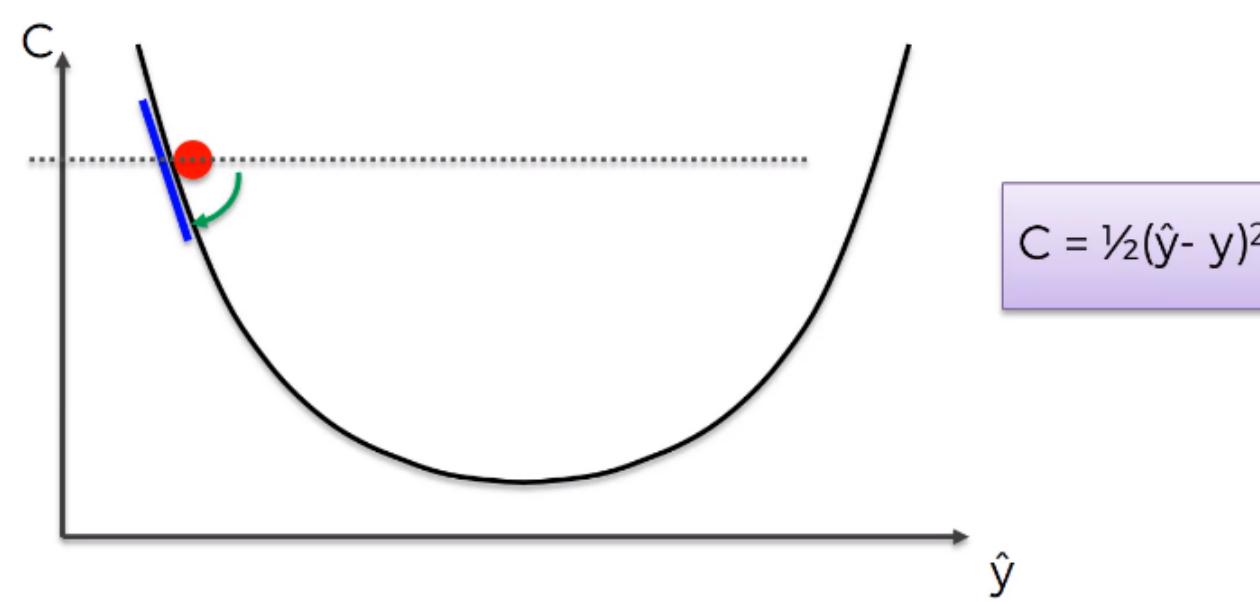
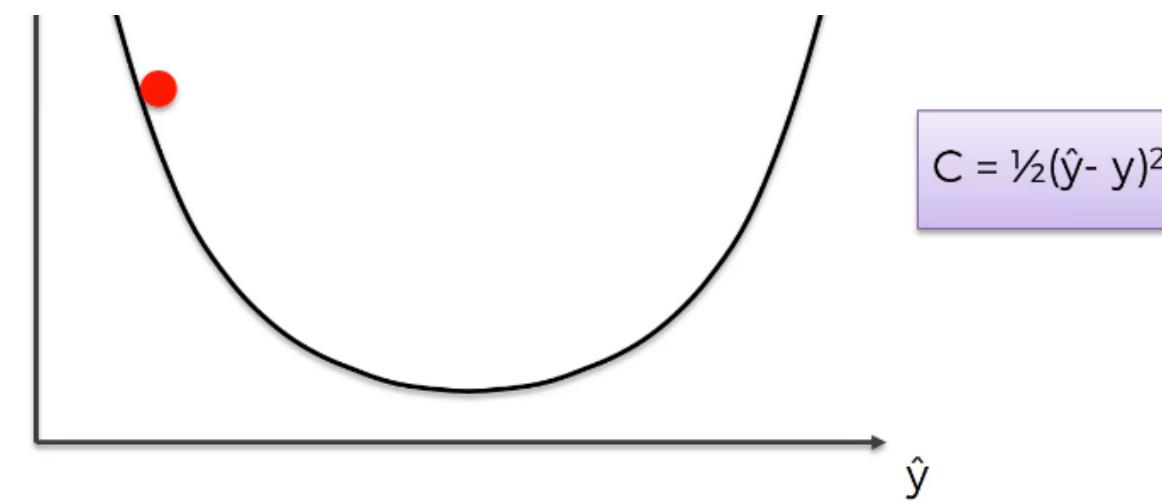
Градиентный спуск



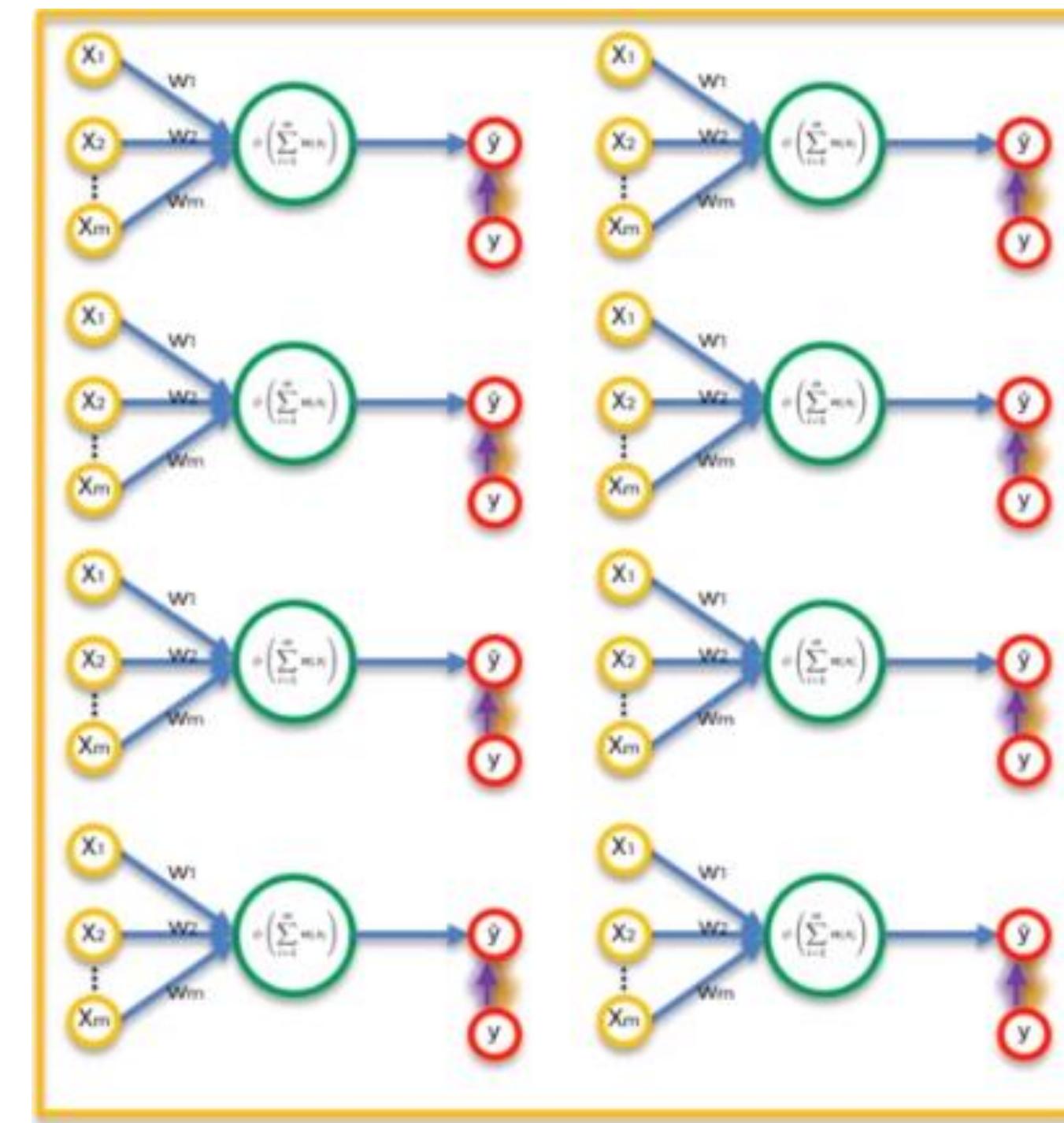
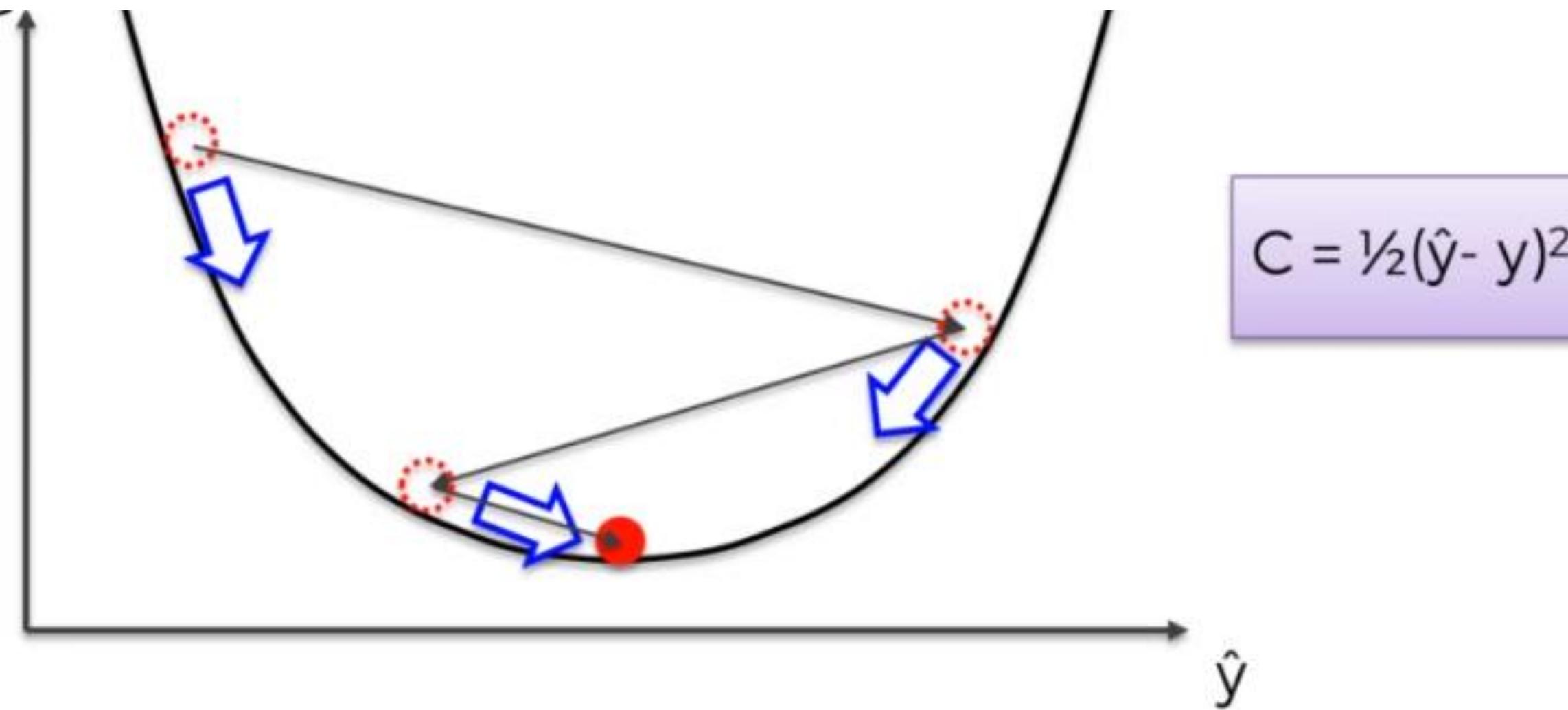
Градиентный спуск



Градиентный спуск



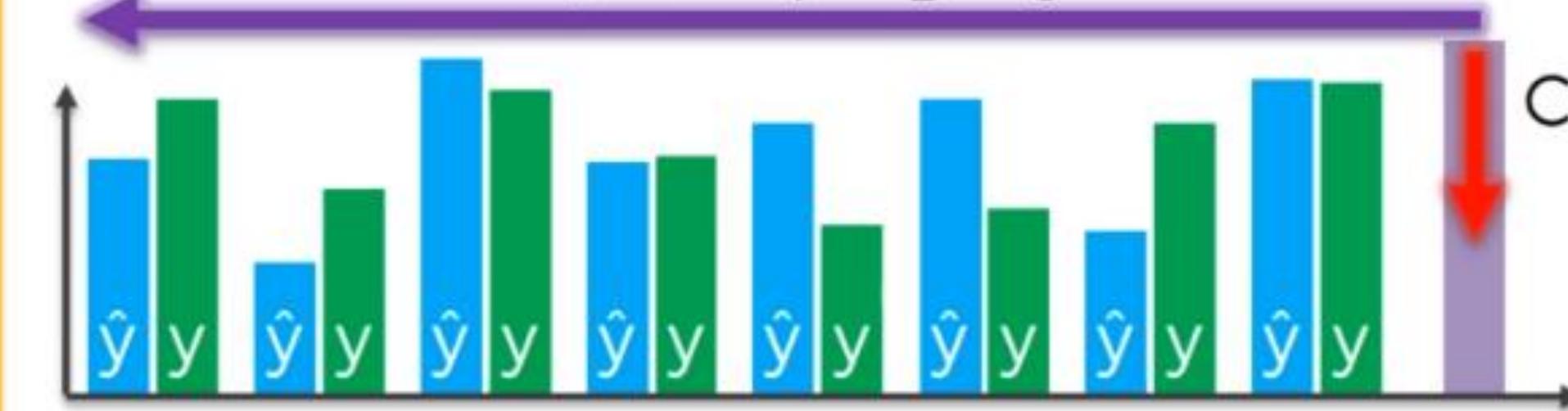
Градиентный спуск



Row ID	Study Hrs	Sleep Hrs	Quiz	Exam
1	12	6	78%	93%
2	22	6.5	24%	68%
3	115	4	100%	95%
4	31	9	67%	75%
5	0	10	58%	51%
6	5	8	78%	60%
7	92	6	82%	89%
8	57	8	91%	97%

$$C = \sum \frac{1}{2}(\hat{y} - y)^2$$

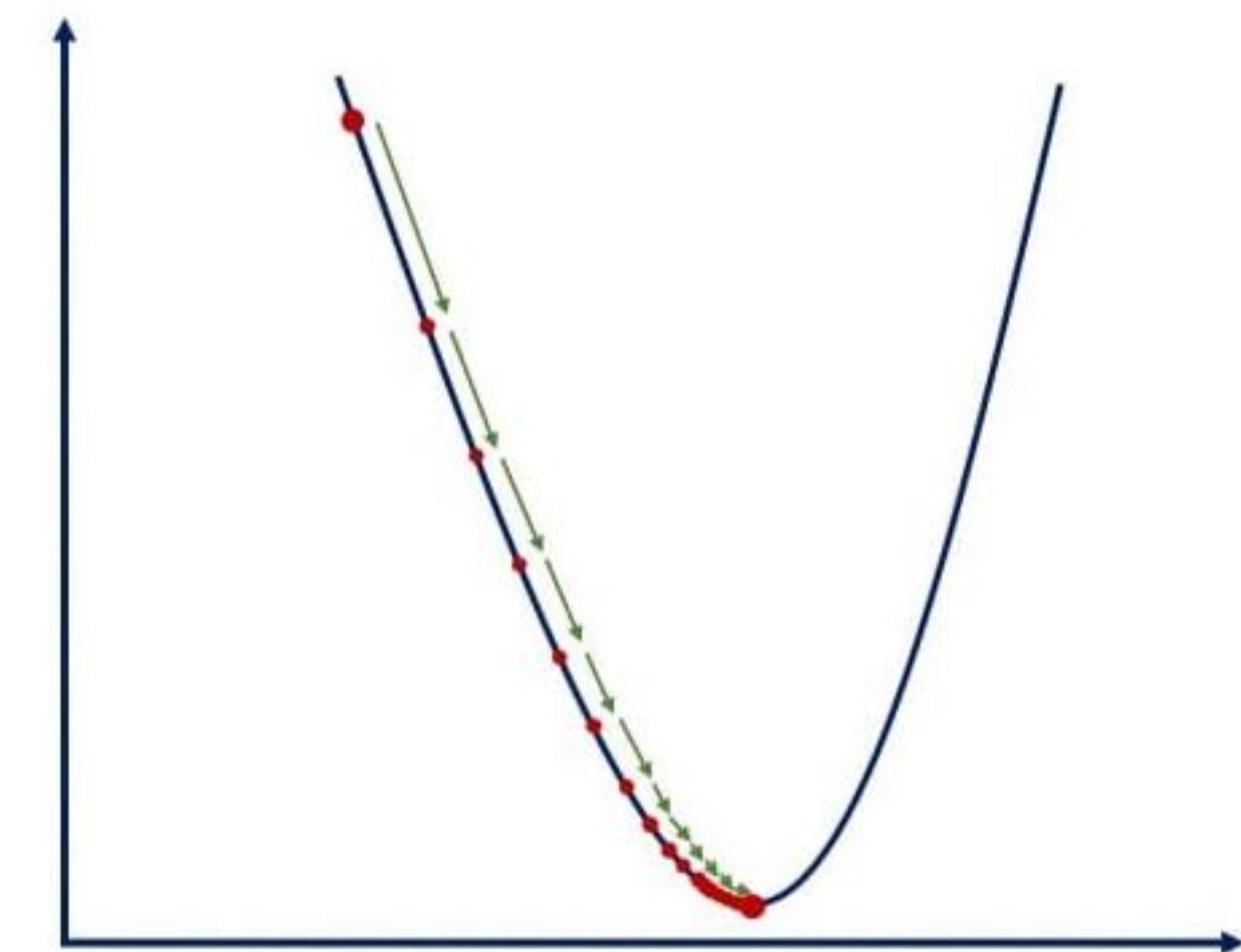
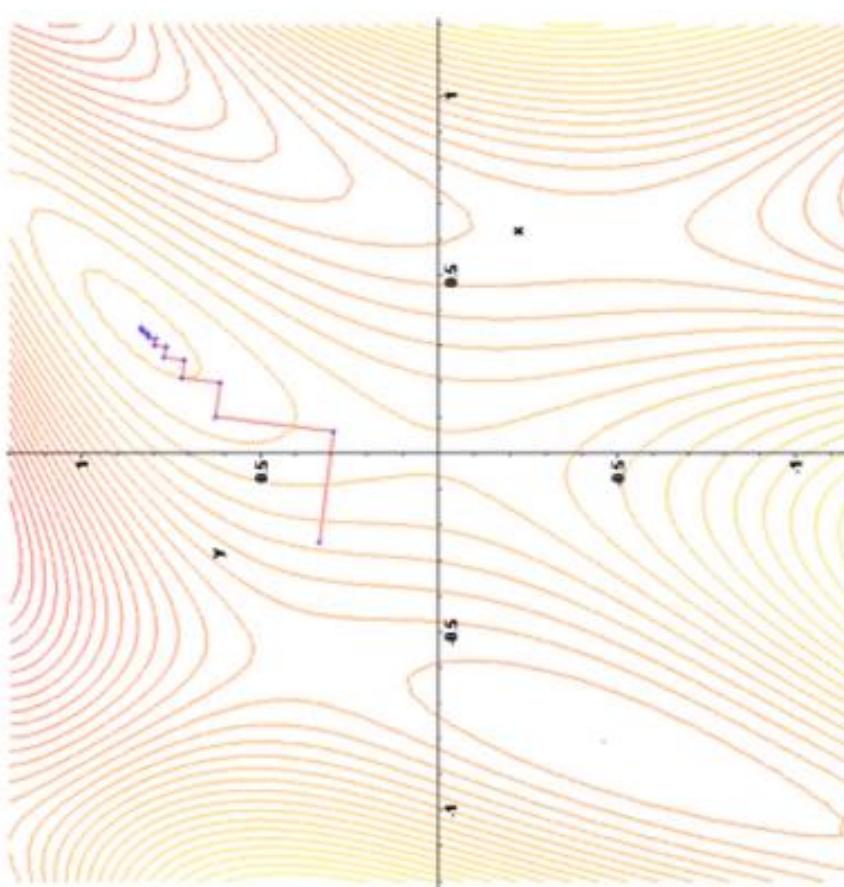
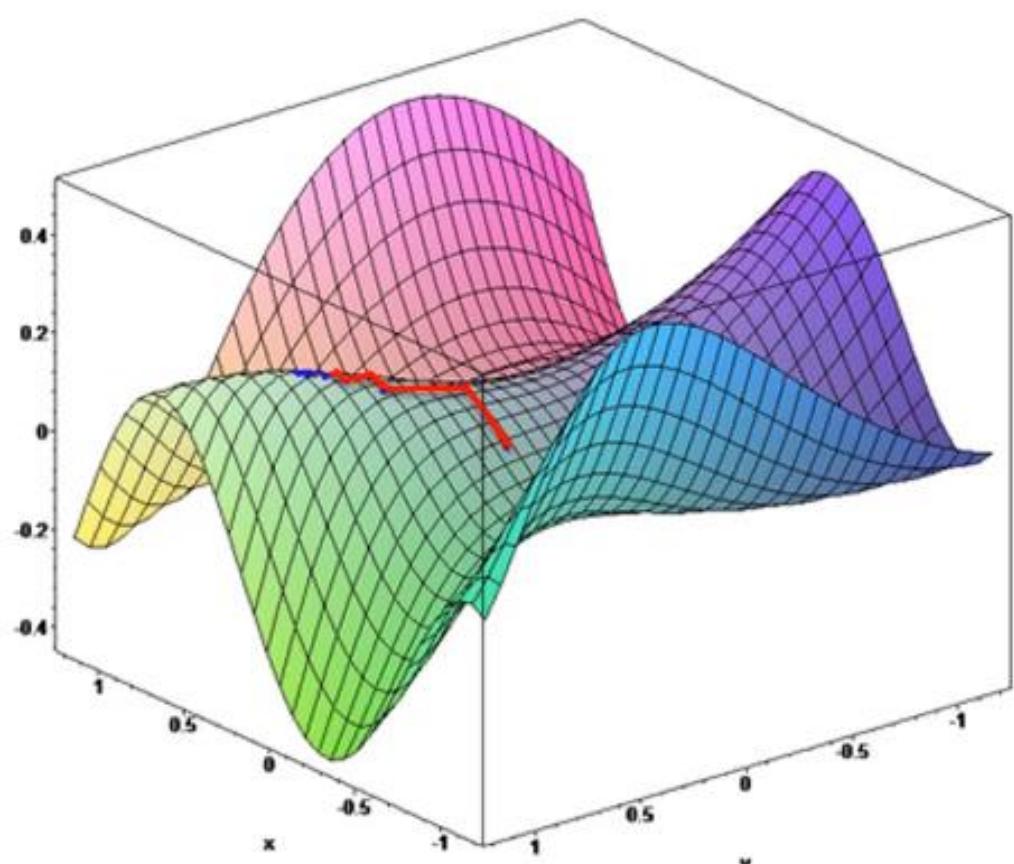
Adjust w_1, w_2, w_3



Upd w's

Row ID	Study Hrs	Sleep Hrs	Quiz	Exam
1	12	6	78%	93%
2	22	6.5	24%	68%
3	115	4	100%	95%
4	31	9	67%	75%
5	0	10	58%	51%
6	5	8	78%	60%
7	92	6	82%	89%
8	57	8	91%	97%

Градиентный спуск



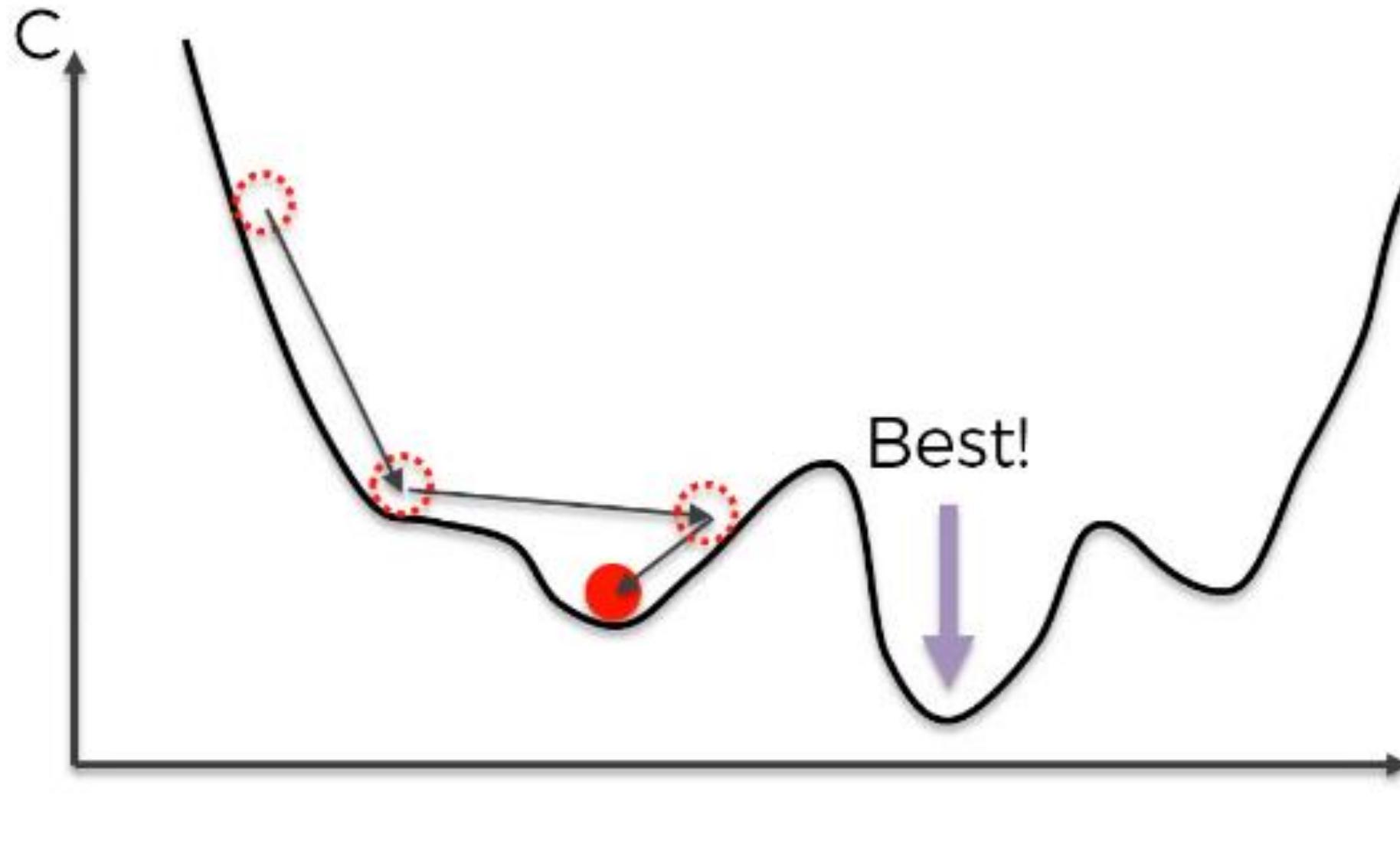
Gradient descent

$$\mathbf{w}_{i+1} = \mathbf{w}_i - \eta \sum_i x_i \delta_i$$

$$\mathbf{b}_{i+1} = \mathbf{b}_i - \eta \sum_i \delta_i$$

$$\delta_i = y_i - t_i$$

Стохастический градиентный спуск

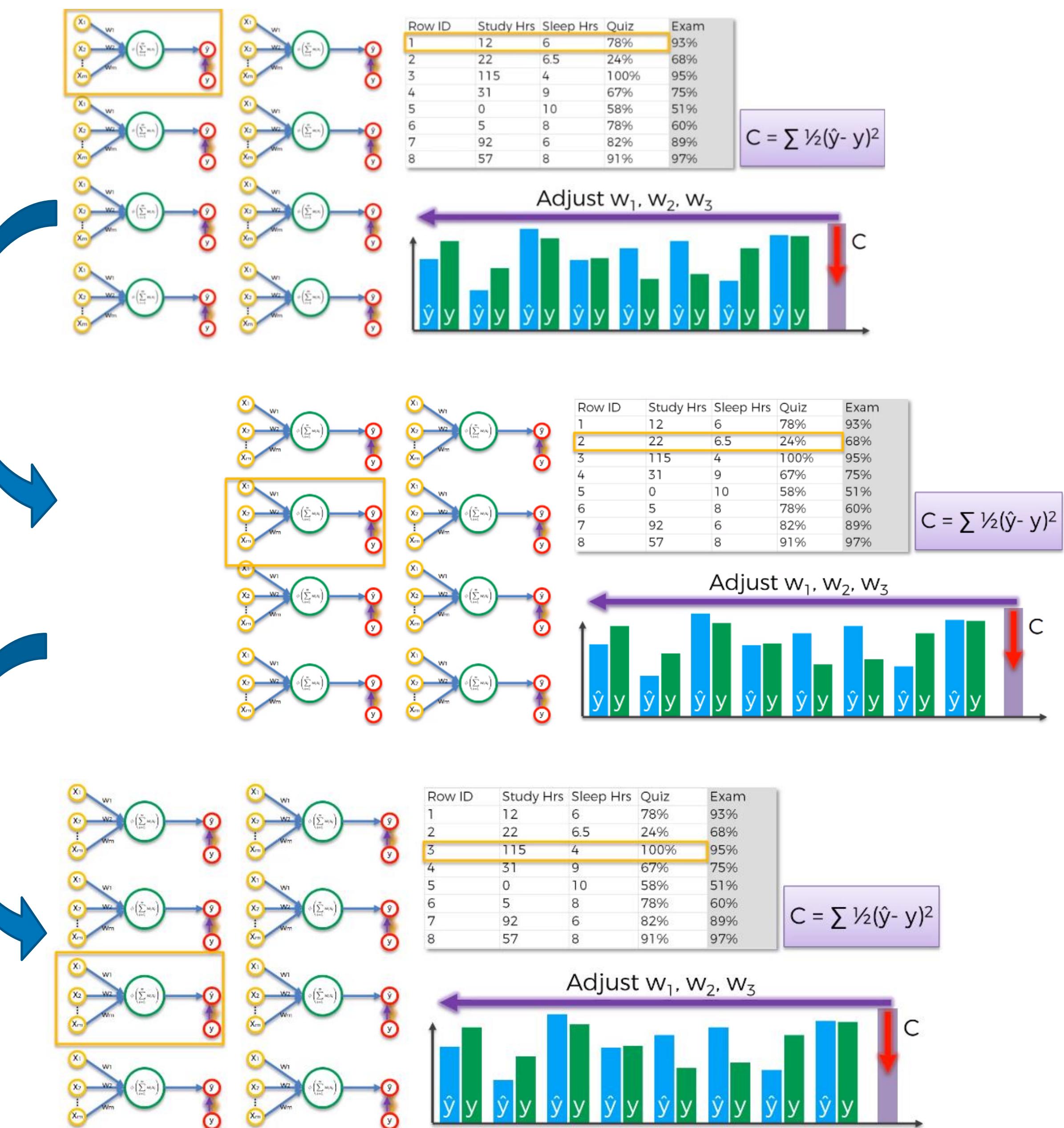


Row ID	Study Hrs	Sleep Hrs	Quiz	Exam
1	12	6	78%	93%
2	22	6.5	24%	68%
3	115	4	100%	95%
4	31	9	67%	75%
5	0	10	58%	51%
6	5	8	78%	60%
7	92	6	82%	89%
8	57	8	91%	97%

Upd w's



Gradient



Part 4: SGD in Neural Networks

So at this point you might be wondering, how does this relate to neural networks and backpropagation? This is the hardest part, so get ready to hold on tight and take things slow. It's also quite important.



That big nasty curve? In a neural network, we're trying to minimize the **error with respect to the weights**. So, what that curve represents is the network's error relative to the position of a single weight. So, if we computed the network's error for every possible value of a single weight, it would generate the curve you see above. We would then pick the value of the single weight that has the lowest error (the lowest part of the curve). I say *single* weight because it's a two-dimensional plot. Thus, the x dimension is the value of the weight and the y dimension is the neural network's error when the weight is at that position.

Stop and make sure you got that last paragraph. It's key.

Let's take a look at what this process looks like in a simple 2 layer neural network.

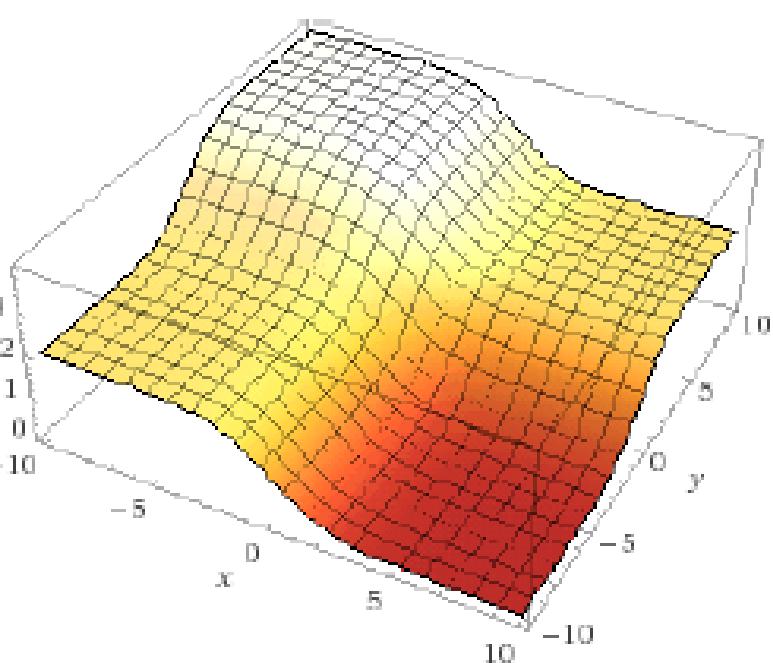
2 Layer Neural Network:

```
01.import numpy as np
02.
03.# compute sigmoid nonlinearity
04.def sigmoid(x):
05.output = 1/(1+np.exp(-x))
06.return output
07.
08.# convert output of sigmoid function to its derivative
09.def sigmoid_output_to_derivative(output):
10.return output*(1-output)
11.
12.# input dataset
13.X = np.array([[0,1],
14.[0,1],
15.[1,0],
16.[1,0]])
17.
18.# output dataset
19.y = np.array([[0,0,1,1]]).T
20.
21.# seed random numbers to make calculation
22.# deterministic (just a good practice)
23.np.random.seed(1)
24.
25.# initialize weights randomly with mean 0
26.synapse_0 = 2*np.random.random((2,1)) - 1
27.
28.for iter in xrange(10000):
```

```
29.
30.# forward propagation
31.layer_0 = X
32.layer_1 = sigmoid(np.dot(layer_0,synapse_0))
33.
34.# how much did we miss?
35.layer_1_error = layer_1 - y
36.
37.# multiply how much we missed by the
38.# slope of the sigmoid at the values in l1
39.layer_1_delta = layer_1_error *sigmoid_output_to_derivative(layer_1)
40.synapse_0_derivative = np.dot(layer_0.T,layer_1_delta)
41.
42.# update weights
43.synapse_0 -= synapse_0_derivative
44.
45.print "Output After Training:"
46.print layer_1
```

So, in this case, we have a single error at the output (single value), which is computed on line 35. Since we have 2 weights, the output "error plane" is a 3 dimensional space. We can think of this as an (x,y,z) plane, where vertical is the error, and x and y are the values of our two weights in syn0.

Let's try to plot what the error plane looks like for the network/dataset above. So, how do we compute the error for a given set of weights? Lines 31,32, and 35 show us that. If we take that logic and plot the overall error (a single scalar representing the network error over the entire dataset) for every possible set of weights (from -10 to 10 for x and y), it looks something like this.



Don't be intimidated by this. It really is as simple as computing every possible set of weights, and the error that the network generates at each set. x is the first synapse_0 weight and y is the second synapse_0 weight. z is the overall error. As you can see, our output data is **positively correlated** with the first input data. Thus, the error is minimized when x (the first synapse_0 weight) is high. What about the second synapse_0 weight? How is it optimal?

How Our 2 Layer Neural Network Optimizes

So, given that lines 31,32, and 35 end up computing the error. It can be natural to see that lines 39, 40, and 43 optimize to reduce the error. This is where Gradient Descent is happening! Remember our pseudocode?

Naive Gradient Descent:

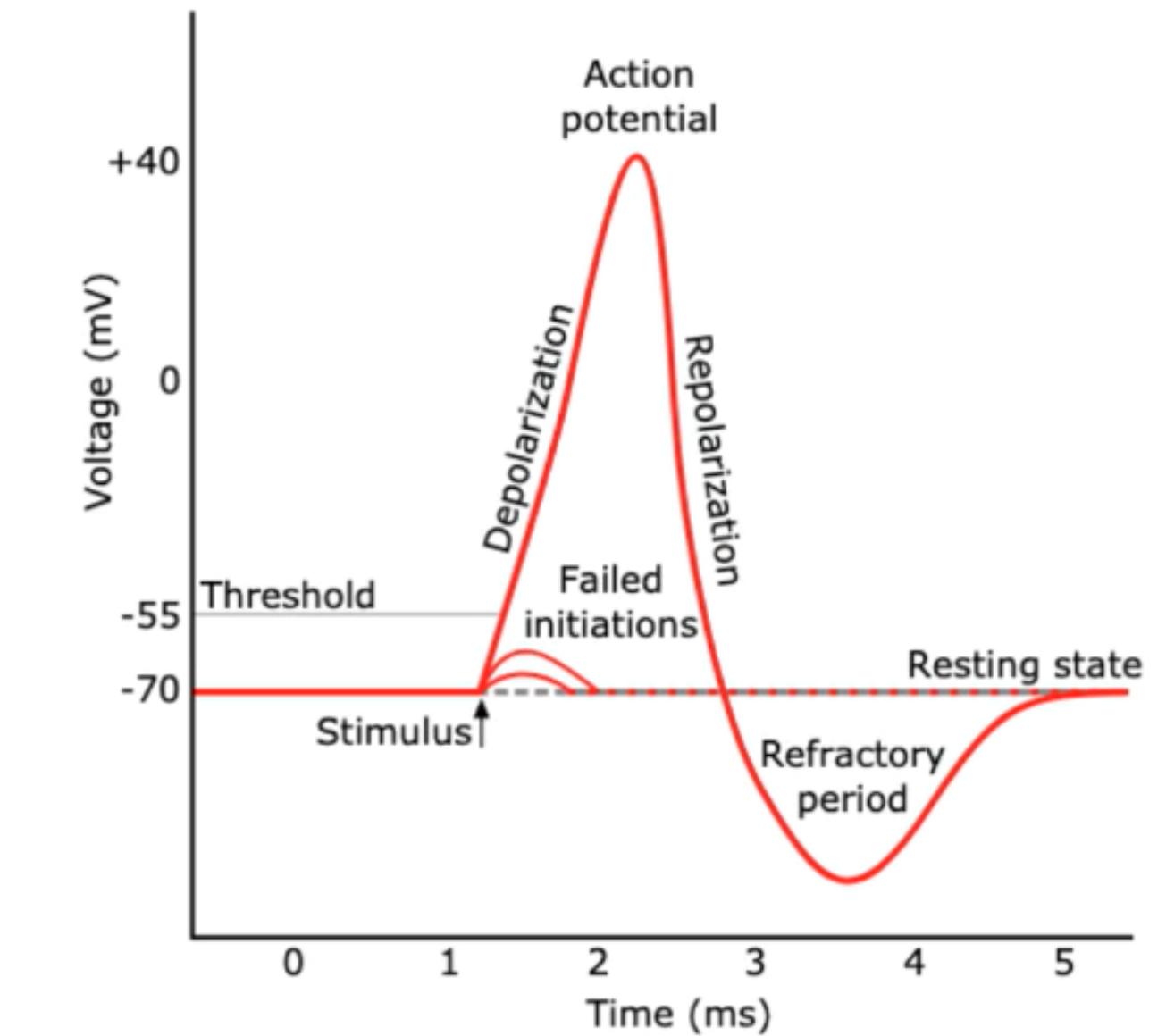
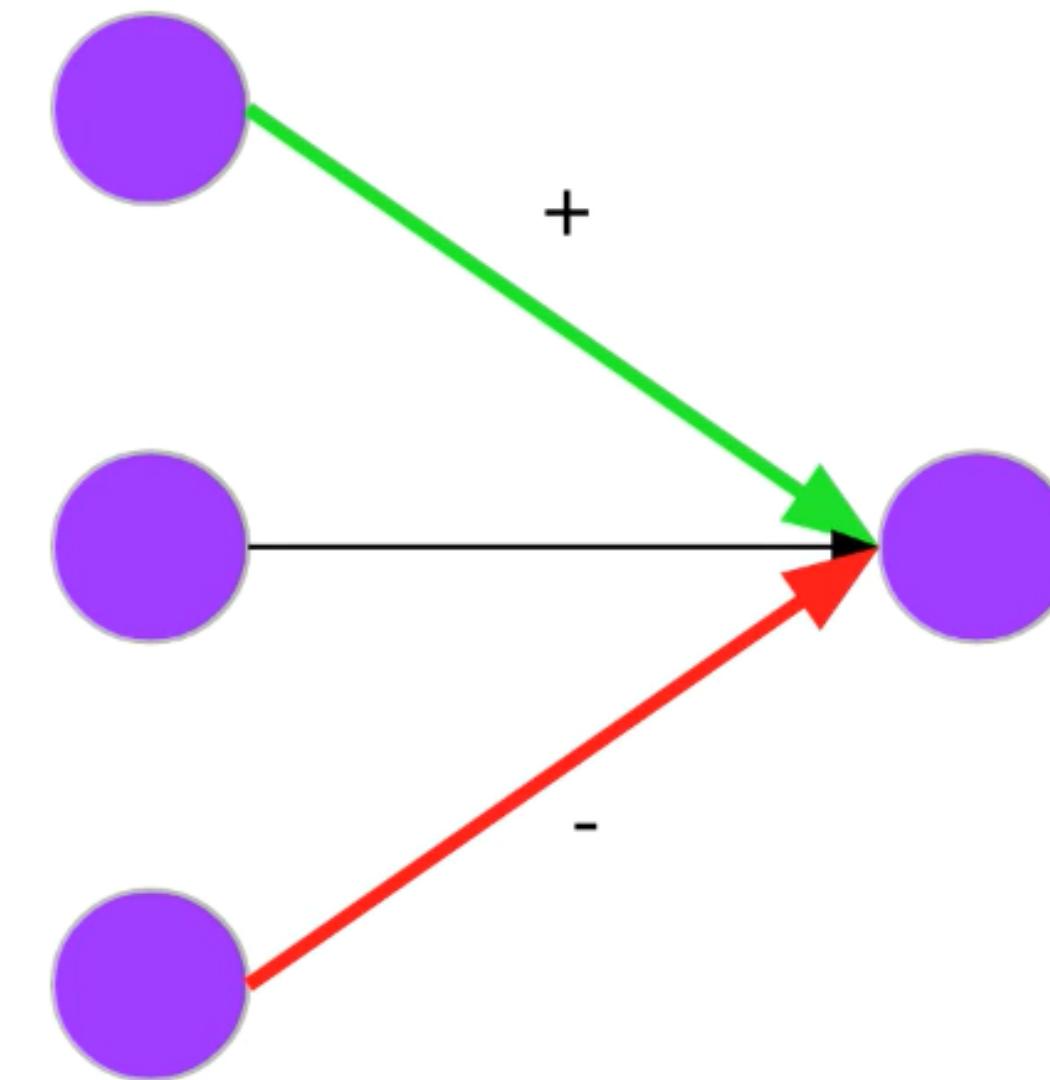
- Lines 39 and 40: Calculate "slope" at current "x" position
- Line 43: Change x by the negative of the slope. ($x = x - \text{slope}$)

A Neural Network in 13 lines of Python
(Part 2 - Gradient Descent)

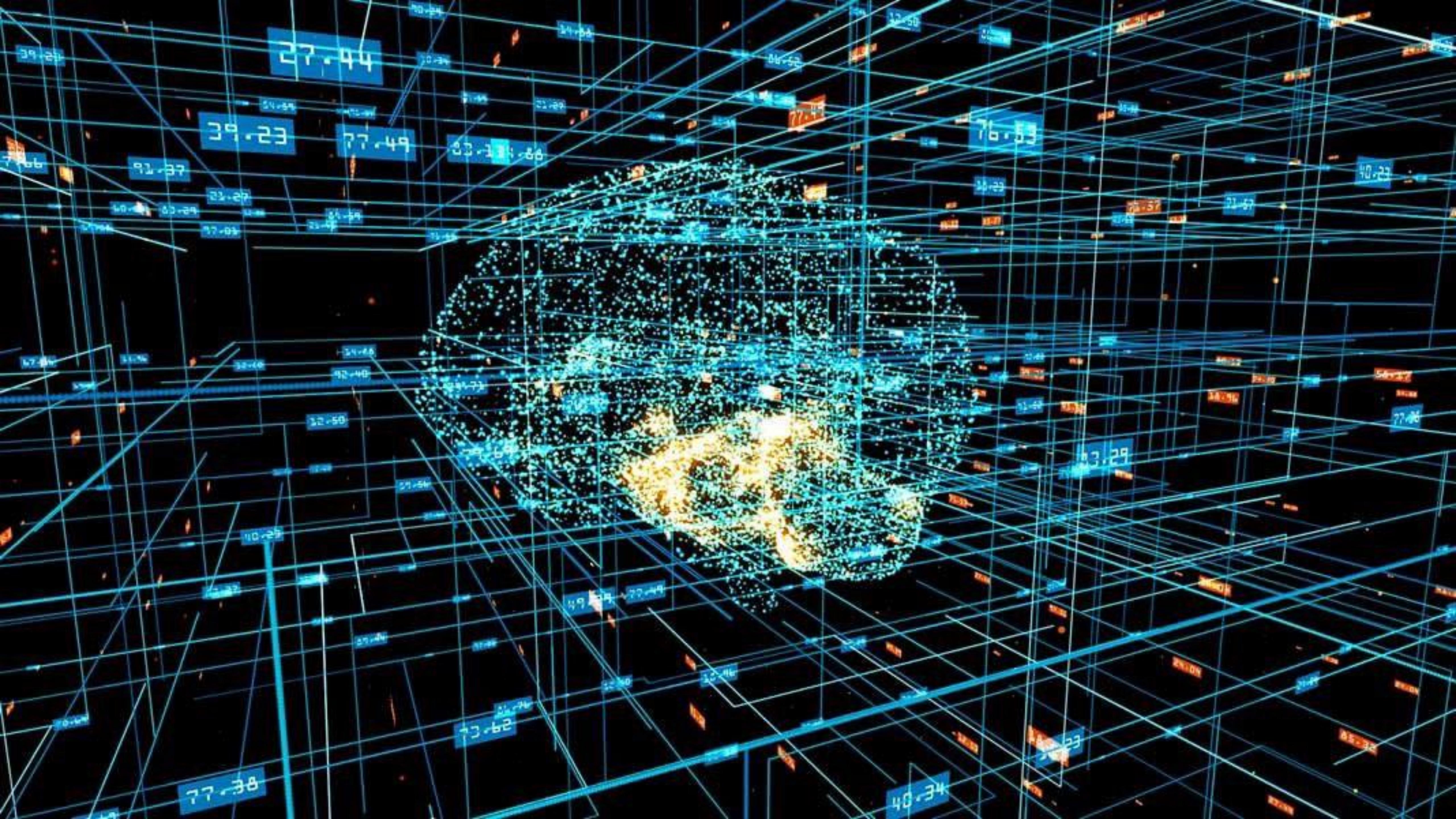
Improving our neural network by
optimizing Gradient Descent Online
available:

<https://iamtrask.github.io/2015/07/27/python-network-part2/>

Нейрон



$$p(y = 1 \mid x) = \sigma(w^T x + b) = \sigma\left(\sum_{d=1}^D w_d x_d + b\right)$$





TensorFlow

Спасибо за внимание –
переходим к практике





ДИСК



Создать



Мой диск



Компьютеры



Доступные мне



Недавние



Помеченные



Корзина



Хранилище

Использовано 41,93 ГБ из
100 ГБ

Купить больше
места



Диск



Поиск на Диске

Папку

Загрузить файлы

Загрузить папку

Google Документы

Google Таблицы

Google Презентации

Google Формы

Ещё

Хранилище

Использовано 41,93 ГБ из
100 ГБ

Купить больше
места

СК

Весь рекомендуемую область

Т-тест

ред

группа

ии

ие типы разделяют двигатели постоянного тока по схеме

и отключки заземления?

заполнение вспомогательных

-тест

тировали за последнюю неделю

ДПТ тест

* Required

ФИО и номер гра

Число:

Код функции

○ программа

○ предприним

ДПТ тес

Вы редактиру

Google Рисунки

Google Мои карты

Google Сайты

Google Apps Script

Google Colaboratory

Google Jamboard

Secure File Encryption

Text Editor

+ Подключить другие приложения



Untitled0.ipynb ☆

Файл Изменить Вид Вставка Среда выполнения Инструменты Справка Изменения сохранены

Комментировать

Поделиться



+ Код + Текст

Подключиться

Редактирование



{x}



CO Untitled0.ipynb ☆

Файл Изменить Вид Вставка

Среда выполнения Инструменты Справка Изменения сохранены

Комментировать Поделиться



Подключиться Редактирование



+ Код + Текст



- Выполнить все Ctrl+F9
- Выполнить до этой Ctrl+F8
- Выполнить код в сфокусированной ячейке Ctrl+Enter
- Запустить выбранный код Ctrl+Shift+Enter
- Выполнить ниже Ctrl+F10
- Прервать выполнение кода Ctrl+M I
- Перезапустить среду выполнения Ctrl+M .
- Перезапустить и выполнить все
- Сбросить настройки среды выполнения
- Сменить среду выполнения**
- Управление сессиями
- Показать журналы среды выполнения

Инструменты Справка Изменения сохранены

Комментарии

Подсказки

Настройки блокнота

Аппаратный ускоритель

None



None

GPU

TPU

вом режиме

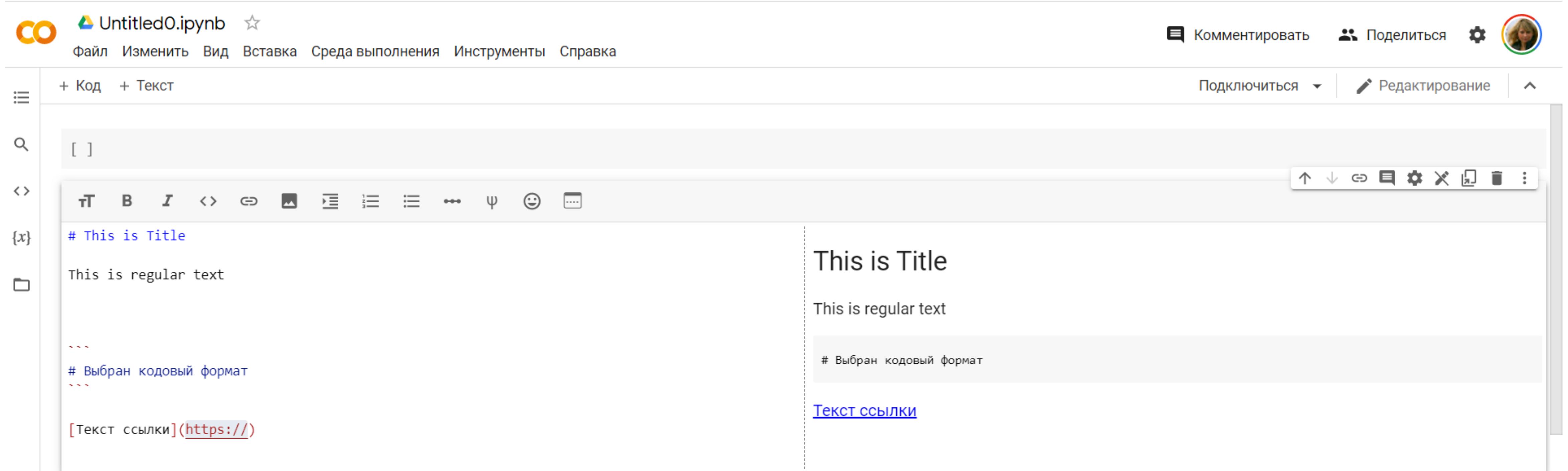
выполнялся, даже когда

вы закроете браузер? [Перейти на Colab Pro+](#)

Исключить выходные данные кодовой ячейки при
сохранении блокнота

Отмена

Сохранить



The screenshot shows a Jupyter Notebook interface with the following details:

- Title Bar:** CO Untitled0.ipynb
- Menu Bar:** Файл, Изменить, Вид, Вставка, Среда выполнения, Инструменты, Справка
- Toolbar:** Кomentировать, Поделиться, Инициализация, Редактирование
- Sidebar:** + Код, + Текст, Search icon, Comparison icon, Title section titled "This is Title" with content "This is regular text", and a code cell with "# Выбран кодовый формат".
- Main Area:** A code cell containing:

```
import numpy as np
import matplotlib.pyplot as plt
```

A blue arrow points from the bottom of this cell to the bottom of another code cell below it.
- Bottom Cell:** A code cell with a green checkmark, a play button, and the text:

```
import r
import n
```

<https://devpractice.ru/numpy-useful-functions/>

<https://pythonworld.ru/novosti-mira-python/scientific-graphics-in-python.html>